Mathematical Modeling of Gas-Phase Organic Air Pollutants

Thesis by

Robert Adam Harley

In Partial Fulfillment of the Requirements

for the Degree of

Doctor of Philosophy

Adviser: Professor Glen Cass

California Institute of Technology

Pasadena, California

1993

(Submitted December 8, 1992)

Acknowledgements

There are many individuals who have provided invaluable assistance and support to me during the last five years. First and foremost, my adviser Dr. Glen Cass has been an unfailing source of encouragement during my stay at Caltech. His insightful comments and suggestions have had a great influence on the research described in this thesis. I have been happy to spend my days as a graduate student in the Environmental Engineering Science department at Caltech. The faculty, staff and my fellow students have all contributed to an outstanding environment for research and learning. I admire particularly the leadership of Dr. Norman Brooks: his commitment to teaching and his energetic efforts to get people together for discussion on a wide range of topics.

Dr. Ted Russell of Carnegie Mellon University provided the foundation and advice along the way as I worked to develop input data fields and enhance the CIT airshed model. His hospitality during several working visits to Pittsburgh is greatly appreciated. Michael Hannigan assisted with the chemical mass balance calculations. Darrell Winner was instrumental in consolidating and implementing the detailed dry deposition algorithm used in the current airshed model. Many others in the department have contributed to the success of this research. In particular, I wish to thank our librarian Rayma Harrison, and Dr. Ken McCue for his assistance on computer-related problems. Dr. Andy Fyfe assisted me in proof-reading this thesis.

I am very grateful for financial support from the Coordinating Research Council and from the Electric Power Research Institute. I also received financial support in the form of Hewlett and C.L. Powell Fellowships.

I wish to acknowledge numerous people outside Caltech who have assisted me with my research. Bart Croes and Paul Allen of the California Air Resources Board provided essential data sets required for this research, and timely answers to my questions about data from the Southern California Air Quality Study. Other individuals who provided data or helpful advice include Dr. Bill Carter of the University of California at Riverside, Dr. Doug Lawson (now at Desert Research Institute), Dr. Julia Lester of the South Coast District, Mike Kulakowksi of Unocal, Dr. Larry Rapp of ARCO, Dr. Fred Stump of the US EPA, and Robert Wendoll of Dunn-Edwards Paint Co.

Dr. Donald Mackay at the University of Toronto first sparked my interest in environmental engineering, and I gratefully acknowledge his help and advice along the way. His interest and concern for the students in the Engineering Science program at U of T rescued me from a career in computer science.

I would like to thank past and present members of the research group for their contributions to a good working environment, and for helping me to maintain my sanity at stressful times. I have spent many happy days together with friends who have been like family here at Caltech: Andy, Annmarie, Barbara, Barry, Chris, Jeremy, Kate, and Steve. They are all true superheroes.

Although I left my family far away in Toronto, the marvels of modern technology have kept us in constant contact (thank you, Bitnet). Still, I wish that we could be together much more often.

Abstract

Volatile organic compounds (VOCs) play a significant role in the production of ozone in urban atmospheres. In addition, VOCs are of concern because some of them are toxic, and because the atmospheric oxidation of directly emitted VOCs can form condensable products which contribute to airborne particulate matter concentrations. In this study, a general model that relates pollutant emissions to ambient VOC concentrations is described. Model performance is evaluated both for ozone and VOCs for the August 27–29, 1987 period in the Los Angeles area using data from the Southern California Air Quality Study (SCAQS).

Improved chemical composition profiles for major VOC emission sources are presented, and use of these profiles results in significant changes to previous emissions estimates for many individual VOCs. Reconciliation of emission data with speciated ambient VOC concentration data from the Los Angeles area indicates that there is much more unburned gasoline in the atmosphere than the emission inventory suggests.

Three photochemical airshed models are presented that predict the ambient concentrations of VOCs. The first model predicts concentrations of lumped VOC classes (e.g. lumped alkanes, monoalkyl benzenes). Satisfactory model performance is obtained only after the VOC emission estimates prepared by the government are scaled up to match emission rates measured in the Van Nuys tunnel. An enhanced airshed model with 53 individual

VOCs represented explicitly also is described and tested. The best performance is obtained for aromatic hydrocarbons which are predicted to within ±20% by the model in most cases; concentrations of most other species are predicted to better than ±50%. Finally, a model for gas-phase toxic organic air pollutants is described and tested for species including aromatics, aldehydes, ketones, and 1,3-butadiene among others. Significant contributions to total ambient concentrations from atmospheric photochemical formation are found for formaldehyde, acetaldehyde, propionaldehyde, acrolein and methyl ethyl ketone. Therefore, control programs for some toxic air pollutants must consider photochemical formation pathways in addition to direct emissions.

The novel aspects of this study include the analysis and improvement of speciated VOC emission estimates, and the development and testing of airshed models for lumped and individual VOCs using data from SCAQS.

Contents

List of Tables

List of Figures

1 Introduction

1.1 Motivation

Volatile organic compounds (VOCs) are an important part of the air pollution problem, in both urban and regional environments. When combined in the atmosphere with oxides of nitrogen (NO_x), VOCs promote the formation of ozone, a key ingredient in photochemical smog, and a widespread air pollution problem [1]. Because of the complex non-linear relationship between ambient ozone concentrations and precursor emissions of VOC and NO_x, it is not immediately obvious whether VOC emissions, NO_x emissions, or both should be controlled to reduce ozone levels [1].

Eulerian photochemical air quality models (airshed models) have been developed and applied to predict the spatial and temporal distribution of ozone concentrations in urban and regional atmospheres based on knowledge of atmospheric chemistry, meteorology, and pollution emission rates [1]. Airshed models have played an important role in the design of air quality improvement plans [2], in particular, in the assessment of the effect of VOC and NO_x emission reductions on ozone levels. Given the costs and time required to implement air quality improvement plans, it is essential that any proposed emission control program be demonstrably effective.

Comparisons between predicted and observed ozone concentrations have been reported in numerous studies, as reviewed by Tesche [3]. Results of such modeling studies have been called into question because of uncertain-

ties in the estimates of pollutant mass emission rates. In particular, it is likely that VOC emission rates have been significantly underestimated by the government [1,4,5,6].

While comparisons between predicted and observed ozone concentrations are presented routinely in photochemical modeling studies, similar analyses are less common for the key ozone precursors (i.e., VOC and NO_x). In the past, only total VOC concentration predictions have been scrutinized, and large negative biases have been found in model predictions relative to atmospheric observations in the few studies where comparisons have been made [7]. If VOC concentrations are indeed underestimated in these modeling studies, this suggests that the apparent good agreement between predicted and observed ozone concentrations that is often reported may be a fortuitous result involving other errors that compensate for understated VOC emissions. This would imply that analyses demonstrating the effectiveness of VOC and/or NO_x emission reduction plans might be flawed as well.

Biogenic hydrocarbons such as isoprene and terpenes are of concern because they represent background sources of VOC emissions to the atmosphere that are not subject to emission controls. The wisdom of ozone control programs that rely on VOC emission reductions has been questioned in several studies [1,8,9] because biogenic emissions may continue to supply enough VOCs to compromise the effectiveness of the control program, even if anthropogenic VOC emissions were to be eliminated.

In the chemical mechanisms typically incorporated into airshed models designed to predict ozone formation, emissions of the many individual VOCs are consolidated into a small number of groupings (on the order of 10 groups is typical) [10,11,12]. While this lumping does not significantly affect the ability

to predict ozone concentrations, it does mean that much of the chemical detail in the representation of VOCs is lost. This means that one also loses the opportunity to use a detailed analysis of VOC concentration predictions to diagnose problems with the model or its associated emissions input data.

Looking beyond the role that VOCs play in promoting ozone formation, there are added reasons why it is desirable to develop models that do treat individual VOCs explicitly. Recent amendments to the Clean Air Act (1990) in the United States require control of 189 individual organic and inorganic species that have been declared to be toxic air pollutants. To verify our overall understanding of the emissions and atmospheric chemistry of individual toxic air pollutants, it is helpful to be able to predict ambient concentrations of these species directly from emissions data using an air quality model. In addition, because some toxic pollutants are formed in the atmosphere as oxidation products of other VOCs, control programs that consider only direct emissions may fail for these cases. It is essential that the relative contributions of direct emissions and atmospheric photochemical formation be understood. Otherwise, programs that seek to reduce toxic pollutants in the atmosphere by mandating emission controls may not produce the expected result.

Even in cases where an individual VOC is not of concern as a toxic air pollutant, it is still useful to track some of these species explicitly in air quality models (instead of lumping them together with other species). For example, combinations of tracers unique to particular emissions sources may be used to diagnose the contributions of these sources to the total region-wide pollutant emission inventory.

Airborne particulate matter constitutes another part of the air pollu-

tion problem. In addition to direct emissions of particulate organic carbon from sources, the gas-phase oxidation of some VOCs can produce low vapor pressure reaction products that condense to form additional secondary aerosol [13,14,15]. If the importance of this secondary organic aerosol is to be assessed, an understanding of the precursor VOC species concentrations is required.

1.2 Research objectives

The major objective of the present research is to develop and test general models for the prediction of VOC concentrations in the atmosphere. Within the scope of this research are assessments of airshed model performance in predicting ozone, VOC, and NO_x species concentrations. Diagnosis and improvement of the pollutant emission inventory procedures used by the government form a necessary part of this work.

Accomplishment of these objectives will contribute to the understanding of VOC emissions, their atmospheric concentrations, and their role in promoting ozone formation. In addition, other elements of the air pollution problem will be addressed including prediction of the concentrations of specific toxic air pollutants and prediction of the concentrations of important secondary organic aerosol precursors.

1.3 Southern California Air Quality Study

An obstacle to more detailed consideration of VOCs in the past has been the scarcity of speciated ambient VOC concentration measurements. In response to this problem, and to improve the understanding of many other aspects of the air pollution problem, a major field study was conducted in the Los

Angeles, California area during the summer and fall of 1987 [16]. This study, referred to as the Southern California Air Quality Study, or SCAQS, provides data that are critical to the development and testing of airshed models that predict ozone and VOC concentrations. Further details of the measurements made during SCAQS have been presented elsewhere [16].

The first step in achieving the research objectives outlined above was to acquire and analyze the meteorolgical and ambient air quality data available from SCAQS. This constitutes an enormous and complex data base assembled from the results reported by numerous investigators. Having gained an understanding of the data available and the prevailing meteorological conditions and air quality, a particular summertime episode from SCAQS was selected for photochemical modeling purposes. This episode, August 27–29, included the highest observed ozone concentrations for any of the SCAQS intensive monitoring periods. A peak one-hour average ozone concentration of 290 parts per billion was measured at the Glendora air monitoring site located 35 kilometers to the east (inland) of downtown Los Angeles, a concentration far above the National Ambient Air Quality Standard for ozone of 120 parts per billion. An additional reason for selecting the August SCAQS episode was that day-specific pollutant emission estimates were available from the government.

1.4 Approach

The purpose of this section is to provide an overview of the remaining chapters of this study. In Chapter 2, improvements to an existing Eulerian photochemical air quality model and application of the model to the prediction of air quality during the August 1987 SCAQS episode are described. Model

performance for ozone and ozone precursors is assessed, and the sensitivity of model predictions to increased on-road vehicle exhaust emissions is investigated.

The chemical composition of VOC emissions from major emission sources is considered in Chapter 3. A set of revised chemical speciation profiles is developed that describes the detailed molecular composition of organic gas emissions from individual source types, and comparisons are made with the official emission inventory and with speciated ambient concentration data acquired in the Los Angeles area. While much current attention is focussed on overall VOC mass emission rates, little attention has been paid in the past to the chemical composition of VOC emissions. The main motivation for the research described in Chapter 3 is to enable further work that requires improved chemical resolution of VOC emission estimates.

In Chapter 4, a detailed comparison of predicted and observed concentrations is reported for each of the lumped VOC species employed in the LCC atmospheric chemical reaction mechanism (Lurmann, Carter and Coyner [11]). Several different emission inventories are used in this analysis: the baseline VOC mass emission estimates prepared by the government, an alternative inventory with increased on-road vehicle exhaust emissions, and the official versus revised (as per Chapter 3) VOC emissions composition profiles.

An airshed model with much more detailed representation of VOCs is described in Chapter 5. This detailed model allows for flexible disaggregation of VOCs from lumped species classes typically used to represent the atmospheric chemistry of VOCs. An evaluation of model performance for each of nearly 50 individual VOCs measured during SCAQS is presented as a means of thoroughly testing the detailed model.

A derivative of this detailed model for individual VOCs is used to investigate the relationships between emissions and air quality for a variety of gas-phase toxic organic air pollutants that are expected to be pervasive in urban environments. The model and its application to the August SCAQS episode are described in Chapter 6. Assessments of the relative contributions of direct emission sources and atmospheric photochemical production to the total concentrations of various toxic organic air pollutants are reported.

Finally, in Chapter 7, the key accomplishments and important results of this research program are summarized. Areas of remaining uncertainty are identified, together with recommendations for future research.

2 Ozone modeling

2.1 Introduction

Concentrations of ozone in the boundary layer of urban and rural atmospheres continue to exceed standards designed to protect human health, despite more than 25 years of effort and billions of dollars of investment in technology to control the emissions of ozone precursors [1]. Mathematical models have been developed that describe the formation and transport of ozone and other components of photochemical smog based on knowledge of atmospheric chemistry, meteorology, and pollutant emissions to the atmosphere [1,17]. In this chapter we describe improvements to an existing Eulerian photochemical air quality model [18,19,20], referred to as the CIT airshed model. Earlier versions of this model have been used to study photochemical smog formation in the Los Angeles area [19,20], formation and control of nitrogen-containing pollutants [20,21], spatial patterns in pollutant responses to emission controls [22], the effects of methanol fuel use in motor vehicles [23], and deposition of nitrogen-containing air pollutants [24].

Reference: Harley, R. A.; Russell, A. G.; McRae, G. J.; Cass, G. R.; Seinfeld, J. H. Photochemical modeling of the Southern California Air Quality Study. *Environ. Sci. Technol.*, **27**, in press, 1993.

This chapter describes the application of the CIT airshed model to the August 27–29, 1987 period in the Los Angeles, California area. This 3-day interval was one of the intensive monitoring periods of the Southern California Air Quality Study (SCAQS; for an overview, see reference [16]) which took place during the summer and fall of 1987. As part of SCAQS, a variety of special meteorological and air quality measurements were carried out to supplement the routine measurements made in the Los Angeles area, thus providing a very detailed ambient data set expressly designed for supporting and testing photochemical airshed models. Data collected during SCAQS will form the basis for many air pollution control decisions in the Los Angeles area over the next decade. In addition, the decisions made in Los Angeles will influence air pollution control policies elsewhere. Several recent studies have questioned the accuracy of the official emission inventory for organic gases and carbon monoxide in the Los Angeles area [1,4,5,6]. If the emissions of organic gases are in fact understated in the official inventory, the air pollution control problem in Los Angeles may be more difficult than was previously thought. It is therefore important that the relationship between emissions and ambient air quality be explored thoroughly for the SCAQS experiment.

In the course of the present study, revisions to the CIT photochemical airshed model have been made. In particular, an extended version of the chemical mechanism of Lurmann et al. [11], and an improved dry deposition module [24] have been incorporated into the model. Further changes have been made to allow for representation of the observed spatial variations in the total and ultraviolet component of the solar radiation flux. These changes are described in greater detail later in the text.

2.2 Model description

Photochemical models such as the CIT airshed model are based on the numerical solution of the atmospheric diffusion equation, which is written repeatedly for each chemical species of interest:

$$\frac{\partial C_i}{\partial t} + \nabla \cdot (\vec{u} C_i) = \nabla \cdot (K \nabla C_i) + R_i + Q_i, \tag{2.1}$$

where C_i is the ensemble mean concentration of species i, $\vec{u}$ is the mean wind velocity, K is the eddy diffusivity tensor (here assumed to be diagonal), R_i is the rate of generation of species i by chemical reactions, and Q_i is a source term for elevated point sources of species i. Boundary and initial conditions, along with meteorological data and emissions fields, complete the specification of the problem. The surface boundary condition sets the upward flux of each pollutant to be equal to direct emissions minus the dry deposition flux:

$$-K_{zz}\frac{\partial C_i}{\partial z} = E_i - v_g^i C_i, \tag{2.2}$$

where K_{zz} is the vertical eddy diffusivity, z is the elevation above ground level, E_i is the ground-level emission flux, and v_g^i is the dry deposition velocity for species i. A no-flux boundary condition is applied at the top of the modeling region. Lateral boundary conditions and initial conditions throughout the modeling region are established using measured pollutant concentration data.

The details of the mathematical model and numerical solution techniques that are used in this study have been described previously [18,20,25]. A number of improvements have been made to an earlier version of this model [20], as described in the following sections. A detailed description of the model, recent enhancements, and performance evaluation is also presented

in reference [25]. A three-volume user's manual for the CIT airshed model has been prepared. These volumes describe installation and operation of the model [26], data preparation and formats [27], and the computer source code [28].

2.2.1 Chemical mechanism

The condensed version of the LCC chemical mechanism (Lurmann, Carter and Coyner [11]) has been incorporated into the CIT airshed model. The published mechanism includes 26 differential and 9 steady-state chemical species.

In addition to the 8 lumped organic classes specified by Lurmann et al. [11], the chemical mechanism has been expanded to include, explicitly, the chemistry of methane, methanol, ethanol, methyl tert-butyl ether (MTBE), isoprene, hydrogen peroxide, and sulfur dioxide. The complete list of chemical species defined in the extended chemical mechanism is shown in Table 2.1. All of the reactions beyond those listed in the published version of the LCC mechanism are shown in Table 2.2. Methane is not followed dynamically in the model, but instead a constant background concentration of 2.2 ppm is applied. Isoprene is used as a surrogate for all biogenic hydrocarbon emissions in the present model. The oxygenated species (methanol, ethanol and MTBE) are of interest as ingredients in alternative or reformulated motor vehicle fuels [23]. The introduction of reformulated motor vehicle fuels containing MTBE did not occur in the Los Angeles area until after the 1987 SCAQS experiment, so therefore there are no emissions of MTBE for the calculations described in the present study.

Table 2.1: List of species defined in the chemical mechanism

Species Code	Species Name	Species Code	Species Name
Differential species:		Steady-state species:	
NO	Nitric oxide	OSD	Oxygen - singlet D
NO2	Nitrogen dioxide	O	Atomic oxygen
O3	Ozone	OH	Hydroxyl radical
HONO	Nitrous acid	RO2R	General RO_2 #1
HNO3	Nitric acid	R2O2	General RO_2 #2
HNO4	Pernitric acid	RO2N	Alkyl nitrate RO_2
N2O5	Dinitrogen pentoxide	RO2P	Phenol RO_2
NO3	Nitrogen trioxide	BZN2	Benzaldehyde N-RO_2
HO2	Hydroperoxy radical	BZO	Phenoxy radical
CO	Carbon monoxide		
HCHO	Formaldehyde	Newly added species (this study):	
ALD2	Acetaldehyde	H2O2	Hydrogen peroxide
MEK	Methyl ethyl ketone	MEOH	Methanol
MGLY	Methyl glyoxal	ETOH	Ethanol
PAN	Peroxyacetyl nitrate	MTBE	Methyl tert-butyl ether
RO2	Total RO_2 radicals	ISOP	Isoprene
MCO3	CH_3CO_3 radical	NH3	Ammonia
ALKN	Alkyl nitrate	NIT	Aerosol nitrate
ALKA	C_4^+ alkanes[a,b]	SO2	Sulfur dioxide
ETHE	Ethene	SO3	Sulfur trioxide
ALKE	C_3^+ alkenes	CH4	Methane
TOLU	Toluene		
AROM	Higher aromatics		
DIAL	Unknown dicarbonyls		
CRES	Cresol		
NPHE	Nitrophenols		

[a]50% of propane emissions also are assigned to the lumped alkane class; the remaining propane emissions are treated as unreactive, as per Lurmann et al. [11].
[b]30% of benzene emissions also are assigned to the lumped alkane class, as per Lurmann et al. [11].

Table 2.2: Chemical reactions added to LCC mechanism

Reaction Number	Chemical Reaction			Rate Constant[a]	Reference
96	H2O2 + hν	$\rightarrow$	2 OH	[b]	[11]
97	H2O2 + OH	$\rightarrow$	HO2 + H2O	$1.36 \times 10^6/T \times e^{-187/T}$	[11]
98	MEOH + OH	$\rightarrow$	HCHO + HO2	$2.81 \times T \times e^{148/T}$	[29]
99	CH4 + OH	$\rightarrow$	HCHO + RO2 + RO2R	$3.06 \times T \times e^{-1282/T}$	[29]
100	ISOP + OH	$\rightarrow$	HCHO + ALD2 + RO2 + RO2R	$1.12 \times 10^7/T \times e^{410/T}$	[29]
101	ISOP + O3	$\rightarrow$	0.5 HCHO + 0.65 ALD2 + 0.21 MEK + 0.16 HO2 + 0.29 CO + 0.06 OH + 0.14 RO2 + 0.14 RO2R	$5.41 \times 10^3/T \times e^{-2013/T}$	[29]
102	ISOP + O	$\rightarrow$	0.4 HO2 + 0.5 MEK + 0.5 ALD2	$2.64 \times 10^7/T$	[29]
103	ISOP + NO3	$\rightarrow$	NO2 + HCHO + ALD2 + RO2 + R2O2	$1.12 \times 10^7/T \times e^{-1121/T}$	[29]
104	ETOH + OH	$\rightarrow$	ALD2 + HO2	$2.72 \times T \times e^{532/T}$	[29]
105	MTBE + 1.4OH[c]	$\rightarrow$	0.4 HCHO + 0.4 MEK + 1.8 RO2 + 1.4 RO2R + 0.4 R2O2 + 0.6 TBF[d]	$3.00 \times T \times e^{460/T}$	[30,31]
106	SO2 + OH	$\rightarrow$	SO3 + HO2	$4.00 \times 10^5/T$ [e]	[29]
107	HNO3 + NH3	$\leftrightarrow$	NIT	[f]	[32,33]

[a] In units of $\text{ppm}^{-1}\ \text{min}^{-1}$, with T specified in degrees Kelvin.

[b] Photolysis rate constant (min^{-1}) depends on light intensity.

[c] The rate expression is simply k[MTBE][OH]. Additional hydroxyl radicals are consumed because an intermediate product is assumed to be oxidized rapidly.

[d] TBF (tertiary butyl formate) is treated as an inert species.

[e] Approximate expression obtained assuming $p = 1$ atm.

[f] Ammonium nitrate aerosol (NIT) is assumed to exist in equilibrium with gas-phase nitric acid and ammonia.

2.2.2 Dry deposition

Because dry deposition fluxes influence atmospheric pollutant concentrations and may adversely affect vegetation and building materials, air quality models should include a thorough calculation of dry deposition velocities. Earlier versions of the CIT airshed model [18,20] calculated a fluid-mechanically determined upper limit value for the dry deposition velocity based on local surface roughness and meteorological conditions, and then applied species-specific linear attenuation factors to estimate the actual deposition velocities for species that are removed by dry deposition at less than the diffusion-limited rate.

A new dry deposition scheme described by Russell et al. [24] has been incorporated into the present version of the model. As before [18], a maximum deposition velocity ($v_{g\ \max}$) is calculated for each grid square assuming that the surface acts as a perfect sink for the depositing pollutant:

$$v_{g\ \max} = \frac{k^2 u(z_r)}{[\int_{z_0}^{z_r} \phi_m(\frac{z}{L})\frac{dz}{z}][2(\frac{\mathrm{Sc}}{\mathrm{Pr}})^{2/3} + \int_{z_0}^{z_r} \phi_p(\frac{z}{L})\frac{dz}{z}]}, \tag{2.3}$$

where k is von Karman's constant, $u(z_r)$ is the wind speed at the reference elevation z_r, z_0 is the surface roughness length, L is the Monin-Obukhov length, Sc is the Schmidt number, and Pr is the Prandtl number. The functions ϕ_m and ϕ_p are based on the momentum and heat flux-profile relationships of Businger et al. [34].

The dry deposition velocity v_g^i for each species is calculated as a function of $v_{g\ \max}$ and a surface resistance term that depends on the surface type (i.e., land use) and the solar radiation flux:

$$v_g^i = \frac{1}{(1/v_{g\ \max}) + r_s^i}, \tag{2.4}$$

where r_s^i is the surface resistance term for chemical species i. Separate values of r_s^i are specified for each chemical species and each of 32 land use types, based on the advice of Sheih et al. [35] and engineering judgement [24].

2.2.3 Solar radiation fields

Rate constants for photolysis reactions are usually estimated using a model that predicts the actinic flux at various wavelengths given the solar zenith angle [36], and from published values of the absorption cross sections and quantum yields for those species that undergo photolysis. The actual photolysis rates may differ from predicted values due to seasonal and local variations in pollutant concentrations and cloud cover. There can also be a pronounced increase in radiation intensity in the vertical direction above ground level [36].

Solar radiometers are available that measure the broadband ultraviolet component (295–385 nm) of the incoming radiation. Data from such instruments can be used to estimate directly the NO_2 photolysis rate [37,38]. This issue will be discussed later in the text with reference to SCAQS.

The CIT airshed model has been modified to accept a spatially and temporally resolved ground level photolysis scaling factor field, plus a single region-wide correction factor that can be applied at the upper boundary of the modeling region. Linear interpolation of the photolysis scaling factors between ground level and the top of the modeling region is used to estimate the vertical variation of photolysis rate constants, creating in effect a three-dimensional ultraviolet radiation field.

The total (as opposed to ultraviolet) solar flux can also exhibit significant variations from predictions that assume clear sky conditions. Within the

model, the total solar radiation flux is first computed as a function of the solar zenith angle assuming clear sky conditions [39]. Then these clear sky solar radiation values are corrected to account for the spatial distribution of cloud cover. Direct measurements of the total radiation flux are the preferable means for computing solar flux scaling factors, but scaling factors can also be estimated based on the fraction of sky covered by clouds using formulas of the form $1 + b_1 \cdot N^{b_2}$ where N is the fraction of sky obscured by clouds, and b_1 and b_2 are empirical constants [39]. The CIT airshed model has been further modified to accept a temporally and spatially resolved total solar radiation scaling factor field.

2.3 Model application to August SCAQS

In this section, the application of the CIT airshed model is described for a 3-day period during summer 1987 in the Los Angeles, California area. The particular days selected encompass one of the intensive monitoring periods of SCAQS: the episode being simulated begins on Thursday, August 27 and continues through Saturday, August 29. The highest measured ozone concentration for this period was observed at Glendora on August 28, with a peak 1-hour average value of 29 pphm reported.

The geographical region under consideration is shown in Figure 2.1. For the purposes of the present air quality modeling calculations, a regular 5 by 5 kilometer square grid system was superimposed on the region, and emissions and meteorological data were specified at each grid square as described later in the text. The modeling region extended to a height of 1100 meters above ground level, with the vertical dimension subdivided into five computational layers. The thicknesses of these five layers, beginning at ground level, were

38, 116, 154, 363, and 429 meters.

2.3.1 Emission inventory

Detailed pollutant emissions data are required for the application of photochemical models. The emission inventory must be both spatially and temporally resolved. A special emission inventory development program for SCAQS has been undertaken [40]. This effort resulted in a set of day-specific data files that specify the emissions of carbon monoxide, oxides of nitrogen, total organic gases, oxides of sulfur, and particulate matter at a spatial resolution of 5 km. The temporal resolution is hourly, although in some cases only daily emissions totals are specified, in which case a source-specific diurnal variation profile is applied to obtain hourly emissions.

The emission inventory used in this study was received from the California Air Resources Board [41]. Mobile source emission estimates were based on a travel demand model and the EMFAC 7E emissions factor model [42]. Stationary source emissions estimates were prepared by the South Coast Air Quality Management District. These estimates include day-specific power plant, aircraft, and refinery emissions. A highly aggregated summary of the emission inventory for August 27 is presented in Table 2.3. The detailed inventory includes emissions from more than 800 source types, with the organic gas emissions broken down into 280 detailed chemical species. The inventory region includes the South Coast Air Basin plus parts of the Southeast Desert Air Basin (to the north and east of the mountains surrounding the Los Angeles area) and parts of Ventura County (to the northwest).

The mobile source emission inventories provided for use in this study are all based on identical weekday traffic flow patterns, even though the last day

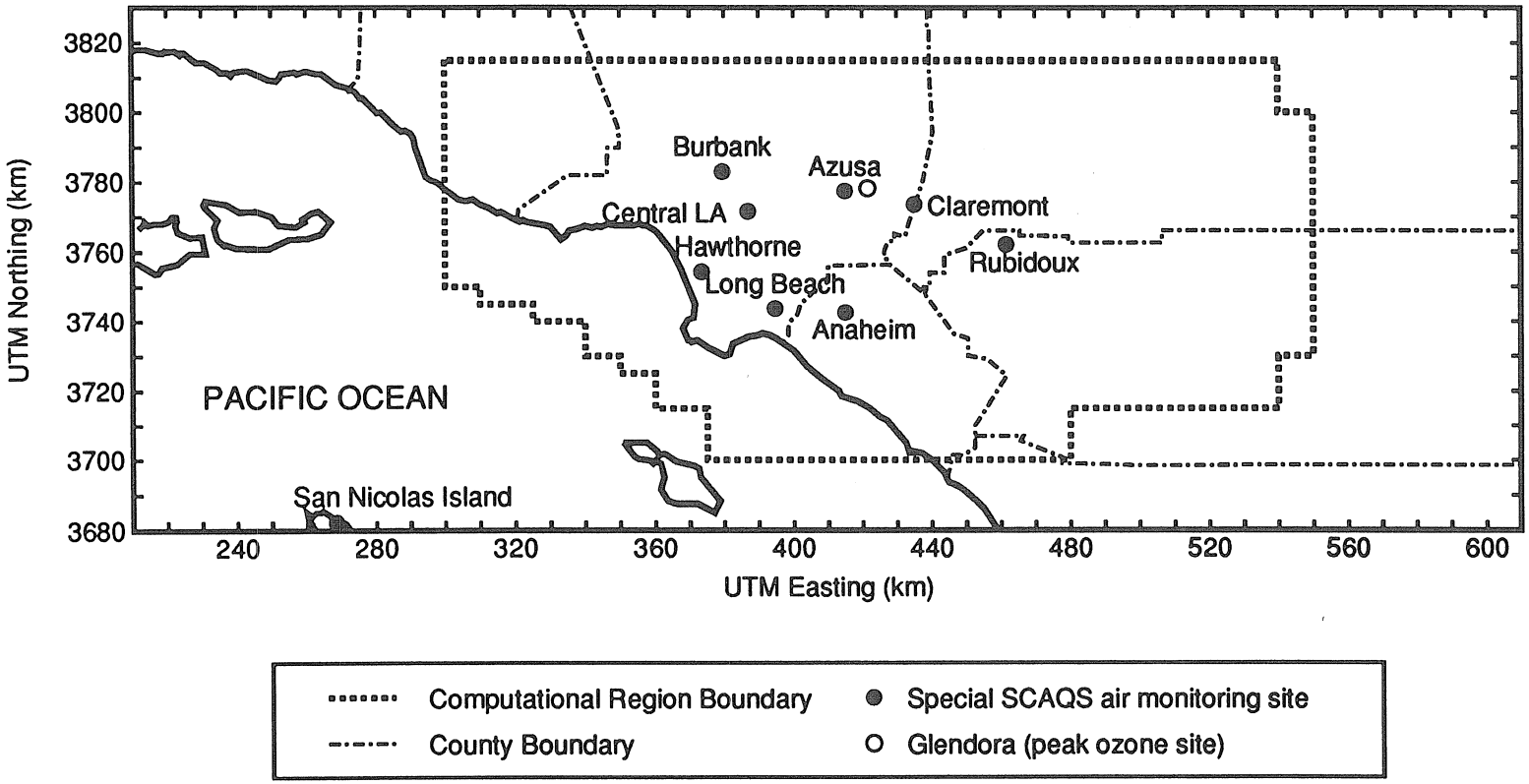

Figure 2.1: Map of the Los Angeles, California area showing the computational region and the locations of special SCAQS air quality monitoring sites.

Table 2.3: Region-wide[a] emissions summary for August 27, 1987

Source type	Base Case Emissions (10^3 kg/day) NMOG[b]	NO_x	CO
On-road vehicle gasoline engines:			
cold exhaust	150	[c]	[c]
hot exhaust	296	[c]	[c]
Evaporative emissions:			
running losses	51	—	—
hot soak	98	—	—
diurnal	24	—	—
On-road diesel engine exhaust	26	[c]	[c]
Subtotal on-road vehicles	645	678	4743
Other mobile sources	61	124	418
Stationary source fuel combustion	29	259	204
Organic solvent emissions:			
surface coatings	363	—	—
domestic products	97	—	—
degreasing & cleaning	109	—	—
pesticides	31	—	—
Biogenic emissions	117	—	—
All other sources	410	77	259
Grand Totals	1745	1138	5624

[a]The inventory region covers most of the area shown in Figure 2.1 which includes portions of the Southeast Desert Air Basin, and portions of Ventura County in addition to the entire South Coast Air Basin

[b]Non-methane organic gases

[c]On-road vehicle NO_x and CO exhaust emissions were not broken down into subcategories in the official inventory

of the modeling period falls on a Saturday. The mobile source inventories are only "day specific" in that they are corrected for spatial and diurnal variations in temperature. Separate stationary source emissions estimates for weekdays and weekends were prepared and were used in this study as appropriate. As a sensitivity test, an alternate emission inventory using increased mobile source exhaust emission factors was prepared. This was done in an attempt to explore the higher on-road vehicle emission rates suggested by a 1987 study of emissions measured within the Van Nuys roadway tunnel in the Los Angeles area [4]. The on-road vehicle hot exhaust emissions of carbon monoxide and organic gases were increased to three times the EMFAC 7E values. Although this exhaust emissions increase is substantial for the particular source categories affected, it is not large in the context of the total organic gas emissions inventory (before being scaled up, the on-road vehicle hot exhaust emissions represented 17% of the total baseline organic gas emissions from all sources combined, as shown in Table 2.3). There are also uncertainties associated with the estimates for mobile source cold start and evaporative emissions, for stationary source emissions, and for biogenic emissions. However, for the purposes of the present hot exhaust emissions sensitivity analysis, emissions from other source categories were not changed.

In addition to the anthropogenic emissions discussed above, there are emissions of isoprene and terpenes from natural and urban vegetation. A study by Winer et al. [43] measured organic gas emission factors for many different plant species found in Southern California, including various urban ornamental plants. A later study investigated organic gas emissions from crops [44]. Based on a new gridded inventory of leaf biomass in the Los Angeles area [45], and temperature and solar radiation data for August 27

and 28, new day-specific biogenic emission inventories were prepared [46]. Because no day-specific biogenic inventory for August 29 was available, the biogenic inventory for August 28 was used for both August 28 and 29.

An ammonia emission inventory also is included in these calculations. The inventory used in this study is the 1982 South Coast Air Basin inventory of Gharib and Cass [47]. The basin-wide emissions of ammonia were estimated to be 164 tons/day, with over half of the emissions coming from livestock waste. A revised ammonia emission inventory is being prepared as part of the SCAQS research effort [48], but was not available for use in this study.

Organic gas speciation profiles have been assigned to each source type and were used to compute detailed emissions of individual organic species from the total organic gas emissions. Speciation of both organic gas emissions and emissions of NO_x and SO_x was based on data supplied with the official emission inventory [41]. The detailed organics (resolved to the level of individual chemical species or isomers of a particular compound) were recombined into a smaller number of lumped organic classes. In this study, assignment of individual organic species to lumped organic classes is extended from Lurmann et al. [11]. In general, compounds with similar chemical properties are lumped together and the chemistry of all compounds assigned to a lumped species group is represented using one or more surrogate species. For example, toluene, ethylbenzene, and other monoalkyl benzenes are lumped together and toluene is used as the surrogate species. The lumping procedure has been revised to account for extensions to the chemical mechanism, so that alcohols are lumped separately from the alkanes, and biogenic alkenes are lumped separately from the other alkenes. Further, the original lumping procedure from Table IV-3 of Lurmann et al. [11] does not include the

complete list of chemical species referenced in the current emission inventory, so lumping assignments were made for the new species by analogy to assignments for existing species.

2.3.2 Meteorological data

The database of routine and special SCAQS measurements was obtained from the California Air Resources Board [49]. Wind, temperature, humidity, solar radiation, air quality, and upper air sounding data were extracted from this database and processed to provide the input data required by the CIT airshed model. To develop spatially complete fields for use in the present study, data values were estimated for each cell in a regular 5 by 5 kilometer square grid system from measured data at nearby monitoring sites, using a weighted interpolation scheme [50,51]. In this scheme, the influence of a monitoring site on interpolated values varies inversely with distance squared between the monitor and the interpolation point. Large topographic features such as mountain ranges are represented by interpolation barriers, so that measured data from stations lying on the far side of a mountain range do not influence interpolated values on the near side.

The interpolation procedures were applied directly to scalar fields such as temperature and humidity. In the case of wind vectors, the interpolation formula was applied separately to the x- and y- components of the wind velocity, and then a smoothing procedure was applied to reduce field divergence [51]. During the development of hourly surface level wind fields, data from 50 wind stations that were reported in an hourly average form were used. Since the interpolation procedures assume that station measurements represent the wind flow over several adjacent model grid squares, wind stations located in

narrow valleys such as Banning Pass and Simi Valley were not used because they are representative of only very local conditions. Special SCAQS wind measurements made on top of hills at Catalina Island, Henninger Flats, Kellogg Hill, and Palos Verdes were not used in the generation of surface level wind fields because these stations were intended to characterize winds aloft as they impinged on major obstacles to flow.

As part of SCAQS, a greatly expanded upper air measurement program was undertaken on all of the intensive monitoring days [52]. Upper air soundings were performed 6 times per day at a network of 8 sites covering the coastal and inland regions of the air basin. Additional upper air sounding data were available at several other sites, but the sampling schedule at these sites called for only 2–3 soundings per day. Data on winds up to 1500 meters above ground level were extracted from these rawinsonde and airsonde measurements, and were input directly to the objective analysis program to generate three-dimensional wind fields [51]. These upper air soundings provide information about winds and temperature structure aloft, and are especially useful in the inland portions of the air basin where upper air soundings seldom are available.

Mixing heights were inferred from plots of the vertical profile of potential temperature derived from the upper air soundings. Typical daytime soundings during the August 27–29 period exhibited well defined inversion layers atop neutral and unstable layers near the surface. Nocturnal ground-based inversions for August 27–29 were only observed at the inland sites of Ontario and Riverside. The condition of the nocturnal boundary layer, as indicated by upper air soundings made at other sites, was generally only slightly stable or neutral. Such behavior is expected in urban areas, where buildings and

heat island effects disturb the boundary layer and inhibit the development of strong ground-based nocturnal inversions [53]. For this reason, the CIT airshed model has been modified to enforce a minimum Monin-Obukhov length of 50 meters at night. Further, the method for calculating the vertical diffusivity profile under stable conditions in the revised CIT airshed model differs slightly from the method specified by McRae et al. [18]. The new profile for K_{zz} is:

$$K_{zz} = \begin{cases} \frac{ku_*z}{0.74+4.7\frac{z}{L}} & \text{for } z < L \\ K_L & \text{for } L \leq z < Z_i, \\ 0.05K_L & \text{for } z \geq Z_i \end{cases} \tag{2.5}$$

where k is Von Karman's constant, u_* is the friction velocity, z is the elevation above ground level, L is the Monin-Obukhov length, and Z_i is the height of the base of the lowest strong inversion layer, and K_L is the vertical diffusivity evaluated at $z = L$ using the first expression above. The nighttime atmosphere is assumed to be slightly stable for elevations below the strong inversion base.

Hourly measurements of dry bulb temperature were reported at 59 sites in the Los Angeles area during the period August 27–29, 1987. In processing these data, isolated missing hours of data were filled in by linear interpolation. Hourly averaged temperature data were reconciled with short averaging time data by interpolating between short term data points to obtain estimates of the hourly average temperature. Relative humidity and dew point measurements reported at 43 sites were converted to absolute water vapor concentrations in parts per million, using a relationship between temperature and the saturation vapor pressure of water [54].

Solar ultraviolet radiometers were operated at 5 locations during the sum-

mer phase of SCAQS. Measurements were made at Long Beach, Central Los Angeles, Rubidoux, Claremont, and on top of Mount Wilson, at an elevation of 1741 meters above sea level. The radiometer data were used to estimate actual NO_2 photolysis rates, according to the following best-fit relationship:

$$J = [0.16(1 - \cos\chi_0) + 0.088] \times \mathrm{E}, \tag{2.6}$$

where χ_0 is the solar zenith angle, E is the measured solar ultraviolet irradiance (mW/cm^2), and J is the NO_2 photolysis rate constant in units of reciprocal minutes. This relationship is based on comparisons of UV radiometer data with simultaneous measurements of the NO_2 photolysis rate [37]. Recently a more general expression relating J to E has been developed that is consistent with radiative transfer theory [38]. Use of this expression results in similar values for J.

In previous modeling studies, the clear sky NO_2 photolysis rate constant J^* generally has been estimated using the expression:

$$J^* = \int_0^\infty \sigma(\lambda)\varphi(\lambda)F(\lambda, \chi_0, z)d\lambda, \tag{2.7}$$

where values of the absorption cross-section σ and the quantum yield φ were derived from experimental data, and values of the actinic flux F (as a function of wavelength λ, solar zenith angle χ_0, and elevation z) were based on the predictions of a radiative transfer model [36]. In the present study, photolysis scaling factors are computed as the ratio of the actual photolysis rate J to the theoretical clear sky value J^* at each station and at each hour where measured irradiance data are available.

Although the photolysis scaling factors computed as described above sometimes show large departures from unity in the early morning and late

afternoon hours, photolysis rates at these times are very low. Typical mid-day values for the UV scaling factor on August 27–29 are: 1.0 at Central Los Angeles, 0.8 at Claremont, 0.65 at Rubidoux, 0.4 at Long Beach, and 1.2 at Mount Wilson. These factors indicate that the actual photolysis rates vary considerably from those calculated using the actinic flux estimates of Peterson [36].

The Long Beach UV measurements for the entire second half of the summer SCAQS experiment (i.e., August and September) were consistently much lower than values reported at other sites, despite reported clear sky conditions at nearby airports. Because of this discrepancy, the Long Beach measurements were not included when constructing the final UV scaling field.

2.3.3 Boundary and initial conditions

Boundary and initial conditions are specified using routine surface-level air quality measurements, aircraft-based measurements acquired during SCAQS [55], and from data in the report by Main et al. [56]. Routine hourly concentration measurements are available for ozone, carbon monoxide, nitric oxide, nitrogen dioxide, sulfur dioxide, and non-methane hydrocarbons (NMHC). Ozone concentration measurements are abundant in the Los Angeles area, with over 50 stations routinely reporting hourly average concentrations. Oxides of nitrogen measurements are reported at about 35 stations, whereas routine hydrocarbon concentration measurements are reported at only 12 sites. There is no detailed chemical speciation reported for the routine hydrocarbon measurements, although in some cases measurements of both total hydrocarbon (THC) and methane concentrations are made, thus permitting direct calculation of NMHC concentrations.

Where only total hydrocarbon (THC) concentrations were reported, without matching methane data, the NMHC concentrations in parts per million of carbon were estimated as:

$$\text{NMHC} = (\text{THC} - 1.7)/1.68 \tag{2.8}$$

based on CH_4/NMHC correlations for Los Angeles [25]. The value 1.7 ppmC is representative of the background methane concentration as measured at San Nicolas Island, and the factor 1.68 accounts for methane emissions within the air basin. The routinely available hydrocarbon concentration measurements specify only THC and sometimes methane, without any further chemical speciation. Therefore, these NMHC concentrations were speciated within the model based on detailed hydrocarbon concentration data measured during SCAQS [57], as shown in a footnote to Table 2.4. Within urban areas, aldehyde and ketone boundary and initial conditions were set proportional to NMHC, and over the ocean were set using aldehyde and ketone concentrations measured upwind at San Nicolas Island [56]. Values for the upwind (inflow) boundary conditions used for the base case model simulation are given in Table 2.4.

2.4 Model results

In the sections above, the CIT model formulation and input data setup procedures have been described. In this section, the model results obtained using the CIT airshed model are presented for the August 27–29, 1987 episode. Model results are presented for ozone and for key ozone precursors including nitrogen dioxide and reactive hydrocarbons. It is important to consider model performance for ozone precursors in addition to ozone itself to

Table 2.4: Upwind[a] boundary condition values (ppb)

Species	Base Case	Increased BC Case[b]
CO	200	200
NO2	1	1
NO	1	1
HCHO	3	24
ALD2	5	5
MEK	4	4
NMHC[c]	100	250
O3	40	100

[a]Downwind boundary conditions are based on the advection flux out of the air basin. The boundary condition at the top of the modeling region (at a height of 1100 meters above ground level in this case) is a zero flux boundary condition such that pollutants are not fed into the model through the top boundary.

[b]Used in a diagnostic model simulation to investigate the effects of increasing the boundary condition values to match those used by the South Coast Air Quality Management District [58].

[c]Non-methane hydrocarbon (NMHC) concentrations are specified in ppbC instead of ppbv. Each ppbC of NMHC is speciated as follows: 0.095 ppbv ALKA, 0.017 ppbv ETHE, 0.018 ppbv ALKE, 0.015 ppbv TOLU, and 0.016 ppbv AROM.

improve confidence in apparent agreement between observed and predicted ozone concentrations. While results are given for all three days, the discussion presented here will focus on predictions for August 28. That is because results on the first day of the calculations (August 27) are sensitive to the choice of initial conditions, and because those for August 29 (a Saturday) are uncertain due to the lack of a mobile source emission inventory that reflects traffic patterns appropriate for Friday evening and Saturday.

The spatial distribution of ground-level 1-hour average ozone concentrations at the time of the observed ozone peak (1400–1500 hours PST on August 28) is presented in Figure 2.2 for the base case calculation. Inspection of Figure 2.2 shows that the model predicts that a substantial fraction of the eastern portion of the South Coast Air Basin exceeds the 12 pphm National Ambient Air Quality Standard. Peak ozone predictions are generally lower than observed concentrations. Ozone predictions obtained using increased organic gas exhaust emissions are presented in Figure 2.3. In this case generally higher ozone concentrations are predicted. The region of high ozone concentrations is shifted westward towards the source-rich coastal and central regions of the air basin.

Time series plots showing diurnal patterns of ozone concentrations over the entire 3-day episode are shown in Figure 2.4. The monitoring stations selected for inclusion in Figure 2.4 were all intensive monitoring sites during SCAQS, and define a cross section taken across the center of the air basin starting at the coast with Hawthorne and proceeding inland to Rubidoux. Using the official emission inventory, the model reproduces the temporal behavior seen in the observed data, but tends to underpredict peak ozone concentrations at the inland sites. The 34% increase in organic gas emissions

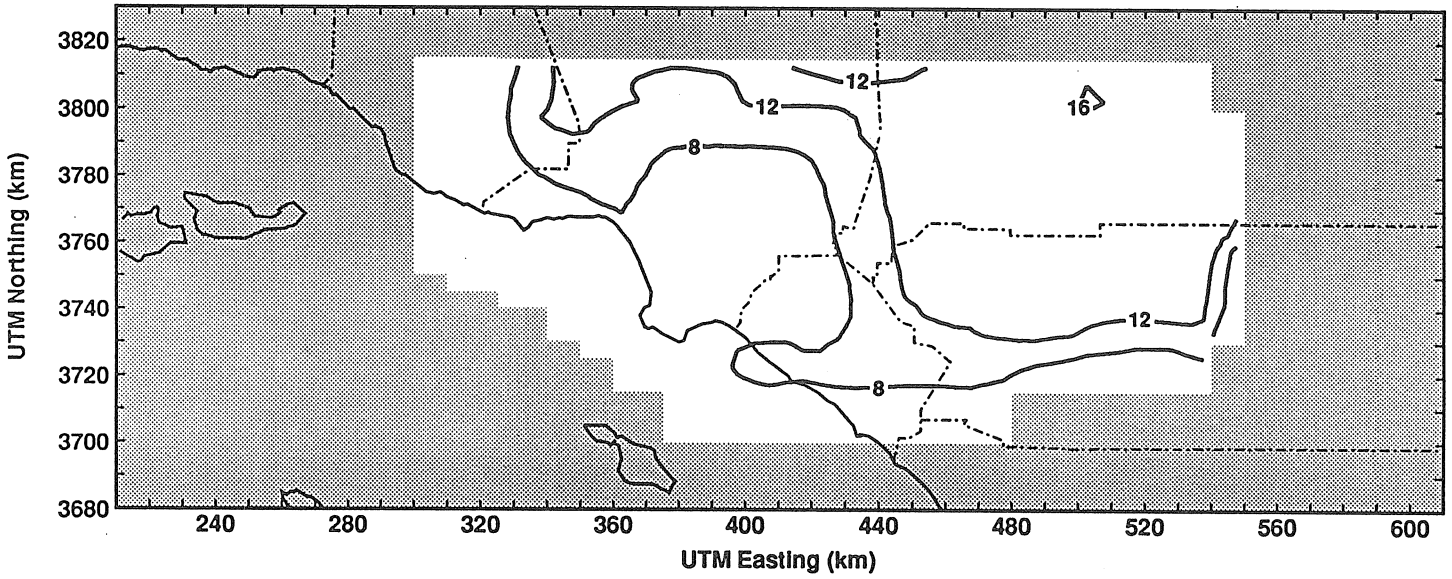

Figure 2.2: Spatial distribution of 1-hour average ozone concentrations at 1400-1500 hours PST on August 28, as calculated using the CIT airshed model and the base case emission inventory.

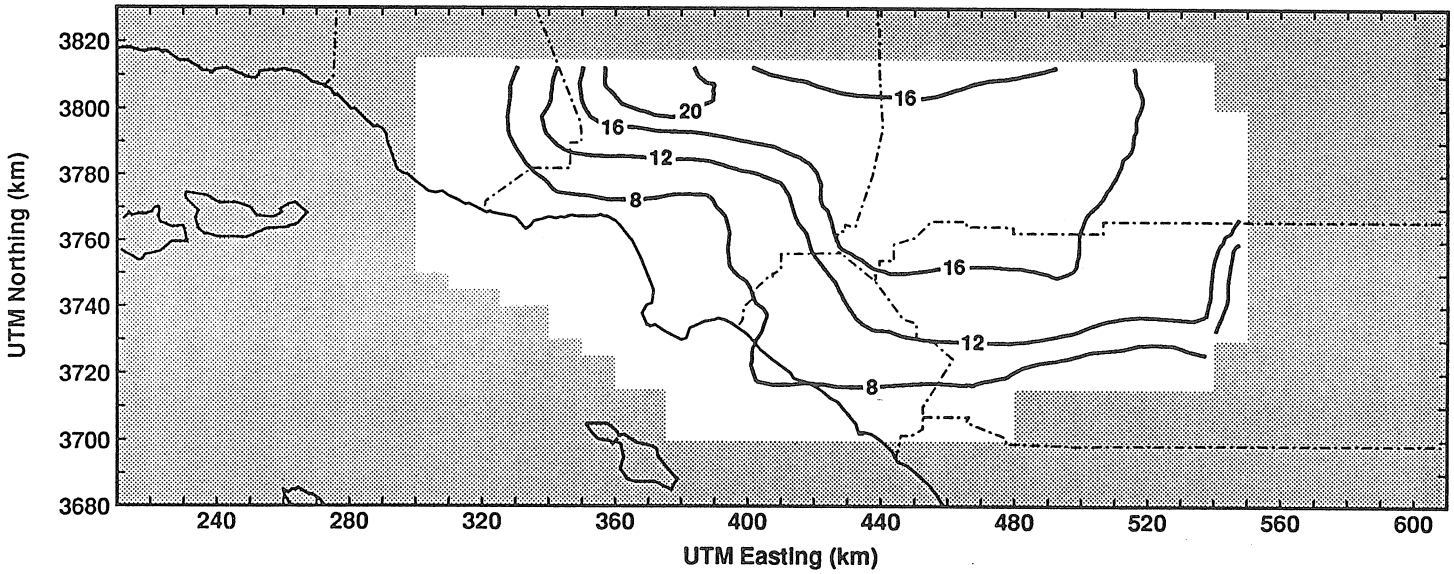

Figure 2.3: Spatial distribution of 1-hour average ozone concentrations at 1400-1500 hours PST on August 28, calculated using increased on-road vehicle hot exhaust emissions of organic gases and carbon monoxide.

represented by the increased exhaust emissions perturbation discussed earlier brings the model into closer agreement with observed ozone levels, especially at sites such as Glendora where observed ozone concentrations were highest and underpredictions in the base case calculation were largest. A statistical comparison of observations and model predictions is presented in Table 2.5. Note that ozone concentration data from 37 air monitoring sites located within the modeling region were used in the statistical comparison, while only a few representative sites are shown in Figure 2.4.

In order to assess model performance for ozone, one must also consider the ability of the model to predict the concentrations of key ozone precursors. In Figure 2.5, comparisons between observed and predicted NO_2 concentrations are presented. The statistical analysis for NO_2 shown in Table 2.6 is based on all available air monitoring data (26 sites). The response of chemiluminescent NO_x monitors to species other than NO and NO_2 has been studied by Winer et al. [59]. It is known that such instruments, when operating in NO_x mode, respond to both NO_2 and other nitrogen-containing species including nitric acid and peroxyacetyl nitrate. For this reason, the model predictions for NO_2 and other reactive nitrogen compounds that are measured as if they were NO_2 were summed to give "total" NO_2 predictions for comparison with observed NO_2 concentrations.

Figure 2.6 shows similar comparisons for the reactive hydrocarbons. Methane, ethane, and acetylene were excluded from this comparison because they are treated as unreactive compounds in the LCC chemical mechanism. The oxygenated species such as aldehydes, alcohols and glycols were lumped separately from the hydrocarbons and have been excluded from this comparison because the data base of measured concentrations does not include all of the

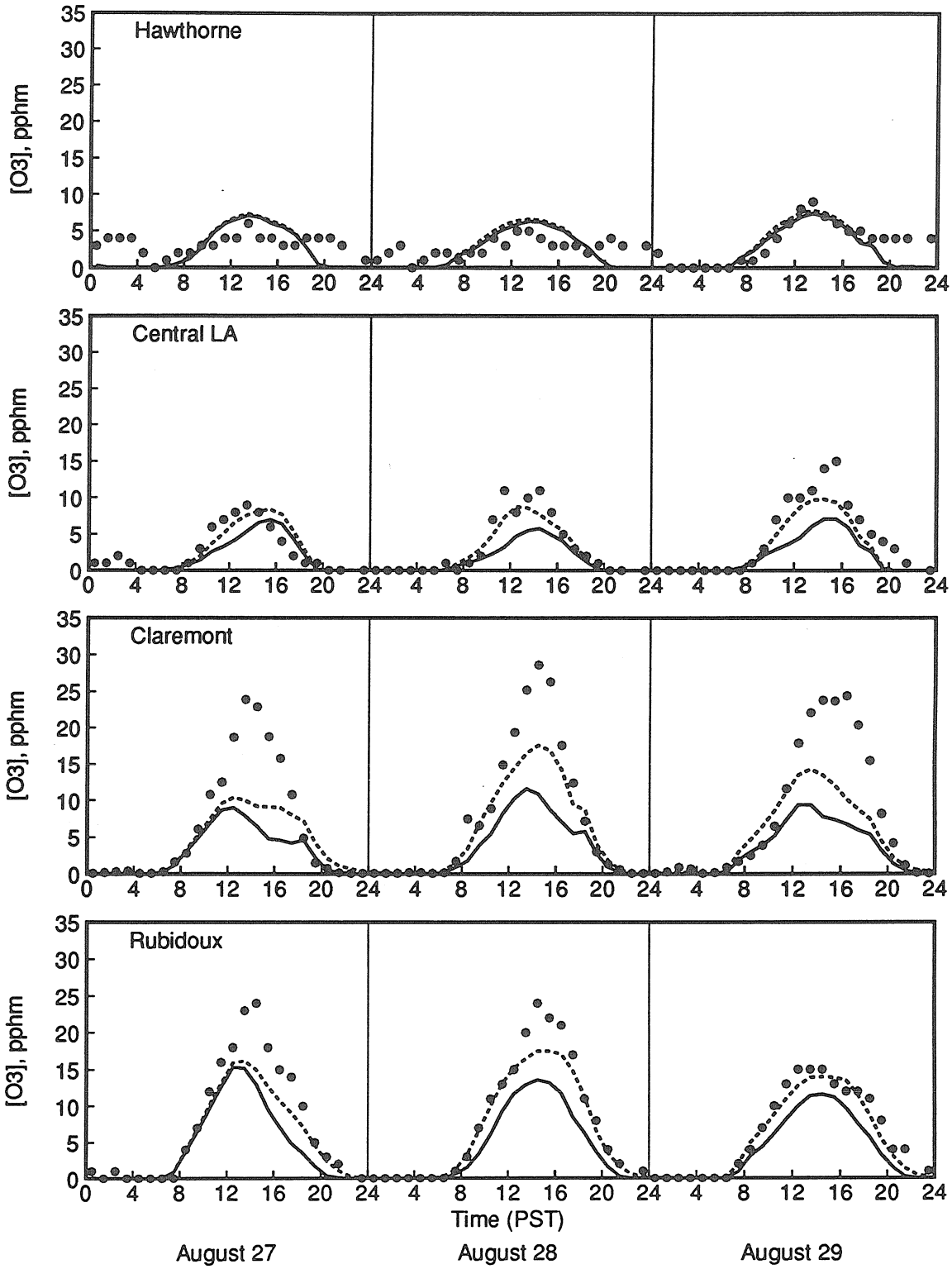

Figure 2.4: Time series plots of observed ozone concentrations (solid circles) and model predictions for the base case (solid line) and for the case of increased on-road vehicle hot exhaust emissions (dashed line).

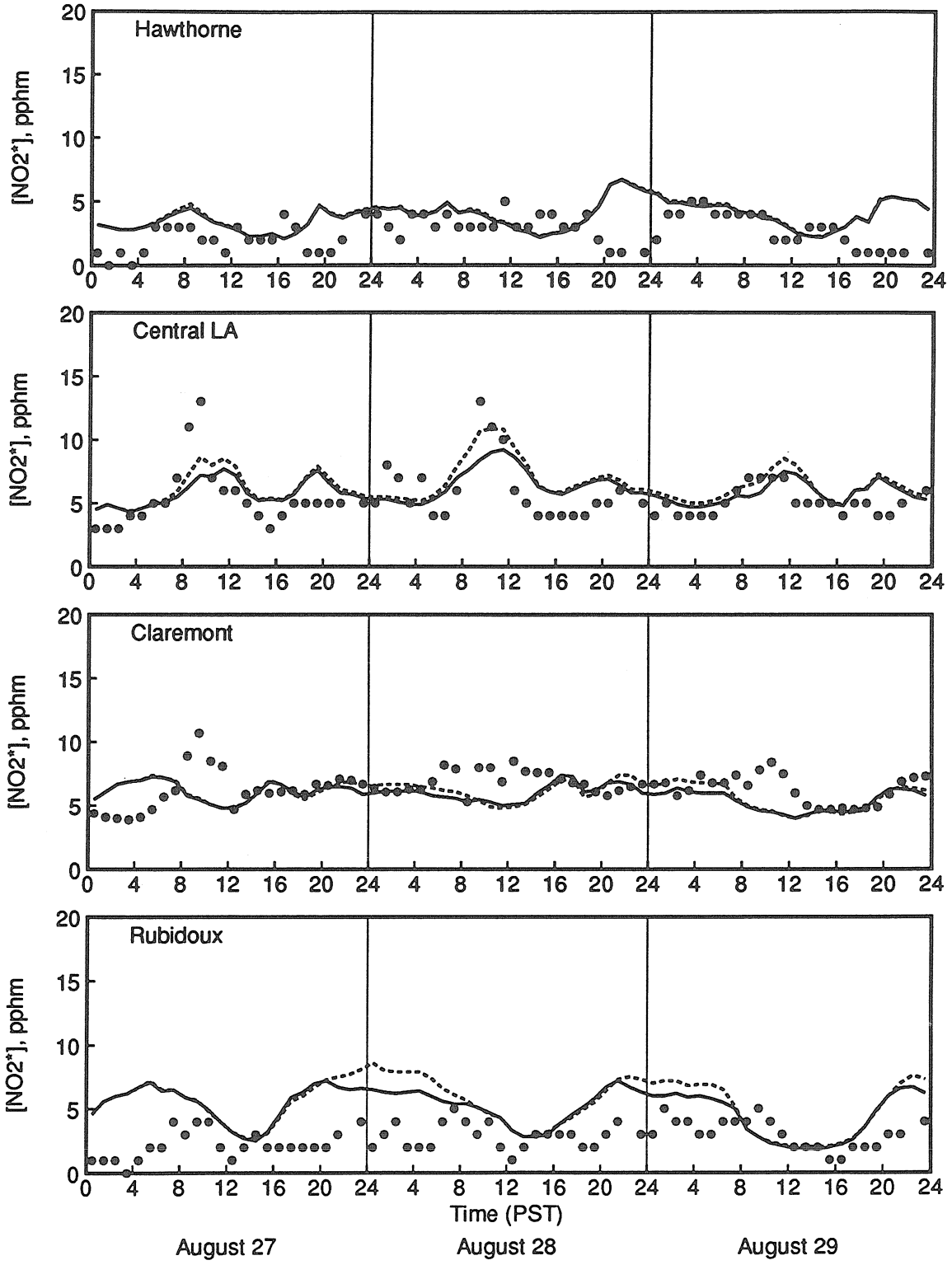

Figure 2.5: Time series plots of observed NO2 concentrations (solid circles) and model predictions for the base case (solid line) and for the case of increased on-road vehicle hot exhaust emissions (dashed line).

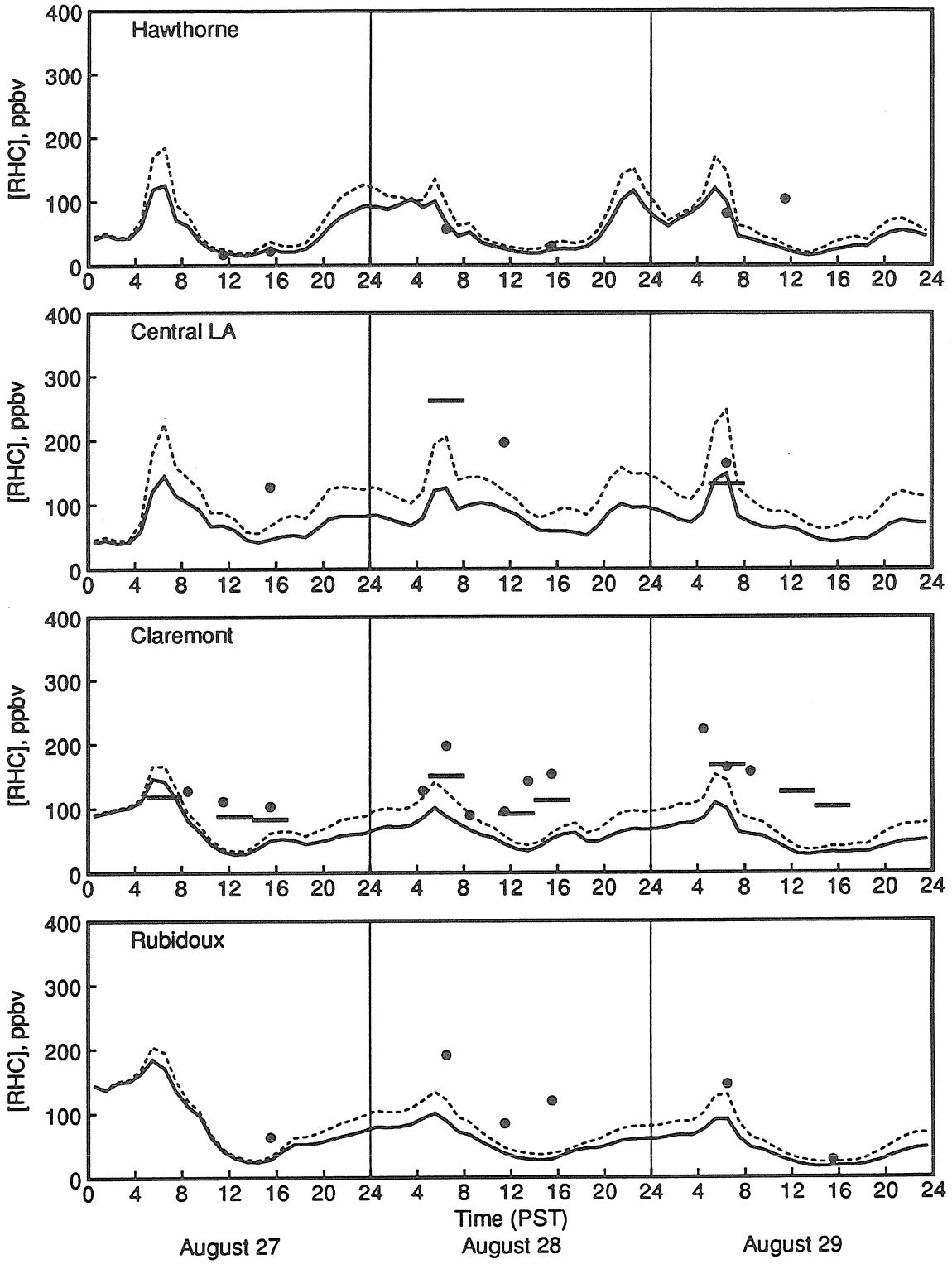

Figure 2.6: Time series plots of observed reactive hydrocarbon concentrations (solid circles are used for data set #1; horizontal bars are used for data set #2) and model predictions for the base case (solid line) and for the case of increased on-road vehicle hot exhaust emissions (dashed line).

relevant oxygenated species. As shown in Figure 2.6, there were two sets of special hydrocarbon concentration measurements made during SCAQS. The first set of measurements (data set #1) was made by Stockburger et al. [57]. A second independent set of measurements (data set #2) was made by Lonneman et al. [60]. The statistical comparison of predicted and observed reactive hydrocarbon concentrations shown in Table 2.6 is based on data set #1 which includes multiple concentration measurements each day at all of the 8 intensive monitoring sites located within the modeling region (see Figure 2.1). The samples in data set #2 were collected over 3-hour intervals with three samples per day at Claremont, and one additional early morning sample collected each day at both the Central Los Angeles and Long Beach City College sites. As shown in Table 2.6, ambient hydrocarbon concentrations are underpredicted when the official emission inventory is used in the base case calculation. The perturbation involving increased on-road vehicle exhaust emissions brings hydrocarbon predictions closer to observed levels.

It should be noted that the case of increased hot exhaust emissions considered here does not represent a complete correction of all possible biases in the emission inventory. The purpose of this analysis was only to examine the effects of increasing on-road vehicle hot exhaust emissions to match emission rates measured in the Van Nuys tunnel [4,5]. Organic gas emissions from other sources could also be understated in the official emission inventory. Further increases in organic gas emissions to the model (beyond the increase in hot exhaust emissions already considered) lead to higher predicted ozone concentrations and better agreement with observed hydrocarbon concentrations.

Table 2.5: Analysis of model performance for ozone on August 28

Statistical Measure[a]	Base Case Model[b]	3× Hot Exhaust Model[c]	Typical Performance[d]
Bias (pphm)	–3.2	–0.4	—
Normalized bias	–23%	+1%	±15%
σ of residuals (pphm)	4.6	3.9	—
Gross error (pphm)	4.3	3.0	—
Normalized gross error	38%	29%	35%
Peak Prediction Accuracy:			
average station ($\overline{A}$)	–26%	–7%	—
basin-wide maximum (A_u)	–54%	–33%	±20%

[a]As per Tesche et al. [61], the statistical measures are calculated using all pairs of predicted and observed concentrations where the observed value is greater than or equal to the cutoff of 6 pphm. The bias is defined as the mean residual (predicted–observed) concentration, and the normalized bias is computed by dividing each residual by the corresponding observed concentration, and then averaging as for the bias. The gross error statistics are computed in the same manner as the bias statistics, except that the absolute values of the residuals are used throughout. The peak prediction accuracy statistics are calculated using only the peak 1-hour observed concentrations. The average station peak prediction accuracy ($\overline{A}$) compares peak observed values with peak predicted values at the same location but not necessarily paired in time. The basin-wide peak accuracy (A_u) focusses on the single site with the highest observed concentration and compares this value with the peak model prediction within a radius of 25 km over a time interval extending from 3 hours before until 3 hours after the time of the observed peak.

[b]From the CIT airshed model using the baseline emission inventory

[c]From the CIT airshed model using scaled up on-road vehicle hot exhaust emissions

[d]Technical guidance for 'typical' ozone model performance [62]

Table 2.6: Analysis of model performance for ozone precursors on August 28

Statistical Measure[a]	Base Case Model[b]	3× Hot Exhaust Model[c]
Total NO_2:[d]		
Bias (pphm)	+0.1	+0.4
Normalized bias	+17%	+22%
σ of residuals (pphm)	2.3	2.4
Gross error (pphm)	1.8	1.8
Normalized gross error	41%	44%
Reactive hydrocarbons:		
Bias (ppbv)	–56	–29
Normalized bias	–35%	–12%
σ of residuals (ppbv)	62	68
Gross error (ppbv)	71	59
Normalized gross error	51%	47%

[a]As per Tesche et al. [61]. The definitions of the statistical measures are presented in the footnotes to Table 2.5. A cutoff value of 2 pphm was used for NO_2; no cutoff was used for reactive hydrocarbons.
[b]From the CIT airshed model using the baseline emission inventory
[c]From the CIT airshed model using scaled up on-road vehicle hot exhaust emissions
[d]Total NO_2 includes NO_2 plus all other reactive nitrogen compounds that are measured as if they were NO_2 by chemiluminescent monitors.

2.5 Sensitivity analysis

As part of any detailed assessment of airshed model performance, a set of diagnostic simulations are recommended [61]. A series of such simulations has been conducted using the CIT airshed model, as described below.

In the first simulation, the model was run using the increased boundary conditions shown in Table 2.4 (see page 28). These values are comparable to those used by the South Coast Air Quality Management District in their modeling of air quality in the Los Angeles area over the same intensive modeling period [58]. The CIT airshed model predicts higher ozone concentrations (higher by 3–7 pphm) generally closer to the observed values, when the increased boundary conditions are used. There is, however, little evidence in the SCAQS data base supporting the use of such high boundary conditions.

Further diagnostic simulations using very clean boundary conditions and initial conditions showed that the base case model predictions described in the previous section were not driven by the boundary conditions, and that model predictions were sensitive to the choice of initial conditions only on the first day of simulation. Use of clean boundary conditions led to model predictions that were virtually identical to those calculated in the base case.

Model sensitivity to dry deposition was examined in a calculation where the deposition of all pollutants was eliminated. Predicted ozone concentrations increased throughout the basin, by about 1 pphm at sites near the coast, and by 2–4 pphm at inland sites. The largest increases were seen at sites located farthest downwind. In another simulation, the surface resistance terms for deposition of ozone and hydrogen peroxide were decreased by factors of 2 and 10, respectively. The dry deposition flux of these pollutants was thereby increased, though not in proportion to the change in surface

resistance values since mass transport considerations provide an upper limit to the dry deposition flux. Predicted ozone concentrations decreased slightly (by 0–2 pphm) following the changes in surface resistance values.

The sensitivity of model predictions to changes in meteorological variables also has been considered. When all wind speeds were reduced by 50% in the model, predicted ozone concentrations at inland sites increased by up to 5 pphm, especially from 1200 to 1600 PST when the sea breeze was strongest. Doubling the mixed layer depth in the model resulted in slight increases in predicted ozone concentrations, whereas predicted carbon monoxide concentrations decreased. When the ground-level photolysis rate scaling factors were removed, and only model-predicted clear sky photolysis rate constants were used as per equation 2.7, predicted ozone concentrations increased by 1–3 pphm. The largest increases were seen near the Rubidoux monitoring site where the base case photolysis scaling factor was lowest.

Predicted ozone concentrations did not increase significantly when the biogenic hydrocarbon emissions to the model were increased to three times the baseline values. This is not surprising given that the emission inventory specifies that the biogenic emissions occur mainly in forested areas in the mountains away from and generally downwind of the urbanized portions of the basin [45].

Finally, a series of diagnostic simulations involving removal of pollutant emissions were performed. The zeroing of NO_x emissions led to virtually background air quality by the second day of the simulation. Similar results were obtained when all pollutant emissions were removed from the model. A simulation with zero organic gas emissions resulted in very low predicted ozone concentrations due to NO_x scavenging of background ozone.

2.6 Discussion

The possibility that the official Los Angeles organic gas emission inventory is understated has been discussed in several recent studies [1,4,5,6]. Results from the present study further suggest that organic gas emissions are in fact understated. The sensitivity of ozone predictions to increased organic gas emissions is greatest at sites showing the largest ozone concentration underpredictions in the base case simulation. The response shown in Figure 2.4 at Claremont to a 34% increase in overall organic gas emissions (the hot exhaust perturbation) is typical of other nearby sites where the peak observed ozone concentrations were underpredicted in the base case simulation. In Figure 2.5, the time series plots for total NO_2 (which includes NO_2 plus other reactive nitrogen compounds that were measured as if they were NO_2) show that the model is carrying approximately the correct total amount of reactive nitrogen compounds.

Night-time concentrations of NO_x and hydrocarbons are generally overpredicted at coastal sites such as Long Beach. Examination of night-time upper air soundings for August 27–29 at Long Beach indicates that the low observed concentrations of primary pollutants result from significant vertical mixing that is not fully reproduced by the model. The upper air soundings show that the nocturnal boundary layer at Long Beach is neutrally stratified, while the model assumes slightly stable conditions. Another possible explanation is that the emission inventory may specify unrealistic levels of night-time source activity in these areas.

In the present study, model simulations using increased on-road vehicle organic gas and carbon monoxide hot exhaust emissions were performed (in addition to simulations using the baseline emission inventory) in order to

approximate the actual motor vehicle emissions as observed in recent roadway tunnel measurements. Use of this scaled up inventory resulted in higher predicted ozone concentrations that were closer to observed values, with increases of up to 8 pphm seen at some sites. Reactive hydrocarbon concentrations were still underpredicted (-12% on average) even after the increase in on-road vehicle hot exhaust emissions. Thus there may be additional organic gas emissions missing from the official inventory, beyond those accounted for by scaling up the mobile source hot exhaust emissions.

2.7 Conclusions

The CIT airshed model has been improved and updated using a new chemical mechanism [11] and a new dry deposition module [24]. Documentation in the form of a user's guide has been prepared [26,27,28].

The CIT model has been applied to the South Coast Air Basin during the August 27–29, 1987 SCAQS intensive monitoring period. In the base case simulation, using the official emission inventory, peak ozone concentrations were substantially underpredicted. When an alternate emission inventory with increased organic gas and carbon monoxide hot exhaust emissions was used to reflect recent measurements of on-road motor vehicle exhaust emissions, the CIT model predicted higher ozone and hydrocarbon concentrations that matched the observed data more closely.

3 Speciation of VOC emissions

3.1 Introduction

Preparation of accurate speciated organic gas emissions inventories is necessary for photochemical modeling calculations and for the design of ozone abatement strategies. Knowledge of organic gas emissions is also required if the concentrations of toxic air contaminants (e.g., formaldehyde, benzene, and 1,3-butadiene) are to be controlled in a systematic fashion.

Current emissions inventories in use in the Los Angeles area specify temporally and spatially resolved organic gas emissions for over 800 source categories. These inventories have been used in the formulation of pollutant abatement strategies [2]. Because the Los Angeles ozone control problem plays a critical role in establishing California and nationwide emission control policies, a correct understanding of the Los Angeles area organic gas emission inventory is very important.

Reference: Harley, R. A.; Hannigan, M. P.; Cass, G. R. Respeciation of organic gas emissions and the detection of excess unburned gasoline in the atmosphere. *Environ. Sci. Technol.*, **26**, in press, 1992.

An organic gas emissions inventory combines source activity factors with pollutant emission factors and speciation profiles. For example, detailed vehicle exhaust emissions are calculated as the product of an activity factor (vehicle miles traveled), emission factors (total organic gas, oxides of nitrogen, and carbon monoxide mass emission rates per mile traveled), and speciation factors for organic gases and oxides of nitrogen (percent by weight of individual compounds). Many of the same chemical composition profiles for organic gas emissions used in the California emission inventory have been incorporated into the United States Environmental Protection Agency (EPA) volatile organic compound speciation data system [63].

In light of recent studies of motor vehicle emissions on the road, a great deal of attention has been focused on mobile source emission factors [4,5,64]. Measurements made in the Van Nuys roadway tunnel in the Los Angeles area suggest that organic gas emissions from vehicles in actual use on the road are up to 3 times higher than those predicted by the EMFAC 7E mobile source emissions model [65]. The EMFAC model is a central part of all mobile source emissions calculations for regulatory planning purposes in California. A comparison of emission inventory and ambient concentration ratios of carbon monoxide, oxides of nitrogen, and non-methane organic gases (NMOG) also suggests that on-road vehicle emissions of CO and NMOG are understated by the EMFAC model [6]. Resolving these emission factor questions is an important step, but both source activity and speciation profile components of the emissions calculation also must be considered.

In the present study, existing speciation profiles for organic gas emissions will be reviewed, and new or updated information will be used to improve the accuracy and level of chemical detail of these profiles. The main mo-

tivation for this study is to improve the emissions estimates for individual organic species, to provide a basis for detailed modeling of the emissions to ambient air quality relationship for the many individual organic species. It is also desirable to check the official state of California emission inventory to determine whether the chemical speciation (and therefore reactivity) of organic gas emissions is defined correctly. For this purpose, a reactivity scale based on reaction rate constants of organic gases with the hydroxyl radical will be used to compare the photochemical reactivity of the revised speciation profiles with the corresponding speciation profiles in the official emissions inventory. Our revised estimate of the composition of basin-wide organic gas emissions then will be compared with ambient organic gas concentration measurements made in the Los Angeles area during recent field studies [66,16].

3.2 Speciation profile development

The South Coast Air Quality Management District and the California Air Resources Board have developed official emission inventories for the South Coast Air Basin. A copy of the current emission inventory for August 27, 1987 was received from the California Air Resources Board [41], and forms the starting point for the present study.

In Table 3.1, the non-methane organic gas emissions associated with selected speciation profiles are presented from the official inventory. Note that emissions from multiple source categories may be assigned to a single speciation profile. Inspection of Table 3.1 indicates that 77% of the anthropogenic non-methane organic gas emissions are assigned to only 13 speciation profiles. Most of the speciation profiles listed in Table 3.1 will be revised in the course

of this study, as discussed in the following sections. The most important of these revised speciation profiles are shown in Table 3.2 for mobile source emissions and in Table 3.3 for various surface coating solvent emissions.

A hydroxyl radical reactivity factor, K_j, has been computed for each speciation profile j, stated relative to a unit mass of organic gas emissions:

$$K_j = \sum_{i=1}^{n} \frac{w_{ij}}{M_i} k_{\mathrm{OH}_i}, \tag{3.1}$$

where w_{ij} is the weight fraction of species i in speciation profile j, M_i is the molecular weight of species i, and k_{OH_i} is the second order hydroxyl radical reaction rate constant for species i. In this study, all reactivities will be expressed relative to the reactivity K_0 of the composite organic gas emissions from all sources combined in the official basin-wide emission inventory:

$$K_0 = \frac{\sum_{i=1}^{n} \frac{E_i}{M_i} k_{\mathrm{OH}_i}}{\sum_{i=1}^{n} E_i}, \tag{3.2}$$

where E_i is the basin-wide emission rate for species i in the official inventory. The reactivity index is computed for each speciation profile as:

$$R_j = \frac{K_j}{K_0}. \tag{3.3}$$

The reactivity scale defined above accounts for differences in the reactivity of individual organic species with the hydroxyl radical, and also for variations in molecular weights leading to different molar emissions at the same total mass emission rate. The values for k_{OH} reported by Carter [29] were used in these calculations. There are other reactivity scales that measure the effect on ozone formation of an incremental addition of a single organic species to an existing mixture of oxides of nitrogen and organic gases [67]. These incremental reactivity scales consider mechanistic as well as kinetic properties of the species in the assessment of reactivity. As well, the incremental

Table 3.1: Non-methane organic gas emissions assigned to selected speciation profiles in the emission inventory for August 27, 1987

Profile description[a]	Non-methane Organic Gas Emissions (tons/day) Official	Revised
Non-catalyst gasoline engine exhaust	346	266
Catalyst-equipped gasoline engine exhaust	256	246
Composite industrial surface coatings	161	206
Solvent-borne architectural surface coatings	120	121
Gasoline vapors	57	115
Whole gasoline	104	108
Domestic solvents	49	90
Industrial adhesives	57	57
Species unknown	94	49
Diesel engine exhaust	44	39
Composite thinning solvent	0	30
Water-borne architectural surface coatings	25	25
Aerosol propellants	57	16
All other anthropogenic	419	412
Total anthropogenic	1789	1780

[a]Note that each speciation profile may be used to speciate organic gas emissions from many different sources. For example, the non-catalyst gasoline engine exhaust profile is used to speciate emissions from on-road vehicles, off-road vehicles, heavy duty equipment, and various other sources.

Table 3.2: Revised mobile source emission speciation profiles

Chemical species	Gasoline Engine Exhaust		Unburned Gasoline (summertime)	
	Non-Catalyst[a]	Catalyst-Equipped[b]	Whole Liquid[c]	Headspace Vapors[d]
	Emissions Composition:[e]			
methane	9.5	15.0	—	—
ethane	0.9	2.9	—	0.2
propane	0.1	0.1	—	2.1
n-butane	1.3	4.4	3.3	30.0
i-butane	0.2	0.5	0.8	11.4
n-pentane	1.9	1.8	2.7	6.3
i-pentane	3.7	4.2	6.9	22.3
n-hexane	0.8	1.0	2.0	1.1
2-methylpentane	1.3	2.1	3.3	2.8
3-methylpentane	1.1	1.3	2.1	1.6
2,2-dimethylbutane	0.3	0.6	0.2	0.3
2,3-dimethylbutane	0.6	1.0	1.1	1.1
n-heptane	0.6	0.3	2.0	0.2
branched C7 alkanes	2.2	3.0	8.8	1.8
n-octane	0.2	0.2	1.0	0.0
branched C8 alkanes	2.8	7.6	9.4	0.8
C9 alkanes	1.4	1.2	4.9	0.1
C10 alkanes	1.8	1.1	1.2	—
C11 alkanes	1.4	0.7	0.2	—
$C12^+$ alkanes	0.3	0.0	0.0	—
cyclopentane	0.2	0.2	0.5	0.5
methylcyclopentane	1.2	0.5	2.5	1.1
cyclohexane	0.4	0.0	0.6	0.3
methylcyclohexane	0.5	0.4	1.0	0.1
other cycloalkanes	0.2	0.3	—	—
acetylene	8.3	2.6	—	—

Table 3.2 (continued):
Revised speciation profiles for mobile source emissions

Chemical species	Gasoline Engine Exhaust		Unburned Gasoline (summertime)	
	Non-Catalyst[a]	Catalyst-Equipped[b]	Whole Liquid[c]	Headspace Vapors[d]
	Emissions Composition:[e]			
ethene	10.2	5.9	—	—
propene	4.3	2.5	—	—
1-butene	0.8	0.4	0.1	1.3
isobutene	1.0	1.3	*	*
cis-2-butene	0.2	0.6	0.1	1.4
trans-2-butene	0.5	0.3	0.1	1.1
C5 terminal alkenes	0.6	0.4	0.4	2.7
C5 internal alkenes	1.5	0.9	2.4	5.1
C6 terminal alkenes	1.6	0.3	0.3	0.2
C6 internal alkenes	*	0.5	2.0	1.1
C7 alkenes	2.3	0.1	0.0	0.1
C8 alkenes	1.1	0.1	0.8	0.0
$C9^+$ alkenes	1.1	0.2	1.0	0.0
cyclopentene	0.2	0.1	0.2	0.3
other cycloalkenes	0.1	0.1	0.5	0.1
1,3-butadiene	1.2	0.2	—	—
other dialkenes	0.6	0.3	0.3	—
benzene	3.6	3.7	1.9	0.7
toluene	5.8	8.9	10.2	0.7
ethylbenzene	1.2	1.3	1.9	0.0
other monoalkylbenzenes	1.2	0.9	1.4	—
o-xylene	1.6	1.3	3.1	0.0
m- & p-xylene	4.2	3.5	8.3	0.1
ethyltoluene isomers	0.5	1.9	3.7	0.0
diethylbenzene isomers	0.3	0.4	0.5	—

Table 3.2 (continued):
Revised speciation profiles for mobile source emissions

Chemical species	Gasoline Engine Exhaust: Non-Catalyst[a]	Gasoline Engine Exhaust: Catalyst-Equipped[b]	Unburned Gasoline (summertime): Whole Liquid[c]	Unburned Gasoline (summertime): Headspace Vapors[d]
	Emissions Composition:[e]			
1,3,5-trimethylbenzene	0.6	1.3	1.2	0.0
1,2,4-trimethylbenzene	1.8	1.9	3.2	0.3
1,2,3-trimethylbenzene	—	0.5	0.9	0.1
other aromatics	1.3	1.7	—	—
formaldehyde	2.30	1.20	—	—
acetaldehyde	0.63	0.62	—	—
propionaldehyde	0.10	0.06	—	—
acrolein	0.47	0.14	—	—
crotonaldehyde	0.12	0.03	—	—
benzaldehyde	0.41	0.20	—	—
other aldehydes	0.21	0.31	—	—
glyoxals	—	—	—	—
acetone	0.14	0.39	—	—
methyl ethyl ketone	0.04	0.08	—	—
other	2.2	2.0	—	—

Asterisk (*) indicates compound not resolved separately from compound listed immediately above

[a]exhaust speciation for gasoline-powered light duty vehicles without catalytic converters

[b]exhaust speciation for catalyst-equipped gasoline-powered light duty vehicles

[c]composition of whole liquid gasoline

[d]composition of gasoline vapors in headspace over liquid fuel

[e]percent by weight of total organic gas emissions

Table 3.3: Revised speciation profiles for surface coatings and adhesives

Chemical species	Architectural Coatings: Solvent-borne	Architectural Coatings: Water-borne	Architectural Coatings: Thinning solvent	Industrial coatings	Industrial adhesives
	Emissions Composition:[a]				
C9$^-$ alkanes	6.4	—	1.0	1.8	11.4
C10 alkanes	20.2	—	3.1	5.7	10.8
C11 alkanes	11.6	—	1.7	3.1	5.8
C12$^+$ alkanes	5.0	—	0.6	1.1	2.1
C9$^-$ cycloalkanes	8.8	—	1.3	2.4	4.6
C10 cycloalkanes	20.5	—	3.2	5.8	11.0
C11 cycloalkanes	3.4	—	0.5	0.9	1.7
C12$^+$ cycloalkanes	3.1	—	0.5	0.9	1.6
toluene	3.2	—	20.7	14.7	5.6
xylene	1.0	—	11.6	15.8	0.1
other aromatics	1.6	—	5.9	4.9	—
acetone	0.1	—	10.3	3.1	2.1
methyl ethyl ketone	1.2	—	16.0	8.1	12.2
methyl isobutyl ketone	1.6	—	0.6	5.9	—
methanol	0.1	—	—	—	0.2
ethanol	0.1	—	11.8	2.7	0.1
isopropanol	2.3	—	5.0	3.5	0.4
butanols	2.2	—	0.3	6.4	—
ethylene gylcol	—	44	—	—	0.2
propylene glycol	—	29	—	—	0.1
glycol ethers[b]	—	27	—	6.6	0.2
ethyl acetate	—	—	3.7	2.0	0.2
propyl acetate	—	—	0.9	1.6	—
n-butyl acetate	2.9	—	1.4	3.1	0.3
1,1,1-trichloroethane	2.2	—	—	—	9.3
dichloromethane	—	—	—	—	1.7
other miscellaneous	1.2	—	—	—	18.2

[a]percent by weight of total organic gas emissions
[b]2-butoxyethanol for example

reactivity scales account for photolysis of species such as formaldehyde, and reactions with other radicals and ozone. However, the detailed chemical reaction mechanisms of many species are still uncertain, while k_{OH} values are well known. Therefore, the R_j index will be used to illustrate differences in reactivity among various speciation profiles, without assuming a particular ambient hydrocarbon-NO_x ratio.

3.2.1 Mobile source evaporative emissions

The composition of whole (liquid) gasoline and gasoline headspace vapors was investigated by Oliver and Peoples [68]. Composites of fuel samples obtained from all of the major oil companies selling gasoline in the Los Angeles area in 1984 were analyzed. Separate analyses were performed for leaded and unleaded fuels, for regular and premium grades, and for summertime and wintertime fuels. The existing Los Angeles emissions inventory uses a composite speciation profile that was back-calculated to reflect the sales of gasoline by grade as they existed in 1979. Since unleaded gasoline sales have increased greatly with the further introduction of catalyst-equipped cars into the vehicle fleet, it is necessary to update the weightings applied to the composition profiles for the different grades of gasoline to reflect 1987 sales [69]. Use of the 1987 grade splits shown in Table 3.4 results in a composite whole gasoline speciation profile with higher aromatic, and lower alkane content. The effect is to increase the reactivity of whole gasoline emissions by 4%. Gasoline vapors that exist in the headspace over the liquid in a gasoline tank are dominated by the higher vapor pressure compounds in the fuel (i.e., butane and pentane). When this gasoline vapor composition is updated to reflect 1987 fuel sales, the reactivity of the gasoline vapors is seen to increase

by 9% relative to the vapor composition for 1979 that is still used in the official emissions inventory.

The volatility of gasoline is seasonally adjusted, with increased vapor pressure during winter months to improve cold weather starting characteristics, and decreased vapor pressure in the summer to reduce evaporative emissions and to prevent vapor locking problems [70]. This reduction in fuel volatility has been achieved by reducing the amount of butane blended into summer gasolines [68,69]. The 1987 composite summertime gasoline is 1% more reactive for whole gasoline and 12% more reactive for gasoline vapors per unit mass of emissions when compared to the wintertime composite fuel for the same year. Revised speciation profiles for summertime whole gasoline and gasoline headspace vapors are given in Table 3.2 and are used elsewhere throughout this study.

3.2.2 Gasoline engine exhaust

There are many published studies detailing the chemical speciation of vehicle exhaust for different vehicle types, driving conditions, and fuel types. These studies include dynamometer-based measurements for non-catalyst [71,72, 73,74], oxidation catalyst [71,72,75,76,77], and three-way catalyst [78,79,80] equipped light duty vehicles. Other measurements of exhaust speciation have been made in highway tunnels [81,82,83,84,85], in a parking garage [85], at the roadside [86], and on board a fleet of non-catalyst vehicles driven over a range of speeds [87].

A number of important conclusions emerge from these studies. The exhaust from non-catalyst light duty vehicles contains a higher percentage of acetylene and alkenes, and a lower percentage of methane than is present

Table 3.4: Share of total gasoline volume sales by grade in Los Angeles

	Year	
Fuel grade	1979	1987
Unleaded regular	40%	55%
Unleaded premium	0%	27%
Leaded regular	38%	18%
Leaded premium	22%	0%

in the exhaust from catalyst-equipped vehicles [71,75,83]. Total organic gas emissions and the chemical composition of these emissions vary with speed. A fleet of 46 vehicles tested on a dynamometer using three different driving cycles (a low-speed city driving cycle, the standard Federal Test Procedure (FTP) cycle, and a higher speed cycle representing conditions on a crowded urban expressway) showed decreased total emissions per mile driven and a higher methane fraction for the exhaust organic gas emissions as average speed increased [77]. For non-catalyst vehicles tested on the road [87], total organic gas emissions decreased with increasing speed up to an average speed of 90 km/h, then began to increase as average vehicle speed was increased beyond this point. The fraction of combustion-derived species such as methane, acetylene, ethene, and propene in the total exhaust emissions increased with increasing speed.

NON-CATALYST VEHICLE EXHAUST

The official inventory for Los Angeles speciates the exhaust emissions from non-catalyst light duty vehicles based on measurements made during the 1970s [75,88]. Since that time, the allowable lead content of gasoline has been reduced, and gasoline suppliers have been forced to use other high octane fuel components to make up for reductions in tetraethyl lead use. The original exhaust speciation measurements did not include aldehydes as part of the exhaust emissions, so the official profile has weight percents of all species summing to 106% resulting from the addition of aldehydes to the list of emitted species. The level of chemical detail in the official profile is limited: only 24 species are listed, whereas more recent speciated exhaust measurements [74,80] have identified 100 or more species.

In the course of evaluating the effect of a reformulated fuel on vehicle emissions, tests on older non-catalyst vehicles were performed by two independent laboratories [74]. These tests were sponsored by the Atlantic Richfield Company (ARCO), and used both a reformulated gasoline and a preexisting (1988) regular leaded gasoline. A revised exhaust speciation profile for non-catalyst gasoline engines burning regular leaded gasoline was created for use in the present study by first averaging the weight percent speciation data for all vehicles tested at each of the two labs used in the ARCO study, and then averaging, with equal weighting, the results reported by each lab to form the final speciation profile. The ARCO exhaust speciation data obtained using the regular leaded gasoline show significantly higher dialkylbenzene content than is indicated in the official speciation profile, while toluene content is lower. The ARCO test data indicate a lower butane content in the exhaust as well, possibly due to use of low volatility fuel prescribed during summer months in California. The official speciation profile for non-catalyst vehicle exhaust does not include any emissions of 1,3-butadiene, whereas the revised profile indicates 1.1% (by weight) of the total organic gas emissions for this species. The revised speciation profile for exhaust from older non-catalyst cars is 7% less reactive than the official speciation profile would indicate.

Catalyst-equipped vehicle exhaust

The official emissions inventory uses the FTP data from the EPA 46-car study [77] to speciate the exhaust emissions from catalyst-equipped gasoline-powered vehicles. More recent studies [78,79,80] have examined vehicles equipped with three-way catalyst systems. A summary of the vehicle fleets tested and fuels used is presented in Table 3.5 for selected exhaust speciation

studies.

Most of the vehicles in the 46-car study were tested using a regular grade gasoline intended for wintertime use. This fuel is not representative of summertime fuels used in Los Angeles. Six vehicles from this study were tested using a premium summer grade gasoline. Exhaust speciation data from these six vehicles have been averaged with data from another EPA study [78,79] and with data for older (1983–1985) vehicles from the Auto/Oil study [80] to form the revised speciation profile, with all vehicles within a single study averaged together to form composite profiles, and a final composite profile obtained by averaging results from each of these studies together, with equal weighting assigned to each study. The one third weighting assigned to the speciation data for the 6 vehicles from the 46-car study tested using premium grade gasoline matches the fraction of unleaded gasoline sales that was premium grade in Los Angeles in 1987 [69]. Consideration of the use of premium grade gasoline is important given the higher aromatic content typical of such fuels (see Table 3.5). The reactivity of the revised speciation profile is 6% lower than that of the official profile.

In the EPA 46-car study [77], benzene and cyclohexane peaks were not resolved separately during the gas chromatographic analysis. The authors estimated "that 50% of the amount stated is benzene," but the more recent EPA [78,79] and Auto/Oil [80] studies indicate that essentially the whole sum should be counted as benzene, so the revised speciation profile counts all of the unresolved cyclohexane and benzene mass reported in the EPA 46-car study [77] as benzene.

The revised speciation profile differs significantly from the official speciation profile in level of chemical detail and in the weight fractions of some

Table 3.5: Summary of selected motor vehicle exhaust speciation experiments

Study Name	ARCO	—EPA 46-Car—		EPA Low Temp	Auto/Oil
Reference(s)	Cohu *et al.* [74]	Sigsby *et al.* [77]		Stump *et al.* [78,79]	Burns *et al.* [80]
Vehicle sample size	20[a]	6[b]	40[b]	20	7[c]
Model years	1970–79	1975–82	1975–82	1984–87	1983–85
Catalyst type	None	Varies[d]	Varies[d]	3-way	Mostly 3-way
Gasoline grade	Regular	Premium	Regular	Regular	Regular
Leaded/unleaded fuel	Leaded[e]	Unleaded	Unleaded	Unleaded	Unleaded
Vapor pressure (RVP)	8.9 psi	8.8 psi	12.2 psi	11.5 psi	8.7 psi
Octane number (R+M)/2	88	92.9	87.1	–	87.3
Fuel % alkanes	60	46	58	62	59
Fuel % alkenes	10	9	11	5	9
Fuel % aromatics	30	44	31	30	32
Fuel % unknown	0	1	0	3	0

[a]Sample includes 4 light duty trucks (1975–79 model years).
[b]The first six vehicles in the 46-car study were tested using premium grade gasoline; the other vehicles were tested using regular grade gasoline.
[c]Includes only the older (1983–85) vehicles tested using industry average gasoline.
[d]The majority are oxidation catalysts.
[e]Lead content is 0.08 grams per gallon.

individual species. In particular, the revised profile specifies less propane (0.1% versus 2.2% in the official profile), more propene (2.5% versus 0.7%), and more benzene (3.7% versus 2.8%) than is specified in the official profile. While 1,3-butadiene is estimated in the revised profile to comprise 0.23% of exhaust emissions from catalyst-equipped vehicles, there are no 1,3-butadiene emissions specified in the official speciation profile. Emissions of 1,3-butadiene from catalyst-equipped vehicles are observed to occur mostly during the cold start phase of the FTP test, because catalytic converters are very effective in removing 1,3-butadiene once they warm up [78,79,89,90].

A recent old car buyback program in the Los Angeles area provided exhaust emission rate measurements for a fleet of pre-1971 cars [91]. These old non-catalyst cars were reported to emit on average 16.5 grams of exhaust hydrocarbons per mile travelled, representing an average exhaust mass emission rate 66 times higher than new (1990) cars equipped with modern catalytic converters [91]. The speciation of emissions from the vehicles in this old car buyback program is not well understood, but if it should turn out that their exhaust composition is similar to that of the other non-catalyst cars tested previously, then these old non-catalyst vehicles may emit over 300 times the mass of 1,3-butadiene per mile driven when compared to new catalyst-equipped vehicles. As shown in Table 3.1, there were comparable NMOG mass emissions from non-catalyst and catalyst-equipped vehicles in Los Angeles for 1987. Therefore the non-catalyst vehicles likely contributed the majority of on-road vehicle emissions of 1,3-butadiene, as can be seen by comparing the speciation profiles given in Table 3.2 for catalyst-equipped and non-catalyst vehicle exhaust.

3.2.3 Diesel engine exhaust

The official inventory uses a speciation profile for diesel engine exhaust based on Table 9–07–021 of the EPA Species Data Manual [92], with additional aldehyde speciation data. The compound n-pentadecane is used as a surrogate for a range of diesel fuel constituents present in the exhaust. The detailed composition of the fuel-derived exhaust emissions is expected to depend strongly on the characteristics of the crude oil from which the diesel fuel was refined [93].

In the revised inventory, we have retained the existing profile for lack of more detailed speciation data. A second diesel exhaust profile that was used in parts of the official inventory indicates a sum of weight fractions exceeding unity when all species are combined, following an assumption that the inventory did not include aldehydes in the total mass emission rates. Since all emission rates are now specified in terms of total organic gas rather than total hydrocarbon mass, all diesel exhaust organic gas emissions are now speciated using the first profile described above.

3.2.4 Jet engine exhaust

The organic gas emissions from aircraft jet engines were investigated by Spicer et al. [94]. Based on these tests and landing and takeoff cycle times for commercial and military aircraft, new and separate speciation profiles for commercial and military jet aircraft exhaust [63] have been used in place of the speciation profile defined in the official emission inventory. The official speciation profile lists only 10 species in jet engine exhaust, whereas the revised profile includes over 50 species. These changes result in a 23% increase in the reactivity of jet engine exhaust emissions.

3.2.5 Surface coatings

The emission inventory for Los Angeles contains significant organic gas emissions attributed to the use of surface coatings, as shown in Table 3.1. The speciation profiles used in the official emission inventory are generally based on limited analyses of surface coating samples, and fail to resolve significant fractions of the sample mass in some cases. Our approach in developing revised speciation profiles for organic gas emissions from surface coatings has been to use manufacturer-supplied data indicating overall usage of organic solvents in various classes of surface coating products. Petroleum distillates (also referred to as mineral spirits) are a common ingredient in many surface coating products. Analyses of the detailed chemical composition of typical petroleum-based solvents were available for several different solvent suppliers [95], and these analyses show that a range of C_8–C_{12} alkanes and cycloalkanes are the main chemical constituents of these solvents. This information has been incorporated in the revised speciation profiles for organic gas emissions from surface coatings.

Industrial surface coatings and adhesives

In the official emission inventory, a composite speciation profile developed by Oliver and Peoples [68] is used to speciate emissions from industrial surface coating activities. This profile is based on direct chemical analyses of composite samples of primers, lacquers, and enamels [68]. In the present study, a profile presented in Table 6.1–1 of Rogozen et al. [96] has been adopted. This profile is based on solvent consumption by the manufacturers of industrial surface coatings. The respeciated emissions are 37% more reactive than is indicated by the official inventory. Further study of the chemical composition

of such coatings is still needed.

Solvents incorporated in industrial adhesives in California are listed in Table 6.5–1 of Rogozen et al. [96]. This listing has been used instead of the existing adhesive speciation profile [68], and results in a 3% increase in reactivity. The official speciation profile lists 56% of the organic gas emissions as isomers of pentane, while the revised profile is dominated by mineral spirits and naphtha (48%), methyl ethyl ketone (15%), and 1,1,1-trichloroethane (11%).

Architectural surface coatings

Architectural surface coatings generally can be classified as either organic solvent- or water-borne. The official emissions inventory for Los Angeles indicates that there are substantial organic gas emissions due to application of both types of coatings (see Table 3.1).

A recent survey by the California Air Resources Board [97] reports the sales volumes, estimated VOC content, and associated thinning solvent usage for 38 different categories of solvent-borne architectural surface coatings. Similar data are reported for water-borne coatings. In the present study, the average organic solvent composition for the major coating categories has been determined from a review of manufacturer-supplied Material Safety Data Sheet (MSDS) information [98,99,100,101,102]. The composite solvent-borne coating speciation profile was developed by averaging the results obtained for each of the major coating categories using the estimated VOC emissions for each coating category [97] as weighting factors. Petroleum-based solvents such as mineral spirits and varnish makers and painters naphtha comprise about 70% of the volatile organic ingredients used in solvent-borne archi-

tectural coatings. One solvent-borne coating category, lacquer, contains a completely different set of chemical compounds. The detailed chemical composition of lacquers was determined from manufacturer-supplied MSDS information, with the major organic ingredients being acetates, alcohols, and ketones.

The official speciation profile (from Table 9–35–103 in the EPA Species Data Manual [92]) uses n-hexane and cyclohexane as surrogates for all of the alkanes contained in mineral spirits. As described previously, mineral spirits contain a range of C_8–C_{12} alkanes and cycloalkanes [95], and this is now reflected in the revised speciation profile. The toluene and xylene content of the revised speciation profile is reduced. The respeciated organic gas emissions from use of solvent-borne architectural coatings are 24% more reactive than the official inventory would suggest.

There are additional organic gas emissions associated with the use of solvent-borne coatings due to cleanup and thinning operations. Chemical analysis of a composite thinning solvent sample [68] provides the basis for speciating these emissions in the official inventory. However, that analysis left 41% of the sample mass unidentified. The composition data for thinners presented in Table 6.1–1 of Rogozen et al. [96] have been used to respeciate these emissions; the reactivity of thinning solvent emissions is found to decrease by 61% after these changes are made.

According to Rogozen et al. [96] and MSDS information, the principal organic cosolvents in water-borne coatings are ethylene glycol, propylene glycol, and a variety of glycol ethers and esters. This list of compounds does not correspond to the major species identified in the existing speciation profile [68]. It may be that low volatility compounds such as the glycols were not

recovered during the distillation step in the analysis of paint samples that is used in the official inventory. A revised speciation profile for water-borne coatings has been developed based on data from Table 6.1–1 of Rogozen et al. [96], and is 117% more reactive than the profile used in the official inventory.

3.2.6 Other changes

In the official inventory for Los Angeles, some source categories have been assigned to a generic "species unknown" profile. In some cases, an alternative profile exists that is better related to the actual source category. Organic gas emissions that occur during cleaning and priming of vehicles prior to repainting, and emissions from other miscellaneous surface coating activities have been reassigned to the composite industrial surface coating profile described previously. Organic solvent usage for thinning and cleanup operations associated with use of architectural surface coatings was also assigned to the "species unknown" profile in the official inventory. In our revised emission inventory, these organic gas emissions are reassigned to the composite thinning solvent profile described earlier. These changes affect 50 tons per day of organic gas emissions.

After reassignment of source categories to alternate speciation profiles, only 49 tons per day of the non-methane organic gas emissions originally assigned to the "species unknown" profile remain in that category. A speciation profile for the organic gas emissions from commercial cooking operations would help to reduce this total still further: presently the official inventory includes 19 tons per day of organic gas emisisons from commercial charbroiling, deep fat frying, and other unspecified operations (excluding baking).

Running evaporative emissions from motor vehicles were mislabelled as

crankcase emissions and assigned to the non-catalyst exhaust speciation profile in the official emission inventory. This source category (56 tons per day of organic gas emissions) was reassigned to the gasoline vapor speciation profile instead.

Organic gas emissions from use of aerosol sprays include both propellant and solvent emissions. The propellants are typically light hydrocarbons such as propane and butane, and synthetic compounds such as dichloromethane. The solvent emissions were speciated as if they were additional propellant. In the revised inventory, the solvent emissions (41 tons per day) have been reassigned to an existing composite domestic solvent speciation profile.

Composite degreasing and cold cleaning solvent speciation profiles were derived from the official emission inventory using all emissions data where the actual degreasing solvent being used was specified. These composite profiles were used to speciate miscellaneous degreasing and cold cleaning emissions where the actual solvent was not known. The old composite profile in the emission inventory referred to solvents such as trichloroethylene which are being phased out.

Evaporative emissions from crude oil production facilities were reassigned from a profile which specified emissions in terms of Carbon Bond mechanism species [12] to another crude oil evaporation profile that gives explicit chemical speciation.

3.2.7 Summary of revisions

The changes in the reactivity of key speciation profiles that occur when the revised speciation data are introduced are summarized in Figure 3.1. The revised speciation profiles have important implications for the evaluation of

emission control proposals because the relative importance of various contributors to the total inventory is now represented better. The largest changes in reactivity for individual speciation profiles were observed for surface coating and solvent usage categories. The reactivity of the overall organic gas emission inventory increases by 4% after respeciation.

While the preceding discussion has focussed on differences in reactivity between official and revised speciation profiles, the main motivation for the respeciation effort conducted in the present study is to advance the ability to compare emission data to ambient air quality for single organic compounds. The adoption of revised speciation profiles has led to major changes in the emissions estimates for many individual chemical compounds. Some of the more striking differences are shown in Figures 3.2 and 3.3. Respeciation of the organic gas emissions results in 14 times greater emissions estimates for 1,3-butadiene, a toxic air contaminant. Emissions of cyclohexane are reduced to 9% of the official inventory estimate.

Use of new speciation profiles has also improved the level of chemical resolution in the inventory. In some cases, emissions of various isomers of a single compound such as hexane or xylene were formerly lumped together as a single sum. The respeciated inventory is more precise in specifying which isomers are emitted.

3.3 Comparison with ambient data

During the period August 10-21, 1986, ambient concentrations of gas-phase organic species were measured downwind of Los Angeles in Glendora, California by R. Rasmussen as part of the Carbonaceous Species Methods Comparison Study [66]. Samples were collected over 4- or 8-hour intervals covering all

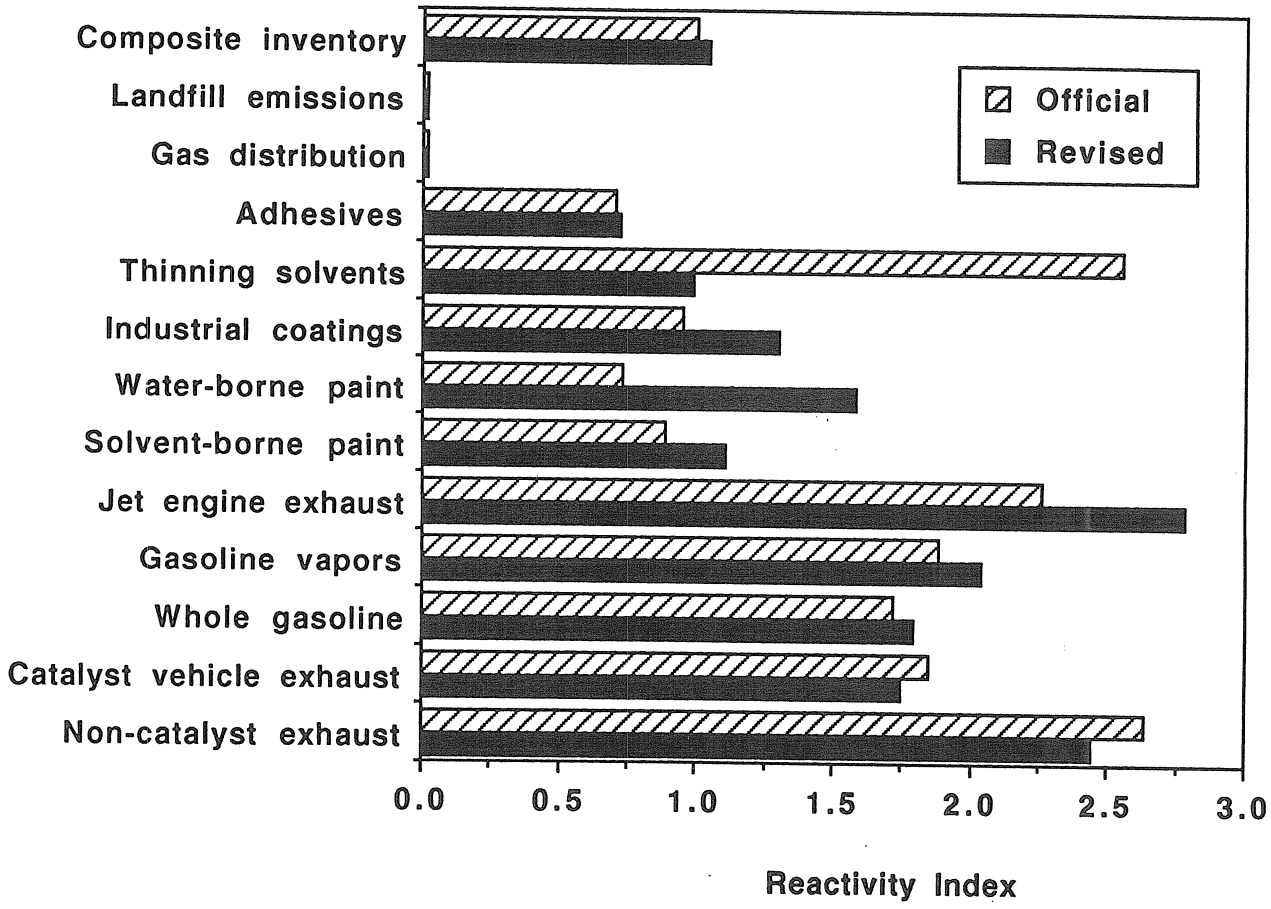

Figure 3.1: Comparison of hydroxyl radical reactivity for organic gas emission speciation profiles in the official and revised emission inventories.

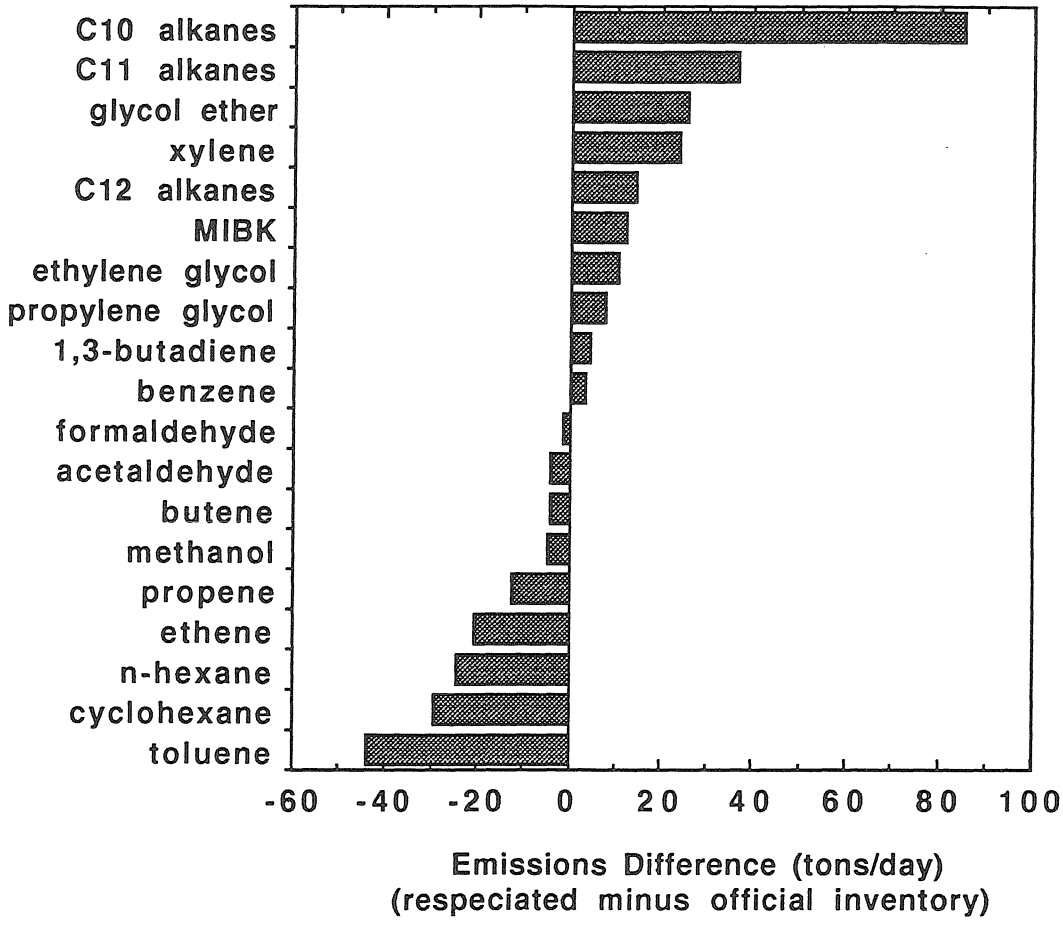

Figure 3.2: Change (tons/day) in basinwide emissions after respeciation for selected compounds.

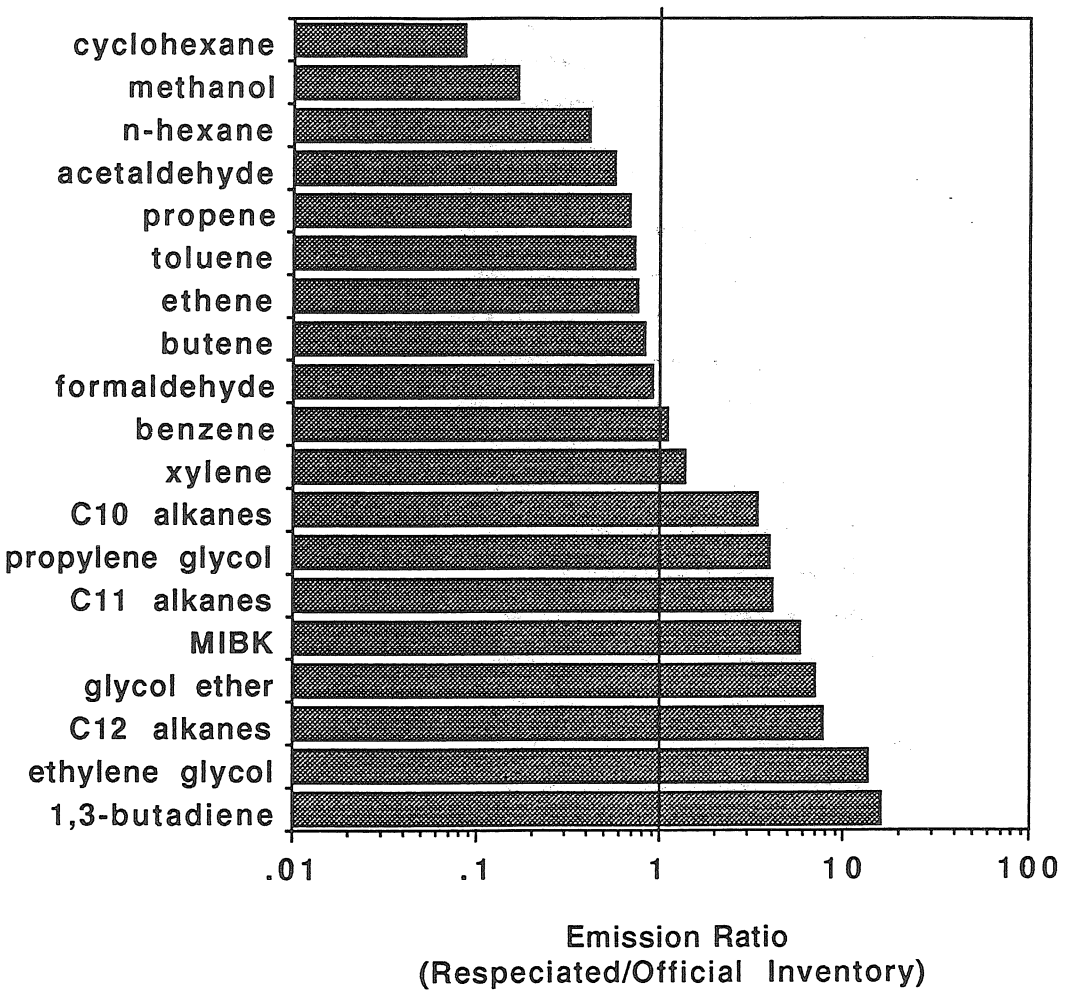

Figure 3.3: Ratio of basinwide emissions in the respeciated versus official emission inventory for selected compounds.

24 hours for each day of the study. Average concentrations for each organic species have been calculated using data from all valid sampling periods and all days. Several of the samples were deleted because of problems with flow rate regulation during filling of the stainless steel sample canisters [103].

Comparisons between the revised basin-wide emission rates for individual compounds and the observed ambient concentrations are presented for selected alkanes in Figure 3.4, and for alkenes, aromatics, and chlorinated compounds in Figure 3.5. In order to reflect only the methane contributed by local emission sources, the average ambient concentration plotted for methane in Figure 3.4 is reduced below the measured value by 1700 ppb, a value representative of upwind background methane levels at San Nicolas Island [56]. The selection of species included in these figures was limited to those that are available in the ambient data base; there are about 200 additional compounds specified in the emission inventory.

The relative positioning of the vertical axes for emissions and ambient concentrations in these figures is arbitrary. The fact that the displacement of ambient concentration points from plotted emissions points for the corresponding species is fairly uniform indicates that the *relative* emission rates of the various species in the revised emission inventory are consistent in order of magnitude with the atmospheric data base.

For the alkanes shown in Figure 3.4, the respeciated inventory generally follows the same trends as the ambient data in terms of the relative abundance of species. Propane, methylcyclopentane, and methylcyclohexane emissions are likely understated relative to emissions of other alkanes, whereas n-nonane emissions appear to be overstated.

In Figure 3.5, similar comparisons are presented for alkenes, acetylene,

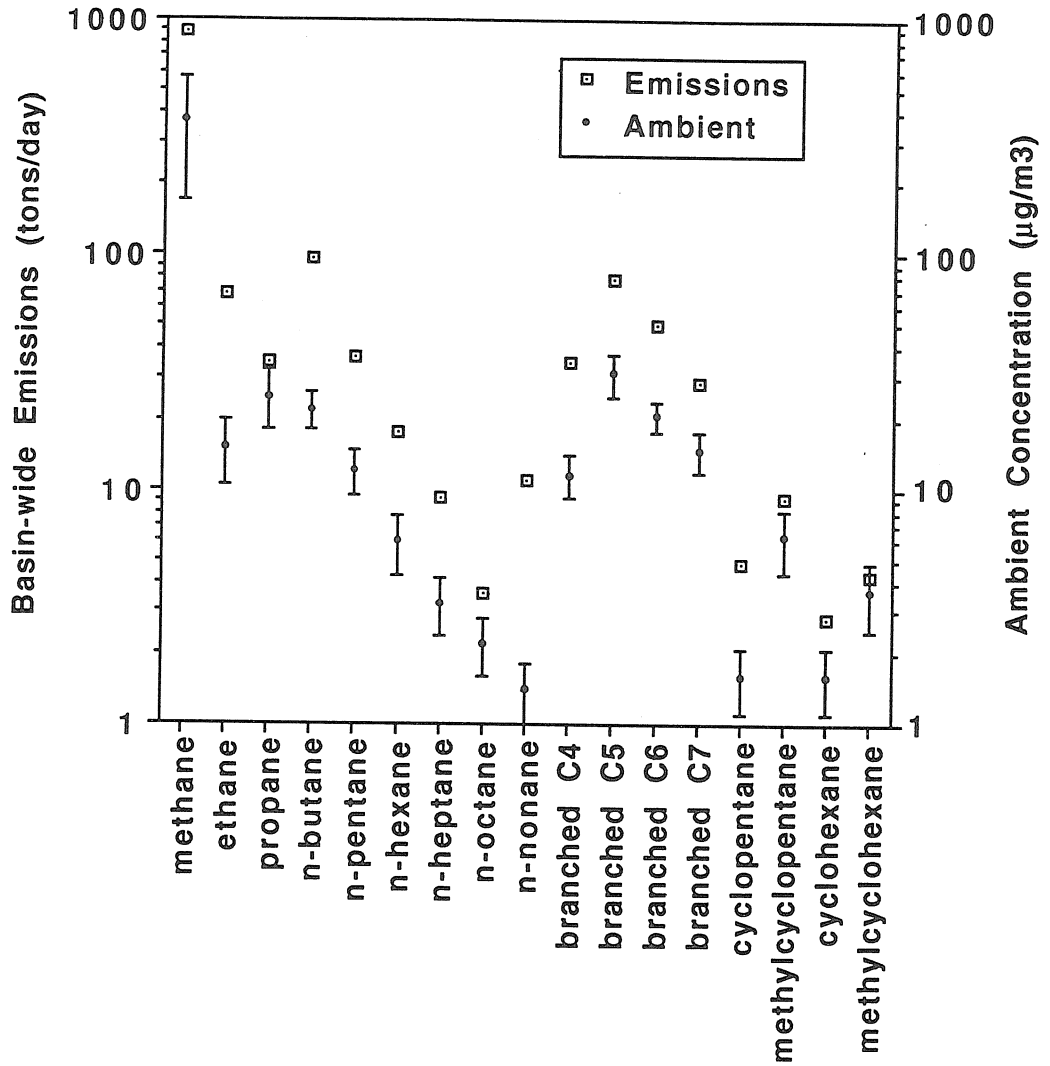

Figure 3.4: Abundance of alkanes in the basinwide emission inventory and in ambient air at Glendora, CA.

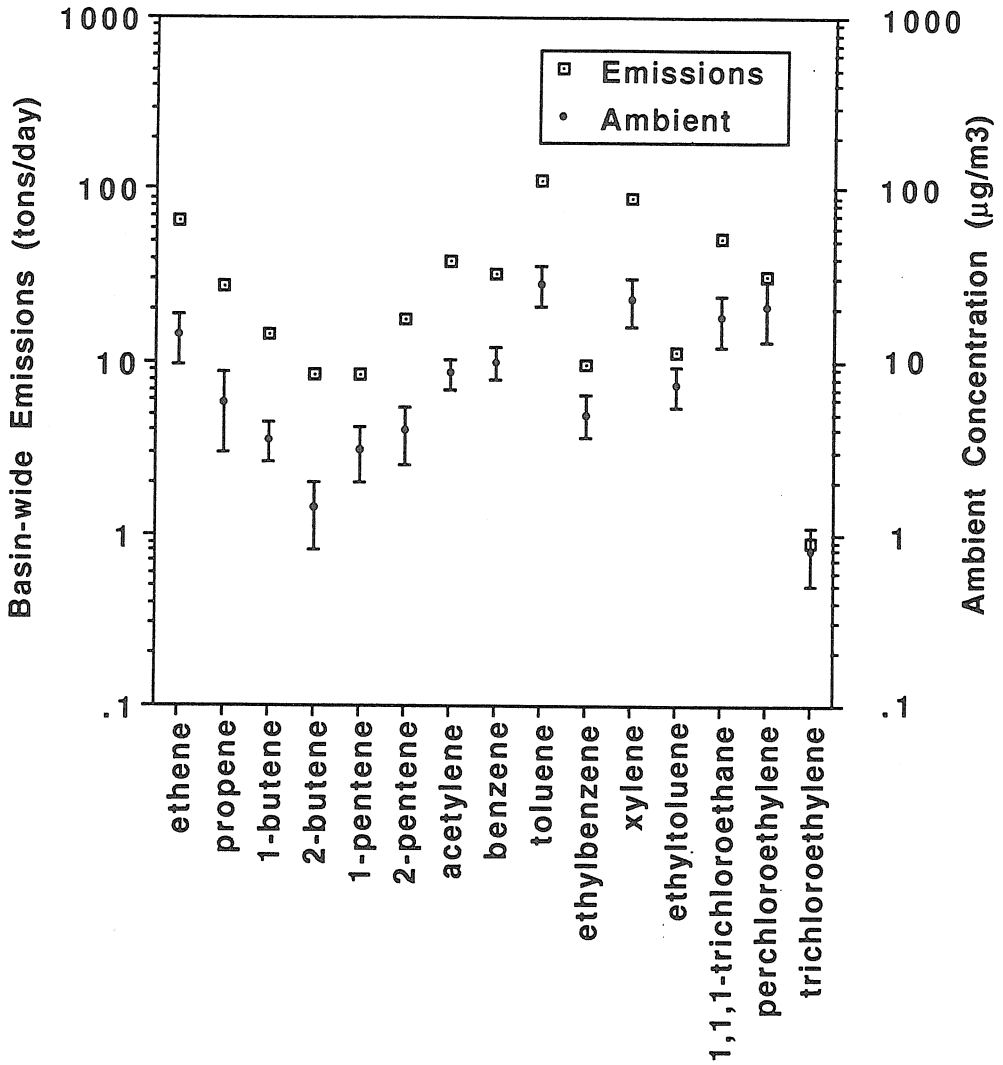

Figure 3.5: Abundance of alkenes, aromatics, and chlorinated species in the basinwide emission inventory and in ambient air at Glendora, CA.

aromatics, and several chlorinated species. The *relative* abundance of these compounds in the respeciated organic gas inventory generally agrees with the ambient data. As shown in Figure 3.5, the actual emissions of ethylbenzene, ethyltoluene, trichloroethylene, and perchloroethylene would appear to be higher than stated in the emission inventory, based on the closer than usual spacing of the emissions and ambient data points for those compounds. The 2-butenes are highly reactive so one should expect that the ambient data point will be displaced further below the emissions point relative to the typical displacement for other species, as seen in Figure 3.5.

3.4 Source-receptor reconciliation

It is highly desirable to have independent methods for checking the accuracy of the emission inventory before using it in photochemical modeling calculations. The chemical mass balance technique [104,105] can be used to determine the contributions of various pollution sources to ambient pollutant concentrations at receptor sites where air quality measurements are available. By using the chemical mass balance model to examine source contributions at many receptors, it is possible to determine whether the emission inventory is accurate in its description of the *relative* importance of the various source types. Such source-receptor reconciliation techniques have been used before for Los Angeles [106], Sydney [107], New Jersey [108], and Chicago [109,110]. Since chemical mass balance models do not directly employ the mass emisison rate data, such an analysis does not determine the absolute magnitude of the source emission rates in tons per day — only the relative importance of the source types is revealed.

As demonstrated by Cass and McRae [111], the tracer species used for

receptor modeling must be selected carefully. The emission inventory for each chemical species should be examined to determine which source categories are thought to be significant contributors to the emissions of each chemical species under consideration. A compound should not be used in the model if the set of source speciation profiles available for use in the receptor model does not include all significant sources of the compound.

In chemical mass balance models, the mass concentration of a species at a receptor air monitoring site is taken to be a linear combination of the emissions of that species from various sources:

$$c_{ik} = \sum_{j=1}^{m} a_{ij} f_{ijk} s_{jk}, \tag{3.4}$$

where c_{ik} is the mass concentration of species i at receptor k, a_{ij} is the weight fraction of species i in the total direct emissions from source j, f_{ijk} is the fractionation coefficient of species i from source j, and s_{jk} is the total mass contribution of all species emitted from source j to air quality observed at receptor k. There are m different source categories, and the unknowns to be determined are the relative source contributions s_{jk}. The fractionation coefficient, f_{ijk}, is the fraction of species i from source j which will reach receptor k. This coefficient is used to account for loss of species mass during transport from source to receptor due to removal processes such as atmospheric chemical reactions and deposition at the earth's surface. For this analysis the organic gas tracer species were selected to exclude highly reactive species so that the fractionation coefficients can be set to unity. For a single receptor k, equation (3.4) is written repeatedly for each of n chemical species. This set of equations forms an over-determined system provided that the number of species is greater than the number of source categories to be resolved.

The system is solved by regression analysis to obtain the best fit combination of source contributions that reproduces the ambient concentrations of all species with minimum squared error.

In this study, the CMB7 source-receptor modeling computer program [112] has been used to solve the set of equations (3.4) at each receptor k. This program requires ambient concentration data (c_{ik}) and source speciation data (a_{ij}) as inputs. Uncertainties to be associated with each data point are also required. The standard deviation of the determination of the weight percent abundance of each species in the ambient data set is used to weight c_{ik} and a_{ij} so that each species is treated relative to the precision with which it can be measured. Without such weighting, species with large ambient concentrations would dominate the calculation, and valuable concentration data obtained for trace species would be ignored. Confidence intervals on the source contribution estimates are computed by the CMB7 program using speciation profile and ambient concentration uncertainty data.

3.4.1 Source, receptor, and species selection

The monitoring sites used in the receptor modeling calculations are shown in Figure 3.6. The list of sites includes Glendora (special monitoring site for the Carbonaceous Species Methods Comparison Study [66], August 10–21, 1986) and Claremont, Long Beach, Anaheim, Azusa, Burbank, Central Los Angeles, Hawthorne, and Rubidoux (intensive monitoring sites during the Southern California Air Quality Study [16], summer and fall 1987). Unlike the samples collected at Glendora which were 4- or 8-hour average samples, the hydrocarbon samples collected during SCAQS were obtained over one-hour sampling intervals. The samples were collected in stainless steel

canisters by Aerovironment [113] at 0600, 1100, and 1500 hours PST, with additional samples collected at the Claremont and Long Beach sites only at 0400, 0800 and 1300 hours PST. The samples were analyzed using gas chromatography by Stockburger et al. [57] and Rasmussen [114].

Average ambient concentrations were determined for each species using all available summertime data at each receptor. The corresponding uncertainties in the ambient concentration data for each species were computed from the standard deviation in the relative abundance of each species on a sample by sample basis. This was done to normalize for meteorological variations that affect the absolute species concentrations but not necessarily the relative abundances.

The number of source categories that can be resolved is limited by availability of tracer species in the ambient data sets and by collinearity among the speciation profiles being used. There are over 800 individual source categories referenced in the emission inventory, and only about 75 species present in the ambient data base that could be used to resolve separately all of these sources. Fortunately, a relatively small number of sources contribute most of the organic gas emissions (see Table 3.1). It is still necessary to lump some of the speciation profiles for different source categories together when there are no appropriate tracer species in the ambient data set for a source category, or when speciation profiles are nearly collinear. Further it is necessary to screen the species used to assure that they react slowly enough in the atmosphere to justify the approximation that f_{ijk} is unity, and also to assure that the few major sources included in the calculation contribute the overwhelming majority of emissions of those compounds such that the material balance of equation (3.4) is in fact observed. The lumping and

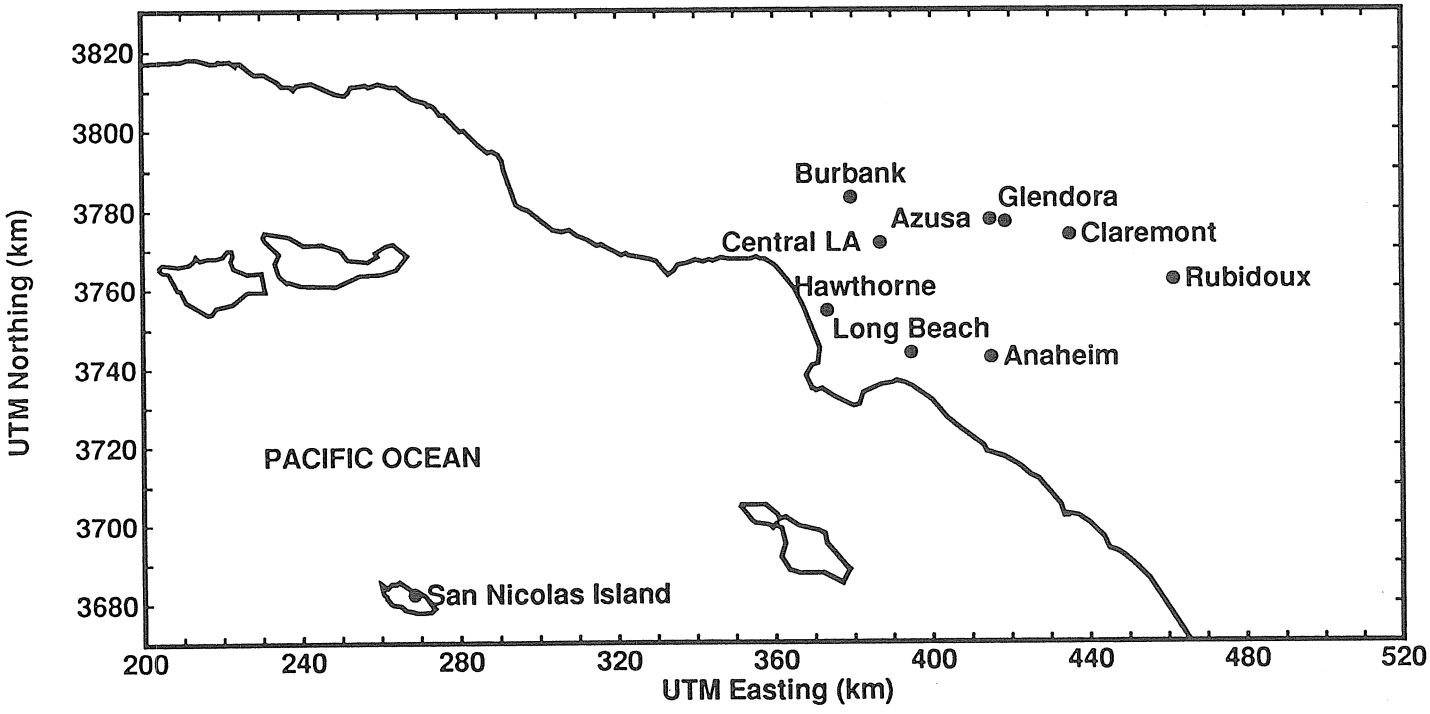

Figure 3.6: Map showing receptor monitoring sites where speciated organic gas concentration measurements were made.

screening procedures employed here follow the emission inventory assisted receptor modeling methods of Cass and McRae [111]. Source categories with similar speciation profiles and similar spatial distribution are pooled. The lumping was carried out using total organic gas emissions (as per the revised emission inventory) to weight the individual speciation profiles to form a composite profile for each lumped group of sources. The lumped sources and their composite speciation profiles are shown in Table 3.6. The standard deviations in Table 3.6 were estimated from speciation uncertainties for each source category and from the uncertainties associated with the lumping procedure. The lumped sources shown in Table 3.6 account for approximately 60% of the anthropogenic non-methane organic gas emissions in the South Coast Air Basin. The source category labelled waste and natural gas includes emissions from methane-rich sources such as natural gas seeps and distribution losses, waste decomposition, oil and gas production, and certain petroleum refinery emissions.

A screening procedure was applied to each candidate tracer species for use in the receptor modeling calculation. The first criterion was that measurements of ambient concentrations for the species must be available. In addition, the species must not be too reactive: assuming a hydroxyl radical concentration of 10^6 molecules/cm^3, the species must have a half-life with respect to hydroxyl radical attack of at least 20 hours. Peak hydroxyl radical concentrations in heavily polluted areas such as Los Angeles may approach 10^7 molecules/cm^3 at midday during the summer, but will be much lower at other times of day [115]. Furthermore, the species should not be formed in appreciable amounts from the atmospheric oxidation of other organic species. Finally, at least 75% (typically more than 80%) of the emissions for the

Table 3.6: Source speciation profiles for use in receptor modeling

Compound[a]	Engine Exhaust	Waste and Natural Gas	Gasoline Headspace Vapors	Whole Gasoline	Dry Cleaning Solvents	Degreasing Solvents
			Emissions Composition:[b]			
methane	11.9 ± 4.0	84.5 ± 15.9	–	–	–	–
ethane	1.9 ± 0.6	4.6 ± 0.5	0.2 ± 0.1	–	–	–
ethene	8.2 ± 2.0	–	–	–	–	–
acetylene	5.3 ± 2.0	–	–	–	–	–
n-butane	2.9 ± 0.8	2.1 ± 0.3	30.0 ± 6.3	3.3 ± 0.6	–	–
n-pentane	1.9 ± 0.4	0.9 ± 0.2	6.3 ± 3.0	2.7 ± 1.4	–	–
isopentane	3.7 ± 1.2	1.1 ± 0.2	22.3 ± 4.9	6.9 ± 1.9	–	–
n-hexane	1.0 ± 0.2	0.5 ± 0.1	1.1 ± 0.3	2.0 ± 0.9	–	–
branched C_6 alkanes	4.1 ± 0.6	0.6 ± 0.1	5.7 ± 1.0	6.7 ± 1.5	–	–
methylcyclopentane	0.8 ± 0.2	–	1.1 ± 0.4	2.5 ± 1.2	–	–
methylcyclohexane	0.4 ± 0.2	–	0.1 ± 0.1	1.0 ± 0.5	–	–
benzene	3.6 ± 0.7	0.2 ± 0.1	0.7 ± 0.1	1.9 ± 0.1	–	–
ethylbenzene	1.2 ± 0.2	–	–	1.9 ± 0.3	–	–
perchloroethylene	–	–	–	–	94 ± 10	11.5 ± 2.7
1,1,1-trichloroethane	–	–	–	–	–	43.5 ± 9.3
all other species	53	6	32	71	6	45

[a]Includes only those species which are present in the ambient data base and meet the other screening criteria described in the text

[b]Percent by weight of total organic gas emissions for the specified lumped source category

species must be accounted for in the source speciation profiles being used. Only those measured species which meet the above criteria appear in Table 3.6.

Initially, all species shown in Figure 3.7 were considered for inclusion in the receptor modeling calculation. Due to the following considerations, some of those compounds and the source classes that they might trace have been eliminated. The fraction of perchloroethylene emissions attributed to 'other' sources in Figure 3.7 results almost entirely from dry cleaning solvent use. Perchloroethylene thus would be an excellent candidate for a fitting compound within our analysis, and could be used to sort out emissions from dry cleaners. However, perchloroethylene concentration data were only available for the Glendora monitoring site. Therefore, at this time, perchloroethylene data cannot be used consistently throughout our analysis. Significant fractions of the emissions of toluene, xylene, and acetone also are attributed to sources other than those listed. Acetone would be a useful tracer for domestic solvent use, except that it is formed in the atmosphere as an oxidation product of other organic gases, and therefore could not be used in the receptor modeling calculation. The domestic solvent speciation profile also includes alcohols and glycols for which no ambient concentration data were available. Surface coating activities emit a complex mixture of organic gases, as shown in Table 3.3. Of these compounds, only toluene and xylene are consistently included in the ambient concentration data base. Xylene does not meet the reactivity criterion specified above, and toluene by itself is not sufficient to act as a tracer for surface coating activity, so the surface coating source category could not be included in the final analysis. As a result, toluene was not used as a fitting compound in the receptor modeling calculations.

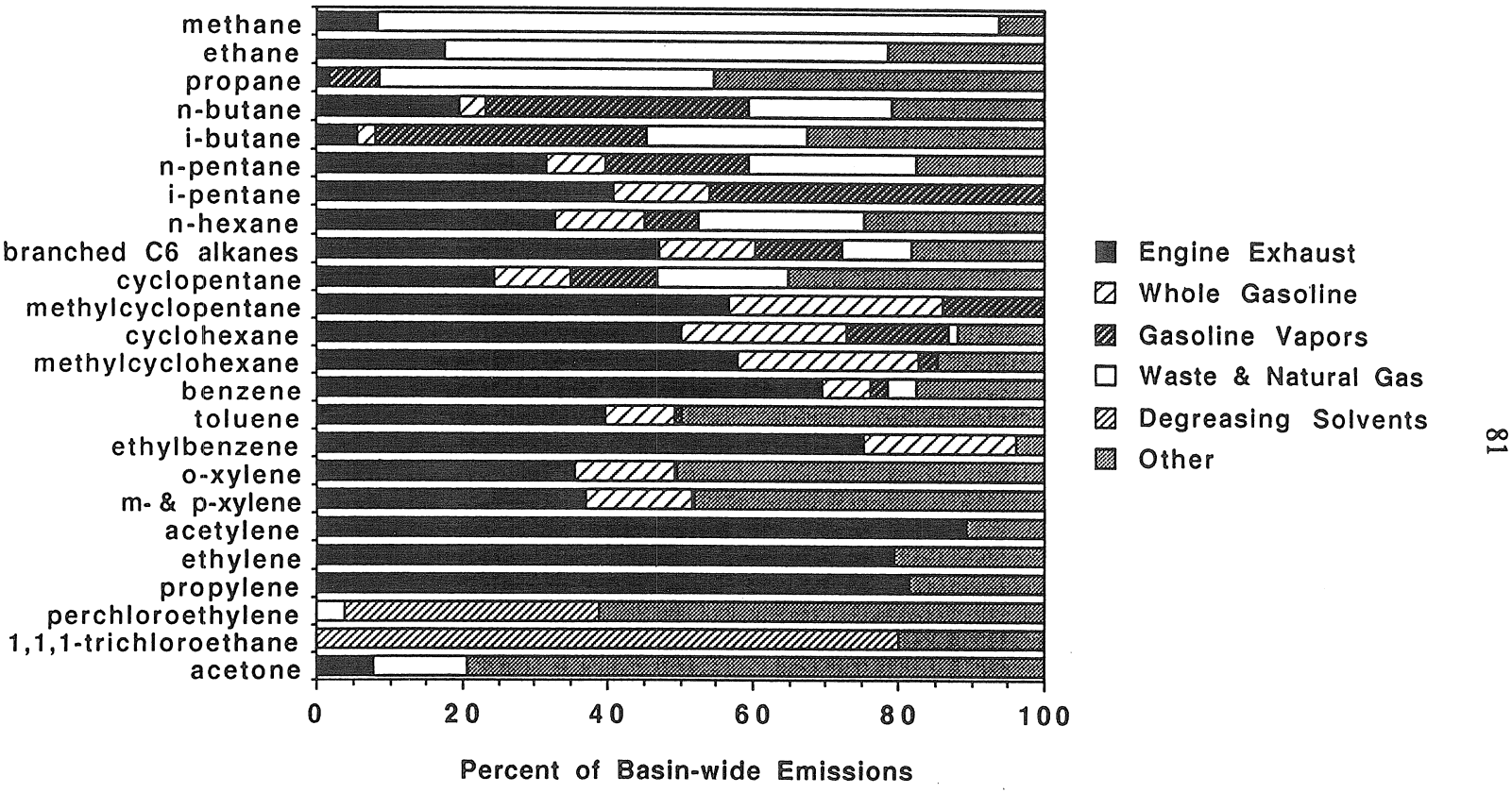

Figure 3.7: Fraction of basinwide emissions of individual species attributed to various source categories.

Having explained why we will not attempt to calculate surface coating and domestic solvent contributions to the ambient organics burden, it is now important to explain why that decision will not result in misidentification of solvent vapors as if they were unburned gasoline emissions. While it is true that certain species are present in both unburned gasoline and surface coating solvents, steps have been taken to guard against such a miscalculation. The main applications of the petroleum distillate solvents are for surface coating, degreasing, and cleaning. In surface coatings and in the Stoddard solvent used for degreasing and cleaning, the bulk of the species are in the C_8 to C_{12} alkane range and these compounds are not used as fitting compounds in the model. In the case of toluene and xylene which are prominent both in gasoline and in some solvents, again the compounds are disqualified as fitting compounds in the model. Solvent emissions from dry cleaning and degreasing can be tracked using chlorinated compounds such as perchloroethylene and 1,1,1-trichloroethane when ambient data are available. The hydrocarbon solvents used by those source categories are carried along with the chlorinated compound tracer analysis, but these hydrocarbons are not used as tracer compounds in a way that could interfere with the identification of unburned gasoline in the atmosphere.

The performance of the chemical mass balance model can be improved when tracer species are available that are unique to a single source category. Carbon monoxide, though not strictly speaking an organic gas, is a very desirable species to include in the analysis because it has a long atmospheric lifetime, is emitted almost entirely from motor vehicle exhaust, and was measured along with gas-phase organic species by gas-chromatographic methods during the special field studies. The mass ratio of carbon monoxide to organic

gas emissions for mobile sources used here is 8.7±3.1, based on measurements made in a Los Angeles area roadway tunnel [4]. This value is consistent with ratios computed for other roadway tunnel experiments [83,116].

Other processes that remove hydrocarbons from the atmosphere have been considered before the final selections of tracer species were made. Dry deposition is the only process other than atmospheric chemical reaction that removes various species from the atmosphere at differing rates. Because species that exhibit high removal rates via dry deposition are highly reactive or highly soluble in water [117], and the hydrocarbons chosen as tracer compounds are not very reactive and typically have low aqueous solubilities, therefore dry deposition is not likely to be a significant removal process for our tracer species over the time scales necessary for the present receptor modeling study.

3.4.2 Source-receptor modeling results

The results of the chemical mass balance model analysis are presented in Table 3.7 and in Figure 3.8. Table 3.7 specifies source contributions to the non-methane organic gas concentrations observed at each receptor. A direct comparison between the sum of computed source contributions and observed organic gas concentrations to determine the residual contribution from other sources is not possible because the emission inventory includes approximately 300 tons per day of oxygenated species such as alcohols and glycols that were not measured in the ambient data base, and because the most reactive compounds (not used as fitting compounds) will be depleted significantly in ambient air relative to the amount emitted.

In Figure 3.8, the relative contributions of 5 lumped sources (engine ex-

Table 3.7: Source contributions[a] to non-methane organic gas concentrations

Receptor:	Engine Exhaust	Waste and Natural Gas	Gasoline Headspace Vapors	Whole Gasoline	Dry Cleaning Solvents	Degreasing Solvents
	Source Contribution ($\mu g/m^3$):					
Glendora	152 ± 34	46 ± 9	21 ± 20	177 ± 46	18 ± 13	49 ± 23
Anaheim	114 ± 32	33 ± 11	43 ± 20	120 ± 36	ND[b]	15 ± 6
Azusa	159 ± 47	45 ± 11	29 ± 32	160 ± 85	ND	39 ± 21
Burbank	211 ± 43	58 ± 17	52 ± 35	217 ± 60	ND	43 ± 16
Central LA	208 ± 51	38 ± 13	45 ± 23	264 ± 67	ND	37 ± 25
Claremont	143 ± 35	47 ± 10	35 ± 22	137 ± 45	ND	26 ± 13
Hawthorne	70 ± 24	25 ± 7	32 ± 17	73 ± 27	ND	14 ± 10
Long Beach	105 ± 36	44 ± 10	42 ± 20	107 ± 45	ND	40 ± 65
Rubidoux	119 ± 29	49 ± 11	27 ± 19	124 ± 38	ND	17 ± 11

[a]Source contributions to non-methane organic gas concentrations at each receptor are reported with associated standard errors (± one standard deviation).
[b]Not determined, as the perchloroethylene concentration data needed were not available at these sites.

haust, waste and natural gas, whole gasoline, gasoline headspace vapors, and degreasing solvents) at each receptor are compared with the relative importance of these sources as specified in the basin-wide emission inventory. Note that a significant fraction of the basin-wide organic gas emissions, including biogenic emissions, domestic solvent use, and architectural and industrial surface coating activities, is not shown in Figure 3.8, and therefore the relative source contributions are relative only to the sum of the five sources mentioned, not the total inventory. Inspection of Figure 3.8 reveals that the relative source contributions are fairly similar at all of the receptors.

When compared to the relative source contributions specified in the emission inventory, the results at all of the receptors indicate that the emission inventory understates the emissions of whole (unburned) gasoline relative to exhaust emissions. The receptor model results do not, however, pinpoint the source of such excess unburned gasoline emissions, and there are many possible sources including understated evaporative emissions (e.g., additional hot soak emissions or fuel spillage), and more unburned gasoline in tailpipe exhaust than is suggested by FTP-based testing. Possible mechanisms that would lead to additional emissions of unburned fuel in tailpipe exhaust include difficult cold starts and misfiring engine cylinders. Excess gasoline emissions might also occur during off-cycle conditions such as rapid decelerations that are not represented in FTP-based tests. A recent remote surveillance study has confirmed that a small fraction of the vehicle fleet contributes a disproportionately large share of the total exhaust emissions [64]. Such vehicles are also important in determining the overall speciation of the exhaust emissions, but measurements made to date have not investigated the chemical speciation of exhaust emissions from the highest-emitting vehicles. Further

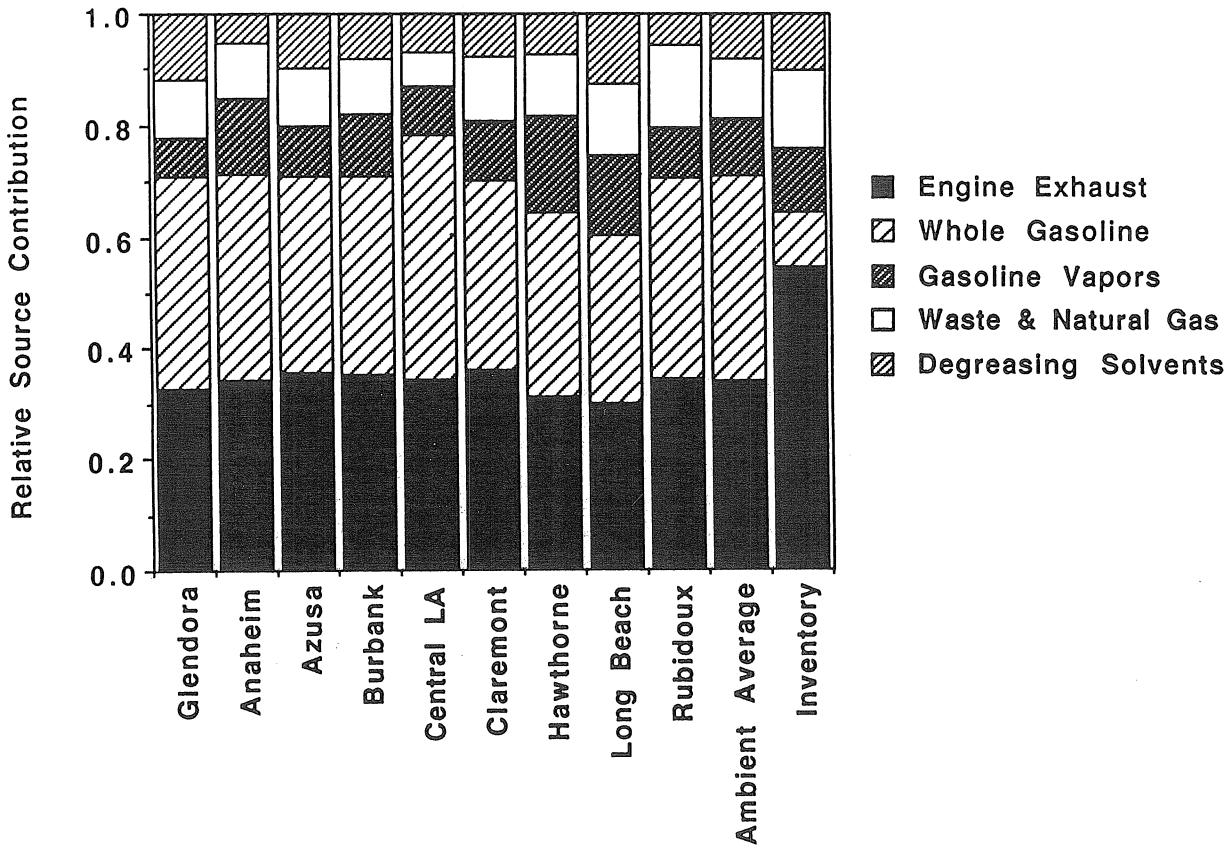

Figure 3.8: Relative source contributions to non-methane organic gas concentrations at various receptor monitoring sites.

study of the many potential sources of the excess emissions described above is recommended.

The results of Figure 3.8 are expressed in terms of percentage contributions to the ambient concentrations and do not explicitly determine the actual tonnage of gasoline vapors and exhaust emitted. However, if one were to assume that the exhaust emissions in the official emission inventory at least are not overstated, then the receptor modeling results suggest that the absolute emissions of unburned gasoline to the atmosphere are much greater than previously thought. For example, if the mass of non-methane organic gas emissions assigned to gasoline and diesel engine exhaust in the respeciated emission inventory (550 tons per day) were correct, then the approximate one to one ratio of unburned whole gasoline to FTP-determined tailpipe exhaust found in the atmosphere suggests an emission rate of unburned gasoline of about 550 tons per day compared to only 108 tons per day in the current emission inventory. Since the exhaust emissions themselves may be understated [5,64,65,6], the actual mass emission rate of unburned gasoline could be even greater than the value just calculated. Resolution of this issue is complicated because the newly recognized emissions of unburned gasoline could be emitted in the tailpipe exhaust under conditions not represented by conventional FTP exhaust speciation tests. Such conventional FTP tests have already identified a 50% contribution of unburned fuel components to engine-out and tailpipe exhaust for 3 catalyst-equipped vehicles [90]. The results of the present study suggest that this contribution might be even higher for the vehicle fleet and driving patterns typical of Los Angeles in 1987.

3.5 Conclusions

Respeciation of the organic gas emission inventory has resulted in large changes in the basin-wide emission estimates for many important organic gases. The hydroxyl radical reactivity of individual speciation profiles has changed significantly. The reactivity of the overall organic gas emissions inventory showed only a modest increase of about 4% after respeciation, which may explain why photochemical models for ozone production have worked reasonably well in spite of major errors in the composition of the actual emissions. The relative abundance of individual species and species groupings in the respeciated emission inventory corresponds to the patterns seen in ambient concentration measurements taken at Glendora during August 1986.

Receptor modeling calculations indicate that the current emission inventory for the Los Angeles area understates the emissions of unburned gasoline relative to combustion-derived hydrocarbons such as ethene and acetylene. Excess unburned fuel may be emitted in tailpipe exhaust under driving conditions not represented in current FTP-based tests, or if the vehicles used in speciated exhaust measurement studies are not truly representative of the on-road vehicle fleet. As well, evaporative emissions including hot soaks and fuel spillage may be underestimated relative to exhaust emissions in the official emission inventory.

It was not possible to determine source contributions in these receptor modeling calculations for biogenic hydrocarbon emissions (due to their short atmospheric lifetime), or for surface coating and domestic solvent use (due to lack of ambient concentration data for key marker compounds). There is a need for further study of the chemical composition of industrial sur-

face coatings, and the detailed composition of petroleum distillate solvents incorporated in surface coatings.

In the future, it is recommended that speciated organic gas measurement programs include alcohols (especially methanol, ethanol, isopropanol, and butanols), glycols (ethylene glycol and propylene glycol), and glycol ethers (e.g., ethylene glycol monobutyl ether) as part of the ambient concentration data sets. Availability of such data for these species would help to resolve the contributions from organic gas emission sources such as surface coatings and domestic solvent use. In addition to the alcohols and glycols, other species such as methyl *tert*-butyl ether should be measured as they are incorporated in reformulated motor vehicle fuels.

4 Modeling lumped VOCs

4.1 Introduction

Emissions of volatile organic compounds (VOCs) contribute to the formation of photochemical smog, in particular ozone. Control of VOC emissions, together with controls on the emissions of oxides of nitrogen (NO_x), are the means by which major urban areas such as Los Angeles hope to solve their ozone air quality problems [1].

The ability to account for the emissions and ambient concentrations of gas-phase organic compounds is an essential step in the development of mathematical models for use in studying regional ozone control problems. Good agreement between ozone model predictions and observations must be viewed with skepticism if predicted VOC and NO_x concentrations are incorrect, yet previous attempts to model VOC concentrations generally have yielded poor results. In the few cases where model performance for VOC was examined (summarized by Tesche [61,7]), large negative biases (on the order of –50%) in predictions relative to observations have been seen. The source of these biases is uncertain because comparison of predictions to observations for individual organic species has not been achieved; only total VOC concentrations have been examined.

Reference: Harley, R. A.; Russell, A. G.; Cass, G. R. Mathematical modeling of the concentrations of volatile organic compounds: model performance using a lumped chemical mechanism. Submitted to *Environ. Sci. Technol.*, 1992.

One of the reasons that detailed models for the prediction of organic gas concentrations have not been proposed and evaluated in the past is that speciated ambient VOC concentration data are scarce. During the 1987 Southern California Air Quality Study (SCAQS; for an overview, see Lawson [16]), a detailed set of speciated organic gas concentration measurements were made at a network of 9 monitoring sites in the Los Angeles area. In the present study, the ability of an Eulerian photochemical air quality model to predict ambient concentrations of individual organic species and lumped species groups is evaluated. Model predictions are compared against measurements of organic species concentrations made during the 27–29 August 1987 intensive monitoring period of SCAQS. The effects of present uncertainties in on-road motor vehicle hot exhaust mass emission rates are examined, and an improved description of the chemical composition of the VOC emission inventory is explored.

4.2 Model description

The CIT airshed model is an Eulerian photochemical air quality model that has been used to calculate the transport and chemical reactions of pollutants in the atmosphere. The theoretical basis of the CIT airshed model and its numerical implementation have been described previously [18,20,25]. In brief, the model solves numerically the atmospheric diffusion equation for a set of reacting chemical species:

$$\frac{\partial C_i}{\partial t} + \nabla \cdot (\vec{u} C_i) = \nabla \cdot (K \nabla C_i) + R_i + Q_i, \tag{4.1}$$

where C_i is the concentration of species i, $\vec{u}$ is the wind velocity, K is the eddy diffusivity tensor (here assumed to be diagonal), R_i is the rate of generation

of species i by chemical reactions, and Q_i is a source term for elevated point sources of species i. A system of coupled non-linear equations is obtained when the above equation is written repeatedly for each of the chemical species tracked by the model. Initial conditions and lateral boundary conditions are set using measured pollutant concentration data. The ground-level boundary condition sets upward pollutant fluxes equal to direct emissions minus dry deposition. The concentration gradient for each species is set to zero at the top boundary, so that there is no vertical transport of pollutants through the top of the modeling region.

Typical photochemical reaction mechanisms that are used within regional air quality models simplify the treatment of the volatile organic compounds by aggregating the emissions of hundreds of individual species into a much smaller number of lumped species classes. In the LCC mechanism (Lurmann, Carter and Coyner [11]), the organic species are lumped by molecule, with compounds having similar structure and reactivity grouped together. The chemistry of all molecules within a single lumped class is then represented using one or more surrogate species (e.g., toluene is used to represent the chemistry of all monoalkyl benzenes).

In the present study, the condensed version of the LCC chemical mechanism [11] with extensions to treat the alcohols and biogenic alkenes separately (described in Chapter 2) has been used to represent the atmospheric chemistry of the organic gases and the relevant inorganic species including ozone and the oxides of nitrogen. The extended mechanism includes 106 chemical reactions involving 35 inorganic and organic species. A list of the the lumped organic species groups and the corresponding surrogate species is shown in Table 4.1. The chemical mechanism includes separate reactions with the

hydroxyl radical for each of the organic species listed in Table 4.1. In addition, the mechanism includes the reactions of ethene, lumped C_3^+ alkenes, and isoprene with ozone, the nitrate radical, and atomic oxygen. Photolysis reactions involving the aldehydes and ketones also are represented in the chemical mechanism. Further details concerning the chemical mechanism used in the present study can be found elsewhere [11].

In the present study, the mechanism has been further extended to track the direct emissions of formaldehyde separately from the formaldehyde that is produced by the atmospheric oxidation of other organic gases, in order to study the contributions of direct emissions versus photochemical production to total formaldehyde concentrations. The extension of the mechanism was accomplished by introducing a specially tagged species that is used to track directly emitted formaldehyde (this tagged species participates in chemical reactions identical to those of the pre-existing formaldehyde species in the LCC mechanism). Total predicted formaldehyde concentrations for comparison with ambient data are computed by summing the concentrations of the directly emitted and photochemically generated formaldehyde model species.

The removal of pollutants at the earth's surface by dry deposition is included in the model. Dry deposition velocities are computed using local meteorological, surface roughness and land use data in each grid square [24]. First, resistances r_a and r_b to dry deposition are calculated based solely on fluid mechanical considerations. These resistances are due respectively to turbulent transport in the atmospheric boundary layer and to molecular diffusion through a laminar sublayer near the ground. Then, a surface resistance term (r_s^i) specific to the pollutant and land use type is included to account

Table 4.1: LCC[a] lumped organic classes and surrogate species

Species Code	Lumped species description	Surrogate species[b]
ALKA	C_4^+ alkanes[c,d]	n-butane, n-pentane, isobutane, isopentane, n-hexane, n-heptane, n-octane, 2-methylpentane, 2,3-dimethylbutane, 2,3-dimethylpentane, isooctane
ETHE	ethene	ethene
ALKE	C_3^+ alkenes	propene, trans-2-butene
TOLU	monoalkyl benzenes	toluene
AROM	di- and trialkyl benzenes	m-xylene; 1,3,5-trimethylbenzene
HCHO	formaldehyde	formaldehyde
ALD2	C_2^+ aldehydes	acetaldehyde
MEK	ketones	methyl ethyl ketone
MEOH	methanol	methanol
ETOH	C_2^+ alcohols	ethanol
ISOP	biogenic alkenes	isoprene

[a]Based on the chemical mechanism of Lurmann et al. [11], with extensions to treat the alcohols and biogenic alkenes separately from the other organics.
[b]Where more than one surrogate species is listed, the rate constant(s) and oxidation product yields for the corresponding lumped species are calculated based on a mixture of the listed surrogate species.
[c]50% of propane emissions also are assigned to the lumped alkane class; the remaining propane emissions are treated as unreactive, as per Lurmann et al. [11].
[d]30% of benzene emissions also are assigned to the lumped alkane class, as per Lurmann et al. [11].

for pollutant-surface interactions:

$$v_g^i = \frac{1}{r_a + r_b + r_s^i}, \tag{4.2}$$

where v_g^i is the actual deposition velocity for species i used in the model. Surface resistance values are derived from the recommendations of Sheih et al. [35] and engineering judgement [24]. Land use characteristics can be specified using detailed maps or satellite data. Dry deposition velocities for the hydrocarbons, though rarely measured, are generally thought to be low because most hydrocarbons are neither highly reactive nor highly soluble in water, and therefore surface resistance terms for these species are large [117]. In the present study, surface resistance values of 50 s/cm have been used for all of the lumped hydrocarbon species in the model, thereby limiting dry deposition velocities for these species to a maximum of 0.02 cm/s. Dry deposition surface resistance terms for formaldehyde and higher aldehydes are scaled relative to the surface resistance values for SO_2: formaldehyde surface resistance values are set to 0.5 times the values used for SO_2; a scaling factor of 2.0 relative to SO_2 is used for acetaldehyde and higher aldehydes [24]. The surface resistance for peroxyacetyl nitrate (PAN) has been set to a value of 4.5 s/cm [118]. The dry deposition surface resistance term for ketones has been set to a high value of 50 s/cm, the same as is used for the hydrocarbons, based on the low atmospheric reactivity of ketones.

4.3 Ambient organics concentrations

In this section, the speciated gas-phase organics concentration data acquired during SCAQS are described. These data, when lumped to match the LCC mechanism species groupings, provide the basis for comparison of organic

species model predictions with observations. There are two independent data sets available.

The first of these two data sets consists of six 1-hour average samples per day taken at the Long Beach and Claremont sites, and three 1-hour average samples per day at the seven additional sites shown in Figure 4.1, giving a total of 33 samples per day. Samples were collected only during SCAQS intensive monitoring periods; this represents a total of 11 days during the summer and 6 days during the fall. Hydrocarbon samples were collected in evacuated stainless steel canisters and stored for later analysis [113]. The samples were analyzed by gas chromatography and gas chromatography/mass spectrometry by Stockburger et al. [57] and Rasmussen [114]. Carbonyl sampling was performed using 2,4-dinitrophenylhydrazine (DNPH) impregnated cartridges [113,119]. As described by Lurmann and Main [120], the above measurements were consolidated into a single data base, and the identification of the hydrocarbons was extended using relative retention time information derived by Fujita from analyses by Lonneman et al. [60]. In the present study, these data will be referred to as data set #1.

A second SCAQS data set consisting of speciated C_2–C_{10} hydrocarbon concentration measurements was reported by Lonneman et al. [60]. Data set #2 consists of three-hour average samples, with measurements made at Central Los Angeles, Long Beach, and Claremont. Early morning samples were collected at all three sites at 0500 hours, with additional samples taken at the Claremont site only at 1100 hours and 1400 hours PST, for a combined total of 5 samples per day. Samples were collected on each of 34 summer days between the dates of June 15 and September 4, 1987, including the summertime intensive monitoring periods of SCAQS.

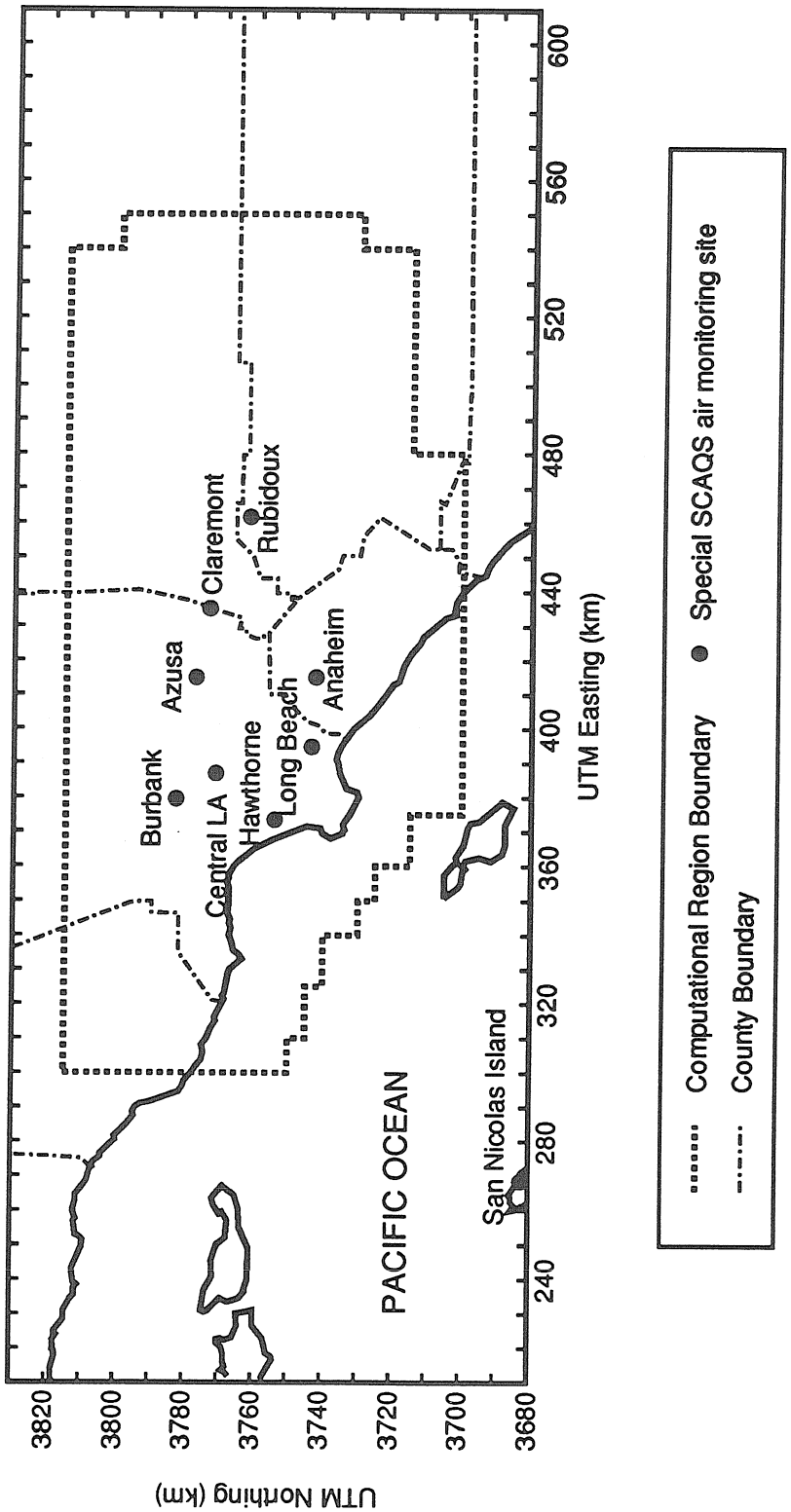

Figure 4.1: Map of the Los Angeles, California area showing the computational region and the locations of special SCAQS air quality monitoring sites.

Using sample scrubbing techniques [121] to remove certain compound classes from a sample, the unidentified fraction of each sample in data set #2 was subdivided into unknown alkanes, alkenes, and aromatics. The alkane and alkene fractions can be assigned unambiguously to lumped species classes within the LCC mechanism. The assignment of the unknown aromatics is less certain, but since the major monoalkyl benzene species were consistently identified in the ambient samples, the unknown aromatics were assigned to the lumped di- and trialkyl benzene class. The inclusion of the unidentified alkanes in the lumped alkane class did not result in a large change in ambient concentrations: typically the unidentified alkanes amounted to about 10% (on a mole basis) of the sum of all other identified alkanes. The contribution of the unidentified aromatics to the corresponding lumped class was higher — typically 30%. The assignment of unidentified alkenes to the lumped alkene class caused a significant increase in lumped species concentrations — sometimes by as much as a factor of two or three, but typically by about 40%. This assignment of the unidentified fraction from each sample was not possible for data set #1 because the sample scrubbing techniques were not used. The relative increase in lumped ambient concentrations in data set #2 due to unidentified compounds is probably greatest for alkenes and di- and trialkyl benzenes; the increments due to unidentified compounds are small for ethene, the alkanes, and the monoalkyl benzenes.

A comparison of the two independent data sets via linear regression analysis is presented in Table 4.2. For the purposes of this comparison, the unidentified fraction for samples in data set #2 was not included in the lumped species assignments because comparable data were not available for data set #1. In later comparisons with model predictions, the unidentified

compounds from data set #2 are included with the appropriate lumped hydrocarbon concentrations. As shown in Table 4.2, correlation coefficients of 0.87 or higher were computed for each of the lumped hydrocarbon species being compared (however, as discussed in the next paragraph, lower correlation coefficients were computed for formaldehyde). This indicates reasonable agreement between the two hydrocarbon data sets, given the different averaging times over which the samples were collected.

In addition to the DNPH cartridge measurements of carbonyl concentrations [119] that form part of data set #1, spectroscopic measurements of ambient formaldehyde concentrations were made at Claremont and Long Beach. Winer et al. [122] made measurements using differential optical absorption spectroscopy (DOAS), and Mackay et al. [123] used tunable diode laser absorption spectroscopy (TDLAS). The spectroscopic methods have been compared [122], and a correlation coefficient of 0.76 was computed for measurements made at Claremont by the two independent spectroscopic methods. Comparisons between the DOAS and DNPH-based formaldehyde measurements from the summertime monitoring periods at Claremont and Long Beach were made as part of the present study. The summertime formaldehyde measurements made at Long Beach using DOAS and DNPH-impregnated cartridges are well correlated, whereas the measurements made at Claremont using the same two techniques do not agree, as shown in Table 4.2. Note that the formaldehyde comparisons were made using a limited number of samples (there were 11 paired samples at Long Beach and 19 paired samples at Claremont). The reasons for the differences in observed formaldehyde concentrations are unclear.

Ambient peroxyacetyl nitrate (PAN) concentrations were measured by

Table 4.2: Comparison of two independent lumped ambient organics data sets[a]

Species Code	Number of Cases	Slope	Intercept (ppbv)	R
ALKA	38	0.96 ± 0.09	5.1 ± 21	0.87
ETHE	34	0.96 ± 0.07	2.9 ± 2.9	0.93
ALKE	34	1.08 ± 0.07	1.5 ± 2.7	0.93
TOLU	37	1.26 ± 0.12	-1.8 ± 2.1	0.88
AROM	38	0.92 ± 0.06	-0.8 ± 2.3	0.94
HCHO:[b]				
Long Beach	11	0.98 ± 0.23	-0.5 ± 2.1	0.81
Claremont	19	0.43 ± 0.25	5.8 ± 3.5	0.37

[a]For the ALKA, ETHE, ALKE, TOLU, and AROM lumped species, the combined data of Stockburger et al. [57] and Rasmussen [114] (data set #1) are regressed on the data of Lonneman et al. [60]. All valid paired summertime samples are used in these comparisons.

[b]HCHO measurements of Fung [119] from data set #1 are regressed on the spectroscopic measurements of Winer et al. [122].

Williams and Grosjean [124] using electron capture gas chromatography. Data were collected at Anaheim, Azusa, Burbank, Central Los Angeles, Claremont, Long Beach, and Rubidoux during the August intensive monitoring period of SCAQS. Independent measurements of PAN at Claremont were reported by Lonneman et al. [60]. Both of these data sets appear on the time series plots presented later. Large systematic differences between the two data sets were observed. It is likely that difficulties in calibrating the instruments are the cause of these differences, since high precision was achieved for measurements made using a single instrument [125]. Therefore large uncertainties must be associated with the ambient concentration data for PAN.

The lumping of the ambient data proceeds by analogy with the method used to lump VOC emissions to the model: each individual organic species is assigned to a lumped class according to its chemical properties as per Lurmann et al. [11], and the lumped species concentrations are accumulated according to the measured concentrations of individual species. Ambient concentrations of hydrocarbons reported in parts per billion of carbon (ppbC) were first converted to parts per billion by volume (ppbv) by dividing by the number of carbon atoms for each individual species. Then the converted concentrations were added to the appropriate lumped molecule species group. Therefore, the comparisons between model predictions and ambient data presented later are based on counts of molecules. This is the appropriate comparison because the LCC chemical mechanism preserves the number of emitted molecules, but not the number of carbon atoms.

4.4 Model application

The present study focusses on the August 27–29, 1987 SCAQS intensive monitoring period. The CIT airshed model has been used to predict ozone and precursor concentrations in the Los Angeles area over the entire 3-day period (see Chapter 2). To perform these calculations, meteorological and pollutant emissions data are required. These data are specified for each 5 km by 5 km grid square of a regular grid system within the modeling region shown in Figure 4.1. The vertical extent of the modeling region is 1100 meters, subdivided into five layers of thicknesses 38, 116, 154, 363, and 429 meters.

Meteorological fields were developed from an extensive data base of routine and special SCAQS surface level and upper air measurements [16,49]. The same meteorological input data fields and setup procedures described in Chapter 2 were used in the present study. The boundary condition values used in the present study are shown in Table 4.3. These values are based on measurements made during SCAQS at San Nicolas Island [113] and measurements made by aircraft over the ocean upwind of the modeling region [56].

An emission inventory supplied by the California Air Resources Board (ARB) was used in this study [41]. Mobile source emission estimates were developed by the ARB using results from a travel demand model and the EMFAC 7E emissions factor model [42]. Stationary source emissions estimates were prepared by the South Coast Air Quality Management District (SCAQMD). Day-specific biogenic emission inventories were provided by the SCAQMD for August 27 and 28 based on a new gridded inventory of leaf biomass in the Los Angeles area [45]. The August 28 biogenic inventory

Table 4.3: Upwind[a] boundary condition values (ppb)

Species	Boundary Condition
CO	200
NO2	1
NO	1
HCHO	3
ALD2	5
MEK	4
NMHC[b]	100
O3	40

[a]Downwind boundary conditions are based on the advection flux out of the air basin. The boundary condition at the top of the modeling region (at a height of 1100 meters above ground level in this case) is a zero flux boundary condition such that pollutants are not fed into the model through the top boundary.

[b]Non-methane hydrocarbon (NMHC) concentrations are specified in ppbC instead of ppbv. Each ppbC of NMHC is speciated as follows: 0.095 ppbv ALKA, 0.017 ppbv ETHE, 0.018 ppbv ALKE, 0.015 ppbv TOLU, and 0.016 ppbv AROM.

was used for both August 28 and 29 because no day-specific inventory was available for the 29th. The official inventory includes a set of 225 chemical composition profiles used to speciate the total VOC mass emissions from over 800 source types. Each speciation profile gives the detailed chemical composition in terms of weight percent for each organic species found in the total VOC emissions from a specific source type. Key speciation profiles have been reviewed and updated as described in Chapter 3. Summaries of the official and respeciated emission inventory for August 27 are presented in Table 4.4. The major differences between the official and respeciated VOC emission inventories arise because of the introduction of new speciation profiles described in Chapter 3. Additional changes, also described in Chapter 3, result from reassigning source emissions with unknown speciation to the most appropriate existing speciation profile. This is discussed in more detail in the following paragraph. The largest differences between these two VOC emission inventories are seen at the individual compound level, where for some species such as 1,3-butadiene and cyclohexane, order of magnitude changes were found in the basin-wide emissions estimates.

In the official emission inventory, in cases where detailed knowledge of the chemical composition of the VOC emissions from a particular source was not available, the emissions were speciated using a 'species unknown' profile that is a composite of the basin-wide emissions from all sources. In the respeciated inventory, the total mass of VOC emissions assigned to this profile has been reduced by 48% by reassigning the emissions from some sources to other more appropriate speciation profiles. The sources that have been reassigned include organic solvent emissions from surface coating thinning and cleanup (16 tons/day of VOC emissions) and from cleaning and pretreat-

ment of vehicles prior to repainting (38 tons/day of VOC emissions). There are currently no appropriate alternative speciation profiles for the remaining 'species unknown' VOC emissions from sources such as commercial cooking (charbroiling, deep fat frying, and other unspecified emissions), manufacture of plastics and plastic products, and a large number of unusual sources with less than 1 ton/day of emissions. VOC emissions from these sources may include a range of complex organic molecules that were not included in the ambient concentration measurements, and probably do not resemble the speciation of the composite inventory for the entire air basin which is dominated by mobile source and surface coating emissions and light hydrocarbons such as methane. Therefore, in the respeciated VOC emission inventory, the remaining 'species unknown' emissions have been assigned to the lumped C_2^+ alcohol species to prevent interferences with the analysis of model performance for the lumped hydrocarbons, while still providing an approximate representation of the reactivity of these emissions. Development of appropriate speciation profiles for these sources would provide the best solution to uncertainties in the chemical composition of these VOC emissions. About half of the increase in C_2^+ alcohol emissions shown in Table 4.4 can be attributed to the assignment of 'species unknown' emissions to this lumped class. The use of revised speciation profiles for VOC emissions from industrial surface coatings and water-borne architectural surface coatings also contributes to the increase in C_2^+ alcohol emissions beyond the amount suggested in the official emission inventory.

Both the official and respeciated emission inventories contain a separate accounting of over 250 organic compounds, which provides a much higher level of chemical detail than is carried in the lumped mechanism used in these

Table 4.4: Region-wide[a] chemical emissions summary for August 27, 1987

Species Code	Lumped species	Base Case Inventory (10^3 kg/day) Official[b] Speciation	Base Case Inventory (10^3 kg/day) Revised[c] Speciation	3× Hot Exhaust Inventory (10^3 kg/day) Official[b] Speciation	3× Hot Exhaust Inventory (10^3 kg/day) Revised[c] Speciation
ALKA	C_4^+ alkanes	799	698	1016	884
ETHE	ethene	83	60	151	114
ALKE	C_3^+ alkenes	100	104	182	190
TOLU	monoalkyl benzenes	162	118	228	178
AROM	di/trialkyl benzenes	118	146	184	218
HCHO	formaldehyde	20	19	35	31
ALD2	C_2^+ aldehydes	13	13	23	24
MEK	ketones	28	49	29	51
MEOH	methanol	5	1	5	1
ETOH	C_2^+ alcohols	91	223	91	235
ISOP	biogenic alkenes	117	117	117	117
ROG	reactive organic gases	1536	1548	2062	2042
NONR	nonreactive[d]	1028	989	1175	1129
CO	carbon monoxide	5624	5624	10867	10867
NO_x	oxides of nitrogen	1138	1138	1138	1138

[a]The inventory region includes most of the mapped area shown in Figure 4.1, which extends beyond the South Coast Air Basin into Ventura County and the Southeast Desert Air Basin.
[b]Using the chemical composition profiles supplied with the official emission inventory.
[c]Using the respeciated VOC emission inventory.
[d]Nonreactive compounds in the LCC mechanism include methane, ethane, acetylene, and various chlorinated compounds.

photochemical modeling calculations. Sometimes there are a small number of species which dominate the emissions assigned to a lumped organic class: for example, the lumped monoalkyl benzene class is dominated by toluene (approximately 90% of assigned emissions), with smaller amounts of ethylbenzene and propylbenzene. The di- and trialkyl benzenes are dominated by emissions of isomers of xylene, ethyltoluene, and trimethylbenzene. The ETHE species used in the model represents ethene emissions almost exclusively, with small amounts of chlorinated alkenes also included (these chlorinated alkenes account for less than 1% of assigned emissions). The lumped alkene class is dominated by emissions of propene, with smaller amounts of 1-butene and other isomers of butene and pentene. In contrast, the lumped alkane class encompasses significant emissions of many different straight-chain and branched alkanes as well as cycloalkanes. The aldehyde and ketone species classes are used in the LCC mechanism to represent both the direct emissions of such compounds as well as their formation in the atmosphere as the oxidation products of other emitted organic species. The aldehyde emissions are made up mostly of formaldehyde and acetaldehyde, with smaller amounts of other aldehydes including propionaldehyde, benzaldehyde, and acrolein (propenal). The ketone emissions are made up of acetone, methyl ethyl ketone, and methyl isobutyl ketone. Only small amounts of methanol are included in the current VOC emission inventory. Emissions of higher alcohols include significant amounts of ethanol, isopropanol, and glycols and glycol ethers from stationary sources such as surface coating and solvent use. The emissions of biogenic alkenes, which are lumped separately from other alkenes in the model, are dominated by isoprene, α-pinene, and β-pinene.

In addition to using both the official and respeciated VOC emission in-

ventories in this study, a sensitivity analysis of the effects of using increased on-road vehicle hot exhaust emissions has been performed. Based on measurements made in a roadway tunnel during SCAQS [4], it was found that actual emissions of carbon monoxide and organic gases from motor vehicles in Los Angeles were significantly higher than suggested by the EMFAC model [4,5]. To account for a possible understatement of such vehicular emissions, alternate emission inventories were created in which the carbon monoxide and organic gas hot exhaust emissions from on-road vehicles were increased to three times the base case values, as suggested by the results of the tunnel study. This change represents an increase in reactive organic gas emissions of about 500 tons per day over the entire mapped region shown in Figure 4.1.

In order to apply the LCC chemical mechanism to a particular urban area, there are three parameters that should be set to match local conditions. The parameters are: the fraction of total C_4^+ alkanes made up of C_4–C_5 alkanes, the terminal alkene fraction of total C_3^+ alkenes, and the dialkyl benzene fraction of total di- and trialkyl benzenes. Default values for these parameters specified by the LCC mechanism are 0.43, 0.60 and 0.60 respectively, but Lurmann et al. [11] recommend that these parameters should be set using location-specific emissions data or speciated ambient concentration measurements. These parameters affect both the reaction rate constants and the oxidation product yields for the corresponding lumped hydrocarbon species. In the present study, these parameters were calculated using the distribution of species indicated in the organic gas emission inventory for the South Coast Air Basin, as described below.

The default value (0.43) for the C_4–C_5 fraction of total C_4^+ alkanes was used in all cases and was not significantly different from the values indicated

by analysis of the official and respeciated emission inventories. The terminal alkene fraction of total C_3^+ alkenes is ambiguous in the official emission inventory because a large fraction of alkene emissions are listed as unspecified isomers of butene and pentene, without distinction between isomers with terminal and internal double bonds. The respeciated VOC emission inventory is more specific in listing exactly which alkene isomers are emitted, and although some ambiguity remains, the default value appears to agree with the value calculated using the respeciated emission inventory. Therefore, the default terminal alkene fraction (0.60) of total C_3^+ alkenes recommended by Lurmann et al. [11] was used in the present study. In the case of the di- and trialkyl benzenes, the default dialkyl benzene fraction (0.60) was not used in the present study. Values of this parameter were calculated to be 0.72 using the official emission inventory, and 0.81 using the respeciated emission inventory. This implies that the dialkyl benzenes comprise a larger fraction of total di- and trialkyl benzene emissions in the Los Angeles area than is reflected by the default value of the corresponding parameter in the LCC chemical mechanism.

4.5 Results

The CIT airshed model has been applied to the August 27–29 period using the meteorological and emissions input data described above. In this section, statistical and graphical comparisons of model predictions and observations are presented.

Statistical model performance measures are presented in Table 4.5 for ozone, total reactive hydrocarbons (RHC), and total NO_2 concentrations (nitrogen dioxide plus other nitrogen-containing species that are measured as if

they are NO_2 by chemiluminescent NO_x monitors). A more detailed analysis of model performance for these species, including time series plots of observed and predicted concentrations has already been presented in Chapter 2.

In the base case calculation using the official emission inventory, ozone and RHC concentrations are underpredicted (normalized biases of -23% and -35% respectively), whereas NO_2 concentrations are overpredicted by 17% on average. Predicted ozone and NO_2 concentrations do not change significantly when the revised speciation profiles are used in place of the official profiles, but the underprediction of RHC concentrations becomes larger, as shown in Table 4.5. This can be explained by noting the increases in alcohol and ketone emissions and simultaneous decreases in alkane and monoalkyl benzene emissions in the respeciated inventory compared with the official base case emission inventory (see Table 4.4). Note that alcohol, aldehyde and ketone species were not included in the analysis of model performance for total RHC.

Table 4.6 shows statistical comparisons of model performance for each of the lumped species defined in Table 4.1 except the alcohols for which no ambient data are available, and the biogenic alkenes because the monoterpenes were not measured in the ambient data sets (only isoprene was detected). All performance statistics shown in Table 4.6 were calculated using observed organic species concentrations from data set #1. Data set #1 provides a large number of samples and good spatial coverage of the modeling region for the SCAQS intensive monitoring days, whereas only 5 samples are available from data set #2 on any given day. Observations from data set #2 are shown on time series plots described later in the text, and these data are consistent with observations from data set #1.

Table 4.5: Model performance for ozone, NO_2 and total reactive hydrocarbons on August 28

Statistical Measure[e]	Species	Base Case Inventory[a] Official[c] Speciation	Base Case Inventory[a] Revised[d] Speciation	3× Hot Exhaust Inventory[b] Official[c] Speciation	3× Hot Exhaust Inventory[b] Revised[d] Speciation
Bias:[f]	Ozone	−3.2	−3.3	−0.4	−0.8
	NO_2	+0.1	+0.1	+0.4	+0.4
	RHC	−56	−69	−29	−46
Normalized bias:	Ozone	−23%	−25%	+1%	−2%
	NO_2	+17%	+16%	+22%	+21%
	RHC	−35%	−46%	−12%	−26%
Gross error:[f]	Ozone	4.3	4.4	3.0	3.1
	NO_2	1.8	1.8	1.8	1.8
	RHC	71	80	59	70
Gross error:	Ozone	38%	38%	29%	29%
(normalized)	NO_2	41%	41%	44%	44%
	RHC	51%	57%	47%	53%

[a]From the CIT airshed model using the base case total mass emissions.
[b]From the CIT airshed model using scaled up on-road vehicle hot exhaust emissions.
[c]Using the chemical composition profiles supplied with the official inventory.
[d]Using the respeciated VOC emission inventory described in Chapter 3.
[e]Bias is defined as the mean residual (predicted minus observed) concentration. Gross error is the mean of the absolute residuals. Normalized statistics are calculated by dividing each residual by the corresponding observed concentration before averaging.
[f]Unnormalized bias and gross error statistics are stated in units of parts per hundred million (pphm) for ozone and NO_2 and in units of parts per billion by volume for total reactive hydrocarbons (RHC).

Table 4.6: Model performance for lumped organic species on August 28

Statistical Measure[e]	Species Code	Base Case Inventory[a] Official[c] Speciation	Base Case Inventory[a] Revised[d] Speciation	3× Hot Exhaust Inventory[b] Official[c] Speciation	3× Hot Exhaust Inventory[b] Revised[d] Speciation
Bias (ppbv):	ALKA	−28	−38	−18	−30
	ETHE	−2.7	−4.7	+6.6	+2.6
	ALKE	−4.1	−4.1	−1.0	−1.3
	TOLU	−3.0	−4.5	−0.2	−2.0
	AROM	−5.3	−4.5	−3.8	−2.9
	HCHO	−1.7	−2.0	+3.1	+1.9
	ALD2	−9.9	−10.1	−6.3	−6.9
	MEK	−6.4	−6.0	−4.9	−4.7
	PAN[f]	−3.3	−3.3	−1.0	−1.1
Normalized bias:	ALKA	−27%	−41%	−12%	−29%
	ETHE	−8%	−26%	+74%	+41%
	ALKE	−45%	−45%	−4%	−7%
	TOLU	−12%	−30%	+22%	+2%
	AROM	−56%	−45%	−35%	−22%
	HCHO	−1%	−4%	+46%	+35%
	ALD2	−46%	−46%	−17%	−21%
	MEK	−15%	−12%	−7%	−4%
	PAN[f]	−37%	−36%	+6%	+4%

[a] From the CIT airshed model using the base case total mass emissions.
[b] From the CIT airshed model using scaled up on-road vehicle hot exhaust emissions.
[c] Using the chemical composition profiles supplied with the official inventory.
[d] Using the respeciated VOC emission inventory described in Chapter 3.
[e] Bias is defined as the mean residual (predicted minus observed) concentration. Gross error is the mean of the absolute residuals. Normalized statistics are calculated by dividing each residual by the corresponding observed concentration before averaging.
[f] A cutoff concentration of 2 ppb was used when computing performance statistics for PAN; no cutoff was used for the other species.

Table 4.6 (continued): Model performance for lumped organic species on Aug. 28

Statistical Measure[e]	Species Code	Base Case Inventory[a] Official[c] Speciation	Base Case Inventory[a] Revised[d] Speciation	3× Hot Exhaust Inventory[b] Official[c] Speciation	3× Hot Exhaust Inventory[b] Revised[d] Speciation
Gross error:	ALKA	40	48	36	44
(ppbv)	ETHE	4.9	6.4	7.0	5.3
	ALKE	5.5	5.5	5.0	5.0
	TOLU	4.0	5.2	3.9	4.3
	AROM	5.8	5.0	5.1	4.4
	HCHO	3.2	3.4	4.1	3.6
	ALD2	10.2	10.3	8.1	8.3
	MEK	7.6	7.6	6.5	6.8
	PAN[f]	3.6	3.5	2.1	2.1
Gross error:	ALKA	47%	55%	45%	51%
(normalized)	ETHE	43%	52%	79%	60%
	ALKE	70%	71%	77%	78%
	TOLU	37%	46%	50%	48%
	AROM	67%	56%	64%	54%
	HCHO	32%	34%	53%	46%
	ALD2	54%	54%	49%	48%
	MEK	41%	43%	38%	41%
	PAN[f]	49%	48%	37%	36%

[a]From the CIT airshed model using the base case total mass emissions.
[b]From the CIT airshed model using scaled up on-road vehicle hot exhaust emissions.
[c]Using the chemical composition profiles supplied with the official inventory.
[d]Using the respeciated VOC emission inventory described in Chapter 3.
[e]Bias is defined as the mean residual (predicted minus observed) concentration. Gross error is the mean of the absolute residuals. Normalized statistics are calculated by dividing each residual by the corresponding observed concentration before averaging.
[f]A cutoff concentration of 2 ppb was used when computing performance statistics for PAN; no cutoff was used for the other species.

For the base case simulation using the official state of California emission inventory and emission speciation profiles, the statistical performance analysis shows that model predictions are generally within 30% of observed concentrations, but tend towards underprediction in all cases. The underpredictions are largest (about –50% normalized bias) for the di- and trialkyl benzenes, C_3^+ alkenes, and C_2^+ aldehydes.

When the respeciated VOC emission inventory is used in place of the official inventory, predicted alkane, ethene, and monoalkyl benzene concentrations decrease, while di- and trialkyl benzene concentrations increase, and the remaining lumped species stay about the same. Predicted ozone concentrations decrease very slightly when the respeciated VOC emission inventory is used, as shown in Table 4.5.

When the calculations are repeated using the official speciation profiles and increased on-road vehicle hot exhaust emissions as suggested by the SCAQS tunnel study [4], predicted ozone and RHC concentrations increase to match observed values more closely as shown in Table 4.5. Predicted NO_2 concentrations increase slightly. Detailed analysis of the various lumped organic compounds shown in Table 4.6 indicates that model performance generally improves, except for ethene and formaldehyde which become overpredicted.

Finally, when both the increased exhaust emissions and the revised emissions composition profiles are used simultaneously, the overprediction of ethene and formaldehyde concentrations is reduced. Concentrations of all other lumped organic species are predicted to within $\pm 30\%$ of observed values in this case. There is little change in predicted ozone and NO_2 concentrations compared to the calculations using scaled up exhaust emissions and

the official emission speciation profiles. Changes in predicted RHC concentrations using the revised versus official emission emission speciation profiles are similar to those found previously using the base case emission inventory.

Time series plots of observed and predicted concentrations for the entire 3-day period are shown in Figure 4.2 for the alkanes, in Figure 4.3 for ethene, and in Figure 4.4 for di- and trialkyl benzenes. Only model predictions based on the revised speciation profiles are shown. The monitoring sites shown in these figures represent a transect drawn from west to east across the air basin from Hawthorne at the coast through central Los Angeles to Claremont and Rubidoux inland. Similar trends in the comparisons between model predictions and observations are seen at the other 4 sites where speciated organics measurements were made (although measurements also were made at San Nicolas Island, this site lies outside of the modeling region and so comparisons with observations at this site were not possible). Nighttime model predictions at Long Beach are higher than the observed concentrations, because stable conditions and highly restricted vertical mixing were assumed by the model at night, while actual temperature soundings at night in this location show that the atmosphere was neutrally stratified, possibly due to urban heat island effects.

Predicted and observed concentrations of the lumped alkane species (see Figure 4.2) are the highest of all lumped organic species defined in the LCC mechanism. Concentrations tend to be underpredicted in all of the emission cases considered in this study, and the changes in model predictions are relatively small for the lumped alkane species when on-road vehicle exhaust emissions are scaled up. Ethene concentrations shown in Figure 4.3 show good agreement between the base case predictions and observations;

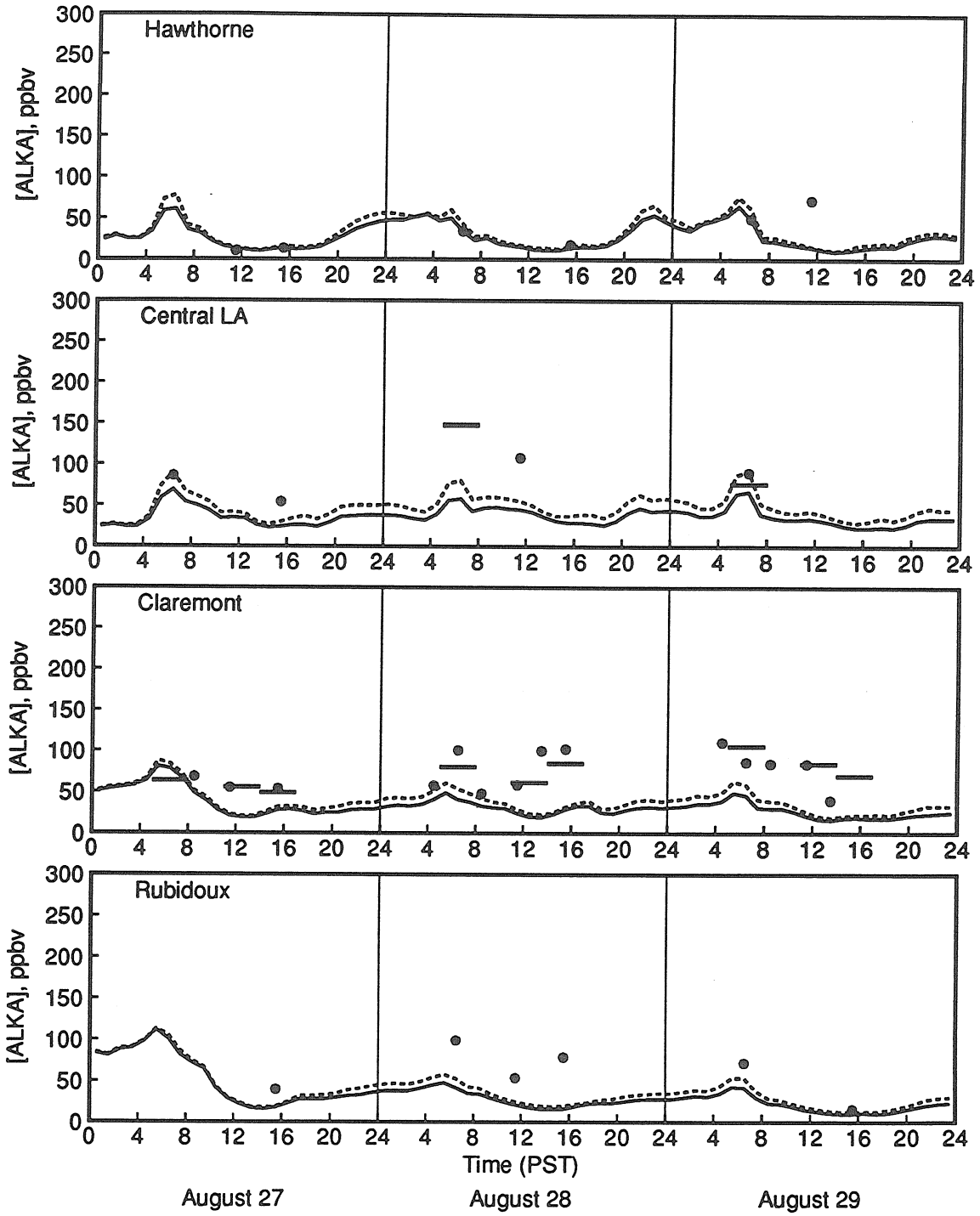

Figure 4.2: Time series plots of observed lumped alkane concentrations (measurements from data set #1 plotted as solid circles; 3-hour average samples from data set #2 plotted as horizontal bars) and model predictions for the base case (solid line) and for the case of increased on-road vehicle hot exhaust emissions (dashed line). Only results obtained using the respeciated VOC emission inventory are shown.

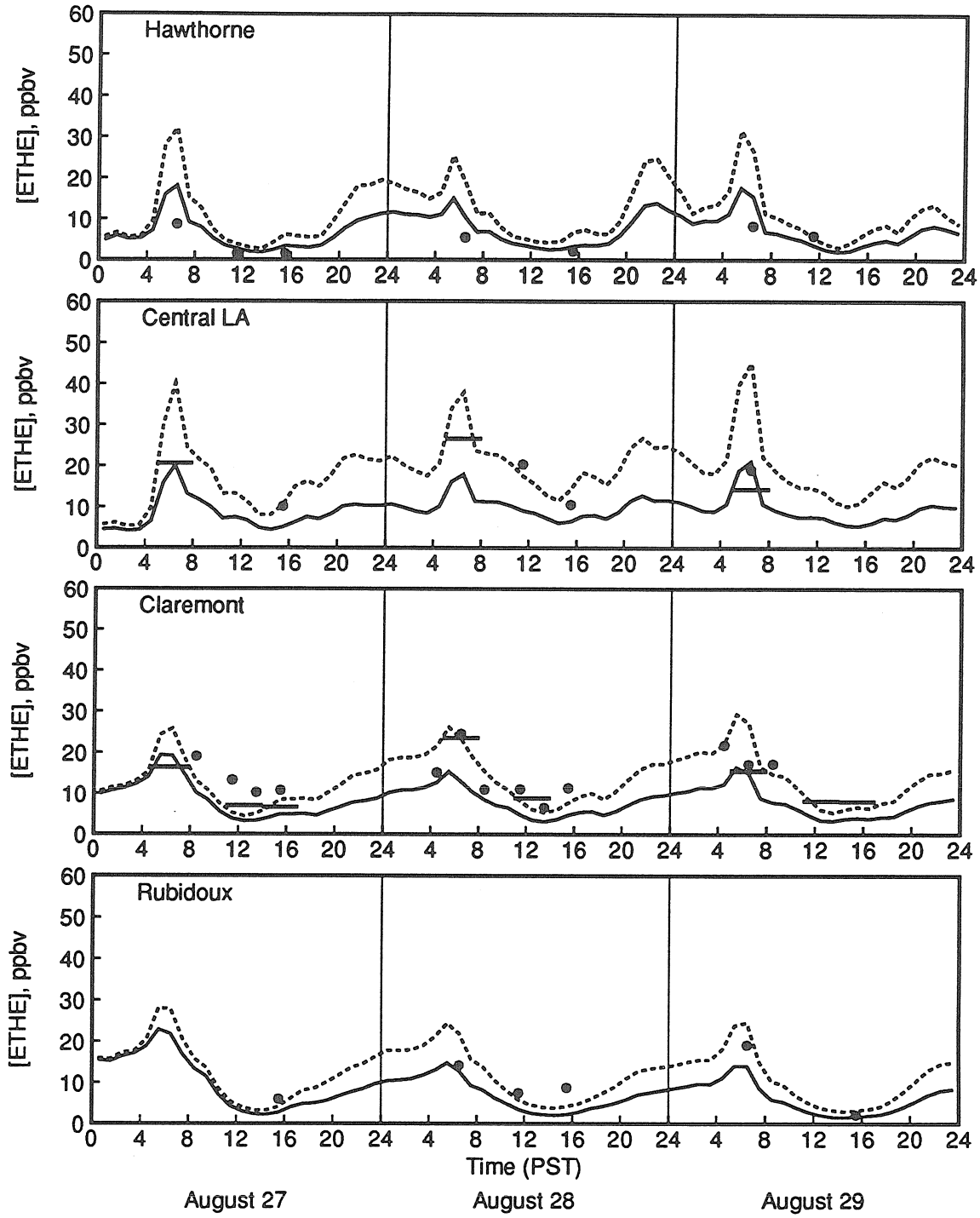

Figure 4.3: Time series plots of observed ethene concentrations (measurements from data set #1 plotted as solid circles; 3-hour average samples from data set #2 plotted as horizontal bars) and model predictions for the base case (solid line) and for the case of increased on-road vehicle hot exhaust emissions (dashed line). Only results obtained using the respeciated VOC emission inventory are shown.

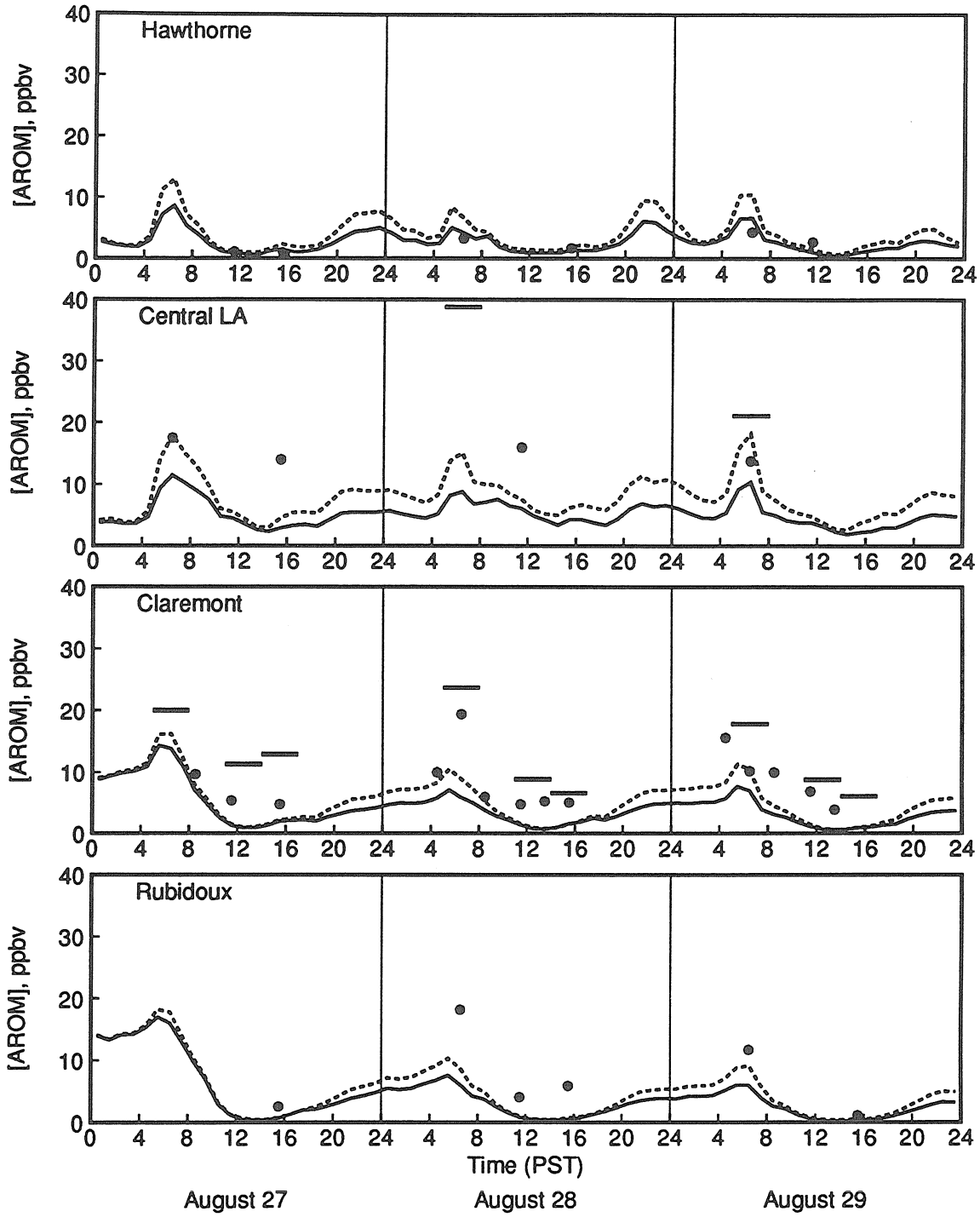

Figure 4.4: Time series plots of observed di/trialkyl benzene concentrations (measurements from data set #1 plotted as solid circles; 3-hour average samples from data set #2 plotted as horizontal bars) and model predictions for the base case (solid line) and for the case of increased on-road vehicle hot exhaust emissions (dashed line). Only results obtained using the respeciated VOC emission inventory are shown.

overpredictions are seen for the case of scaled up exhaust emissions. Both model predictions and observations show that peak ethene concentrations occur during the morning rush hour. The di- and trialkyl benzenes shown in Figure 4.4 also exhibit peaks in predicted and observed concentrations during the morning rush hour. Concentrations of this lumped species tend to be underpredicted in the base case calculation; the underpredictions are reduced when on-road vehicle exhaust emissions are scaled up. Concentrations of di- and trialkyl benzenes fall to very low values during the early to mid-afternoon hours.

Base case model predictions and observed formaldehyde concentrations are shown in Figure 4.5. The observed and predicted formaldehyde concentrations were higher at the inland sites. Only model results using the updated VOC emissions speciation profiles and the base case mass emissions are shown in this figure. Minor differences in model results for formaldehyde were found when the official emission inventory speciation profiles were used. The directly emitted component of total formaldehyde concentrations is also presented in Figure 4.5, based on model calculations using the extended chemical mechanism described previously. Inspection of Figure 4.5 shows that most of the atmospheric formaldehyde is formed by atmospheric reactions rather than being directly emitted. Similar behavior is seen throughout the land area included in the modeling region. The percentage contribution of direct emissions to total formaldehyde concentrations was found to increase overnight, and to reach a peak during the morning rush hour. The contribution of direct formaldehyde emissions becomes negligible during the late morning hours through late afternoon. The relative importance of direct formaldehyde emissions is predicted to be highest at the coastal (upwind)

sites.

Model predictions and observations for peroxyacetyl nitrate (PAN) are shown in Figure 4.6. The diurnal pattern and nighttime concentrations seen in the observed data are reproduced by the model. Predicted PAN concentrations agree approximately with observations at central LA and Rubidoux, but daytime peak concentrations are underpredicted at Claremont. The model predictions shown in Figure 4.6 were calculated using the respeciated VOC emission inventory. Predicted PAN concentrations were not significantly different when the official emission inventory speciation profiles were used.

4.6 Discussion

An important feature of the statistical analysis shown in Table 4.6 is that model performance varies from one lumped organic species to another. Therefore, attempts to compensate for possible bias in the VOC emission inventory by simply scaling up all emissions by a uniform factor will result in a chemical distribution of the emissions that does not match the speciation of the ambient data, even if the total mass of VOC emissions in the scaled up inventory is correct.

Use of the respeciated VOC emission inventory along with the base case mass emissions estimates resulted in improved model performance for di- and trialkyl benzenes, while large underpredictions for many of the remaining hydrocarbon classes still were observed. In some cases, model results for lumped organic species using the base case inventory indicated larger biases when the revised speciation profiles were used in place of the official profiles. However, since the total VOC mass emissions in the base case inventory are probably understated, it should not be concluded that the revised speciation

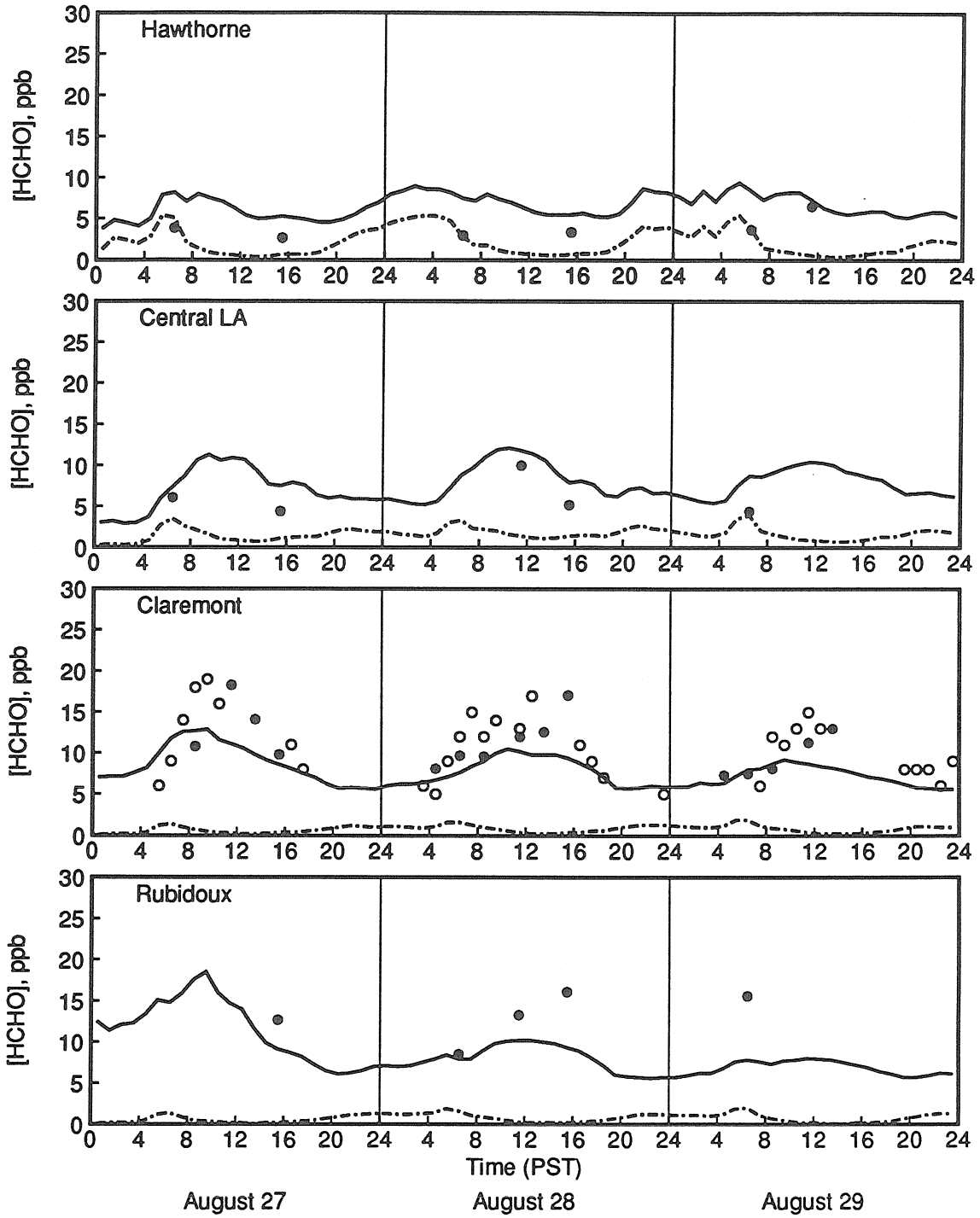

Figure 4.5: Time series plots of observed formaldehyde concentrations (plotted as solid circles (DNPH) and open circles (DOAS)) and model predictions using the base case emissions (solid line). The directly emitted component of predicted formaldehyde concentrations is also shown (dash-dotted line). Only the base case calculation using the respeciated VOC emission inventory is shown.

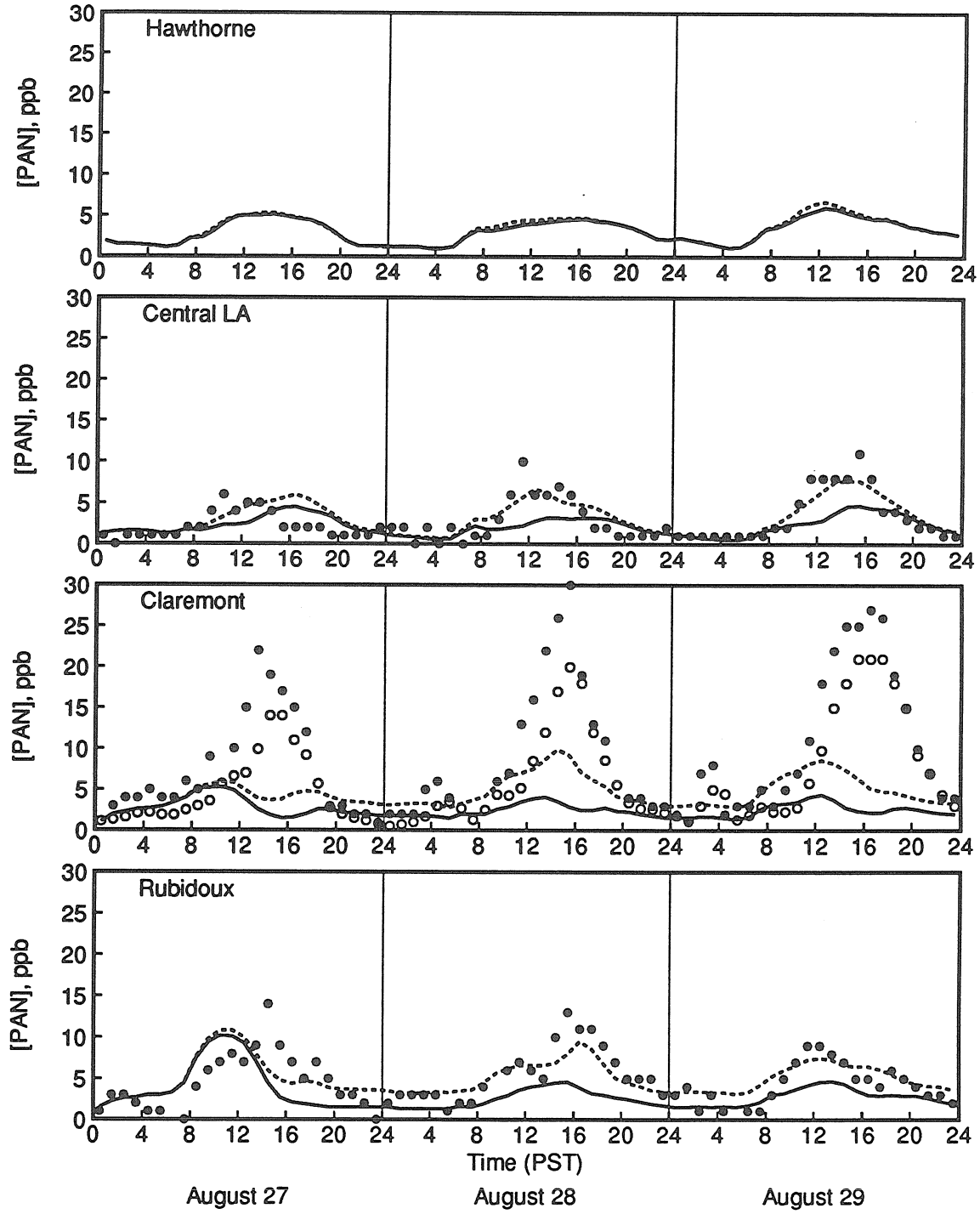

Figure 4.6: Time series plots of observed peroxyacetyl nitrate (PAN) concentrations (measurements reported by Williams and Grosjean [124] plotted as solid circles; measurements reported by Lonneman [60] at Claremont plotted as open circles) and model predictions for the base case (solid line) and for the case of increased on-road vehicle hot exhaust emissions (dashed line). Only results obtained using the respeciated VOC emission inventory are shown.

profiles are inferior to the official speciation profiles. In fact, when the on-road vehicle hot exhaust emissions were increased to reflect measured emission rates in the Van Nuys tunnel [4], use of the revised speciation profiles instead of the official inventory speciation resulted in better agreement with observed concentrations. Predicted ozone concentrations were sensitive to the change in VOC mass emissions, but not to the change in the chemical composition of VOC emissions. Similarly, predicted NO_2 concentrations were somewhat sensitive to the change in VOC mass emissions, but not to the changes in VOC emission speciation. However, the change in VOC chemical composition did result in significant changes in model performance for the lumped organic species.

For this summertime air pollution episode in the Los Angeles area, the contribution of direct emissions to total formaldehyde concentrations is less important than photochemical production of formaldehyde in the atmosphere. The contribution of direct formaldehyde emissions during the middle of the day is generally very small. This finding implies that programs to control atmospheric formaldehyde concentrations must focus not only on direct emission sources, but also on reducing photochemical production in the atmosphere. The contribution of direct formaldehyde emissions is likely to be more significant during winter months when the level of photochemical activity is lower.

Predicted PAN concentrations at the coastal and mid-basin sites (i.e., Long Beach and central Los Angeles) are close to observed values, but peak midday PAN concentrations at sites located further inland (i.e., Azusa, Burbank, and Claremont) are underpredicted by the model. Peak ozone concentrations are underpredicted at these sites as well, even after on-road vehicle

hot exhaust emissions to the model were increased. The underpredictions of PAN concentrations could be due to a combination of factors including inadequate photochemical production or understated emissions of acetaldehyde (a PAN precursor), or a general understatement of all organic gas emissions into the model. The LCC mechanism includes other PAN analogs in the predicted PAN concentrations, so, if anything, the underprediction of observed peak PAN concentrations is larger than the performance statistics suggest due to approximations in the LCC mechanism. In comparisons of predictions made using the LCC mechanism with results of smog chamber experiments, good agreement between measured and predicted ozone concentrations was found, but predictions of other secondary species such as PAN and formaldehyde were less accurate [11]. Therefore, a final possible explanation for differences between predicted and observed PAN concentrations in the present study is uncertainty in the LCC chemical mechanism itself.

4.7 Conclusions

The application of a model to predict the transport and chemical reactions of volatile organic compounds in the atmosphere has been described for the August 27–29 SCAQS episode. In the model, the many individual organics are aggregated into 11 lumped organic species classes. Model predictions have been compared with speciated organic gas concentration measurements made during SCAQS that have been lumped according to the same procedures used to lump organic gas emissions within the model.

For the base case calculation using the official State of California emission inventory and chemical speciation profiles, ethene, monoalkyl benzene and formaldehyde concentrations were predicted to within $\pm 10\%$ of observed

values, while the other lumped species concentrations tended to be underpredicted. The largest underpredictions were found for the di- and trialkyl benzenes, C_2^+ aldehydes, and PAN.

Introduction of updated VOC emission speciation profiles resulted in significant changes in model performance for the organics, while predicted ozone concentrations did not differ appreciably from those obtained using the VOC speciation profiles supplied by the government with the official emission inventory. Use of increased hot exhaust emissions from on-road vehicles approximating the actual emission rates measured in a Los Angeles area roadway tunnel [4,5] resulted in significant changes in the predicted concentrations of both lumped organics and ozone. Finally, the combined use of increased hot exhaust emissions and updated VOC speciation profiles resulted in the best model performance of the four emissions cases considered.

Model calculations indicate that during this summertime air pollution episode in the Los Angeles area, photochemical formation in the atmosphere is a more important source of formaldehyde than direct emissions, especially during the late morning and all afternoon hours. Therefore, any program to control formaldehyde concentrations in the Los Angeles atmosphere must consider photochemical formation pathways in addition to the control of direct emission sources.

5 Modeling individual VOCs

5.1 Introduction

In previous air quality models designed to predict ozone formation, individual organic species were typically lumped into a relatively small number of species classes on the basis of similarities in their chemical properties. For example, the lumped organic species defined in the LCC chemical mechanism [11] include C_4^+ alkanes, ethene, C_3^+ alkenes, monoalkyl benzenes, di- and trialkyl benzenes, formaldehyde, C_2^+ aldehydes, and ketones. This level of detail in the representation of the atmospheric chemistry of VOCs has proved adequate for the prediction of ozone formation, and advantageous computationally because the number of organic species that must be tracked is reduced substantially [11]. However, a much greater level of detail in the representation of individual VOCs is required if emissions to air quality relationships are to be assessed for individual toxic air pollutants, biogenic hydrocarbons, and tracer species unique to particular sources. Therefore, in the present study, a model is developed in which many individual organic species are represented explicitly. The model is tested using an extensive data base of speciated VOC concentration measurements acquired in the Los Angeles, California area during 1987.

5.2 Model description

The CIT airshed model is an Eulerian photochemical air quality model that predicts spatially and temporally resolved ambient pollutant concentrations given pollutant emission rates, meteorological conditions, and knowledge of the relevant chemical reactions taking place in the atmosphere. In Chapters 2 and 4, model predictions of ambient ozone and lumped organics concentrations have been presented, and comparisons have been made with measured pollutant concentrations for a 3-day period during the summer of 1987 in the Los Angeles area. The implementation of the LCC chemical mechanism [11] used in the CIT airshed model is such that flexible disaggregation of individual organic species from the lumped organic classes cannot be performed in an efficient manner. Therefore, an enhanced version of the model has been developed for use in the present study.

The chemical mechanism used in this study represents the reactions of 53 individual organic species explicitly. These species were chosen based on the availability of ambient concentration data and detailed emissions estimates, and the list of species can be expanded easily if desired. The 53 compounds treated explicitly in the present study account for approximately 75% of the total emissions of all non-methane volatile organic compounds in Los Angeles. In addition to the explicit species, there are 4 lumped alkane classes, 2 lumped olefins, and 3 lumped aromatics, a lumped aldehyde, and a lumped ketone species used to account for the remaining organic species that are not treated explicitly in the mechanism. This mechanism provides a much greater level of chemical resolution than is normally used to represent the organic species in chemical mechanisms intended for use in urban scale photochemical air quality models [11,12]. The chemical mechanism compiler of

Carter [126] is used to generate the necessary mechanism-dependent Fortran model subroutines and data files.

The explicit and lumped organic species tracked by the model and their corresponding hydroxyl radical reaction rate constants are shown in Table 5.1. Additional reactions of alkenes, aldehydes, and ketones included in the model are shown in Table 5.2. The mechanism also includes photolysis reactions for each of the aldehydes and ketones, as per Carter [29]. The oxidation product yields of the reactions listed in Tables 5.1 and 5.2, the subseqeuent reactions of the oxidation products, and reactions involving the inorganic species are as described by Carter [29]. The importance of the lumped organic species is greatly reduced because approximately 75% of the emissions of non-methane organics are treated explicitly in the detailed mechanism used in the present study. Although the details of the oxidation mechanism of many of the individual organic species represented in the model are uncertain, the rates of initial reaction with the hydroxyl radical are known [31]. Since the goal of this study is to predict the atmospheric concentrations of directly emitted organic species, the details of the oxidation mechanisms are not as important as the rate of the initial reactions that represent the first step in the atmospheric oxidation of directly emitted species.

As in earlier versions of the CIT model, the atmospheric diffusion equation governs the transport, reactions, emissions, and deposition of the chemical species represented in the model:

$$\frac{\partial C_i}{\partial t} + \nabla \cdot (\vec{u} C_i) = \nabla \cdot (K \nabla C_i) + R_i, \tag{5.1}$$

where C_i is the concentration of species i, $\vec{u}$ is the wind velocity, K is the eddy

Table 5.1: List of organic species represented in the detailed model

Species	Region-wide Emissions[a] (kmol/day)	k_{OH} at 300K (cm^3 $molec^{-1}$ s^{-1})	kinetic parameters[b] A	E_a (kcal/mol)	B
methane	53940	8.71E-15	6.255E-13	2.548	2
ethane	2294	2.74E-13	1.278E-12	0.918	2
acetylene	2735	7.82E-13	1.700E-12	0.463	0
propane	662	1.17E-12	1.350E-12	0.087	2
n-butane	1575	2.56E-12	1.359E-12	–0.378	2
n-pentane	652	4.11E-12	1.890E-12	–0.463	2
n-hexane	264	5.63E-12	1.350E-11	0.521	0
n-heptane	119	7.21E-12	1.960E-11	0.596	0
n-octane	41	8.76E-12	3.150E-11	0.763	0
n-nonane	86	1.03E-11	2.170E-11	0.447	0
isobutane	544	2.35E-12	9.360E-13	–0.550	2
isopentane	1107	3.95E-12	5.110E-12	0.154	0
2-methylpentane	338	5.66E-12	8.212E-12	0.222	0
3-methylpentane	242	5.76E-12	6.680E-12	0.088	0
2,2-dimethylbutane	65	2.36E-12	2.840E-11	1.484	0
2,3-dimethylbutane	170	5.50E-12	4.592E-12	–0.108	0
2-methylhexane	108	6.87E-12	1.066E-11	0.262	0
3-methylhexane	107	7.24E-12	9.337E-12	0.152	0
2,3-dimethylpentane	115	7.29E-12	6.194E-12	–0.097	0
2,4-dimethylpentane	100	6.92E-12	6.898E-12	–0.002	0
2,2,4-trimethylpentane	243	3.72E-12	1.610E-11	0.874	0
cyclopentane	63	5.19E-12	1.917E-12	–0.594	2
cyclohexane	50	7.54E-12	2.394E-12	–0.684	2
methylcyclopentane	169	8.10E-12	1.253E-11	0.260	0
methylcyclohexane	68	1.03E-11	1.337E-11	0.155	0

Table 5.1 (continued):

Species	Region-wide Emissions[a] (kmol/day)	k_{OH} at 300K (cm^3 $molec^{-1}$ s^{-1})	kinetic parameters[b] A	E_a (kcal/mol)	B
benzene	665	1.28E-12	2.500E-12	0.397	0
toluene	1562	5.91E-12	1.810E-12	–0.705	0
ethylbenzene	154	7.10E-12	7.100E-12	0.000	0
isopropylbenzene	19	6.50E-12	6.500E-12	0.000	0
n-propylbenzene	67	6.00E-12	6.000E-12	0.000	0
m-xylene	411	2.36E-11	2.360E-11	0.000	0
o-xylene	353	1.37E-11	1.370E-11	0.000	0
p-xylene	331	1.43E-11	1.430E-11	0.000	0
1,3,5-trimethylbenzene	98	5.75E-11	5.750E-11	0.000	0
1,2,3-trimethylbenzene	30	3.27E-11	3.270E-11	0.000	0
1,2,4-trimethylbenzene	208	3.25E-11	3.250E-11	0.000	0
ethene	3911	8.43E-12	1.960E-12	–0.870	0
propene	1099	2.60E-11	4.850E-12	–1.001	0
1-butene	193	1.38E-12	6.550E-12	0.928	0
trans-2-butene	116	6.30E-11	1.010E-11	–1.091	0
cis-2-butene	104	5.58E-11	1.100E-11	–0.968	0
isobutene	220	5.09E-11	9.470E-12	–1.002	0
1,3-butadiene	170	6.59E-11	1.480E-11	–0.890	0
styrene	19	5.73E-11	1.070E-11	–1.000	0
isoprene	767	9.97E-11	2.540E-11	–0.815	0
α-pinene	354	5.31E-11	1.210E-11	–0.882	0
β-pinene	80	7.82E-11	2.380E-11	–0.709	0
1,1,1-trichloroethane[c]	351	1.23E-14	3.100E-12	3.299	0
perchloroethylene[c]	169	1.72E-13	9.400E-12	2.385	0
formaldehyde	968	9.80E-12	1.130E-12	–1.288	2

Table 5.1 (continued):

Species	Region-wide Emissions[a] (kmol/day)	k_{OH} at 300K (cm^3 $molec^{-1}$ s^{-1})	kinetic parameters[b] A	E_a (kcal/mol)	B
acetaldehyde	207	1.56E-11	5.550E-12	–0.618	0
benzaldehyde	37	1.29E-11	1.290E-11	0.000	0
acetone	350	2.31E-13	1.920E-13	–0.110	2
Total explicit species	24930				
Lumped alkane 1[d]	150	1.93E-12			
Lumped alkane 2[d]	2074	4.38E-12			
Lumped alkane 3[d]	1191	9.20E-12			
Lumped alkane 4[d]	2339	1.50E-11			
Lumped aromatic 1[d]	64	6.14E-12			
Lumped aromatic 2[d]	327	2.31E-11			
Lumped aromatic 3[d]	86	5.08E-11			
Lumped olefin 1[d]	375	3.48E-11			
Lumped olefin 2[d]	720	6.87E-11			
Lumped aldehyde	172	1.97E-11	8.500E-12	–0.500	0
Lumped ketone	628	1.16E-12	2.920E-13	–0.823	2
Total lumped species	8126				

[a]Region-wide emissions on August 27, 1987 from all sources combined, using three times the baseline on-road vehicle hot exhaust emissions of carbon monoxide and VOC, and the revised chemical composition profiles of Chapter 2. The inventory region includes most of the mapped area shown in Figure 5.1, which extends beyond the South Coast Air Basin into Ventura County and the Southeast Desert Air Basin.

[b]As per Carter [29,127]. The rate constant is computed from the kinetic parameters using the expression $k = A \exp(-E_a/RT) \times (T/300)^B$ using R=0.0019872 kcal mol^{-1} K^{-1}.

[c]Kinetic parameters for 1,1,1-trichloroethane and perchloroethylene are from Atkinson et al. [128].

[d]Individual compounds are assigned according to their hydroxyl radical reactivities. The reaction rate constants and oxidation product yields of the lumped species (except for the aldehydes and ketones) are computed based on a weighted average of the properties of individual species assigned to the lumped class, as per Carter [29]. Propionaldehyde and methyl ethyl ketone are used as surrogate species to represent the chemistry of the lumped aldehyde and lumped ketone species.

Table 5.2: Additional reactions of organic species included in the model

Reaction	k at 300K (cm^3 $molec^{-1}$ s^{-1})	kinetic parameters[a] A (cm^3 $molec^{-1}$ s^{-1})	E_a (kcal/mol)
ethene + O3	1.87E-18	1.200E-14	5.226
ethene + NO3	2.15E-16	5.430E-12	6.043
ethene + O	7.42E-13	1.040E-11	1.574
propene + O3	1.19E-17	1.320E-14	4.182
propene + NO3	9.80E-15	4.850E-12	3.699
propene + O	4.01E-12	1.180E-11	0.644
1-butene + O3	1.15E-17	3.460E-15	3.403
1-butene + NO3	1.30E-14	6.550E-12	3.708
1-butene + O	4.22E-12	1.250E-11	0.648
trans-2-butene + O3	2.06E-16	9.080E-15	2.258
trans-2-butene + NO3	3.92E-13	1.098E-13	–0.759
trans-2-butene + O	2.34E-11	2.260E-11	–0.020
cis-2-butene + O3	1.33E-16	3.520E-15	1.953
cis-2-butene + NO3	3.47E-13	9.710E-14	–0.759
cis-2-butene + O	1.79E-11	1.210E-11	–0.235
isobutene + O3	1.26E-17	3.550E-15	3.364
isobutene + NO3	3.40E-13	9.470E-12	1.984
isobutene + O	1.53E-11	1.760E-11	0.085
1,3-butadiene + O3	7.93E-18	3.300E-14	4.968
1,3-butadiene + NO3	1.03E-13	1.480E-11	2.959
1,3-butadiene + O	2.10E-11	2.100E-11	0.000
styrene + O3	1.77E-17	3.460E-15	3.144
styrene + NO3	1.55E-13	6.550E-12	2.233
styrene + O	1.79E-11	1.210E-11	–0.235

Table 5.2 (continued):

Reaction	k at 300K (cm^3 $molec^{-1}$ s^{-1})	kinetic parameters[a] A (cm^3 $molec^{-1}$ s^{-1})	E_a (kcal/mol)
isoprene + O3	1.50E-17	1.230E-14	4.000
isoprene + NO3	6.85E-13	3.030E-12	0.886
isoprene + O	6.00E-11	6.000E-11	0.000
α-pinene + O3	1.00E-16	9.900E-16	1.366
α-pinene + NO3	6.10E-12	1.190E-12	–0.974
α-pinene + O	3.00E-11	3.000E-11	0.000
β-pinene + O3	1.69E-17	3.550E-15	3.187
β-pinene + NO3	2.51E-12	2.510E-12	0.000
β-pinene + O	2.80E-11	2.800E-11	0.000
lumped olefin 1 + O3	1.24E-17[b]		
lumped olefin 1 + NO3	1.37E-14[b]		
lumped olefin 1 + O	4.28E-12[b]		
lumped olefin 2 + O3	2.66E-16[b]		
lumped olefin 2 + NO3	2.54E-12[b]		
lumped olefin 2 + O	2.84E-11[b]		
formaldehyde + HO2	7.79E-14	9.700E-15	–1.242
formaldehyde + NO3	6.38E-16	2.800E-12	5.000
acetaldehyde + NO3	2.84E-15	1.400E-12	3.696
benzaldehyde + NO3	2.61E-15	1.400E-12	3.747
lumped aldehyde + NO3	2.84E-15	1.400E-12	3.696

[a] As per Carter [29,127]. The rate constant is computed from the kinetic parameters using the expression $k = A \exp(-E_a/RT) \times (T/300)^B$ using R=0.0019872 kcal mol^{-1} K^{-1}. B=0 in all cases except for the reaction of trans-2-butene with NO3 where B=2.

[b] The reaction rate constants and oxidation product yields of the lumped species (except for the aldehydes and ketones) are computed based on a weighted average of the properties of individual species assigned to the lumped class, as per Carter [29].

diffusivity tensor (assumed to be diagonal), and R_i is the rate of formation of species i by chemical reactions. Because of the high level of chemical detail used to represent the organic species in the present model, the final equation set obtained by writing equation (5.1) repeatedly for each species tracked by the model is much larger than has been attempted in previous airshed modeling studies, and consists of 96 simultaneous differential equations.

To provide a mathematically complete specification of the problem, boundary conditions and initial conditions are needed. Both lateral boundary conditions and initial conditions are established using measured pollutant concentrations. Boundary conditions also must be specified at ground level and at the top of the modeling region. In the CIT model, the upward flux of each pollutant at ground level is equal to direct emissions minus the dry deposition flux. A no-flux condition is enforced at the top of the modeling region for each species.

The parameterization of dry deposition fluxes used in this study follows the general approach used elsewhere [24]. In brief, the model computes dry deposition velocities in each grid square using local meteorological conditions and surface characteristics specific to 32 different land use types that have been mapped by the United States Geological Survey. Resistances to dry deposition due to turbulent transport in the atmospheric boundary layer (r_a) and diffusion in a laminar sublayer next to the surface (r_b) are computed first. Then these resistances are combined with surface resistance terms (r_s^i) to account for differing rates of pollutant uptake at surfaces:

$$v_g^i = \frac{1}{r_a + r_b + r_s^i} \tag{5.2}$$

to compute the deposition velocity for a particular pollutant (v_g^i). The sur-

face resistance value used for all of the hydrocarbons and ketones in this study is 50 s/cm [24]. If deposition velocities are limited to this extent, then atmospheric chemical reactions will be the major removal process for these species. Surface resistance values for the aldehydes are specified relative to the values used for SO_2 [129]. For formaldehyde, the surface resistances are set at half the corresponding values for SO_2, while for acetaldehyde and higher aldehydes, the surface resistances are set at twice the values for SO_2 [24,129].

5.3 Ambient organics data

As part of the Southern California Air Quality Study (SCAQS; for an overview see Lawson [16]), ambient VOC samples were collected at a network of 9 monitoring sites shown in Figure 5.1 on selected days during the summer and fall of 1987. The samples were stored in stainless steel canisters [113], and then analyzed by gas chromatography and gas chromatography/mass spectrometry [57,114]. Additional air sampling over the same network of 9 sites was performed using 2,4-dinitrophenylhydrazine (DNPH) impregnated cartridges to determine ambient concentrations of aldehydes and ketones [113,119]. Three samples per day were collected over 1-hour sampling intervals at each of the monitoring sites, beginning at 0600, 1100 and 1500 hours PST. Additional samples were collected each day at the Claremont and Long Beach monitoring sites beginning at 0400, 0800, and 1300 hours PST. The above data were consolidated into a single data base and further analyzed by Lurmann and Main [120]. This consolidated set of data will be referred to as data set #1.

The precision of the measured concentration data included in data set #1 has been estimated from analyses of replicate samples. For the hydro-

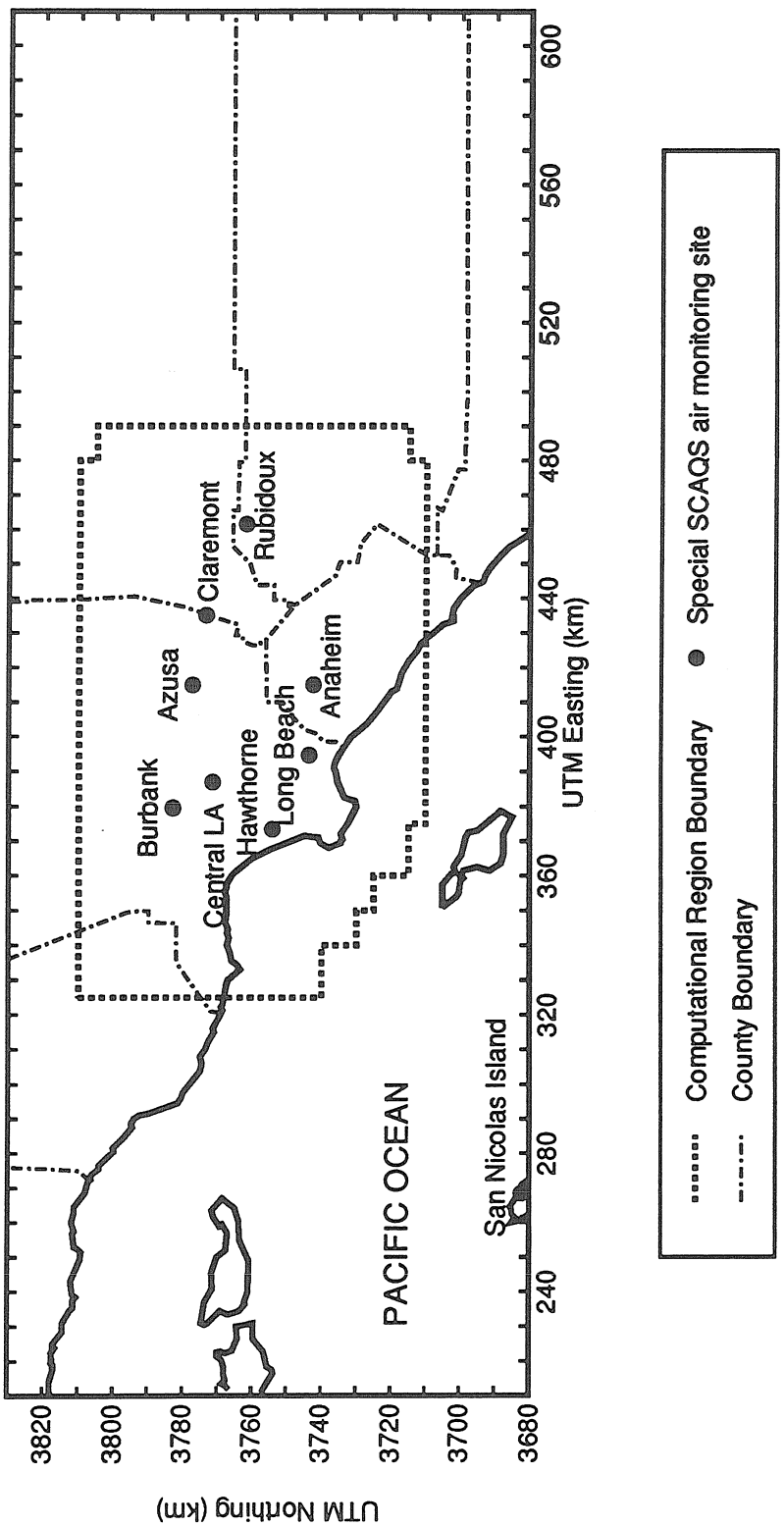

Figure 5.1: Map of the Los Angeles, California area showing the computational region and the locations of special SCAQS air quality monitoring sites.

carbons, the precision was found to be better than ±10% for species with concentrations exceeding 5 parts per billion carbon (ppbC). At lower measured concentrations, the uncertainties increased to as much as ±35% for some species [57]. The effect of storing ambient air samples in stainless steel canisters for extended periods of time (up to 12 weeks) before analysis also has been examined [57]. The concentrations of most species remained stable over time, except for styrene, isoprene and a C_9 aromatic compound; these species were sometimes depleted in later reanalyses of selected samples. This is important because many of the canister samples collected during SCAQS were not analyzed immediately, and therefore the actual concentrations of a few of the most reactive compounds may be understated in data set #1. The precision of the measured carbonyl data was found to be ±8.7% for formaldehyde and ±9.9% for acetaldehyde [119].

Independent speciated non-methane hydrocarbon measurements were made at three sites during the summer of 1987 by Lonneman et al. [60]. Three samples per day were collected at Claremont, beginning at 0500, 1100, and 1400 hours PST. Additional early morning samples were collected each day at the Central Los Angeles and Long Beach monitoring sites beginning at 0500 hours PST. These samples also were collected in stainless steel canisters, but over three-hour sampling intervals instead of the 1-hour intervals used for other measurements described previously. The samples were analyzed by gas chromatography. These measurements will be referred to as data set #2. The measured hydrocarbon concentrations in data set #2 were found to agree reasonably well with measurements from data set #1, given that sample averaging times differ (see Chapter 4 for further details). The only exception during the August 27–29 SCAQS epsiode was that two very low

measured values of 1,3-butadiene are reported in data set #2 that do not agree with the higher values indicated in data set #1.

The extensive data sets described above provide the basis for comparison of model predictions with speciated ambient organic species concentrations, as will be discussed later in section 5.5.

5.4 Model application

Application of the CIT airshed model is now described for a summertime intensive monitoring period of the Southern California Air Quality Study (SCAQS). The particular episode considered is August 27–28, 1987. The main advantages to using this episode include the availability of speciated organic gas concentration measurements for all of the sites shown in Figure 5.1, and the existence of an extensive data base of ground-level and upper air meteorological measurements.

A regular 5 by 5 kilometer grid system has been superimposed on the modeling region shown in Figure 5.1, and meteorological and emissions data are specified as inputs to the model for each grid square and at each hour, as described in previous chapters. The modeling region extends to 1100 meters above ground level, with five computational layers in the vertical direction. Because of the greatly expanded level of detail in the chemical mechanism and the resulting increase in the size of equation set (5.1), the computational region used in the present study is smaller than that used in previous applications of the CIT airshed model to this episode (as described in Chapters 2 and 4). This results in a significant speedup to the overall calculation through a reduction in the number of computational cells. This was achieved by eliminating cells at the edges of the modeling region, mostly

downwind in Ventura County to the northwest, and in the Coachella Valley at the far eastern edge of the modeling region. These areas were orginally added to the computational region to assess the rate of transport of pollutants from the South Coast air basin to these neighboring areas. Elimination of the outlying areas from the computational region does not change the predicted pollutant concentrations within the remaining region shown in Figure 5.1, although model predictions are no longer available for the areas that have been eliminated. The computational region used here is comparable in spatial extent to the region used in earlier photochemical modeling studies [20,21].

Boundary condition values used in the present study are shown in Table 5.3. These values are based on measured pollutant concentrations upwind of the modeling region over the Pacific Ocean [56]. Initial conditions are set using measured pollutant concentrations at the appropriate hour. Downwind boundary values are determined by the concentrations in the predicted flux out of the modeling region. When inflow boundary conditions are required for the northern or eastern edge of the modeling region, those values are based on interpolated values using measurements from nearby air quality monitoring sites at each hour. When total non-methane hydrocarbons (NMHC) are used to help establish initial or boundary conditions, they are speciated using the average summertime NMHC composition measured during SCAQS, as per Table 5–5 of Lurmann and Main [120]. This breakdown of NMHC into individual species tracked in the model is shown in Table 5.4.

The CIT airshed model also requires emissions data with spatial resolution matching the computational grid (5 by 5 kilometer squares in this case), and hourly temporal resolution. High-resolution emission inventories of this type have been prepared by the California Air Resources Board (CARB) and

Table 5.3: Upwind boundary condition values over the ocean[a]

Species	Boundary Condition (ppbv)
CO	200
NO2	1
NO	1
methane	1700
NMHC	100
formaldehyde	3
acetaldehyde	5
acetone	4
O3	40

[a]Based on measurements made at San Nicolas Island and by aircraft flights over the ocean [56,120].

Table 5.4: Non-methane hydrocarbon speciation[a]

Species	Relative Composition of NMHC (ppbv/ppmC)
ethane	21.0
acetylene	13.8
propane	25.0
n-butane	14.3
n-pentane	6.9
n-hexane	2.7
n-heptane	1.3
isobutane	6.5
isopentane	14.5
2-methylpentane	3.6
3-methylpentane	3.1
2,2-dimethylbutane	0.2
2,3-dimethylbutane	1.0
2-methylhexane	1.4
3-methylhexane	1.4
2,4-dimethylpentane	1.4
2,3-dimethylpentane	1.4
2,2,4-trimethylpentane	1.5
cyclopentane	0.8
methylcyclopentane	2.6
cyclohexane	0.7
methylcyclohexane	1.5
ethene	19.4
propene	5.2
1-butene	0.8

Table 5.4 (continued):

Species	Relative Composition of NMHC (ppbv/ppmC)
trans-2-butene	0.4
cis-2-butene	0.4
isobutene	0.8
1,3-butadiene	0.6
isoprene	0.5
benzene	4.3
toluene	10.4
ethylbenzene	1.5
isopropylbenzene	0.1
n-propylbenzene	0.1
m- + p-xylene	5.6
o-xylene	2.2
1,3,5-trimethylbenzene	1.2
1,2,4-trimethylbenzene	1.2
styrene	0.6
lumped alkane 1	0.0
lumped alkane 2	0.0
lumped alkane 3	4.2
lumped alkane 4	13.8
lumped aromatic 1	1.3
lumped aromatic 2	5.0
lumped aromatic 3	1.3
lumped olefin 1	0.8
lumped olefin 2	1.9

[a]Based on average non-methane hydrocarbon composition measured during SCAQS [120].

the South Coast Air Quality Management District (SCAQMD). The mobile source mass emission rates were calculated by CARB using the EMFAC 7E emission factor model and typical weekday traffic patterns. Stationary source and biogenic emission estimates were prepared by the SCAQMD. This emission inventory [41] provides the starting point for the emission inventory used in the present study. The inventory specifies separate mass emission rates for carbon monoxide, oxides of nitrogen, oxides of sulfur, volatile organic compounds (VOC), and particulate matter for over 800 different source types.

Several recent studies have concluded that the official emission inventory understates the mobile source emissions of carbon monoxide and VOC [1,4,5,6]. Therefore, to correct at least some of the negative bias in the official emission inventory, we have increased the hot exhaust emissions of CO and VOC from on-road vehicles to three times the baseline values, as suggested by local measurements of actual on-road vehicle emission rates in the Van Nuys tunnel during SCAQS [4]. This change represents an increase of 5800 tons/day in CO emissions above the baseline inventory, and an increase of 670 tons/day in VOC emissions. In a previous photochemical modeling study using the LCC lumped chemical mechanism [11] and the same meteorological and emissions data as used here, it was found that the best agreement between model predictions and observations for both ozone and the lumped hydrocarbon species defined in the LCC mechanism was obtained when this scaled up on-road vehicle hot exhaust emissions inventory was used (see Chapter 4). However, even after this increase in hot exhaust emissions, it is possible that there are additional pollutant emissions still missing from the inventory (e.g., cold start emissions; running loss, hot soak, and diurnal evaporative emissions; stationary source emissions; biogenic emissions).

The total VOC mass emissions from individual sources are speciated using a set of 225 chemical composition profiles. The composition profiles supplied with the official inventory have been reviewed and updated as described in Chapter 3. New profiles have been introduced for catalyst-equipped and non-catalyst light duty vehicle engine exhaust, for whole (liquid) gasoline and gasoline headspace vapors, and for various surface coating solvent emissions. Further changes were made to the speciated VOC emission inventory by reassigning individual emission sources to new composition profiles. For example, solvent emissions occurring cleaning and priming of vehicles prior to repainting were reassigned from a catch-all 'species unknown' profile to a composite industrial surface coating profile. When compared to the official VOC emission inventory, the most significant changes in the respeciated inventory are seen at the level of individual chemical compounds. Because the focus of the present study is on individual organic species, these improvements to VOC emission speciation represent an important correction to the emission inventory being used here. A summary of the region-wide emission estimates for each emitted organic species tracked in the model is presented in Table 5.1.

5.5 Results

A statistical analysis of model predictions for each of the individual organic species is presented in Table 5.5 using the observations from data set #1 on August 28 as the basis for comparison. Note that the individual species are listed in order of descending average ambient concentration. The model predicts the concentrations of all but 7 individual species with a normalized bias of 50% or less, as shown in Table 5.5. Both observed concentrations and

model predictions for many species reach peak values during the morning rush hour while the level of photochemical activity is still low.

The mean normalized biases for most of the aromatic hydrocarbons, including benzene, toluene, ethylbenzene, m/p-xylene, and o-xylene are within ±20%. This represents almost all of the aromatics that were included in data set #1. The model underpredicts the concentrations of two other aromatics that are listed in Table 5.5 (i.e., 1,2,4-trimethylbenzene and n-propylbenzene). Time series plots for toluene are presented in Figure 5.2. The monitoring sites shown in these Figures represent a cross section drawn across the air basin beginning at the coast (Hawthorne), and proceeding inland through central Los Angeles to Claremont and Rubidoux farther to the east. The model overpredicts the nighttime concentrations of many of the individual organic species at the Long Beach monitoring site, but this probably occurs because the model does not follow the upper air sounding data for this area which shows no stably stratified layer near the ground at night.

There are numerous alkanes for which ambient concentration data are available for this episode. An example of model performance for one such alkane (2,3-dimethylpentane) is shown in Figure 5.3. As indicated in Table 5.5, the predicted concentrations of most alkanes tend to be lower than the observed values.

There are not as many alkenes as there are alkanes in the ambient data sets, and measured concentrations of alkenes with 4 or more carbon atoms (except the combination of 1-butene and isobutene) are below 4 ppbC for this episode. Predicted concentrations for these alkenes are in the same range of low values. Model predictions and observations for propene are presented in Figure 5.4.

Table 5.5: Analysis of model performance for individual organic species[a]

Species	Average Ambient Conc. (ppbC)	Bias[b] (ppbC)	Bias[b] (%)	Gross Error[c] (ppbC)	Gross Error[c] (%)
methane	2245.7	−228.6	−9	326.8	14
propane	73.4	−51.0	−66	55.4	70
isopentane	67.9	−36.0	−44	39.0	51
toluene	60.7	−10.3	+2	21.8	38
n-butane	57.3	−15.2	−16	31.5	48
ethane	34.2	−6.2	−5	16.0	44
n-pentane	31.0	−7.2	−18	18.8	53
m/p-xylene	29.3	−8.5	−13	12.0	38
acetone	27.4	−2.3	+17	8.7	46
ethene	26.0	+5.7	+41	10.4	52
isobutane	23.6	−4.3	−10	13.2	50
benzene	21.6	−0.6	+17	6.9	41
2-methylpentane	20.5	−10.2	−41	11.0	49
acetylene	20.4	+7.9	+63	9.9	67
acetaldehyde	19.0	−3.7	−2	6.5	37
3-methylpentane	14.1	−6.4	−38	7.5	49
n-hexane	13.6	−3.7	−18	8.1	55
methylcyclopentane	11.8	−6.9	−22	7.7	83
o-xylene	11.5	−1.0	+9	4.1	41
formaldehyde	11.0	+0.7	+22	3.0	37
iso-octane	10.8	−1.0	+12	4.7	48
3-methylhexane	10.2	−6.3	−54	6.7	60
1,2,4-trimethylbenzene	10.1	−4.4	−32	5.4	49
methylcyclohexane	10.0	−7.7	−68	7.8	69

Table 5.5 (continued):

Species	Average Ambient Conc. (ppbC)	Bias[b] (ppbC)	Bias[b] (%)	Gross Error[c] (ppbC)	Gross Error[c] (%)
propene	9.5	0.0	+24	4.8	55
ethylbenzene	9.2	-3.4	-22	4.3	47
n-heptane	8.2	-3.3	-19	5.3	55
1,1,1-trichloroethane	8.1	-4.6	-41	4.8	53
2-methylhexane	7.5	-3.6	+4	4.4	90
2,3-dimethylpentane	5.8	-1.8	-16	2.8	48
2,3-dimethylbutane	5.3	-0.2	+10	2.2	44
styrene	4.8	-4.2	-85	4.2	85
1-butene	4.5	-0.6	+8	2.2	50
cyclohexane	4.2	-2.7	-54	2.8	58
2,4-dimethylpentane	4.1	-0.4	+16	1.9	56
n-octane	3.8	-2.1	-40	2.7	59
cyclopentane	3.6	-2.0	-47	2.1	54
n-nonane	2.4	+0.5	+42	1.2	61
n-propylbenzene	2.2	+0.5	+50	1.0	63
isoprene	1.6	-1.0	-38	1.0	59
2,2-dimethylbutane	1.4	+0.4	+38	0.5	45
1,3-butadiene	1.2	+0.3	+54	0.7	79
cis-2-butene	1.0	-0.2	+1	0.6	65
trans-2-butene	1.0	-0.3	-2	0.7	75

[a]Using all valid measured concentrations from data set #1 on August 28. A total of 26 samples were available for this day at the sites shown in Figure 5.1 (does not include samples from San Nicolas Island which is located outside of the modeling region).
[b]Bias is defined as the mean residual (predicted minus observed) concentration. The percent bias statistic is computed by normalizing each residual to the corresponding observed concentration before averaging.
[c]Gross error is defined as the mean absolute value of the residuals.

Acetylene and ethene are interesting species because they provide tracers for engine exhaust emissions: they are formed during combustion, but are not present in unburned gasoline or diesel fuel. As shown in Figure 5.5, predicted acetylene concentrations exceed measured values somewhat, as is also the case for ethene.

Peak observed and predicted concentrations of the species shown in Figures 5.2–5.5 occur during the morning rush hours. The lowest concentrations are seen in the afternoon from 1200–1600 hours PST. Similar behavior is seen for most of the other hydrocarbons tracked in the model. This is not the case for oxygenated compounds (i.e., aldehydes and ketones) which generally reach their highest concentrations in the afternoon.

Isoprene is the only biogenic hydrocarbon that was observed during SCAQS [120]. Predicted isoprene concentrations at most sites are in agreement with low observed values of no more than 2 ppbC. However, higher ambient isoprene concentrations of up to 6 ppbC were observed at Claremont. Given the high reactivity of isoprene, this suggests that local isoprene emissions near Claremont must have been much higher than was typical elsewhere in other urban portions of the air basin. The model underpredicts both isoprene and ozone concentrations at this site. Time series plots for isoprene are presented in Figure 5.6. Note that the highest observed isoprene concentrations at Claremont are seen in the afternoon.

Ozone concentrations predicted using the detailed chemical mechanism of the present study are very similar to predictions obtained for the same episode using the LCC lumped chemical mechanism [11] and the same overall VOC mass emissions described in Chapter 2. In the present study, the mean normalized bias in predicted ozone concentrations is -9% using the in-

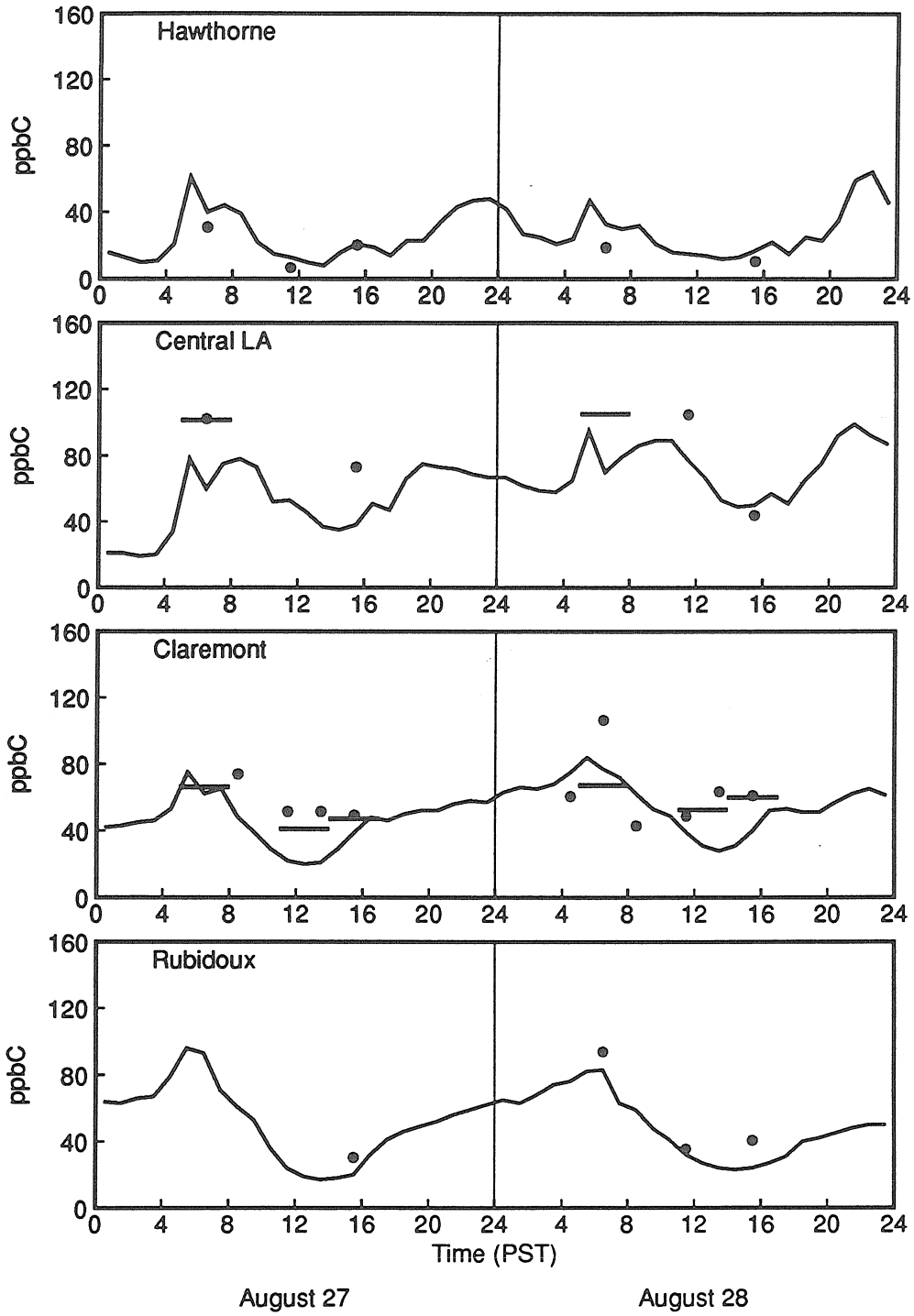

Figure 5.2: Time series plots of observed toluene concentrations (plotted as circles for data set #1 and horizontal bars for data set #2) and model predictions (solid line).

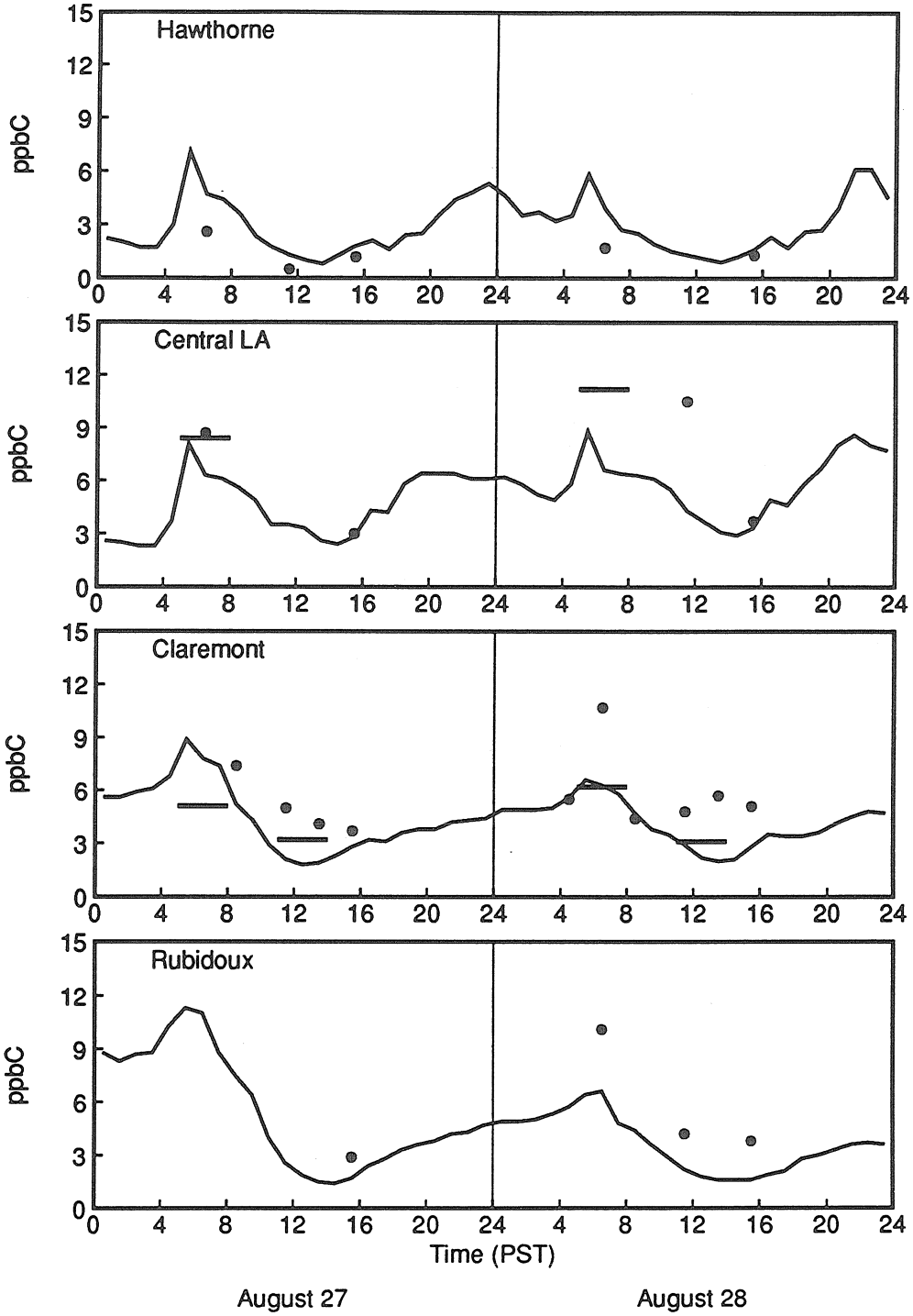

Figure 5.3: Time series plots of observed 2,3-dimethylpentane concentrations (plotted as circles for data set #1 and horizontal bars for data set #2) and model predictions (solid line).

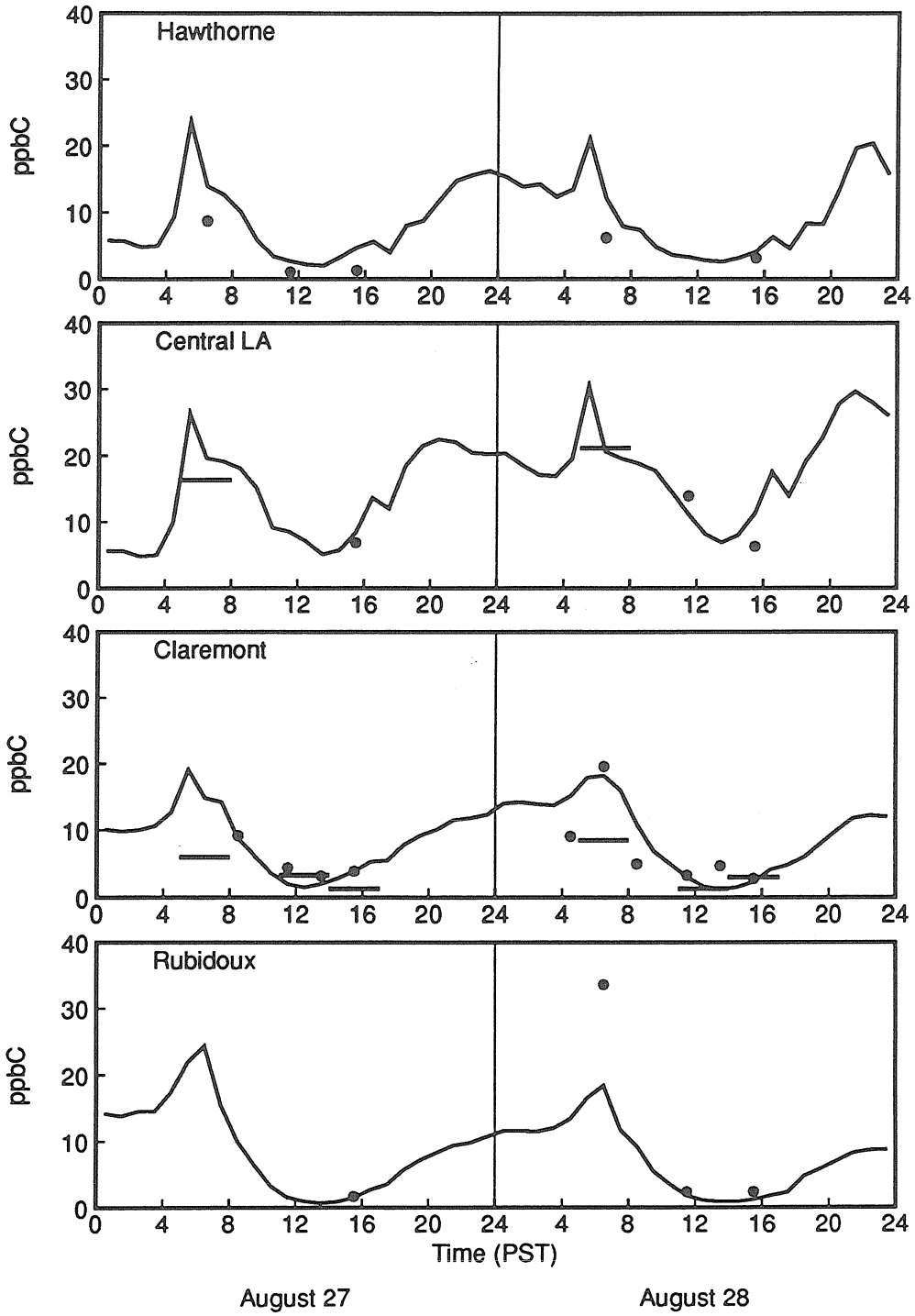

Figure 5.4: Time series plots of observed propene concentrations (plotted as circles for data set #1 and horizontal bars for data set #2) and model predictions (solid line).

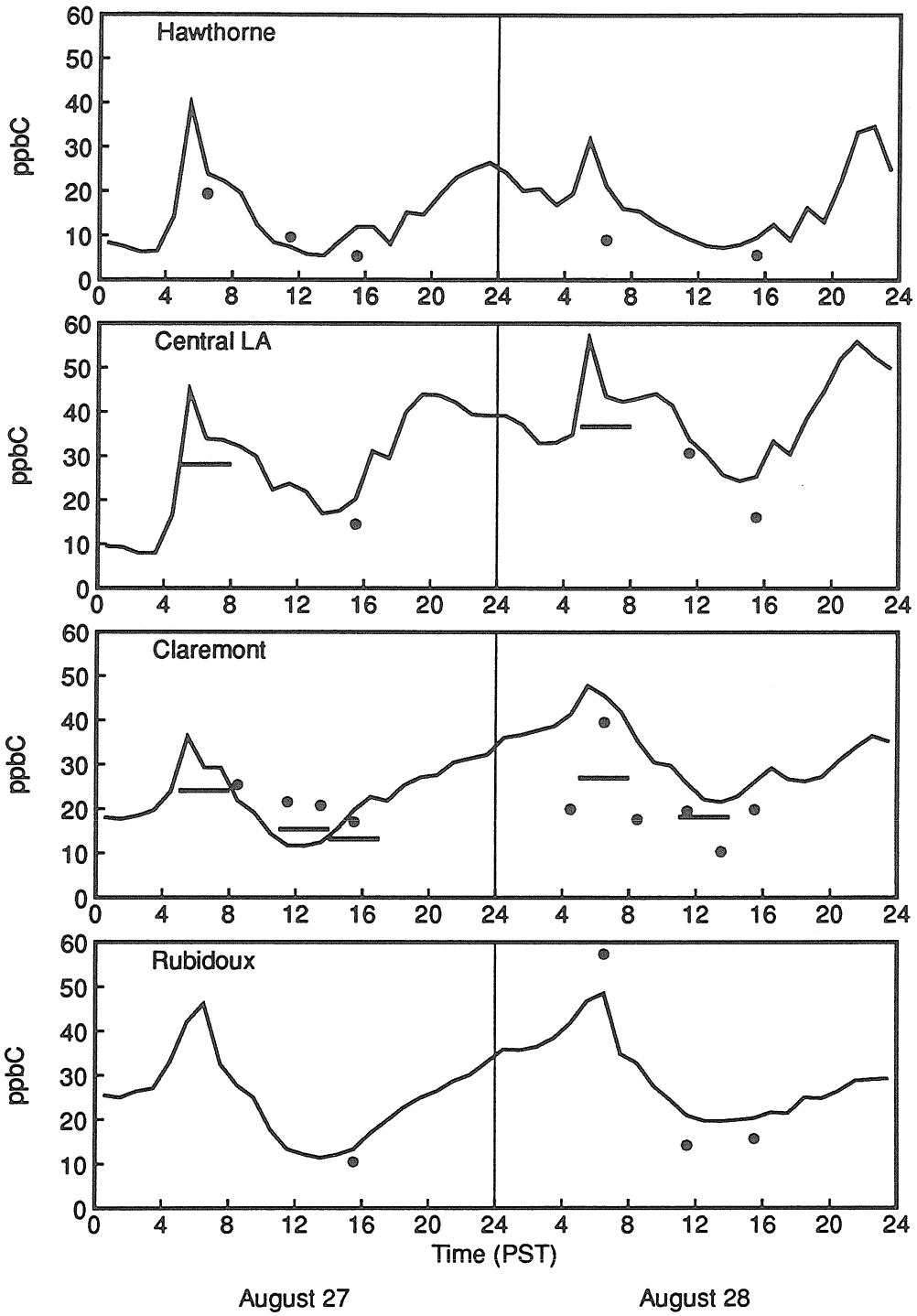

Figure 5.5: Time series plots of observed acetylene concentrations (plotted as circles for data set #1 and horizontal bars for data set #2) and model predictions (solid line).

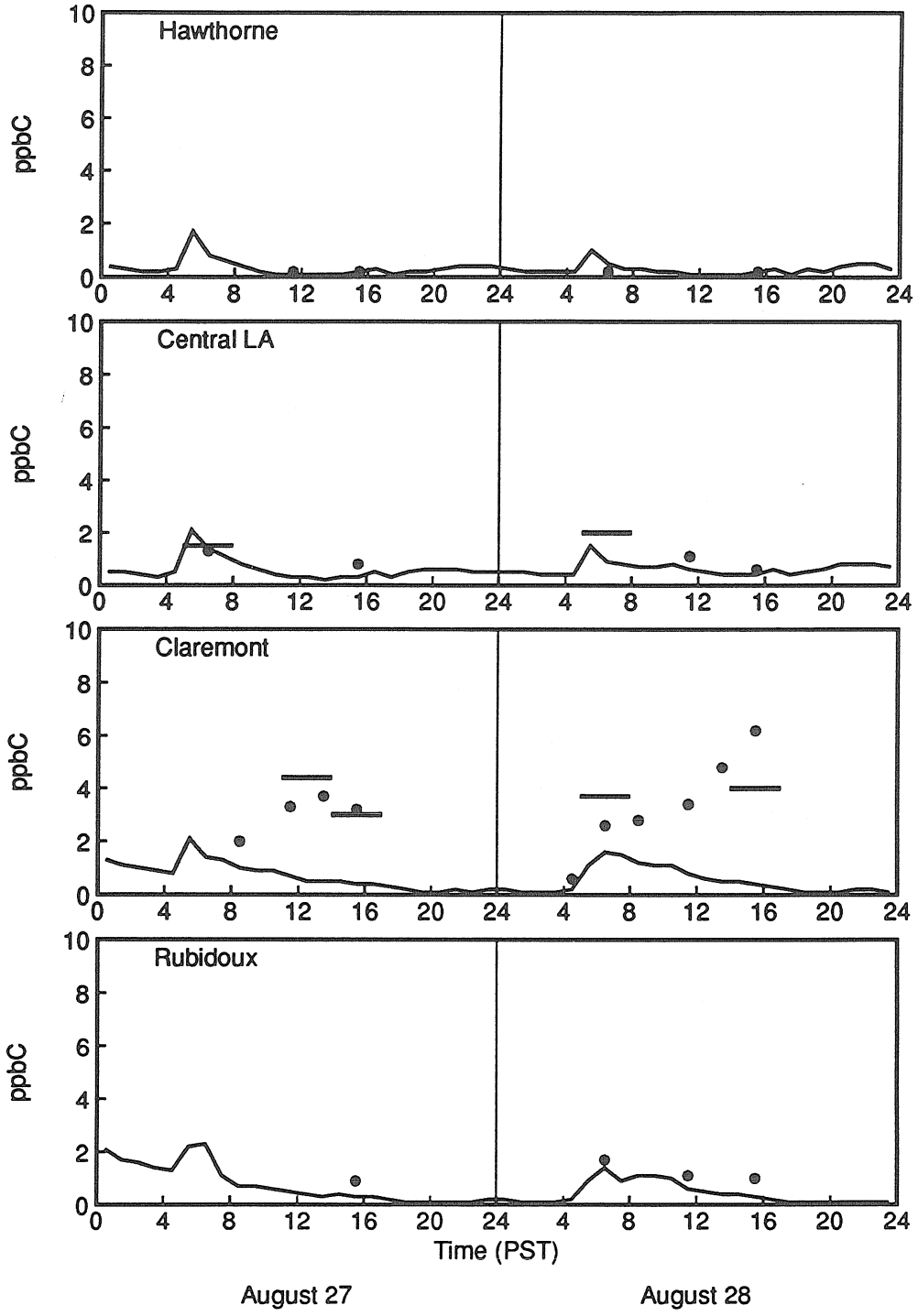

Figure 5.6: Time series plots of observed isoprene concentrations (plotted as circles for data set #1 and horizontal bars for data set #2) and model predictions (solid line).

creased motor vehicle VOC hot exhaust emissions and revised VOC emission composition profiles. The largest underpredictions of ozone concentrations by the model occur near the Claremont monitoring site where observed ozone concentrations are highest.

5.6 Discussion

The results of the present study are consistent with previous results indicating that the atmosphere contains more unburned gasoline and less of the combustion-derived species than is suggested by the VOC emission inventory, as discussed in Chapter 2. Observed concentrations of combustion-derived species including ethene, propene and acetylene are usually lower than predicted by the model, while observed concentrations of most unburned gasoline components tend to be a bit higher than predicted by the model. For some species such as benzene that are present in both unburned gasoline and in engine exhaust, model performance may reflect some compensating errors in the emission inventory that overstate exhaust emissions and understate emissions of unburned fuel.

An important result of the present study is the comparison between observed and predicted isoprene concentrations, which shows that for this episode the model is carrying the correct amount of isoprene at most sites where ambient concentration data are available. However, at one site (Claremont) where peak ozone concentrations are among the highest measured anywhere in the basin, both isoprene and ozone concentrations are underpredicted by the model. This implies that biogenic emissions may be much higher in this area than the emission inventory suggests. If it is true that biogenic emissions are in fact seriously understated near Claremont, this could

help to explain the underprediction of ozone concentrations by the model near Claremont. Furthermore, the effectiveness of a VOC-based ozone control strategy may be limited at least near Claremont by elevated concentrations of biogenic hydrocarbons such as isoprene. Further study of this issue is needed and should include a comprehensive biogenic hydrocarbon emissions and ambient concentration measurement program, followed by modeling calculations designed to determine the importance of biogenic hydrocarbon emissions to the Los Angeles ozone problem.

5.7 Conclusions

An Eulerian photochemical air quality model has been developed using explicit representation of the atmospheric chemistry of key volatile organic compounds. Model performance has been evaluated using speciated ambient concentration data acquired during SCAQS. A normalized bias of better than $\pm 50\%$ was calculated using model predictions and observed concentrations on August 28, 1987, for all except 7 individual organic species examined in the present study. Even better performance was observed for most of the aromatic hydrocarbons that were measured during SCAQS. Observed concentrations of combustion-derived species are lower than predicted by the model and its associated emission inventory, while observed concentrations of many species that are derived directly from unburned fuel tend to be higher than predicted by the model and the emission inventory.

Comparison of model predictions with measured data for isoprene show that the model is carrying about the correct amount of this biogenic compound at most locations. However, high measured isoprene concentrations at Claremont that are not reproduced by the model raise further questions

about the importance of biogenic emissions in the Los Angeles area. This issue has important implications for ozone control strategies, and should be studied further.

6 Modeling toxic VOCs

6.1 Introduction

Volatile organic compounds (VOCs) are pervasive in indoor and outdoor air [130,131]. This is of concern because VOCs promote the photochemical formation of ozone and other oxidants [1], and because some individual VOCs are known or suspected to have adverse effects on human health [132,133]. In the United States, recent amendments to the Clean Air Act (1990) require reductions in the emissions of compounds that have been identified as toxic air contaminants. The state of California and other jurisdictions also have initiated programs to identify toxic air contaminants and to gather data on the emissions, atmospheric chemistry, ambient concentrations, and health effects of these compounds. Numerous studies have been published that examine individual compounds of concern; for examples see refs [134]–[141].

In order to verify our understanding of the emissions and atmospheric concentrations of individual toxic air pollutants, it is important to be able to predict the ambient concentrations of toxic pollutants directly from emissions data and to compare these results against measured concentration data. However, in past studies, data on ambient concentrations generally have been analyzed separately from pollutant emissions data. Some toxic pollutants may be formed in the atmosphere as oxidation products of other VOCs. In all but a few past studies, formation pathways are identified without exploring in detail how important photochemical production might be in determin-

ing ambient concentrations. In those cases where photochemical production has been considered, it has been found to be important. A study of aldehydes and ketones (carbonyls) in Los Angeles air conducted by Grosjean et al. [142] did conclude that photochemical production of carbonyls dominates over direct emissions, based on changes in the measured ratios of carbonyl to carbon monoxide concentrations in ambient air. An analysis of carbonyl and non-methane hydrocarbon concentration data acquired during the summer of 1987 in the Los Angeles area indicates low carbonyl to hydrocarbon ratios in early morning samples, with much higher ratios later in the day [120]. This result also indicates significant photochemical formation of carbonyls during the daytime.

The objectives of the present study are to assess the contributions of various sources to the total direct emissions of individual toxic air contaminants, to model the emissions to air quality relationship for these species, and to investigate the relative importance of direct emissions versus atmospheric photochemical production in determining the atmospheric concentrations of toxic air contaminants. For this purpose, an Eulerian photochemical air quality model is described that tracks the transport and chemical reactions of pollutants emitted to the atmosphere. This model is applied to the Los Angeles, California area for a summertime period in 1987.

6.2 Selection of species studied

Title III of the the Clean Air Act Amendments of 1990 specifies a list of 189 inorganic and organic species that are declared to be toxic air contaminants. This list includes: various organic solvents; pesticides and herbicides; chemical process feedstocks, intermediates, products and by-products; some

of the hydrocarbons present in gasoline; and combustion-derived species such as formaldehyde and acetaldehyde. In addition to direct emission sources, some of the toxic species such as aldehydes, ketones, phenol and cresols are formed in the atmosphere as oxidation products of other directly emitted VOCs [31,143,144]. Twenty-one species appearing in the Clean Air Act list that are ubiquitous in urban areas are considered in the present study, as shown in Table 6.1. Many of the species listed in Table 6.1 are emitted directly in motor vehicle exhaust [81,82,89].

6.3 Model description

The CIT airshed model [18,20] is an Eulerian photochemical air quality model that solves the atmospheric diffusion equation:

$$\frac{\partial C_i}{\partial t} + \nabla \cdot (\vec{u} C_i) = \nabla \cdot (K \nabla C_i) + R_i \tag{6.1}$$

to predict the spatial and temporal distribution of pollutant concentrations in the atmosphere. The variables referred to in equation (6.1) are defined as follows: C_i is the ensemble mean concentration of species i, $\vec{u}$ is the wind velocity vector, K is the eddy diffusivity tensor, R_i is the rate of generation of species i by chemical reactions, and t is time. At ground level, the boundary condition is:

$$-K_{zz}\frac{\partial C_i}{\partial z} = E_i - v_g^i C_i, \tag{6.2}$$

where K_{zz} is the vertical eddy diffusivity, E_i is the emission flux, and v_g^i is the dry deposition velocity for species i. A no flux boundary condition is applied at the top of the modeling region, and lateral boundary conditions are set using measured pollutant concentrations. Initial conditions also are set using measured data.

6.3.1 Chemical mechanism

The gas-phase atmospheric reactions of VOC, NO_x, and other pollutants are represented in the model using the chemical mechanism of Carter [29]. Reaction rate constants with the hydroxyl (OH) radical are listed in Table 6.1 for individual toxic organic species that are tracked in the present study. Additional reaction rate constants of toxic organic species with ozone, the nitrate radical, and monatomic oxygen are listed in Table 6.2. Photolysis reactions for formaldehyde, acetaldehyde, propionaldehyde, acetone, and methyl ethyl ketone are included in the mechanism as per Carter [29]. The photolysis of acrolein is neglected [145].

Reactions of the toxic organic species form part of a much larger photochemical reaction mechanism used in this study. Other organic species not listed in Table 6.1 are represented in the model using 4 lumped alkane species, 3 lumped aromatics, 3 lumped olefins, and additional explicit model species for methane, ethane, ethene, isoprene, α-pinene, β-pinene, and acetone. The atmospheric oxidation product yields for the organic species are as per Carter [29]. The mechanism has a total of 78 active chemical species and 230 reactions.

Some of the species listed in Table 6.1 can be formed photochemically in the atmosphere. The aldehydes and ketones are produced in numerous reactions involving many different VOC precursors. The yields of these carbonyl products are taken from Carter [29]. Acrolein (propenal) is formed as a product of reactions of 1,3-butadiene with the hydroxyl radical and ozone [138]. In the model, one molecule of acrolein is produced for each molecule of 1,3-butadiene that reacts with OH or ozone. Formation of ring-retaining products in the atmospheric oxidation of benzene and toluene has been stud-

Table 6.1: Toxic organic species and hydroxyl radical reaction rate constants

Species	k_{OH} at 300K (cm^3 $molec^{-1}$ s^{-1})	kinetic parameters[a] A	E_a (kcal/mol)	ref
benzene	1.28E-12	2.500E-12	0.397	[29]
toluene	5.91E-12	1.810E-12	–0.705	[29]
ethylbenzene	7.10E-12	7.100E-12	0.000	[29]
isopropylbenzene	6.50E-12	6.500E-12	0.000	[29]
o-xylene	1.37E-11	1.370E-11	0.000	[29]
m-xylene	2.36E-11	2.360E-11	0.000	[29]
p-xylene	1.43E-11	1.430E-11	0.000	[29]
styrene	5.73E-11	1.070E-11	–1.000	[127]
phenol	2.63E-11	2.630E-11	0.000	[146]
o-cresol	4.20E-11	4.200E-11	0.000	[146]
p-cresol	4.70E-11	4.700E-11	0.000	[146]
formaldehyde	9.80E-12	1.130E-12	–1.288	[29]
acetaldehyde	1.56E-11	5.550E-12	–0.618	[29]
propionaldehyde	1.97E-11	8.500E-12	–0.500	[29]
acrolein	1.99E-11	1.990E-11	0.000	[31]
methyl ethyl ketone	1.15E-12	2.92E-13	–0.823	[29]
methyl isobutyl ketone	1.41E-11	1.410E-11	0.000	[31]
ethylene glycol	7.70E-12	7.700E-12	0.000	[29]
1,1,1-trichloroethane	1.23E-14	3.100E-12	3.299	[128]
perchloroethylene	1.72E-13	9.400E-12	2.385	[128]
1,3-butadiene	6.59E-11	1.480E-11	–0.890	[29]

[a]The hydroxyl radical reaction rate constant is computed from the kinetic parameters using the expression $k_{OH} = A \exp(-E_a/RT) \times (T/300)^B$ using R=0.0019872 kcal mol^{-1} K^{-1}. B=0 in all cases except formaldehyde and methyl ethyl ketone for which B=2.

Table 6.2: Additional reactions of toxic species included in the model

Reaction	k at 300K (cm^3 $molec^{-1}$ s^{-1})	kinetic parameters[a] A	E_a (kcal/mol)	ref
styrene + O3	1.77E-17	3.460E-15	3.144	[127]
styrene + NO3	1.55E-13	6.550E-12	2.233	[127]
styrene + O	1.79E-11	1.210E-11	–0.235	[127]
phenol + NO3	3.92E-12	3.920E-12	0.000	[146]
o-cresol + NO3	1.37E-11	1.370E-11	0.000	[146]
p-cresol + NO3	1.07E-11	1.070E-11	0.000	[146]
formaldehyde + HO2	7.79E-14	9.700E-15	–1.242	[29]
formaldehyde + NO3	6.38E-16	2.800E-12	5.000	[29]
acetaldehyde + NO3	2.84E-15	1.400E-12	3.696	[29]
propionaldehyde + NO3[b]	2.84E-15	1.400E-12	3.696	[29]
acrolein + O3	2.80E-19	2.800E-19	0.000	[31]
acrolein + NO3	1.20E-15	1.200E-15	0.000	[31]
1,3-butadiene + O3	7.93E-18	3.300E-14	4.968	[29]
1,3-butadiene + NO3	1.03E-13	1.480E-11	2.959	[29]
1,3-butadiene + O	2.10E-11	2.100E-11	0.000	[29]

[a]The rate constant is computed from the kinetic parameters using the expression $k = A \exp(-E_a/RT)$ using R=0.0019872 kcal mol^{-1} K^{-1}.
[b]Rate constant is assumed to be the same as that for reaction of acetaldehyde with NO3 radical, as per Carter [29].

ied by Atkinson et al. [143] among others. The yield of phenol from the reaction of benzene with OH was measured to be 0.236 ± 0.044. For the reaction of toluene with OH, cresol (methylphenol) yields of 0.204 ± 0.027 for o-cresol and 0.048 ± 0.009 for the sum of m- and p-cresol were measured. Earlier work by Gery et al. [147] showed similar cresol yields from toluene oxidation, and a ratio of p- to m-cresol of 17:2. Therefore, because m-cresol is a minor product, only o- and p-cresol are represented explicitly in the model, and m-cresol is lumped together with p-cresol. Subsequent reactions of phenol and cresols have been studied [146], and rate constants are shown in Tables 6.1 and 6.2.

Emissions of carbonyl species (formaldehyde, acetaldehyde, propionaldehyde, acrolein, acetone, and methyl ethyl ketone) are specially tagged in the model so that the contribution of direct emission sources can be resolved separately from the generation of these species by photochemical reactions. This tagging procedure has been accomplished by using two species to represent each of the carbonyls in the model: one species for the directly emitted fraction, and a separate twin species for the photochemically derived fraction. All chemical reactions are identical in the model for both of the twin species in each pair. Total concentrations for comparison with ambient concentration data are computed by summing the concentrations of the species in each pair. Primary and secondary phenol concentrations are tracked in an analagous manner.

6.3.2 Dry deposition

Dry deposition velocities are computed in the model using a three-resistance scheme [24] that includes turbulent transport through the atmospheric bound-

ary layer (r_a), diffusion through a laminar sublayer (r_b), and a surface resistance term (r_s^i) to account for differences in pollutant-surface interactions. The deposition velocity v_g^i for species i is given by:

$$v_g^i = \frac{1}{r_a + r_b + r_s^i}. \tag{6.3}$$

The atmospheric resistances (r_a and r_b) are computed in each model grid square using local surface roughness characteristics and meteorological conditions. Surface resistance values for the hydrocarbons and ketones listed in Table 6.1 are set to 50 s/cm throughout, and therefore dry deposition velocities for these species are limited to a low value of 0.02 cm/s. Surface resistances are lower for species that are highly reactive and more soluble in water [117]. Approximate surface resistance values for phenol and the cresols have been set to match the values used for SO_2. For formaldehyde, the surface resistances are set at half the corresponding values used for SO_2, and to double the SO_2 surface resistance values for the other aldehydes [129]. Atmospheric reaction and advection out of the air basin rather than dry deposition are likely to be the major removal process for the organic species considered here.

6.4 Model application

The model is applied to the Los Angeles, California area for the period August 27–28, 1987 as described in the previous chapter. The modeling region is shown in Figure 6.1. Boundary and initial condition values are set using measured pollutant concentration data. There is no significant input of these toxic organic air pollutants at the upwind boundary of the modeling region, except for formaldehyde (3 ppb) and acetaldehyde (5 ppb). The model is ex-

ecuted over a two day period; the first of these two days (August 27) is used to reduce the effect of uncertainties in specification of the initial conditions. Analysis of model results will focus on the second day (August 28).

An emission inventory for the Los Angeles area has been prepared by the California Air Resources Board and the South Coast Air Quality Management District [41], and forms the starting point for the emission inventory used in the present study. The inventory specifies hourly emission rates of carbon monoxide, oxides of nitrogen, and volatile organic compounds (VOC) for over 800 source types. These emission estimates are resolved spatially over a 5 by 5 kilometer square grid system. Mobile source emissions are estimated using the EMFAC 7E emission factor model and typical weekday traffic patterns developed using a travel demand model [42].

Numerous studies have concluded that the official emission inventory prepared by the government for the 1987 period studied here understates the emissions of VOCs and CO [1,4,5,6]. Emissions of VOCs and CO from on-road vehicles measured in the Van Nuys tunnel during 1987 were found to be up to three times higher than the values computed by the EMFAC 7E emissions model [65]. Therefore, to compensate at least in part for understated emissions, the on-road vehicle hot exhaust emissions of VOC and CO were scaled up to three times the baseline (EMFAC 7E) values, to reflect better the measured emission rates in the Van Nuys tunnel.

For the purposes of mapping total VOC emissions to individual organic species, each source is assigned to one of 225 chemical composition profiles. The composition profiles supplied with the official emission inventory have been updated as described in Chapter 3.

The available speciation profiles described above do not include phenol

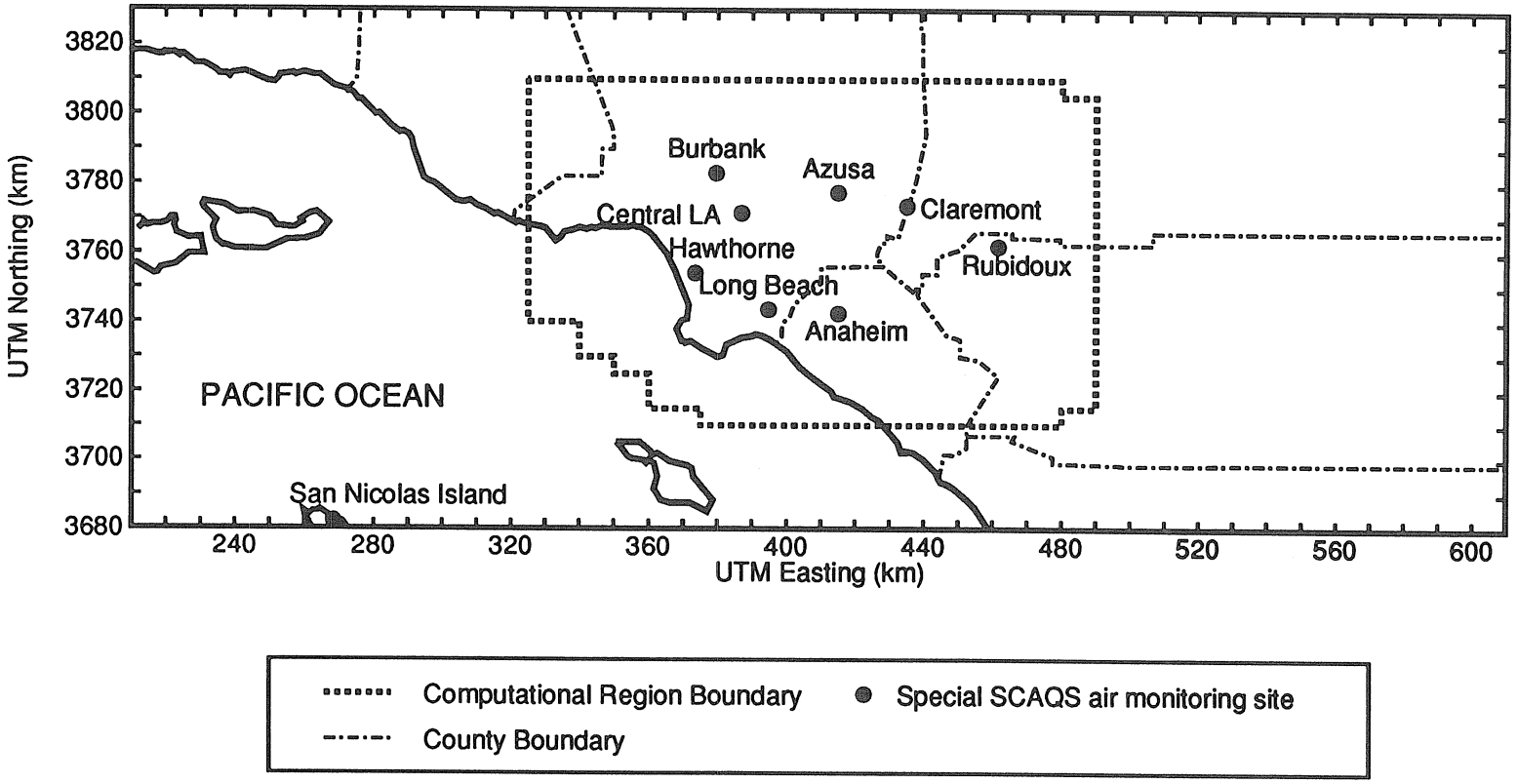

Figure 6.1: Map of the Los Angeles, California area showing the computational region and the locations of special SCAQS air quality monitoring sites.

emissions, and only include styrene emissions for catalyst-equipped vehicles. Average phenol emission rates of 3.0 mg/km for gasoline-powered vehicles, and 4.5 mg/km for diesel trucks, were measured in the Allegheny tunnel [82]. In the same study, styrene emission rates of 6.6 mg/km and 1.8 mg/km were measured for gasoline-powered vehicles and diesel trucks respectively. Using these data and total hydrocarbon emission rates measured in the same tunnel in a separate study [116], phenol and styrene were added to the engine exhaust speciation profiles as shown in Table 6.3. Acrolein was missing from the official diesel engine exhaust speciation profile, so a value of 1.4% by weight relative to total organic gas emissions was added based on test results for a heavy duty diesel engine [148]. Results of emission tests for 2 light duty diesel vehicles [149] were used to establish a content of 1.6% by weight of 1,3-butadiene in diesel engine exhaust. Further study of the emissions from heavy duty diesel engines is recommended.

Total emissions from all sources combined within the entire region mapped in Figure 6.1 for each of the toxic organic species tracked in the present study are presented in Table 6.4. The contribution of individual sources to the total emissions of benzene, toluene, xylenes, acrolein, and 1,3-butadiene are detailed in Table 6.5. Inspection of Table 6.5 shows that on-road vehicle exhaust is the biggest contributor to the total emissions of each species listed. Hot soak evaporative emissions contribute significantly to the emissions of the aromatic hydrocarbons. Diurnal and running loss evaporative emissions are enriched in the high volatility compounds such as butane found in gasoline, and hence are lower in aromatic content. There are significant contributions to toluene and xylene emissions from industrial surface coating activities (e.g., product finishes). Further analysis of the emission inventory

and the technical literature (see Chapter 3 and references therein) indicates that methyl ethyl ketone and methyl isobutyl ketone are used as solvents, and that mobile source emissions of these compounds are negligible. Ethylene glycol is used as an organic cosolvent in water-borne paints [96]; this compound also is used as a cosolvent in automotive cooling systems, but the emission inventory does not include ethylene glycol emissions from mobile sources. Trichloroethane is used as an industrial degreasing solvent, especially for metal parts prior to painting, and perchloroethylene is used both as a degreasing solvent and as a solvent for dry cleaning of clothes. The other compounds listed in Table 6.4 including aldehydes, ethylbenzene, isopropylbenzene, styrene, and phenol are all emitted primarily in the exhaust of on-road vehicle engines.

One caveat in the emissions estimates for the species considered here is that sources such as wood combustion in fireplaces and stoves and cigarette smoking have not been included in the emission inventory. Phenol and cresols among other species have been measured in emissions associated with residential wood combustion [150]. However, in Los Angeles for the hot summertime episode being considered in this study, emissions from fireplaces and woodstoves are of minor importance. Cigarette smoke contributes significantly to the indoor concentrations and human exposure to some toxic organic pollutants [151].

6.5 Ambient concentration data

On selected days during the summer and fall of 1987, speciated hydrocarbon concentration measurements were made at a network of 9 monitoring sites shown in Figure 6.1, as part of the Southern California Air Quality

Table 6.3: Content of selected toxic species in direct source emissions

Species	Gasoline Engine Exhaust: Non-Catalyst[a]	Gasoline Engine Exhaust: Catalyst-Equipped[b]	Unburned Gasoline (summertime): Whole Liquid[c]	Unburned Gasoline (summertime): Headspace Vapors[d]	Diesel Engine Exhaust
	Emissions Composition:[e]				
benzene	3.6	3.7	1.9	0.66	1.7
toluene	5.8	8.9	10.2	0.65	1.8[f]
ethylbenzene	1.2	1.3	1.9	0.03	0.1
isopropylbenzene	0.3	0.1	0.2	—	0.1
o-xylene	1.6	1.3	3.1	0.04	0.6
m- & p-xylene	4.2	3.5	8.3	0.13	0.3
styrene	0.66	0.21	—	—	0.06
phenol	0.30	0.30	—	—	0.14
formaldehyde	2.30	1.20	—	—	8.8
acetaldehyde	0.63	0.62	—	—	3.0
propionaldehyde	0.10	0.06	—	—	1.8
acrolein	0.47	0.14	—	—	1.4
methyl ethyl ketone	0.04	0.08	—	—	—
1,3-butadiene	1.2	0.2	—	—	1.6

[a]Exhaust speciation for gasoline-powered light duty vehicles without catalytic converters [74].
[b]Exhaust speciation for catalyst-equipped gasoline-powered light duty vehicles [77,78,79,80].
[c]Composition of whole liquid gasoline [68].
[d]Composition of gasoline vapors in headspace over liquid fuel [68].
[e]Percent by weight relative to total organic gas emissions.
[f]Toluene content of diesel engine exhaust may be overstated in this speciation profile. However, contribution of diesel exhaust to overall toluene emissions is still minor when the value stated above is used, as shown in Table 6.5.

Table 6.4: Region-wide emission totals for selected toxic organic species[a]

Species	Region-wide Emissions (10^3 kg/day)
benzene	52
toluene	144
ethylbenzene	16
isopropylbenzene	2.3
total xylenes	116
styrene	8.5
phenol	3.6
formaldehyde	29
acetaldehyde	9.1
propionaldehyde	5.8
acrolein	4.6
methyl ethyl ketone	35
methyl isobutyl ketone	14
ethylene glycol	10
1,1,1-trichloroethane	47
perchloroethylene	28
1,3-butadiene	10

[a]Emission inventory region includes most of the area shown in Figure 6.1. The on-road gasoline-powered vehicle hot exhaust emissions of all VOCs including toxic species have been scaled up to three times the official state of California emission inventory (EMFAC 7E) values, as suggested by on-road vehicle emission rates measured in the Van Nuys tunnel [4].

Table 6.5: Source contributions to total emissions of selected toxic organic species within the southern California study area shown in Figure 6.1

Source	Total VOC emissions	benzene	toluene	total xylenes	acrolein	1,3-butadiene
			(10^3 kg/day)			
On-road vehicles						
engine exhaust						
non-catalyst[a]	590	21.4	34.5	33.7	2.8	6.9
catalyst[a]	528	19.6	47.0	25.4	0.7	1.2
diesel	26	0.4	0.5	0.2	0.4	0.4
evaporative						
hot soak	98	1.8	10.0	11.2		
diurnal	24	0.2	0.2	0.0		
running loss	51	0.3	0.3	0.1		
Other exhaust[b]	74	2.2	3.1	2.9	0.7	1.0
Solvent emissions						
house paints						
water-borne	23					
solvent-borne	110		3.5	1.1		
industrial						
coatings	198		29.1	31.3		
adhesives	52		3.4	0.1		
thinning solvents	27		5.6	3.2		
All other sources	735[c]	5.9	6.7	7.1	0.0	0.6
TOTAL	2536[d]	52	144	116	4.6	10

[a]On-road vehicle hot exhaust emissions have been scaled up to three times the values found in the official state of California emission inventory in order to reflect better the results of measurements made in the Van Nuys tunnel [4].
[b]Includes off-road mobile sources such as aircraft, boats, trains, and construction equipment.
[c]Includes 634×10^3 kg/day of methane from natural gas leaks and waste decomposition.
[d]Total includes 791×10^3 kg/day of methane emissions.

Study (SCAQS; for an overview see Lawson [16]). Samples were collected in stainless steel canisters [113], and then analyzed by gas chromatography and gas chromatography/mass spectrometry [57,114]. Aldehyde and ketone sampling was performed over the same network of 9 sites, using 2,4-dinitrophenylhydrazine (DNPH) impregnated cartridges [119]. These data were consolidated into a single data base and further analyzed by Lurmann and Main [120], and provide the principal means for assessing the accuracy of model predictions. These data will be referred to as data set #1. In addition to the formaldehyde concentration measurements available as part of data set #1, concentration data for nitrogen dioxide (NO_2), nitrous acid and formaldehyde acquired using differential optical absorption spectroscopy are available at the Long Beach and Claremont sites [122].

An independent set of speciated non-methane hydrocarbon concentration data was acquired by Lonneman et al. [60] at the Long Beach, central Los Angeles, and Claremont sites. These data will be referred to as data set #2. Peroxyacetyl nitrate, trichloroethane, and perchloroethylene concentrations were monitored continuously at the sites shown in Figure 6.1 using electron capture gas chromatography [124,152,153,154].

In summary, ambient concentration data for most of the species listed in Table 6.1 are available for the locations and dates of interest in this study. Unfortunately, however, no measurements of phenol, cresol, ethylene glycol, and acrolein concentrations were made during SCAQS. Styrene concentrations reported in data set #1 may be unreliable [57]. An unspecified C6 carbonyl routinely reported in data set #1 may in fact be methyl isobutyl ketone, but this identification could not be confirmed.

6.6 Results

Statistical comparisons between predicted and observed concentrations for individual toxic organic species tracked in the model are presented in Table 6.6. The range of predicted 24-hour average concentrations for each species over the eight mainland sites shown in Figure 6.1 also is indicated in Table 6.6. The statistical measures of model performance could not be computed for some species where ambient concentration data were not available.

Inspection of Table 6.6 shows that the mean bias in the predicted concentrations of aromatic hydrocarbons is within $\pm 25\%$ in all cases except styrene which is underpredicted by a larger amount (-36%). While ambient concentration data for isopropylbenzene were not available, the predicted concentrations for this species are much lower than predictions for other aromatic hydrocarbons such as benzene, toluene, ethylbenzene, and the xylenes.

Predicted 24-hour average concentrations shown in Table 6.6 for the aromatic hydrocarbons, 1,3-butadiene, and acrolein were all highest at the central Los Angeles site where there is a high level of motor vehicle activity. In contrast, predicted aldehyde and ketone concentrations were highest at the inland sites (Azusa, Claremont, and Rubidoux). The lowest predicted concentrations for almost all of the toxic organic pollutants were seen at a coastal site (Hawthorne). Two highly reactive pollutants (1,3-butadiene and styrene) were predicted to have low concentations far inland at Rubidoux.

Time series plots of predicted and observed concentrations are shown for four sites starting at the coast with Hawthorne and proceeding inland through central Los Angeles to Claremont and Rubidoux. Figure 6.2 (benzene) and Figure 6.3 (o-xylene) indicate that the highest concentrations of the aromatic hydrocarbons occur during the morning rush hour period. Concentrations

Table 6.6: Statistical analysis of model performance[a]

Species	Range[b] of predicted concentrations (ppbC)	Bias[c] (ppbC)	Bias[c] (%)	Gross Error[d] (ppbC)	Gross Error[d] (%)
benzene	14–29	–0.5	+17	6.9	41
toluene	28–72	–10.2	+2	21.8	38
ethylbenzene	4–9	–3.4	–22	4.3	47
isopropylbenzene	0.4–1.2	ND[e]	ND	ND	ND
o-xylene	6–16	–1.0	+9	4.1	41
m- & p-xylene	14–35	–8.5	–13	11.9	38
styrene	0.8–4.0	–3.2	–36	3.6	83
phenol	0.24–0.96	ND	ND	ND	ND
o-cresol[f]	0.08–0.29	ND	ND	ND	ND
p-cresol[f]	0.02–0.07	ND	ND	ND	ND
formaldehyde	8–12	+0.8	+24	3.1	39
acetaldehyde	8–16	–3.6	–2	6.4	36
propionaldehyde	3–12	–11.7	–33	13.0	59
acrolein	1.1–2.1	ND	ND	ND	ND
methyl ethyl ketone	9–62	+9.4	+40	18.8	54
methyl isobutyl ketone	0.8–3.2	ND	ND	ND	ND
ethylene glycol	0.2–2.0	ND	ND	ND	ND
1,1,1-trichloroethane	3.4–4.6	–4.7	–41	4.9	53
perchloroethylene	0.8–2.3	–1.2	–33	1.4	46
1,3-butadiene	1.1–3.3	+0.4	+65	0.8	85

[a]Using all valid measured 1-hour average concentrations from data set #1 on August 28.
[b]Lowest and highest predicted 24-hour average concentration for August 28 over the 8 SCAQS intensive monitoring sites shown in Figure 6.1.
[c]Bias is defined as the mean residual (predicted minus observed) concentration. The percent bias values shown are computed by normalizing each residual to the corresponding observed concentration before averaging.
[d]Gross error is defined as the mean absolute value of the residuals.
[e]No measured data are available.
[f]Photochemical production only; there are no direct cresol emissions included in the model.

of these species fall to lower values by midday. Similar diurnal patterns are observed for other aromatics. In Figure 6.4, time series plots are presented for 1,3-butadiene. Again, concentrations are highest during the morning rush hour, and fall to low values at midday. There is one low observed value of 1,3-butadiene reported at Claremont and another low value at Long Beach in data set #2 for August 28 that disagree with higher observed values reported in data set #1.

Additional time series data have been plotted for species that are both formed in the atmosphere and emitted directly. Observed and predicted formaldehyde and acetaldehyde concentrations are shown in Figures 6.5 and 6.6 respectively. The directly emitted component of the total predicted concentration is indicated in these figures by the dashed line; the sum of directly emitted and photochemically generated contributions is indicated by the solid line. Figures 6.5 and 6.6 show that photochemical production contributes significantly to total formaldehyde and acetaldehyde concentrations. The contribution of direct emissions is small during daylight hours. Similar results were obtained for propionaldehyde and methyl ethyl ketone. In relative terms, direct emissions of acetaldehyde are less important than direct emissions of formaldehyde as a fraction of the total concentrations of the respective aldehyde, although photochemical production dominates the total concentrations for both species.

As shown in Figure 6.7, direct emissions and photochemical production both make roughly comparable contributions to total predicted acrolein concentrations. For the case of phenol, direct emissions dominate greatly over the fraction of total phenol concentrations contributed by atmospheric benzene oxidation, as shown in Figure 6.8. Unfortunately, ambient concentra-

tion measurements of acrolein and phenol were not made during the SCAQS episodes; therefore the accuracy of total predicted concentrations for these species is not known.

6.7 Discussion

Airshed model calculations for formaldehyde, acetaldehyde, propionaldehyde, acetone, methyl ethyl ketone, and acrolein indicate significant atmospheric photochemical formation of these species. This is important because programs designed to reduce ambient concentrations of these species may fail to achieve the desired results if the control programs only target direct emissions. In contrast, photochemical production of phenol is of minor importance when compared to direct emissions. Results reported here are for a sunny summertime episode in Los Angeles where there is a high level of photochemical activity. Photochemical production of toxic organic species may be less important during the winter months.

Direct emissions were found to be a smaller contributor to total acetaldehyde concentrations than is the case for direct emissions of formaldehyde. This can be explained by noting that acetaldehyde is less abundant than formaldehyde in vehicle exhaust (see Table 6.3). Furthermore, at least for the case of representative alkane mixtures, acetaldehyde is a major oxidation product whereas formaldehyde yields are small [144].

As shown in Figure 4 and Table 6.6, 1,3-butadiene concentrations predicted by the model are somewhat higher than observed values. While butadiene is emitted in engine exhaust, it is not present in unburned fuel. Analysis of ambient concentration data and source emissions signatures (see Chapter 3) suggests that the atmosphere contains more unburned gasoline

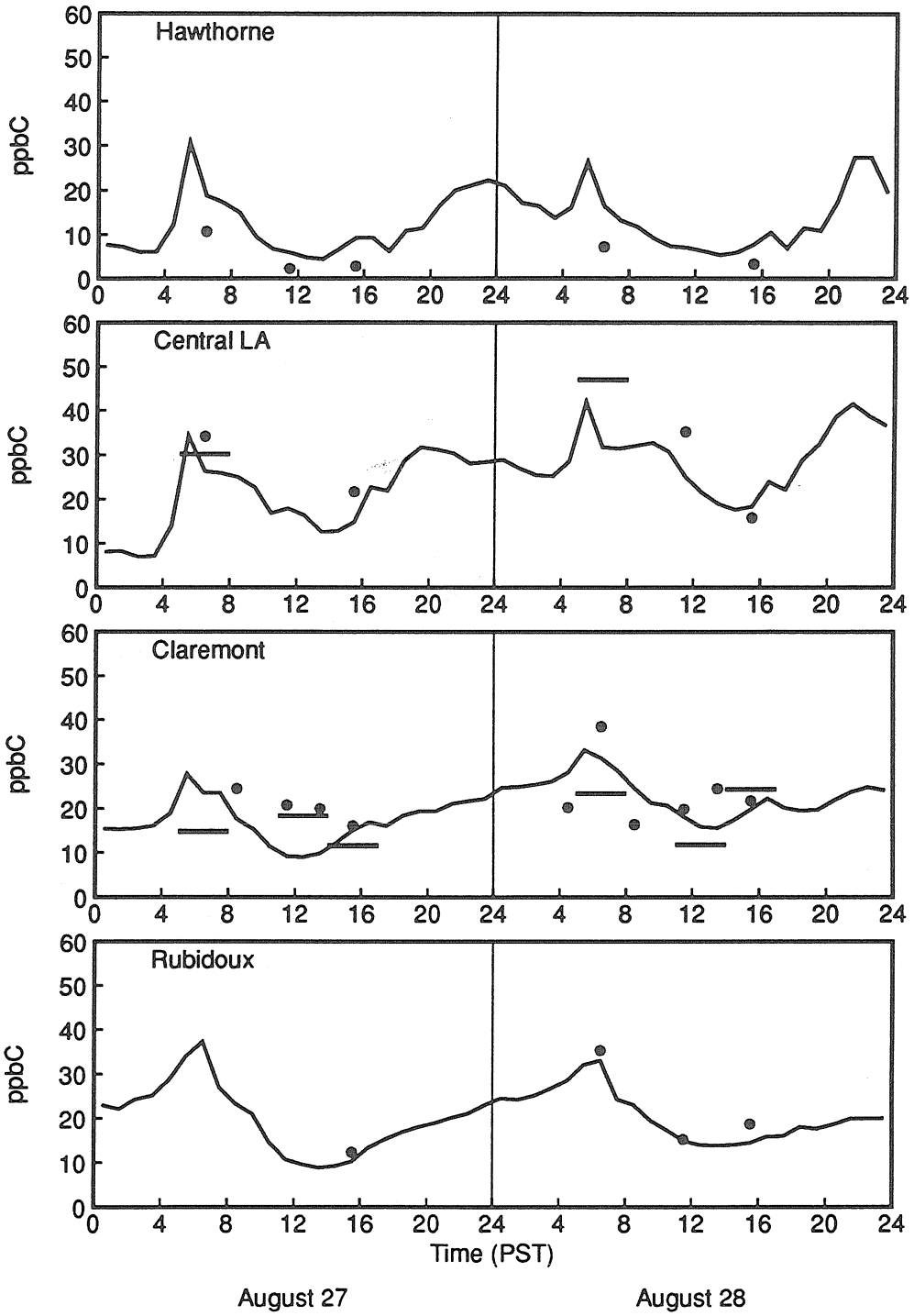

Figure 6.2: Time series plots of observed benzene concentrations (plotted as circles for data set #1 and horizontal bars for data set #2) and model predictions (solid line).

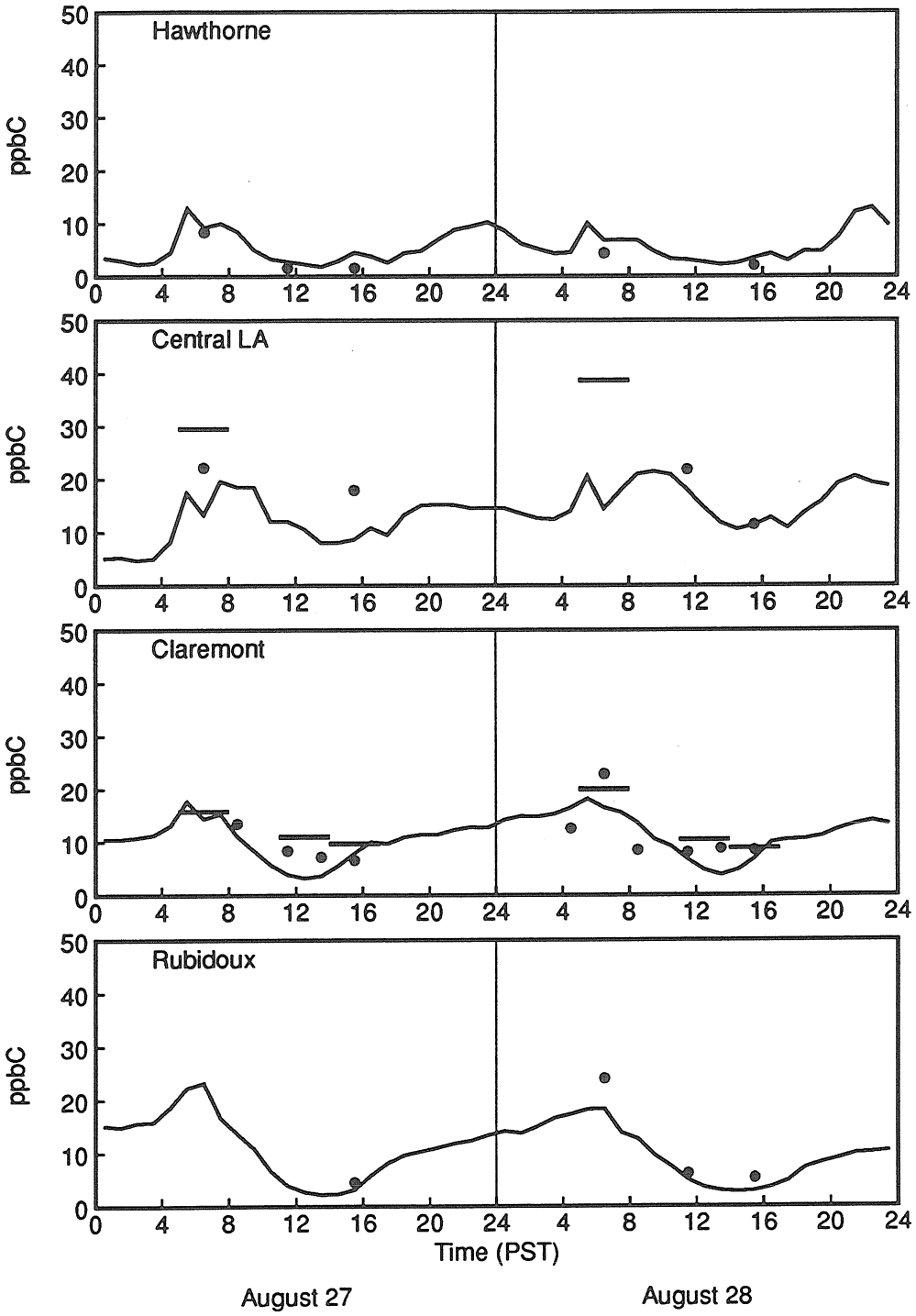

Figure 6.3: Time series plots of observed o-xylene concentrations (plotted as circles for data set #1 and horizontal bars for data set #2) and model predictions (solid line).

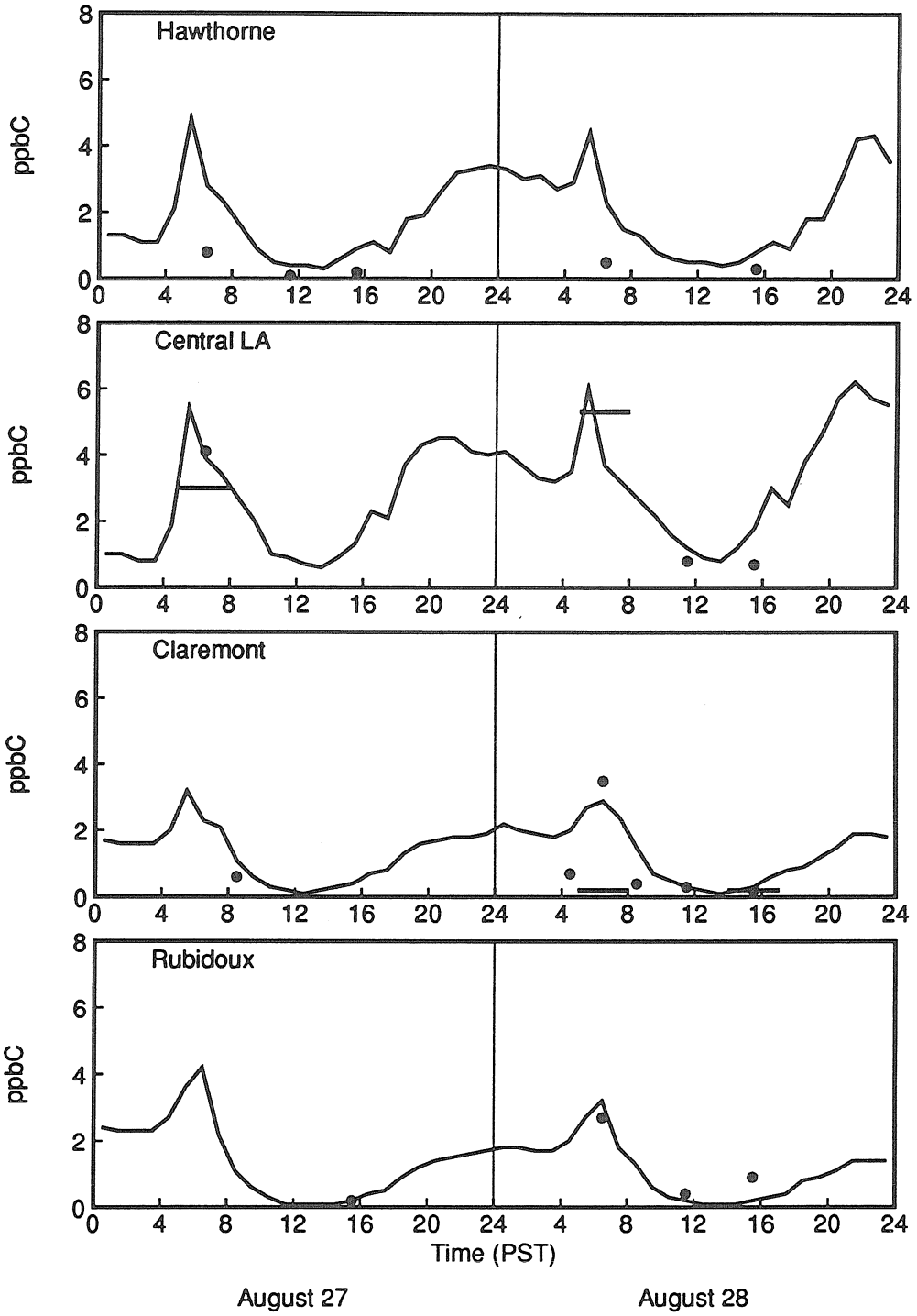

Figure 6.4: Time series plots of observed 1,3-butadiene concentrations (plotted as circles for data set #1 and horizontal bars for data set #2) and model predictions (solid line).

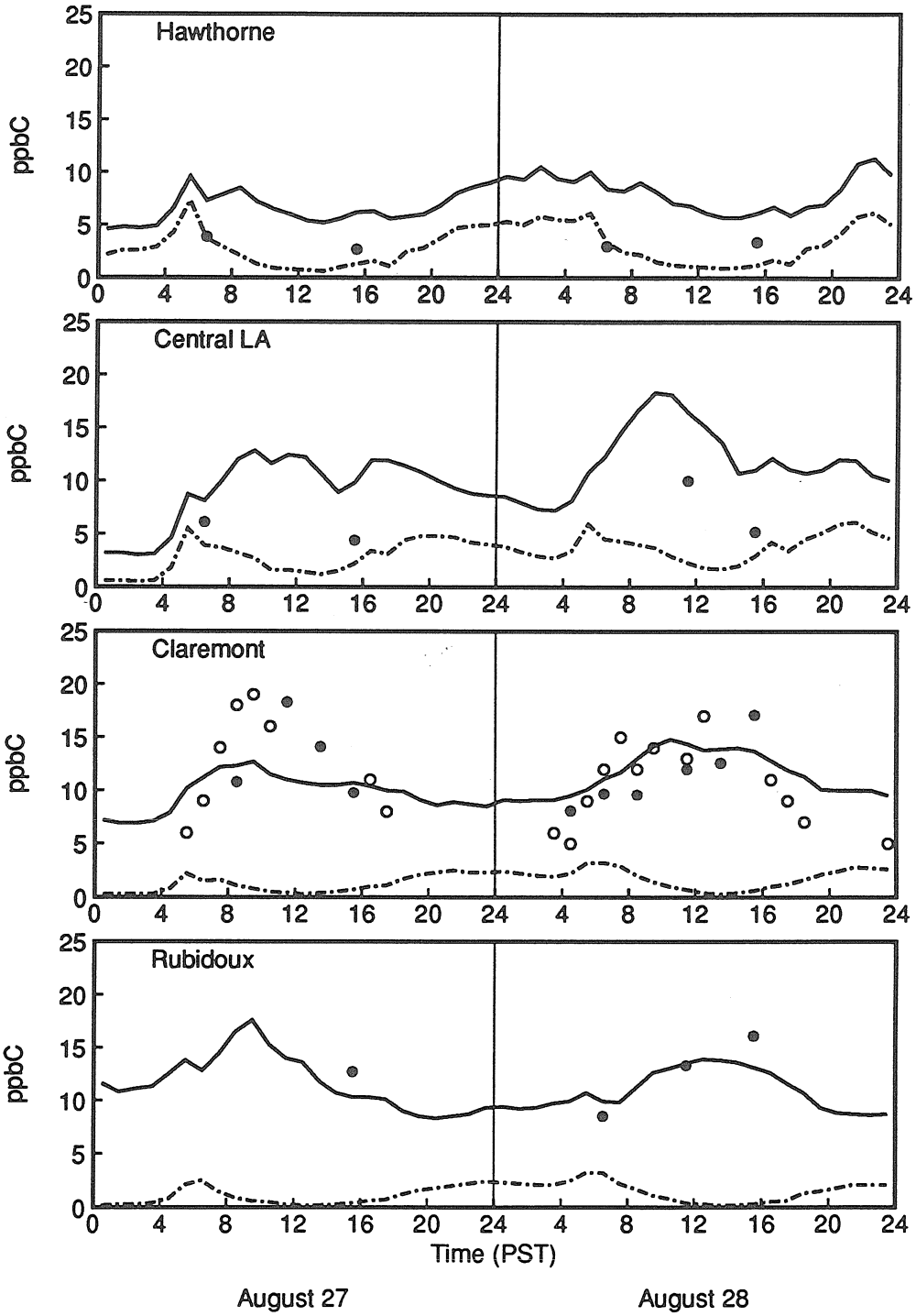

Figure 6.5: Time series plots of observed formaldehyde concentrations (plotted as solid circles (DNPH) and open circles (DOAS)) and model predictions for total formaldehyde (solid line) and the contribution from direct emissions (dot-dashed line).

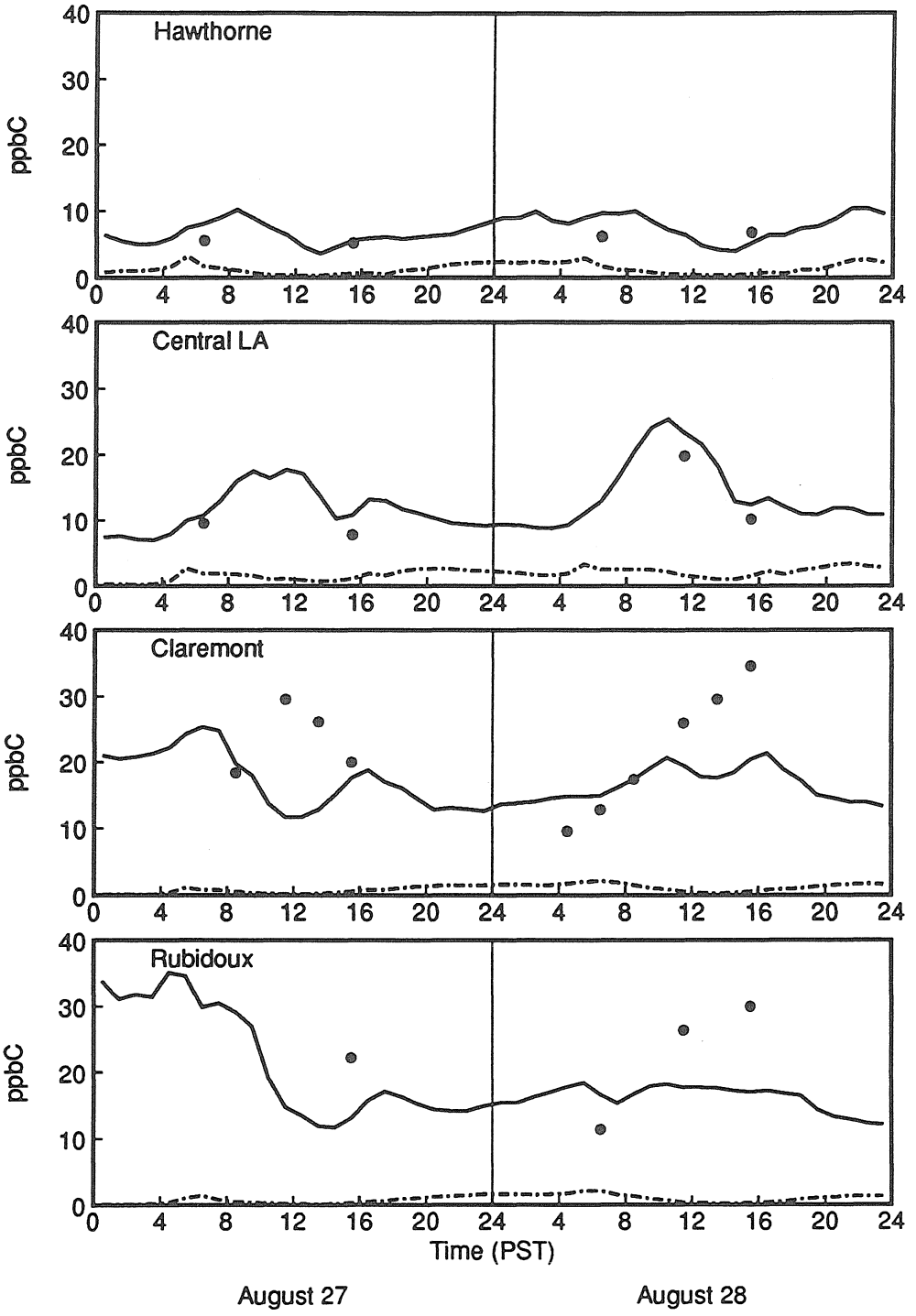

Figure 6.6: Time series plots of predicted acetaldehyde concentrations showing the directly emitted component (dot-dashed line) and the total predicted concentration (solid line). Observations from data set #1 are plotted using circles.

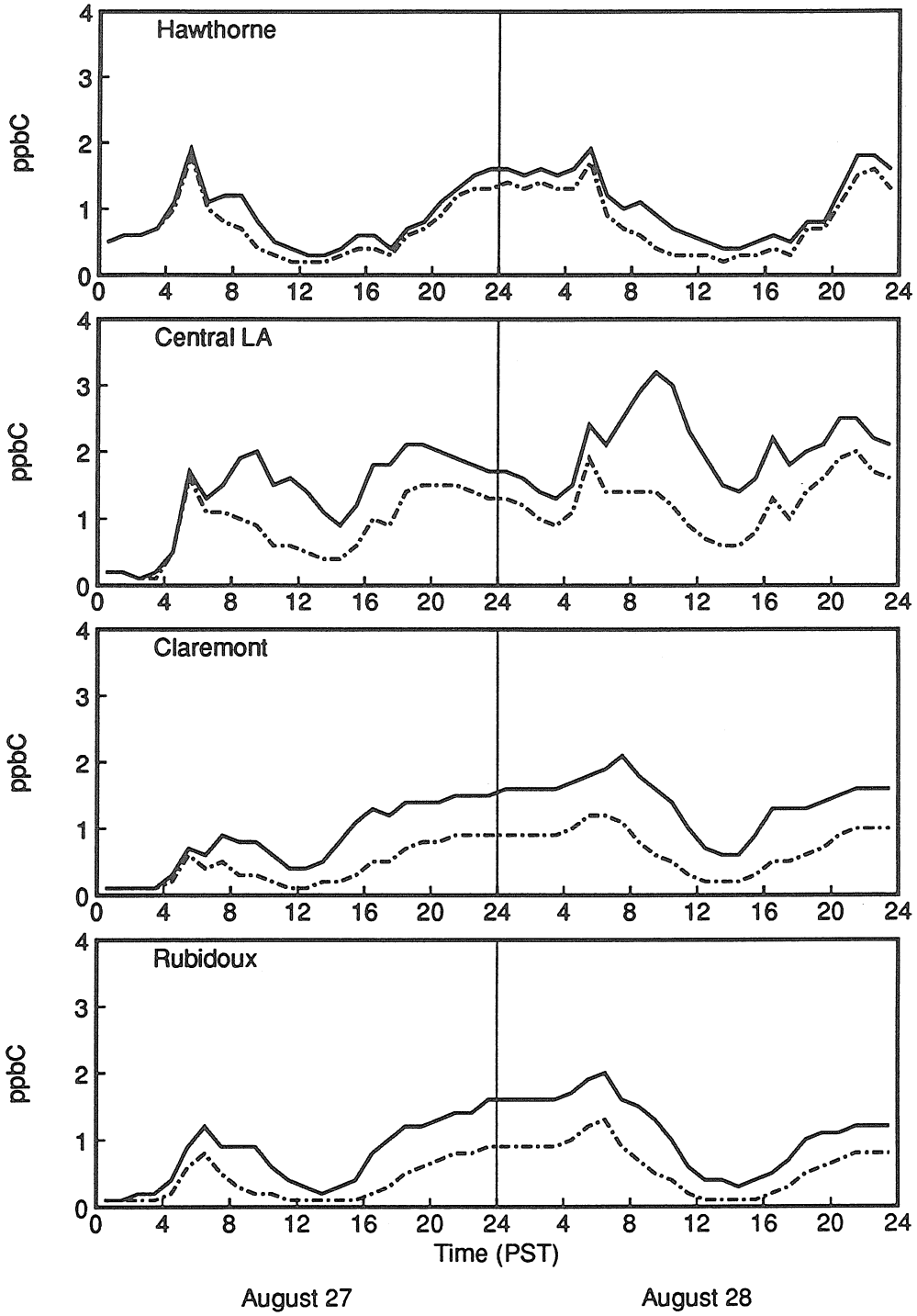

Figure 6.7: Time series plots of predicted acrolein concentrations showing the directly emitted component (dot-dashed line) and the total predicted concentration (solid line). Acrolein concentrations were not measured during SCAQS.

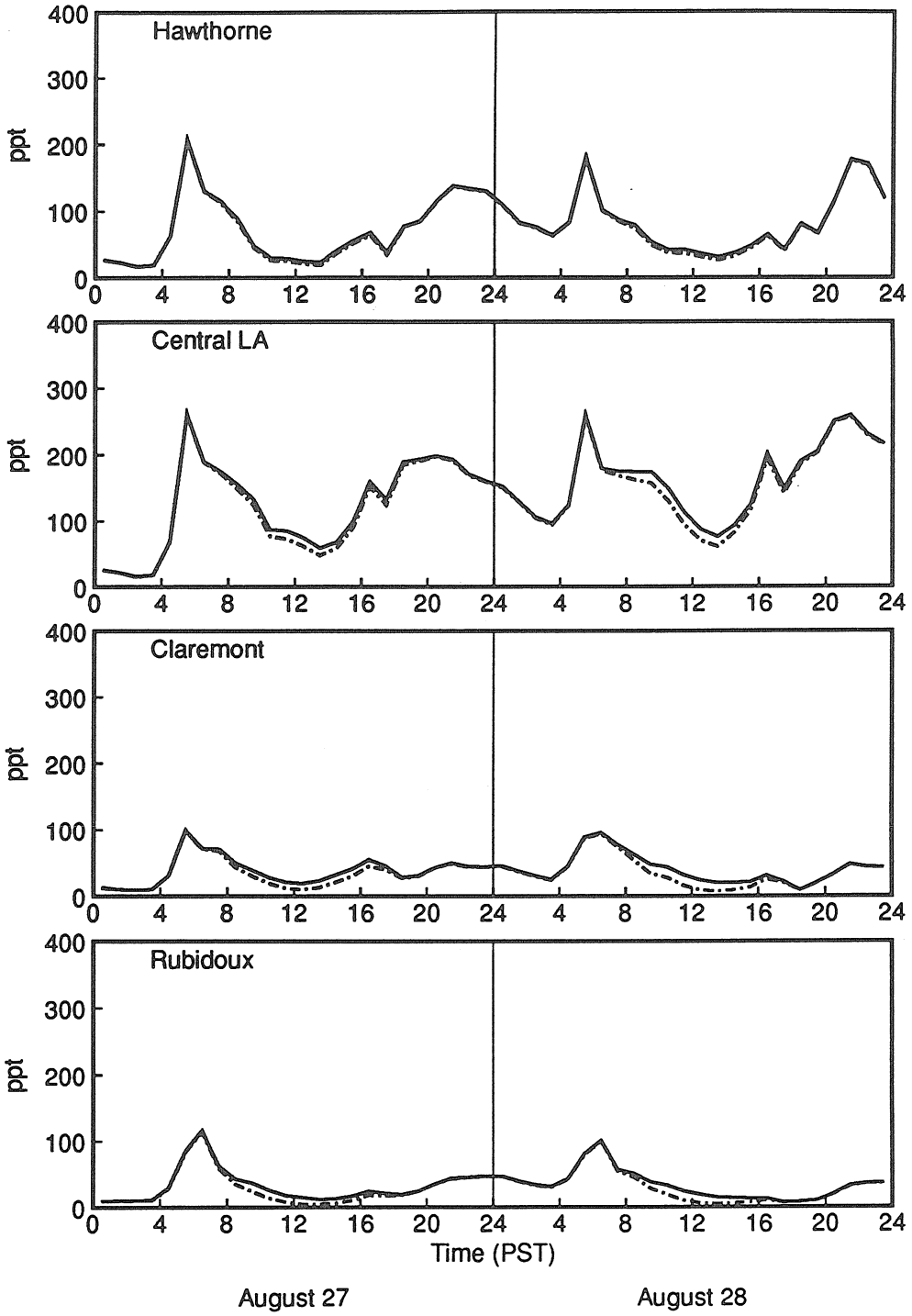

Figure 6.8: Time series plots of predicted phenol concentrations showing the directly emitted component (dot-dashed line) and the total predicted concentration (solid line). Phenol concentrations were not measured during SCAQS.

(and less of the combustion-derived species which would include butadiene) than is indicated by the emission inventory. Therefore, it is possible that butadiene emissions to the model are overstated. There are also uncertainties in the ambient concentration data for this compound.

Given that butadiene concentrations predicted by the model are somewhat higher than observed values, the rate of formation of acrolein as an oxidation product also may be overstated. However, secondary formation of acrolein will likely remain significant even if butadiene levels in the model are reduced to match observed concentrations. If butadiene emissions are controlled because butadiene is itself a toxic pollutant, then it appears that such controls would have additional benefits in the form of reduced secondary formation of acrolein.

Turning to other toxic organic species included in the model, it should be noted that in some cases, model predictions have been reported for species that were not measured during SCAQS. An assessment of model predictions for some of these species still can be performed using measurements reported in other studies, although the comparisons are less definitive. Ambient concentration data for acrolein, summarized by Grosjean [137], ranged up to 14 parts per billion by volume (ppbv) during the 1960s in the Los Angeles area, while more recent measurements suggest values on the order of 1 ppbv, in agreement with the predictions of the present study shown in Table 6.6. Measured concentrations of phenol as high as 420 ppb have been reported near point sources such as phenolic resin factories; values in the range 0.1–1 ppbv are more typical of urban areas [139]. The predicted phenol concentrations of the current study lie in the same range as other measured data for urban areas.

Cresols have been measured in the gas phase and in rainwater in Portland, OR [155]. Average gas-phase concentrations of 16 parts per trillion by volume (ppt) for o-cresol and 30 ppt for the sum of m- and p-cresol were reported; significant scavenging of these species by rain droplets also was reported. These measured concentrations are lower than the concentrations of cresols predicted in the present study based solely on formation of cresols from toluene oxidation. However, it is not surprising that predicted cresol concentrations in this study are higher than those observed in the study in Portland, given the lower precursor emissions and level of photochemical activity in Portland, and the fact that scavenging by rain events occurred in Portland whereas it did not rain on the days modeled in Los Angeles. A study of direct phenol and cresol emissions from non-catalyst, diesel, and various types of catalyst-equipped light duty motor vehicles indicates that phenol emission rates are higher by a factor of 10 or more than the corresponding cresol emission rates [156]. While photochemical generation of phenol by benzene oxidation was found to be negligible compared to direct emissions (see Figure 8), the combination of higher cresol production rates from toluene oxidation and lower direct emission rates from motor vehicles implies that photochemical production will be a more signficant relative contributor to cresol concentrations than is the case for phenol. However, the contribution of atmospheric formation to total cresol concentrations could still be quite small compared to direct emissions.

Since benzene and toluene are listed as toxic air contaminants, emissions of these species may be reduced in response to the Clean Air Act requirements. Results of this study suggest that toluene emission controls will reduce ambient cresol concentrations by about 100 parts per trillion by

volume. Benzene emission controls are not expected to affect ambient phenol concentrations significantly.

6.8 Conclusions

An Eulerian photochemical air quality model has been described that enables prediction of ambient concentrations of individual gas-phase toxic organic air pollutants based on knowledge of direct pollutant emission rates, meteorological conditions, and atmospheric chemistry. The model has been tested against measurements of speciated VOC concentrations for the August 27–28, 1987 period in the Los Angeles area.

Analysis of the direct emissions to the atmosphere in southern California indicates a signficiant mobile source contribution to the total direct emissions of many toxic organic species including the aromatic hydrocarbons, the aldehydes, and 1,3-butadiene. Given the presence of large numbers of motor vehicles in cities, similar findings can be expected in most urban areas.

Further analysis indicates that for the summertime conditions considered here, the total ambient concentrations of certain toxic organics are significantly affected by the contribution from atmospheric photochemical formation that begins with the emissions of other VOC precursors. Photochemical formation is more important than direct emissions for acetaldehyde, formaldehyde, propionaldehyde, acetone and methyl ethyl ketone under the Los Angeles summertime conditions studied here. Direct emissions and photochemical formation contribute in roughly equal amounts to acrolein concentrations. Photochemical formation may contribute significantly to cresol concentrations. In contrast, despite the existence of a pathway for phenol formation as a product of benzene oxidation in the atmosphere, ambient phe-

nol concentrations are dominated by direct emissions. These results indicate that the control of toxic organic species in the atmosphere in several cases must consider both direct emissions and atmospheric chemical formation.

7 Conclusions

7.1 Summary of results

An Eulerian photochemical air quality model that relates emissions of volatile organic compounds (VOCs) to ambient air quality has been described. The performance of this model has been evaluated for the Los Angeles area using data from the Southern California Air Quality Study (SCAQS).

The overall research program described in this thesis includes a major effort to diagnose errors present in the VOC emission inventory that is maintained by the government and to improve the accuracy of that inventory. In agreement with other recent studies [1,4,5,6], the results of this study indicate that total VOC mass emissions are significantly understated in the official 1987 emission inventory for the Los Angeles area. Improved chemical composition profiles for important VOC emission sources have been presented, and use of these profiles results in significant changes to the official VOC emission inventory, especially at the individual species level. Further insight into the emission inventory has been obtained by reconciling VOC emission source signatures with speciated ambient VOC concentration data in Los Angeles. It appears that the atmosphere contains much more unburned gasoline than is present in the emission inventory. This finding provides a useful clue to future research projects that seek to identify the origins of excess VOC emissions that are not included in current emission inventories. It also implies that control of photochemical smog in Los Angeles will be more difficult

than was previously thought because the actual VOC emissions that must be reduced are higher than previously estimated.

A major achievement of this research program is the incorporation of numerous data sets acquired during SCAQS into the unifying framework of the CIT airshed model. The airshed model has been used to gain new insight into the problem of ozone formation in urban atmospheres. Model performance has been analyzed in detail for the August 27–29, 1987 period in the Los Angeles area. In the base case calculations using the official emission inventory, both ozone and reactive hydrocarbon concentrations were underpredicted. When hot exhaust emissions of VOCs were scaled up to three times the baseline values in order to reflect on-road vehicle emissions measurements in the Van Nuys tunnel, then model predictions for both ozone and hydrocarbons increased to match observed values more closely.

Airshed model formulations capable of predicting ambient VOC concentrations at progressively increasing levels of detail have been described. In Chapter 2, predictions for total reactive hydrocarbon concentrations in the model were analyzed. This study is comparable to the most sophisticated analyses of performance for VOCs reported in past studies in the few cases where VOC predictions were examined at all. In Chapter 4 of this study, model performance has been assessed for the lumped organic species defined in the LCC chemical mechanism [11]. A model that predicts the level of individual VOCs has been reported in Chapter 5. An important finding of these assessments is that while total VOC concentrations were underpredicted when the base case emission inventory prepared by the government was used, bias in model predictions relative to observations was not uniform from species to species. Therefore efforts to correct perceived bias in the

VOC emission inventory will require more sophistication than simple scaling of total VOC mass emissions. When corrections were made to the emissions data based on recent source speciation measurements and tunnel study results, then VOC concentrations predicted by the model improved greatly.

A general purpose model for relating emissions of gas-phase toxic air pollutants to ambient air quality has been described. The model has been tested for a variety of toxic species with widely different emissions characteristics and chemical properties. Application of the model to the Los Angeles area suggests that atmospheric photochemical formation contributes significantly to the ambient concentrations of some toxic organic air pollutants, including formaldehyde, acetaldehyde, propionaldehyde, methyl ethyl ketone, and acrolein. This is important because programs designed to control toxic air pollutants will not achieve the expected results if they consider only direct emissions in the many cases where atmospheric formation is also significant.

7.2 Recommendations for future research

Further improvements need to be made to the pollutant emission inventories required for photochemical modeling. Without a good understanding of the underlying emission rates, it is difficult to predict pollutant concentrations, or to make informed decisions about control program plans. While much of the effort to improve the emission inventory seems to focus on mass emission factors for on-road vehicles, it is important that all aspects of the emission inventory be considered. This means further work to characterize the chemical composition of pollutant emissions, and improved assessments of the level of source activity (e.g., number of vehicle trips, diurnal and weekly traffic patterns, fuel and solvent consumption rates, and so on).

Given the changes in gasoline composition that have occurred in recent years and given that further changes are expected in the future, and because the chemical composition of tailpipe exhaust is dependent on fuel composition, it would be useful to survey routinely (say once every 3 years for both summer and winter seasons) the properties of gasolines being used as motor vehicle fuels. This survey should extend beyond bulk fuel properties to include quantitative data on the abundance of each individual compound present in gasoline. It would also be very useful to be able to predict the complete composition of tailpipe exhaust as a function of fuel composition.

Future programs to measure speciated ambient VOC concentrations must consider more than the traditional list of hydrocarbons present in gasoline. With major changes to gasoline composition already underway, changes to both vehicle emissions and ambient concentrations of individual VOCs are inevitable. In addition, the likelihood of signifcant emissions of polar organic compounds such as alcohols and glycols from surface coating and consumer product solvents has been mentioned. However, since concentrations of these species were not measured during SCAQS (and are not commonly measured in other studies either), it has not been possible to verify emission estimates from several types of important stationary sources.

Finally, more study of the emissions and atmospheric behavior of toxic air pollutants is needed to improve the effectiveness of proposed control programs. Because toxic species are often trace constituents in the overall VOC emissions from a source, these compounds are sometimes missing from VOC emission source test data, and hence are not incorporated into some of the speciation profiles used for photochemical modeling. Therefore, to improve the understanding of the contributions to direct emissions of toxic pollutants,

further characterization of direct emission sources is needed. In addition, for toxic organic species such as formaldehyde and acetaldehyde where atmospheric photochemical formation represents a signficant fraction of total ambient concentrations, approaches for controlling the secondary (i.e., photochemically derived) fraction should be studied.

Bibliography

[1] National Research Council. *Rethinking the ozone problem in urban and regional air pollution.* National Academy Press, Washington, D.C., 1991.

[2] Air quality management plan for the South Coast Air Basin. South Coast Air Quality Management District, El Monte, CA, 1991.

[3] Tesche, T. W. *J. Environ. Eng.* **1988**, *114*, 739–752.

[4] Ingalls, M. N.; Smith, L. R.; and Kirksey, R. E. Measurement of on-road vehicle emission factors in the California South Coast Air Basin. Volume I: regulated emissions. Southwest Research Institute, San Antonio, TX, 1989. Report to the Coordinating Research Council under project SCAQS-1.

[5] Pierson, W. R.; Gertler, A. W.; and Bradow, R. L. *J. Air Waste Manage. Assoc.* **1990**, *40*, 1495–1504.

[6] Fujita, E. M.; Croes, B. E.; Bennett, C. L.; Lawson, D. R.; Lurmann, F. W.; and Main, H. H. *J. Air Waste Manage. Assoc.* **1992**, *42*, 264–276.

[7] Tesche, T. W. Alpine Geophysics, Crested Butte, CO, 1991. Personal communication.

[8] Chameides, W. L.; Lindsay, R. W.; Richardson, J.; and Kiang, C. S. *Science.* **1988**, *241*, 1473–1475.

[9] Chameides, W. L.; Fehsenfeld, F.; Rodgers, M. O.; Cardelino, C.; Mar-

tinez, J.; Parrish, D.; Lonneman, W.; Lawson, D. R.; Rasmussen, R. A.; Zimmerman, P.; Greenberg, J.; Middleton, P.; and Wang, T. *J. Geophys. Res.* **1992**, *97*(D5), 6037–6055.

[10] Falls, A. H. and Seinfeld, J. H. *Environ. Sci. Technol.* **1978**, *12*, 1398–1406.

[11] Lurmann, F. W.; Carter, W. P. L.; and Coyner, L. A. A surrogate species chemical reaction mechanism for urban-scale air quality simulation models. Volumes I and II. ERT Inc., Newbury Park, CA and Statewide Air Pollution Research Center, University of California, Riverside, CA, 1987. Report to the US Environmental Protection Agency under contract 68-02-4104.

[12] Gery, M. W.; Whitten, G. Z.; Killus, J. P.; and Dodge, M. C. *J. Geophys. Res.* **1989**, *94*(D10), 12925–12956.

[13] Grosjean, D. Aerosols. In *Ozone and other photochemical oxidants*, chapter 3, pages 45–125, National Academy of Sciences, Washington, D.C., 1977.

[14] Grosjean, D. and Seinfeld, J. H. *Atmos. Environ.* **1989**, *23*, 1733–1747.

[15] Izumi, K. and Fukuyama, T. *Atmos. Environ.* **1990**, *24A*, 1433–1441.

[16] Lawson, D. R. *J. Air Waste Manage. Assoc.* **1990**, *40*, 156–165.

[17] Seinfeld, J. H. *J. Air Pollut. Control Assoc.* **1988**, *38*, 616–645.

[18] McRae, G. J.; Goodin, W. R.; and Seinfeld, J. H. *Atmos. Environ.* **1982**, *16*, 679–696.

[19] McRae, G. J.; Goodin, W. R.; and Seinfeld, J. H. *Atmos. Environ.* **1983**, *17*, 501–522.

[20] Russell, A. G.; McCue, K. F.; and Cass, G. R. *Environ. Sci. Technol.* **1988**, *22*, 263–271.

[21] Russell, A. G.; McCue, K. F.; and Cass, G. R. *Environ. Sci. Technol.* **1988**, *22*, 1336–1347.

[22] Milford, J. B.; Russell, A. G.; and McRae, G. J. *Environ. Sci. Technol.* **1989**, *23*, 1290–1301.

[23] Russell, A. G.; St. Pierre, D.; and Milford, J. B. *Science.* **1990**, *247*, 201–205.

[24] Russell, A. G.; Winner, D. A.; McCue, K. F.; and Cass, G. R. Mathematical modeling and control of the dry deposition flux of nitrogen-containing air pollutants. EQL Report 29, Environmental Quality Laboratory, California Institute of Technology, Pasadena, CA, 1992. Report to the California Air Resources Board under contract A6-188-32.

[25] Harley, R. A.; Russell, A. G.; McRae, G. J.; McNair, L. A.; Winner, D. A.; Odman, M. T.; Dabdub, D.; Cass, G. R.; and Seinfeld, J. H. Continued development of a photochemical model and application to the Southern California Air Quality Study (SCAQS) intensive monitoring periods: Phase I. Carnegie Mellon University, Pittsburgh, PA and California Institute of Technology, Pasadena, CA, 1992. Report to the Coordinating Research Council under project SCAQS-8.

[26] McRae, G. J.; Russell, A. G.; and Harley, R. A. CIT photochemical airshed model — installation and operation manual. Carnegie Mellon University, Pittsburgh, PA and California Institute of Technology, Pasadena, CA, 1992. Report to the Coordinating Research Council under project SCAQS-8.

[27] McRae, G. J.; Russell, A. G.; and Harley, R. A. CIT photochemical airshed model — data preparation manual. Carnegie Mellon Univer-

sity, Pittsburgh, PA and California Institute of Technology, Pasadena, CA, 1992. Report to the Coordinating Research Council under project SCAQS-8.

[28] McRae, G. J.; Russell, A. G.; and Harley, R. A. CIT photochemical airshed model — systems manual. Carnegie Mellon University, Pittsburgh, PA and California Institute of Technology, Pasadena, CA, 1992. Report to the Coordinating Research Council under project SCAQS-8.

[29] Carter, W. P. L. *Atmos. Environ.* **1990**, *24A*, 481–518.

[30] Japar, S. M.; Wallington, T. J.; Richert, J. F. O.; and Ball, J. C. *Int. J. Chem. Kinet.* **1990**, *22*, 1257–1269.

[31] Atkinson, R. *Atmos. Environ.* **1990**, *24A*, 1–41.

[32] Russell, A. G.; McRae, G. J.; and Cass, G. R. *Atmos. Environ.* **1983**, *17*, 949–964.

[33] Russell, A. G. and Cass, G. R. *Atmos. Environ.* **1986**, *20*, 2011–2025.

[34] Businger, J. A.; Wyngaard, J. C.; Izumi, Y.; and Bradley, E. F. *J. Atmos. Sci.* **1971**, *28*, 181–189.

[35] Sheih, C. M.; Wesely, M. L.; and Walcek, C. J. A dry deposition module for regional acid deposition. Atmospheric sciences laboratory, US Environmental Protection Agency, Research Triangle Park, NC, 1986. EPA-600/3-86-037.

[36] Peterson, J. T. Calculated actinic fluxes (290-700 nm) for air pollution photochemistry applications. US Environmental Protection Agency, Research Triangle Park, NC, 1976. EPA-600/4-76-025.

[37] Zafonte, L.; Rieger, P. L.; and Holmes, J. R. *Environ. Sci. Technol.* **1977**, *11*, 483–487.

[38] Madronich, S. *Atmos. Environ.* **1987**, *21*, 569–578.

[39] Holtslag, A. A. M. and Ulden, A. P. V. *J. Climate Appl. Meteorol.* **1983**, *22*, 517–529.

[40] Mirabella, V. and Nazemi, M. Development of the SCAQS emission inventory: an overview. Paper no. 89-111.4 presented at the 82nd annual meeting of the Air and Waste Management Association, Anaheim, CA, 1989.

[41] Wagner, K. K. and Allen, P. D. SCAQS emissions inventory for August 27–29, 1987 (Tape ARA714). Technical Support Division, California Air Resources Board, Sacramento, CA, 1990. Personal communication.

[42] Yotter, E. E. and Wade, D. L. Development of a gridded motor vehicle emission inventory for the Southern California Air Quality Study. Paper no. 89-137.2 presented at the 82nd annual meeting of the Air and Waste Management Association, Anaheim, CA, 1989.

[43] Winer, A. M. Investigation of the role of natural hydrocarbons in photochemical smog formation in California. Statewide Air Pollution Research Center, University of California, Riverside, CA, 1983. Report to the California Air Resources Board under contract A0-056-32.

[44] Winer, A. M.; Arey, J.; Aschmann, S. M.; Atkinson, R.; Long, W. D.; Morrison, L. C.; and Olszyk, D. M. Hydrocarbon emissions from vegetation found in California's Central Valley. Statewide Air Pollution Research Center, University of California, Riverside, CA, 1989. Report to the California Air Resources Board under contract A732-155.

[45] Horie, Y.; Sidawi, S.; and Ellefsen, R. Inventory of leaf biomass and emission factors for vegetation in the South Coast Air Basin. Valley Research Inc., Van Nuys, CA, 1990. Report to the South Coast Air Quality Management District under contract 90163.

[46] Causley, M. C. and Wilson, G. M. Seasonal and annual average biogenic emissions for the South Coast Air Basin generated by the SCAQMD biogenic data base system. Systems Applications International, San Rafael, CA, 1991. Report to the South Coast Air Quality Management District under contract 90177.

[47] Gharib, S. and Cass, G. R. Ammonia emissions in the South Coast Air Basin. Environmental Quality Laboratory, California Institute of Technology, Pasadena, CA, 1984. Open file report 84-2.

[48] Dickson, R. J. and Oliver, W. R. Approach to developing the SCAQS high-resolution ammonia emission inventory. Paper no. 89-137.6 presented at the 82nd annual meeting of the Air and Waste Management Association, Anaheim, CA, 1989.

[49] Croes, B. E. Research Division, California Air Resources Board, Sacramento, CA, 1990. Personal communication.

[50] Goodin, W. R.; McRae, G. J.; and Seinfeld, J. H. *J. Appl. Meteorol.* **1979**, *18*, 761–771.

[51] Goodin, W. R.; McRae, G. J.; and Seinfeld, J. H. *J. Appl. Meteorol.* **1980**, *19*, 98–108.

[52] Lehrman, D.; Knuth, W.; Alexander, N.; Giroux, H.; and Lehrman, L. SCAQS meteorological support program. Technical & Business Systems, Santa Rosa, CA, 1988. Report to the California Air Resources Board under contract A6-097-32.

[53] Hanna, S. R. and Chang, J. C. *Boundary Layer Meteorol.* **1992**, *58*, 229–259.

[54] McRae, G. J. *J. Air Pollut. Control Assoc.* **1980**, *30*, 394–396.

[55] Anderson, J. A.; Koos, J. C.; and Hammarstrand, R. G. M. Sum-

mary of SCAQS upper air measurements performed by the STI aircraft. Sonoma Technology Inc., Santa Rosa, CA, 1989. Report to the California Air Resources Board under contract A6-098-32.

[56] Main, H. H.; Lurmann, F. W.; and Roberts, P. T. Pollutant concentrations along the western boundary of the South Coast Air Basin. Part I: a review of existing data. Sonoma Technology, Inc., Santa Rosa, CA, 1990. Report to the South Coast Air Quality Management District.

[57] Stockburger, L.; Knapp, K. T.; and Ellestad, T. G. Overview and analysis of hydrocarbon samples during the summer Southern California Air Quality Study. Paper no. 89-139.1 presented at the 82nd annual meeting of the Air and Waste Management Association, Anaheim, CA, 1989.

[58] Ozone modeling — performance evaluation. South Coast Air Quality Management District, El Monte, CA, 1990. Draft Technical Report V-B, Air Quality Management Plan, 1991 Revision.

[59] Winer, A. M.; Peters, J. W.; Smith, J. P.; and Pitts, J. N. *Environ. Sci. Technol.* **1974**, *8*, 1118–1121.

[60] Lonneman, W. A.; Seila, R. L.; and Ellenson, W. Speciated hydrocarbon and NO_x comparisons at SCAQS source and receptor sites. Paper no. 89-152.5 presented at the 82nd annual meeting of the Air and Waste Management Association, Anaheim, CA, 1989.

[61] Tesche, T. W.; Georgopoulos, P.; Seinfeld, J. H.; Cass, G. R.; Lurmann, F. W.; and Roth, P. M. Improvement of procedures for evaluating photochemical models. Radian Corporation, Sacramento, CA, 1990. Report to the California Air Resources Board under contract A832-103.

[62] DaMassa, J. Technical guidance document: photochemical modeling. Technical Support Division, California Air Resources Board, Sacramento, CA, 1992.

[63] VOC/PM speciation data system documentation and user's guide, version 1.32a. Radian Corporation, Research Triangle Park, NC, 1990. EPA-450/2-91-002.

[64] Lawson, D. R.; Groblicki, P. J.; Stedman, D. H.; Bishop, G. A.; and Guenther, P. L. *J. Air Waste Manage. Assoc.* **1990**, *40*, 1096–1105.

[65] Carlock, M. A. Mobile Source Division, California Air Resources Board, El Monte, CA, 1992. Personal communication.

[66] Lawson, D. R. and Hering, S. V. *Aerosol Sci. Technol.* **1990**, *12*, 1–2.

[67] Carter, W. P. L. and Atkinson, R. *Environ. Sci. Technol.* **1989**, *23*, 864–880.

[68] Oliver, W. R. and Peoples, S. H. Improvement of the emission inventory for reactive organic gases and oxides of nitrogen in the South Coast Air Basin. Systems Applications, Inc., San Rafael, CA, 1985. Report to the California Air Resources Board under contract A2-076-32.

[69] Kulakowski, J. M. UNOCAL Refining and Marketing, Los Angeles, CA, 1990. Personal communication.

[70] Gary, J. H. and Handwerk, G. E. *Petroleum refining — technology and economics.* Marcel Dekker, Inc., New York, NY, second edition, 1984. pp. 8–9.

[71] Jackson, M. W. *SAE Tech. Pap. Ser.* **1978**, No. 780624.

[72] Black, F. M. and High, L. E. *J. Air Pollut. Control Assoc.* **1980**, *30*, 1216–1221.

[73] Nelson, P. F. and Quigley, S. M. *Atmos. Environ.* **1984**, *18*, 79–87.

[74] Cohu, L. K.; Rapp, L. A.; and Segal, J. S. EC–1 emission control gasoline. ARCO Products Company, Anaheim, CA, 1989.

[75] Black, F. M. and High, L. E. *SAE Tech. Pap. Ser.* **1977**, No. 770144.

[76] Smith, L. R. Characterization of exhaust emissions from high mileage catalyst-equipped automobiles. Southwest Research Institute, San Antonio, TX, 1981. EPA-460/3-81-024.

[77] Sigsby, J. E.; Tejada, S.; Ray, W.; Lang, J. M.; and Duncan, J. W. *Environ. Sci. Technol.* **1987**, *21*, 466–475.

[78] Stump, F.; Tejada, S.; Ray, W.; Dropkin, D.; Black, F.; Crews, W.; Snow, R.; Siudak, P.; Davis, C. O.; Baker, L.; and Perry, N. *Atmos. Environ.* **1989**, *23*, 307–320.

[79] Stump, F.; Tejada, S.; Ray, W.; Dropkin, D.; Black, F.; Snow, R.; Crews, W.; Siudak, P.; Davis, C. O.; and Carter, P. *Atmos. Environ.* **1990**, *24A*, 2105–2112.

[80] Burns, V. R.; Benson, J. D.; Hochhauser, A. M.; Koehl, W. J.; Kreucher, W. M.; and Reuter, R. M. *SAE Tech. Pap. Ser.* **1991**, No. 912320.

[81] Hampton, C. V.; Pierson, W. R.; Harvey, T. M.; Updegrove, W. S.; and Marano, R. S. *Environ. Sci. Technol.* **1982**, *16*, 287–298.

[82] Hampton, C. V.; Pierson, W. R.; Schuetzle, D.; and Harvey, T. M. *Environ. Sci. Technol.* **1983**, *17*, 699–708.

[83] Lonneman, W. A.; Seila, R. L.; and Meeks, S. A. *Environ. Sci. Technol.* **1986**, *20*, 790–796.

[84] Dannecker, W.; Schroder, B.; and Strechmann, H. *Sci. Total Environ.* **1990**, *93*, 293–300.

[85] Ingalls, M. N. and Smith, L. R. Measurement of on-road vehicle emis-

sion factors in the California South Coast Air Basin. Volume II: unregulated emissions. Southwest Research Institute, San Antonio, TX, 1990. Report to the Coordinating Research Council under project SCAQS-1.

[86] Zweidinger, R. B.; Sigsby, J. E.; Tejada, S. B.; Stump, F. D.; Dropkin, D. L.; Ray, W. D.; and Duncan, J. W. *Environ. Sci. Technol.* **1988**, *22*, 956–962.

[87] Bailey, J. C.; Schmidl, B.; and Williams, M. L. *Atmos. Environ.* **1990**, *24A*, 43–52.

[88] Aldehyde and reactive organic emissions from motor vehicles. Part II – characterization of emissions from 1970 through 1973 model vehicles. US Environmental Protection Agency, Ann Arbor, MI, 1973. APTD-1568b.

[89] Warner-Selph, M. A. Measurements of toxic exhaust emissions from gasoline-powered light-duty vehicles. Southwest Research Institute, San Antonio, TX, 1989. Report to the California Air Resources Board under contract A6-198-32.

[90] Leppard, W. R.; Rapp, L. A.; Burns, V. R.; Gorse, R. A.; Knepper, J. C.; and Koehl, W. J. *SAE Tech. Pap. Ser.* **1992**, No. 920329.

[91] Hirata, A. A. South Coast Recycled Auto Project (SCRAP). Unocal Corporation, Los Angeles, CA, 1990. Personal communication.

[92] Volatile organic compound species data manual (2nd edition). US Environmental Protection Agency, Research Triangle Park, NC, 1980. EPA-450/4-80-015; NTIS PB81-119455.

[93] Bradow, R. L. Bradow & Associates, Raleigh, NC, 1991. Personal communication.

[94] Spicer, C. W. Composition and photochemical reactivity of turbine

engine exhaust. Batelle Columbus Laboratories, Columbus, OH, 1984. Report ESL-TR-84-28 prepared for US Air Force Engineering and Services Center.

[95] Hoekman, S. K. Chevron Research and Technology Company, Richmond, CA, 1991. Personal communication.

[96] Rogozen, M. B.; Rapoport, R. D.; and Shochet, A. Development and improvement of organic compound emissions inventories for California. Science Applications International Corp., Hermosa Beach, CA, 1985. Report to the California Air Resources Board under contract A0-101-32.

[97] Results of the 1988 architectural coatings sales survey. Stationary Source Division, California Air Resources Board, Sacramento, CA, 1991.

[98] Ameritone Products MSDS Manual. Ameritone Paint Corp., Long Beach, CA, 1988.

[99] Material Safety Data Sheets. Old Quaker Paint Co., Victorville, CA, 1991.

[100] Material Safety Data Sheets. Decratrend Paint Co., Industry, CA, 1988.

[101] Material Safety Data Sheets. Dunn-Edwards Co., Los Angeles, CA, 1986.

[102] Material Safety Data Sheets. Sinclair Paint Co., Los Angeles, CA, 1990.

[103] Lawson, D. R. Research Division, California Air Resources Board, Sacramento, CA, 1990. Personal communcation.

[104] Miller, M. S.; Friedlander, S. K.; and Hidy, G. M. *J. Colloid Interface*

Sci. **1972**, *39*, 165–176.

[105] Friedlander, S. K. *Environ. Sci. Technol.* **1973**, *7*, 235–240.

[106] Mayrsohn, H. and Crabtree, J. H. *Atmos. Environ.* **1976**, *10*, 137–143.

[107] Nelson, P. F.; Quigley, S. M.; and Smith, M. Y. *Atmos. Environ.* **1983**, *17*, 439–449.

[108] Scheff, P. A. and Klevs, M. *J. Environ. Eng.* **1987**, *113*, 994–1005.

[109] O'Shea, W. J. and Scheff, P. A. *J. Air Pollut. Control Assoc.* **1988**, *38*, 1020–1026.

[110] Aronian, P. F.; Scheff, P. A.; and Wadden, R. A. *Atmos. Environ.* **1989**, *23*, 911–920.

[111] Cass, G. R. and McRae, G. J. *Environ. Sci. Technol.* **1983**, *17*, 129–139.

[112] Receptor model technical series, Volume III. CMB7 User's Manual. US Environmental Protection Agency, Research Triangle Park, NC, 1990. EPA-450/4-90-004.

[113] Chan, M. and Durkee, K. Southern California Air Quality Study B-Site operations. Aerovironment Inc., Monrovia, CA, 1989. Report to the California Air Resources Board under contract A5-196-32.

[114] Rasmussen, R. A. SCAQS hydrocarbon collection and analyses (Part I). Biospherics Research Corporation, Hillsboro, OR, 1990. Report to the California Air Resources Board under contract A6-179-32.

[115] Finlayson-Pitts, B. J. and Pitts, J. N. *Atmospheric chemistry — fundamentals and experimental techniques.* John Wiley and Sons, New York, NY, first edition, 1986. pp. 313–316.

[116] Gorse, R. A. *Environ. Sci. Technol.* **1984**, *18*, 500–507.

[117] Wesely, M. L. *Atmos. Environ.* **1989**, *23*, 1293–1304.

[118] Garland, J. A. and Penkett, S. A. *Atmos. Environ.* **1976**, *18*, 1737–1750.

[119] Fung, K. Carbonyl observations during the SCAQS. Paper no. 89-152.3 presented at the 82nd annual meeting of the Air and Waste Management Association, Anaheim, CA, 1989.

[120] Lurmann, F. W. and Main, H. H. Analysis of the ambient VOC data collected in the Southern California Air Quality Study. Sonoma Technology Inc., Santa Rosa, CA, 1992. Report to the California Air Resources Board under contract A832-130.

[121] Klosterman, D. L. and Sigsby, J. E. *Environ. Sci. Technol.* **1968**, *1*, 309–314.

[122] Winer, A. M.; Biermann, H. W.; Dinoff, T.; Parker, L.; and Poe, M. P. Measurements of nitrous acid, nitrate radicals, formaldehyde, and nitrogen dioxide for SCAQS by differential optical absorption spectroscopy. Statewide Air Pollution Research Center, University of California, Riverside, CA, 1989. Report to the California Air Resources Board under contract A6-146-32.

[123] Mackay, G. I.; Karecki, D. R.; and Schiff, H. I. SCAQS: tunable diode laser absorption spectrometer measurements of H2O2 and H2CO at the Claremont and Long Beach "A" sites. Unisearch Associates, Concord, Ontario, Canada, 1988. Report to the California Air Resources Board under contract A732-073.

[124] Williams, E. L. and Grosjean, D. *Atmos. Environ.* **1990**, *24A*, 2369–2377.

[125] Fujita, E. M. Research Division, California Air Resources Board, Sacramento, CA, 1991. Personal communication.

[126] Carter, W. P. L. and Atkinson, R. Development and implementation of an up-to-date photochemical mechanism for use in airshed modeling. Statewide Air Pollution Research Center, Riverside, CA, 1988. Report to the California Air Resources Board under contract A5-122-32.

[127] Carter, W. P. L. Statewide Air Pollution Research Center, University of California, Riverside, CA, 1992. Personal communication.

[128] Atkinson, R.; Baulch, D. L.; Cox, R. A.; Hampson, R. F.; Kerr, J. A.; and Troe, J. *Atmos. Environ.* **1991**, *26A*, 1187–1230.

[129] Chang, J. S.; Brost, R. A.; Isaksen, I. S. A.; Madronich, S.; Middleton, P.; Stockwell, W. R.; and Walcek, C. J. *J. Geophys. Res.* **1987**, *92*(D12), 14681–14700.

[130] Shah, J. J. and Singh, H. B. *Environ. Sci. Technol.* **1988**, *22*, 1381–1388.

[131] Evans, G. F.; Lumpkin, T. A.; Smith, D. L.; and Somerville, M. C. *J. Air Waste Manage. Assoc.* **1992**, *42*, 1319–1323.

[132] Goldstein, B. D. *J. Air Pollut. Control Assoc.* **1983**, *33*, 454–467.

[133] Goldstein, B. D. *J. Air Pollut. Control Assoc.* **1986**, *36*, 367–370.

[134] National Research Council. *The alkyl benzenes.* National Academy Press, Washington, D.C., 1981.

[135] National Research Council. *Formaldehyde and other aldehydes.* National Academy Press, Washington, D.C., 1981.

[136] Grosjean, D. *J. Air Waste Manage. Assoc.* **1990**, *40*, 1397–1402.

[137] Grosjean, D. *J. Air Waste Manage. Assoc.* **1990**, *40*, 1522–1531.

[138] Grosjean, D. *J. Air Waste Manage. Assoc.* **1990**, *40*, 1664–1668.

[139] Grosjean, D. *Sci. Total Environ.* **1991**, *100*, 367–414.

[140] Hughes, K. Proposed identification of 1,3-butadiene as a toxic air con-

taminant. Part A: exposure assessment. Stationary Source Division, California Air Resources Board, Sacramento, CA, 1992.

[141] Hughes, K. Proposed identification of 1,3-butadiene as a toxic air contaminant. Part B: health assessment. Stationary Source Division, California Air Resources Board, Sacramento, CA, 1992.

[142] Grosjean, D.; Swanson, R. D.; and Ellis, C. *Sci. Total Environ.* **1983**, *29*, 65–85.

[143] Atkinson, R.; Aschmann, S. M.; Arey, J.; and Carter, W. P. L. *Int. J. Chem. Kinet.* **1989**, *21*, 801–827.

[144] Altshuller, A. P. *J. Atmos. Chem.* **1991**, *12*, 19–61.

[145] Gardner, E. P.; Sperry, P. D.; and Calvert, J. G. *J. Phys. Chem.* **1987**, *91*, 1922–1930.

[146] Atkinson, R.; Aschmann, S. M.; and Arey, J. *Environ. Sci. Technol.* **1992**, *26*, 1397–1403.

[147] Gery, M. W.; Fox, D. L.; Jeffries, H. E.; Stockburger, L.; and Weathers, W. S. *Int. J. Chem. Kinet.* **1985**, *17*, 931–955.

[148] Westerholm, R. N.; Almén, J.; Li, H.; Rannug, J. U.; Egebäck, K.; and Grägg, K. *Environ. Sci. Technol.* **1991**, *25*, 332–338.

[149] Smith, L. R. Characterization of exhaust emissions from trap-equipped light-duty diesels. Southwest Research Institute, San Antonio, TX, 1989. Report to the California Air Resources Board under contract A5-159-32.

[150] Hawthorne, S. B.; Krieger, M. S.; Miller, D. J.; and Mathiason, M. B. *Environ. Sci. Technol.* **1989**, *23*, 470–475.

[151] Wallace, L. A. *Environ. Health Perspect.* **1989**, *82*, 165–169.

[152] Williams, E. L. and Grosjean, D. SCAQS: peroxyacetyl nitrate (PAN)

measurements. DGA Inc., Ventura, CA, 1989. Report to the California Air Resources Board under contract A6-099-32.

[153] Hisham, M. W. M. and Grosjean, D. Southern California Air Quality Study: toxic air contaminants, task I. DGA Inc., Ventura, CA, 1990. Report to the California Air Resources Board under contract A832-152.

[154] Hisham, M. W. M. and Grosjean, D. *Environ. Sci. Technol.* **1991**, *25*, 1930–1936.

[155] Leuenberger, C.; Ligocki, M. P.; and Pankow, J. F. *Environ. Sci. Technol.* **1985**, *19*, 1053–1058.

[156] Mulawa, P. A. and Cadle, S. H. *Analytical Letters.* **1981**, *14*, 671–687.

A LCC chemical mechanism

In this appendix, a complete listing of the condensed version of the LCC chemical mechanism (Lurmann, Carter, and Coyner [11]) is presented. Reaction rate constants are expressed in $ppm^{-1}\ min^{-1}$ units, with the temperature specified in degrees Kelvin.

```
1.    NO2  + HV          ----> 1.0 NO   + 1.0 O
         RK(  1) =  depends on light intensity
2.    O                  ----> 1.0 O3
         RK(  2) = 6.30E+04*EXP(1282/TEMP)
3.    O    + NO2         ----> 1.0 NO
         RK(  3) = 4.083E+06/TEMP
4.    O    + NO2         ----> 1.0 NO3
         RK(  4) = 48890/TEMP*EXP(894/TEMP)
5.    NO   + O3          ----> 1.0 NO2
         RK(  5) = 7.93E+05/TEMP*EXP(-1370/TEMP)
6.    NO2  + O3          ----> 1.0 NO3
         RK(  6) = 5.285E+04/TEMP*EXP(-2450/TEMP)
7.    NO   + NO3         ----> 2.0 NO2
         RK(  7) = 3.52E+06/TEMP*EXP(252/TEMP)
8.    NO   + NO          ----> 2.0 NO2
         RK(  8) = 7.22E-03/TEMP*EXP(529/TEMP)
9.    NO2  + NO3         ----> 1.0 N2O5
         RK(  9) = 2.035E+05/TEMP*EXP(273/TEMP)
```

```
10.   N2O5              ----> 1.0 NO2  + 1.0 NO3
         RK( 10) = 7.98E+16*EXP(-11379/TEMP)
11.   N2O5 + H2O        ----> 2.0 HNO3
         RK( 11) = 4.41E-04/TEMP
12.   NO2  + NO3        ----> 1.0 NO   + 1.0 NO2
         RK( 12) = 1.10E+04/TEMP*EXP(-1229/TEMP)
13.   NO3  + HV         ----> 1.0 NO
         RK( 13) =  depends on light intensity
14.   NO3  + HV         ----> 1.0 NO2  + 1.0 O
         RK( 14) =  depends on light intensity
15.   O3   + HV         ----> 1.0 O
         RK( 15) =  depends on light intensity
16.   O3   + HV         ----> 1.0 OSD
         RK( 16) =  depends on light intensity
17.   OSD  + H2O        ----> 2.0 OH
         RK( 17) = 9.69E+07/TEMP
18.   OSD               ----> 1.0 O
         RK( 18) = 4.32E+10
19.   NO   + OH         ----> 1.0 HONO
         RK( 19) = 1.78E+05/TEMP*EXP(833/TEMP)
20.   HONO + HV         ----> 1.0 NO   + 1.0 OH
         RK( 20) =  depends on light intensity
21.   NO2  + H2O        ----> 1.0 HONO + -1. NO2  + 1.0 HNO3
         RK( 21) = 1.76E-06/TEMP
22.   NO2  + OH         ----> 1.0 HNO3
         RK( 22) = 4.22E+05/TEMP*EXP(737/TEMP)
23.   HNO3 + OH         ----> 1.0 NO3
         RK( 23) = 4.14E+03/TEMP*EXP(778/TEMP)
```

```
24.   CO   + OH          ----> 1.0 HO2
         RK( 24) = 9.60E+04/TEMP
25.   O3   + OH          ----> 1.0 HO2
         RK( 25) = 7.05E+05/TEMP*EXP(-942/TEMP)
26.   NO   + HO2         ----> 1.0 NO2  + 1.0 OH
         RK( 26) = 1.63E+06/TEMP*EXP(240/TEMP)
27.   NO2  + HO2         ----> 1.0 HNO4
         RK( 27) = 4.493E+04/TEMP*EXP(773/TEMP)
28.   HNO4               ----> 1.0 NO2  + 1.0 HO2
         RK( 28) = 2.61E+15*EXP(-10103/TEMP)
29.   HNO4 + OH          ----> 1.0 NO2
         RK( 29) = 1.76E+06/TEMP
30.   O3   + HO2         ----> 1.0 OH
         RK( 30) = 6.17E+03/TEMP*EXP(-579/TEMP)
31.   HO2  + HO2         ----> 1.0 H2O2
         RK( 31) = 1.00E+05/TEMP*EXP(771/TEMP)
32.   HO2  + HO2  + H2O ----> 1.0 H2O2
         RK( 32) = 1.054/(TEMP*TEMP)*EXP(2971/TEMP)
33.   NO3  + HO2         ----> 1.0 HNO3
         RK( 33) = 1.00E+05/TEMP*EXP(771/TEMP)
34.   NO3  + HO2  + H2O ----> 1.0 HNO3
         RK( 34) =  1.054/(TEMP*TEMP)*EXP(2971/TEMP)
35.   RO2  + NO          ----> 1.0 NO
         RK( 35) = 1.85E+06/TEMP*EXP(180/TEMP)
36.   RO2  + HO2         ----> 1.0 HO2
         RK( 36) = 1.32E+06/TEMP
37.   RO2  + RO2         ---->
         RK( 37) = 441.0/TEMP
```

```
38.   RO2  + MCO3        ---->
         RK( 38) = 1.32E+06/TEMP
39.   HCHO + HV          ----> 2.0 HO2  + 1.0 CO
         RK( 39) =  depends on light intensity
40.   HCHO + HV          ----> 1.0 CO
         RK( 40) =  depends on light intensity
41.   HCHO + OH          ----> 1.0 HO2  + 1.0 CO
         RK( 41) = 3.93E+06/TEMP
42.   HCHO + NO3         ----> 1.0 HNO3 + 1.0 HO2  + 1.0 CO
         RK( 42) = 2.64E+05/TEMP*EXP(-2060/TEMP)
43.   HCHO + HO2         ----> 1.0 RO2R + 1.0 RO2
         RK( 43) = 4.41E+03/TEMP
44.   ALD2 + OH          ----> 1.0 MCO3
         RK( 44) = 3.039E+06/TEMP*EXP(250/TEMP)
45.   ALD2 + HV          ----> 1.0 CO   + 1.0 HCHO + 1.0 RO2R   + 1.0 HO2
                                       + 1.0 RO2
         RK( 45) =  depends on light intensity
46.   ALD2 + NO3         ----> 1.0 HNO3 + 1.0 MCO3
         RK( 46) = 1.32E+05/TEMP*EXP(-1427/TEMP)
47.   MCO3 + NO          ----> 1.0 NO2  + 1.0 HCHO + 1.0 RO2R + 1.0 RO2
         RK( 47) = 1.85E+06/TEMP*EXP(180/TEMP)
48.   MCO3 + NO2         ----> 1.0 PAN
         RK( 48) = 1.23E+06/TEMP*EXP(180/TEMP)
49.   MCO3 + HO2         ----> 1.0 HCHO
         RK( 49) = 1.32E+06/TEMP
50.   MCO3 + MCO3        ----> 2.0 HO2  + 2.0 HCHO
         RK( 50) = 1.1E+06/TEMP
51.   PAN                ----> 1.0 MCO3 + 1.0 NO2
```

```
      RK( 51) = 1.2E+18*EXP(-13542/TEMP)
52.   MEK  + HV          ----> 1.0 MCO3 + 1.0 ALD2 + 1.0 RO2R + 1.0 RO2
      RK( 52) =  depends on light intensity
53.   MEK  + OH          ----> 1.2 R2O2 + 1.2 RO2  + 1.0 MCO3 + .5 ALD2
                                      + 0.5 HCHO
      RK( 53) = 5.285E+06/TEMP*EXP(-745/TEMP)
54.   MGLY + HV          ----> 1.0 MCO3 + 1.0 HO2  + 1.0 CO
      RK( 54) =  depends on light intensity
55.   MGLY + OH          ----> 1.0 MCO3 + 1.0 CO
      RK( 55) = 7.48E+06/TEMP
56.   MGLY + NO3         ----> 1.0 HNO3 + 1.0 MCO3 + 1.0 CO
      RK( 56) = 1.321E+05/TEMP*EXP(-1427/TEMP)
57.   ALKA + OH          ----> BO1 HCHO + BO2 ALD2 + BO3 MEK + BO4 RO2N
                               BO5 RO2R + BO6 R2O2 + BO7 RO2
      RK( 57) = 4.40E+17/TEMP*
        (1.053E-11*EXP(-354/TEMP)*X + 1.62E-11*EXP(-289/TEMP)*XT)
58.   ALKN + OH          ----> 1.0 NO2  + 0.15 MEK  + 1.53 ALD2 + 0.16 HCHO
                                      + 1.39 R2O2 + 1.39 RO2
      RK( 58) = 9.65E+06/TEMP*EXP(-709/TEMP)
59.   RO2N + NO          ----> 1.0 ALKN
      RK( 59) = 1.85E+06/TEMP*EXP(180/TEMP)
60.   RO2N + HO2         ----> 1.0 MEK
      RK( 60) = 1.32E+06/TEMP
61.   RO2N + RO2         ----> 1.0 RO2  + 1.0 HO2  + 1.0 MEK
      RK( 61) = 441.0/TEMP
62.   RO2N + MCO3        ----> 1.0 HCHO + 1.0 HO2  + 1.0 MEK
      RK( 62) = 1.32E+06/TEMP
63.   R2O2 + NO          ----> 1.0 NO2
```

```
      RK( 63) = 1.85E+06/TEMP*EXP(180/TEMP)
64.   R2O2 + HO2          ---->
      RK( 64) = 1.32E+06/TEMP
65.   R2O2 + RO2          ----> 1.0 RO2
      RK( 65) = 441.0/TEMP
66.   R2O2 + MCO3         ----> 1.0 HCHO + 1.0 HO2
      RK( 66) = 1.32E+06/TEMP
67.   RO2R + NO           ----> 1.0 NO2  + 1.0 HO2
      RK( 67) = 1.85E+06/TEMP*EXP(180/TEMP)
68.   RO2R + HO2          ---->
      RK( 68) = 1.32E+06/TEMP
69.   RO2R + RO2          ----> 0.5 HO2  + 1.0 RO2
      RK( 69) = 441.0/TEMP
70.   RO2R + MCO3         ----> 1.0 HO2  + 1.0 HCHO
      RK( 70) = 1.32E+06/TEMP
71.   ETHE + OH           ----> 1.0 RO2R + 1.0 RO2  + 1.56 HCHO + 0.22 ALD2
      RK( 71) = 9.47E+05/TEMP*EXP(411/TEMP)
72.   ETHE + O3           ----> 1.0 HCHO + 0.12 HO2 + 0.42 CO
      RK( 72) = 5.28E+03/TEMP*EXP(-2634/TEMP)
73.   ETHE + O            ----> 1.0 RO2R + 1.0 RO2  + 1.0 CO  + 1.0 HCHO
                                          + 1.0 HO2
      RK( 73) = 4.58E+06/TEMP*EXP(-792/TEMP)
74.   ETHE + NO3          ----> 1.0 RO2  + 1.0 NO2  + 2.0 HCHO + 1.0 R2O2
      RK( 74) = 8.81E+05/TEMP*EXP(-2925/TEMP)
75.   ALKE + OH           ----> 1.0 RO2  + 1.0 RO2  + B08 HCHO + B09 ALD2
      RK( 75) = 4.40E+17/TEMP*
        (4.85E-12*EXP(504/TEMP)*Y + 1.01E-11*EXP(549/TEMP)*YT)
76.   ALKE + O3           ----> B10 HCHO + B11 ALD2 + B12 RO2R + B12 RO2
```

```
                                    + B13 HO2  + B14 OH   + B15 CO
      RK( 76) = 4.40E+17/TEMP*
        (1.32E-14*EXP(-2105/TEMP)*Y + 9.08E-15*EXP(-1137/TEMP)*YT)
77.   ALKE + O          ----> B16 CO   + B17 MEK  + B18 HCHO + B19 ALD2
                                    + B20 HO2  + B21 RO2R + B21 RO2
      RK( 77) = 4.40E+17/TEMP*
        (1.18E-11*EXP(-324/TEMP)*Y + 2.26E-11*EXP(10/TEMP)*YT)
78.   ALKE + NO3        ----> 1.0 NO2  + B08 HCHO + B09 ALD2 + 1.0 R202
                                    + 1.0 RO2
      RK( 78) = 4.40E+17/TEMP*
        (5.00E-12*EXP(-1935/TEMP)*Y + 1.00E-11*EXP(-975/TEMP)*YT)
79.   TOLU + OH         ----> 0.16 CRES + .16 HO2  + .84 RO2R + .4 DIAL
                                    + .84 RO2  + .144MGLY
                                    + .114 HCHO +  .114CO
      RK( 79) = 9.25E+05/TEMP*EXP(322/TEMP)
80.   AROM + OH         ----> 0.17 CRES + .17 HO2  + .83 RO2R + .83 RO2
                                    + B22 DIAL + B23 MGLY + B24 CO
                                    + B24 HCHO
      RK( 80) = 4.40E+17/TEMP*
          (1.66E-11*EXP(116/TEMP)*Z + 6.20E-11*ZT)
81.   DIAL + OH         ----> 1.0 MCO3
      RK( 81) = 1.32E+07/TEMP
82.   DIAL + HV         ----> 1.0 HO2  + 1.0 CO   + 1.0 MCO3
      RK( 82) =  depends on light intensity
83.   CRES + OH         ----> 0.2 MGLY + 0.15 RO2P + 0.85 RO2R + 1.0 RO2
      RK( 83) = 1.76E+07/TEMP
84.   CRES + NO3        ----> 1.0 HNO3 + 1.0 BZO
      RK( 84) = 9.66E+06/TEMP
```

```
85.   RO2P + NO          ----> 1.0 NPHE
         RK( 85) = 1.85E+06/TEMP*EXP(180/TEMP)
86.   RO2P + HO2         ---->
         RK( 86) = 1.32E+06/TEMP
87.   RO2P + RO2         ----> 0.5 HO2  + 1.0 RO2
         RK( 87) = 441.0/TEMP
88.   RO2P + MCO3        ----> 1.0 HCHO + 1.0 HO2
         RK( 88) = 1.32E+06/TEMP
89.   BZO  + NO2         ----> 1.0 NPHE
         RK( 89) = 6.62E+06/TEMP
90.   BZO  + HO2         ---->
         RK( 90) = 1.32E+06/TEMP
91.   BZO                ---->
         RK( 91) = 0.06
92.   NPHE + NO3         ----> 1.0 HNO3 + 1.0 BZN2
         RK( 92) = 1.68E+06/TEMP
93.   BZN2 + NO2         ---->
         RK( 93) = 6.62E+06/TEMP
94.   BZN2 + HO2         ----> 1.0 NPHE
         RK( 94) = 1.32E+06/TEMP
95.   BZN2               ----> 1.0 NPHE
         RK( 95) = 0.06
96.   H2O2 + HV          ----> 2.0 OH
         RK( 96) =  depends on light intensity
97.   H2O2 + OH          ----> 1.0 HO2
         RK( 97) = 1.36E+06/TEMP*EXP(-187/TEMP)
98.   MEOH + OH          ----> 1.0 HCHO + 1.0 HO2
         RK( 98) = 2.81*TEMP*EXP(148/TEMP)
```

```
99.   CH4  + OH          ----> 1.0 HCHO + 1.0 RO2 + RO2R
        RK( 99) = 3.06E+00*TEMP*EXP(-1282/TEMP)
100.  ISOP + OH          ----> HCHO + ALD2 + RO2R + RO2
        RK(100) = 1.12E+07/TEMP*EXP(410/TEMP)
101.  ISOP + O3          ----> 0.5 HCHO + 0.65 ALD2 + 0.21 MEK + 0.16 HO2
                                + 0.29 CO + 0.06 OH + 0.14 RO2R + 0.14 RO2
        RK(101) = 5.41E+03/TEMP*EXP(-2013/TEMP)
102.  ISOP + O           ----> 0.4 HO2 + 0.5 MEK + 0.5 ALD2
        RK(102) = 2.64E+07/TEMP
103.  ISOP + NO3         ----> NO2 + HCHO + ALD2 + R2O2 + RO2
        RK(103) = 1.12E+07/TEMP*EXP(-1121/TEMP)
104.  ETOH + OH          ----> ALD2 + HO2
        RK(104) = 2.72*TEMP*EXP(532/TEMP)
105.  MTBE + 1.4 OH      ----> 0.6 TBF + 0.4 HCHO + 0.4 MEK +
                                + 1.4 RO2R + 0.4 R2O2 + 1.8 RO2
        RK(105) = 3.00*TEMP*EXP(460/TEMP)
106.  SO2  + OH          ----> SO3  + HO2
        RK(106) = 4.0E+05/TEMP
```

Reactions 96 et seq. are not part of the published LCC mechanism. Refer to Table 2.2 on page 13 for a description of these extensions to the mechanism. Product yield coefficients for several of the lumped organic species depend on the mix of individual species assigned to the lumped groups. In particular, a lumped alkane parameter (X) defines the mol fraction of C_4–C_5 alkanes of the total C_4^+ alkanes. Similarly, parameter Y defines the fraction of internal alkenes of the total C_3^+ alkenes. Finally, parameter Z defines the mol fraction of dialkyl benzenes relative to total di- plus trialkyl benzenes.

The hydrocarbon product yield coefficients are set based on the mol frac-

tion parameters X, Y, and Z and the complements XT=1–X, YT=1–Y, and ZT=1–Z. The lumped alkane (ALKA) product yield coefficients are computed as a function of X, XT and temperature as follows:

```
B01 = CT(TEMP,0.197,0.189,0.188)*X + CT(TEMP,0.005,0.023,0.054)*XT
B02 = CT(TEMP,0.282,0.481,0.826)*X + CT(TEMP,0.236,0.281,0.377)*XT
B03 = CT(TEMP,0.489,0.442,0.267)*X + CT(TEMP,0.765,0.882,0.891)*XT
B04 = CT(TEMP,0.114,0.073,0.050)*X + CT(TEMP,0.288,0.190,0.126)*XT
B05 = CT(TEMP,0.886,0.927,0.950)*X + CT(TEMP,0.701,0.810,0.873)*XT
B06 = CT(TEMP,0.446,0.599,0.807)*X + CT(TEMP,0.651,0.837,1.004)*XT
B07 = B05 + B06
```

The lumped C_3^+ alkene product yields are computed as follows:

```
B08 = Y
B09 = Y       + 2.00*YT
B10 = 0.64*Y
B11 = 0.50*Y +       YT
B12 = 0.13*Y + 0.27*YT
B13 = 0.17*Y + 0.21*YT
B14 = 0.06*Y + 0.12*YT
B15 = 0.28*Y
B16 = 0.40*Y
B17 =                YT
B18 = 0.40*Y
B19 = 0.20*Y
B20 = 0.20*Y + 0.40*YT
B21 = 0.60*Y
```

Finally, the lumped aromatic (AROM) oxidation product yields are calculated as a function of Z and ZT:

```
  B22 = 0.650*Z + 0.49*ZT

  B23 = 0.316*Z + 0.86*ZT

  B24 = 0.095*Z
```

The Fortran function CT provides interpolated values depending on the temperature specified. The function is listed below:

```
      FUNCTION CT(TEMP, C1, C2, C3)
C.....LINEAR INTERPOLATION FOR 3 VALUE TABULATED FUNCTION
      T1=270.
      T2=300.
      T3=330.
      IF (TEMP .LE. T1) THEN
        CT = C1
      ELSEIF (TEMP .GE. T3) THEN
        CT = C3
      ELSEIF (TEMP .LT. T2) THEN
        SLOPE = (C2-C1)/(T2-T1)
        CT = C1 + SLOPE*(TEMP-T1)
      ELSE
        SLOPE = (C3-C2)/(T3-T2)
        CT = C2 + SLOPE*(TEMP-T2)
      ENDIF
      RETURN
      END
```

B Detailed chemical mechanisms

The chemical mechanisms used in Chapters 5 and 6 are assembled using the chemical mechanism compiler of Carter [126]. The base mechanism representing the gas phase atmospheric chemistry of inorganic species and lumped organic species is documented elsewhere [29]. The extensions to this base mechanism developed for use in the present study are documented below.

B.1 Mechanism for individual VOCs

The reactions of 53 individual VOCs that are explicitly represented (as listed in Chapter 5) are presented below. The kinetic and product yield data are from Carter [29,127].

```
!-----------------------------------------------------------------------
! UNBUNDLE.RXN:
!-----------------------------------------------------------------------
!
.ACT
!         ---- Defaults for ----
!       Conc(0)  Mwt    #C's  #N's
!
CH4       0.0    16.04   1.0    0     methane
C2H6      0.0    30.07   2.0    0     ethane
C2H2      0.0    44.10   2.0    0     acetylene
C3H8      0.0    44.10   3.0    0     propane
N-C4      0.0    58.12   4.0    0     n-butane
N-C5      0.0    72.15   5.0    0     n-pentane
N-C6      0.0    86.18   6.0    0     n-hexane
N-C7      0.0   100.20   7.0    0     n-heptane
N-C8      0.0   114.23   8.0    0     n-octane
N-C9      0.0   128.26   9.0    0     n-nonane
2MC3      0.0    58.12   4.0    0     isobutane (2-methylpropane)
2MC4      0.0    72.15   5.0    0     isopentane (2-methylbutane)
```

```
2MC5      0.0     86.18    6.0    0      2-methylpentane
3MC5      0.0     86.18    6.0    0      3-methylpentane
22C4      0.0     86.18    6.0    0      2,2-dimethylbutane
23C4      0.0     86.18    6.0    0      2,3-dimethylbutane
2MC6      0.0    100.20    7.0    0      2-methylhexane
24C5      0.0    100.20    7.0    0      2,4-dimethylpentane
23C5      0.0    100.20    7.0    0      2,3-dimethylpentane
I-C8      0.0    114.23    8.0    0      isooctane (2,2,4-trimethylpentane)
CYC5      0.0     70.13    5.0    0      cyclopentane
MCY5      0.0     84.16    6.0    0      methylcyclopentane
CYC6      0.0     84.16    6.0    0      cyclohexane
MCY6      0.0     98.19    7.0    0      methylcyclohexane
3MC6      0.0    100.20    7.0    0      3-methylhexane
ETHE      0.0     28.05    2.0    0      ethene
PRPE      0.0     42.08    3.0    0      propene
BUTE      0.0     56.11    4.0    0      butene
T2BU      0.0     56.11    4.0    0      trans-2-butene
C2BU      0.0     56.11    4.0    0      cis-2-butene
IBTE      0.0     56.11    4.0    0      isobutene
BD13      0.0     56.10    4.0    0      1,3-butadiene
ISOP      0.0     70.13    5.0    0      isoprene
APIN      0.0    136.24   10.0    0      alpha-pinene
BPIN      0.0    136.24   10.0    0      beta-pinene
C6H6      0.0     78.11    6.0    0      benzene
TOLU      0.0     92.14    7.0    0      toluene
ETBZ      0.0    106.17    8.0    0      ethylbenzene
IPBZ      0.0    120.19    9.0    0      isopropylbenzene
NPBZ      0.0    120.19    9.0    0      n-propylbenzene
XYLM      0.0    106.17    8.0    0      m-xylene
XYLO      0.0    106.17    8.0    0      o-xylene
XYLP      0.0    106.17    8.0    0      p-xylene
T135      0.0    120.19    9.0    0      1,3,5-trimethylbenzene
T123      0.0    120.19    9.0    0      1,2,3-trimethylbenzene
T124      0.0    120.19    9.0    0      1,2,4-trimethylbenzene
STYR      0.0    104.15    8.0    0      styrene
MTBE      0.0     88.15    5.0    0      methyl tert-butyl ether
TCA       0.0    133.40    2.0    0      1,1,1-trichloroethane
PERC      0.0    165.83    2.0    0      perchloroethylene
!
!
!       Format of Rate Parameter Input:
!
!       Default rate parameter input is
!               A, E, B
!       where
!               k = A * (T/TREF)**B * exp (-E/RT)
!       TREF=300K, k and A are in cm - molecule - sec units, and
```

```
!       E is in kcal/mole.
!       (The units are converted to ppm - minute units prior to passing
!       the rate parameters to the integration program.  The conversion
!       used is:
!               A (ppm-min units) =
!                       A (cm-molec-sec units) * 60 *
!                                       [(7.3395E+15)/tref)] ** order-1
!               B (ppm-min units) = B (cm-molec-sec units) - order-1
!       where "order" is the order of the reaction.)
!
!
.RXN
EEOH) 1.960E-12 -0.870  0.000 ;ETHE + HO. = RO2-R. + RO2. + #1.56 HCHO &
                                 + #.22 CCHO
!
EEO3) 1.200E-14  5.226  0.000 ;ETHE + O3 = #.12 HO2. + HCHO + #.44 CO &
                                 + #.56 -C + #.37 O3OL-SB + #.12 OLE-RI
!
EEN3) 5.430E-12  6.043  0.000 ;ETHE + NO3 = R2O2. + RO2. + #2 HCHO + NO2
!
EEOA) 1.040E-11  1.574  0.000 ;ETHE + O = RO2-R. + HO2. + RO2. + HCHO + CO &
                                 + #2 OLE-RI
!
PEOH) 4.850E-12 -1.001  0.000 ;PRPE + HO. = RO2-R. + RO2. + HCHO + CCHO
!
PEO3) 1.320E-14  4.182  0.000 ;PRPE + O3 = #.135 RO2-R. + #.165 HO2. &
                                 + #.135 RO2. + #.65 HCHO + #.5 CCHO + #.14 MEK &
                                 + #.295 CO + #.495 -C + #.06 HO. &
                                 + #.285 O3OL-SB + #.36 OLE-RI
!
PEN3) 4.850E-12  3.699  0.000 ;PRPE + NO3 = R2O2. + RO2. + HCHO + CCHO &
                                 + NO2
!
PEOA) 1.180E-11  0.644  0.000 ;PRPE + O = #.4 HO2. + #.5 RCHO + #.5 MEK &
                                 + #-0.5 -C + #.4 OLE-RI
!
BUOH) 6.550E-12 -0.928  0.000 ;BUTE + HO. = RO2-R. + RO2. + HCHO + RCHO
!
BUO3) 3.460E-15  3.403  0.000 ;BUTE + O3 = #.135 RO2-R. + #.165 HO2. &
                                 + #.135 RO2. + #.5 HCHO + #.15 CCHO + #.5 RCHO &
                                 + #.21 MEK + #.295 CO + #.565 -C + #.06 HO. &
                                 + #.285 O3OL-SB + #.36 OLE-RI
!
BUN3) 6.550E-12  3.708  0.000 ;BUTE + NO3 = R2O2. + RO2. + HCHO + RCHO &
                                 + NO2
!
BUOA) 1.250E-11  0.648  0.000 ;BUTE + O = #.4 HO2. + #.5 RCHO + #.5 MEK &
```

```
                                + #.5 -C + #.4 OLE-RI
!
T2OH) 1.010E-11 -1.091  0.000 ;T2BU + HO. = RO2-R. + RO2. + #2 CCHO
!
T2O3) 9.080E-15  2.258  0.000 ;T2BU + O3 = #.27 RO2-R. + #.21 HO2. &
                                + #.27 RO2. + #.3 HCHO + CCHO + #.28 MEK &
                                + #.15 CO + #.43 -C + #.12 HO. + #.2 O3OL-SB &
                                + #.6 OLE-RI
!
T2N3) 1.098E-13 -0.759  2.000 ;T2BU + NO3 = R2O2. + RO2. + #2 CCHO + NO2
!
T2OA) 2.260E-11 -0.020  0.000 ;T2BU + O = #.4 HO2. + #.5 RCHO + #.5 MEK &
                                + #.5 -C + #.4 OLE-RI
!
C2OH) 1.100E-11 -0.968  0.000 ;C2BU + HO. = RO2-R. + RO2. + #2 CCHO
!
C2O3) 3.520E-15  1.953  0.000 ;C2BU + O3 = #.27 RO2-R. + #.21 HO2. &
                                + #.27 RO2. + #.3 HCHO + CCHO + #.28 MEK &
                                + #.15 CO + #.43 -C + #.12 HO. + #.2 O3OL-SB &
                                + #.6 OLE-RI
!
C2N3) 9.710E-14 -0.759  0.000 ;C2BU + NO3 = R2O2. + RO2. + #2 CCHO + NO2
!
C2OA) 1.210E-11 -0.235  0.000 ;C2BU + O = #.4 HO2. + #.5 RCHO + #.5 MEK &
                                + #.5 -C + #.4 OLE-RI
!
IBOH) 9.470E-12 -1.002  0.000 ;IBTE + HO. = RO2-R. + RO2. + HCHO + ACET
!
IBO3) 3.550E-15  3.364  0.000 ;IBTE + O3 = #.1 RO2-R. + #.06 HO2. &
                                + #.1 RO2. + #.5 HCHO + #.5 ACET + #.4 MEK &
                                + #.22 CO + #.1 MGLY + #-0.12 -C + #.1 HO. &
                                + #.185 O3OL-SB + #.26 OLE-RI
!
IBN3) 9.470E-12  1.984  0.000 ;IBTE + NO3 = R2O2. + RO2. + HCHO + ACET &
                                + NO2
!
IBOA) 1.760E-11  0.085  0.000 ;IBTE + O = #.4 HO2. + #.5 RCHO + #.5 MEK &
                                + #.5 -C + #.4 OLE-RI
!
BDOH) 1.480E-11 -0.890  0.000 ;BD13 + HO. = RO2-R. + RO2. + HCHO + RCHO
!
BDO3) 3.300E-14  4.968  0.000 ;BD13 + O3 = #.135 RO2-R. + #.165 HO2. &
                                + #.135 RO2. + #.5 HCHO + #.15 CCHO + #.5 RCHO &
                                + #.21 MEK + #.295 CO + #.565 -C + #.06 HO. &
                                + #.285 O3OL-SB + #.36 OLE-RI
!
BDN3) 1.480E-11  2.959  0.000 ;BD13 + NO3 = R2O2. + RO2. + HCHO + RCHO &
```

```
                                + NO2
!
BDOA) 2.100E-11  0.000  0.000 ;BD13 + O = #.4 HO2. + #.5 RCHO + #.5 MEK &
                                + #.5 -C + #.4 OLE-RI
!
SYOH) 1.070E-11 -1.000  0.000 ;STYR + HO. = RO2-R. + RO2. + HCHO + BALD
!
SYO3) 3.460E-15  3.144  0.000 ;STYR + O3 = #.06 HO2. + #.25 R2O2. &
                                + #.25 RO2. + #.5 HCHO + #.47 CO + #.5 BALD &
                                + #2.03 -C + #.25 HO. + #.435 O3OL-SB &
                                + #.31 OLE-RI + #.25 BZ-O.
!
SYN3) 6.550E-12  2.233  0.000 ;STYR + NO3 = R2O2. + RO2. + HCHO + BALD &
                                + NO2
!
SYOA) 1.210E-11 -0.235  0.000 ;STYR + O = #.4 HO2. + #.5 RCHO + #.5 MEK &
                                + #4.5 -C + #.4 OLE-RI
!
CH4) 6.255E-13  2.548  2.000 ;CH4 + HO. = RO2-R. + HCHO + RO2.
!
C2H6) 1.278E-12  0.918  2.000 ;C2H6 + HO. = RO2-R. + CCHO + RO2.
!
C2H2) 1.700E-12  0.463  0.000 ;C2H2 + HO. = #.7 RO2-R. + #.3 HO2. &
                                + #.3 CO + #.3 -C + #.7 GLY + #.7 RO2.
!
C3H8) 1.350E-12  0.087  2.000 ;C3H8 + HO. = #.039 RO2-XN. + #.961 RO2-R. &
                                + #.658 ACET + #.303 RCHO + #.116 -C + RO2.
!
N-C4) 1.359E-12 -0.378  2.000 ;N-C4 + HO. = #.076 RO2-N. + #.924 RO2-R. &
                                + #.397 R2O2. + #.001 HCHO + #.571 CCHO &
                                + #.14 RCHO + #.533 MEK + #-0.076 -C &
                                + #1.397 RO2.
!
N-C5) 1.890E-12 -0.463  2.000 ;N-C5 + HO. = #.12 RO2-N. + #.88 RO2-R. &
                                + #.544 R2O2. + #.007 HCHO + #.08 CCHO &
                                + #.172 RCHO + #.929 MEK + #.001 -C &
                                + #1.544 RO2.
!
N-C6) 1.350E-11  0.521  0.000 ;N-C6 + HO. = #.185 RO2-N. + #.815 RO2-R. &
                                + #.738 R2O2. + #.02 CCHO + #.105 RCHO &
                                + #1.134 MEK + #.186 -C + #1.738 RO2.
!
N-C7) 1.960E-11  0.596  0.000 ;N-C7 + HO. = #.267 RO2-N. + #.733 RO2-R. &
                                + #.727 R2O2. + #.056 RCHO + #1.241 MEK &
                                + #.535 -C + #1.727 RO2.
!
N-C8) 3.150E-11  0.763  0.000 ;N-C8 + HO. = #.333 RO2-N. + #.667 RO2-R. &
```

```
                                + #.706 R2O2. + #.002 RCHO + #1.333 MEK &
                                + #.998 -C + #1.706 RO2.
!
N-C9) 2.170E-11  0.447  0.000 ;N-C9 + HO. = #.373 RO2-N. + #.627 RO2-R. &
                                + #.673 R2O2. + #.001 RCHO + #1.299 MEK &
                                + #1.934 -C + #1.673 RO2.
!
2MC3) 9.360E-13 -0.550  2.000 ;2MC3 + HO. = #.027 RO2-N. + #.973 RO2-R. &
                                + #.744 R2O2. + #.744 HCHO + #.744 ACET &
                                + #.229 RCHO + #.202 -C + #1.744 RO2.
!
2MC4) 5.110E-12  0.154  0.000 ;2MC4 + HO. = #.064 RO2-N. + #.002 RO2-XN. &
                                + #.933 RO2-R. + #.734 R2O2. + #.614 CCHO &
                                + #.611 ACET + #.133 RCHO + #.303 MEK &
                                + #.007 -C + #1.734 RO2.
!
2MC5) 8.212E-12  0.222  0.000 ;2MC5 + HO. = #.122 RO2-N. + #.005 RO2-XN. &
                                + #.873 RO2-R. + #.749 R2O2. + #.006 HCHO &
                                + #.023 CCHO + #.223 ACET + #.545 RCHO &
                                + #.724 MEK + #.137 -C + #1.749 RO2.
!
3MC5) 6.680E-12  0.088  0.000 ;3MC5 + HO. = #.112 RO2-N. + #.888 RO2-R. &
                                + #.86 R2O2. + #.005 HCHO + #.523 CCHO &
                                + #.089 RCHO + #1.003 MEK + #.11 -C &
                                + #1.86 RO2.
!
22C4) 2.840E-11  1.484  0.000 ;22C4 + HO. = #.153 RO2-N. + #.847 RO2-R. &
                                + #.96 R2O2. + #.295 HCHO + #.303 CCHO &
                                + #.295 ACET + #.372 RCHO + #.542 MEK &
                                + #.164 -C + #1.96 RO2.
!
23C4) 4.592E-12 -0.108  0.000 ;23C4 + HO. = #.061 RO2-N. + #.039 RO2-XN. &
                                + #.901 RO2-R. + #.944 R2O2. + #1.584 ACET &
                                + #.128 RCHO + #.096 MEK + #.177 -C &
                                + #1.944 RO2.
!
2MC6) 1.066E-11  0.262  0.000 ;2MC6 + HO. = #.196 RO2-N. + #.803 RO2-R. &
                                + #.858 R2O2. + #.03 HCHO + #.037 CCHO &
                                + #.036 ACET + #.118 RCHO + #1.265 MEK &
                                + #.393 -C + #1.858 RO2.
!
3MC6) 9.337E-12  0.152  0.000 ;3MC6 + HO. = #.182 RO2-N. + #.002 RO2-XN. &
                                + #.815 RO2-R. + #.842 R2O2. + #.127 CCHO &
                                + #.329 RCHO + #1.119 MEK + #.369 -C &
                                + #1.842 RO2.
!
23C5) 6.194E-12 -0.097  0.000 ;23C5 + HO. = #.128 RO2-N. + #.011 RO2-XN. &
```

```
                                  + #.86 RO2-R. + #1.101 R2O2. + #.036 HCHO &
                                  + #.253 CCHO + #.39 ACET + #.185 RCHO &
                                  + #.96 MEK + #.252 -C + #2.101 RO2.
!
24C5) 6.898E-12 -0.002  0.000 ;24C5 + HO. = #.131 RO2-N. + #.002 RO2-XN. &
                                  + #.867 RO2-R. + #.844 R2O2. + #.257 ACET &
                                  + #.772 RCHO + #.682 MEK + #.531 -C &
                                  + #1.844 RO2.
!
I-C8) 1.610E-11  0.874  0.000 ;I-C8 + HO. = #.188 RO2-N. + #.001 RO2-XN. &
                                  + #.811 RO2-R. + #.878 R2O2. + #.115 HCHO &
                                  + #.001 CCHO + #.254 ACET + #.745 RCHO &
                                  + #.573 MEK + #1.65 -C + #1.878 RO2.
!
CYC5) 1.917E-12 -0.594  2.000 ;CYC5 + HO. = #.127 RO2-N. + #.873 RO2-R. &
                                  + #1.745 R2O2. + #.873 RCHO + #.218 MEK &
                                  + #.873 CO + #2.745 RO2.
!
CYC6) 2.394E-12 -0.684  2.000 ;CYC6 + HO. = #.193 RO2-N. + #.807 RO2-R. &
                                  + #.352 R2O2. + #.003 HCHO + #.333 RCHO &
                                  + #.816 MEK + #.003 CO2 + #.765 -C &
                                  + #1.352 RO2.
!
MCY5) 1.253E-11  0.260  0.000 ;MCY5 + HO. = #.153 RO2-N. + #.847 RO2-R. &
                                  + #1.978 R2O2. + #.283 HCHO + #.697 RCHO &
                                  + #.49 MEK + #.564 CO + #.189 CO2 + #.153 -C &
                                  + #2.978 RO2.
!
MCY6) 1.337E-11  0.155  0.000 ;MCY6 + HO. = #.216 RO2-N. + #.784 RO2-R. &
                                  + #.928 R2O2. + #.092 HCHO + #.001 CCHO &
                                  + #.466 RCHO + #.987 MEK + #.003 CO &
                                  + #.046 CO2 + #.432 -C + #1.928 RO2.
!
C6H6) 2.500E-12  0.397  0.000 ;C6H6 + HO. = #.236 PHEN + #.207 GLY &
                                  + #.49 AFG1 + #.764 RO2-R. + #.236 HO2. &
                                  + #3.19 -C + #.764 RO2.
!
TOLU) 1.810E-12 -0.705  0.000 ;TOLU + HO. = #.085 BALD + #.26 CRES &
                                  + #.118 GLY + #.131 MGLY + #.41 AFG2 &
                                  + #.74 RO2-R. + #.26 HO2. + #2.726 -C &
                                  + #.74 RO2.
!
ETBZ) 7.100E-12  0.000  0.000 ;ETBZ + HO. = #.085 BALD + #.26 CRES &
                                  + #.118 GLY + #.131 MGLY + #.41 AFG2 &
                                  + #.74 RO2-R. + #.26 HO2. + #3.726 -C &
                                  + #.74 RO2.
!
```

```
IPBZ) 6.500E-12  0.000  0.000 ;IPBZ + HO. = #.085 BALD + #.26 CRES &
                                + #.118 GLY + #.131 MGLY + #.41 AFG2 &
                                + #.74 RO2-R. + #.26 HO2. + #4.726 -C &
                                + #.74 RO2.
!
NPBZ) 6.000E-12  0.000  0.000 ;NPBZ + HO. = #.085 BALD + #.26 CRES &
                                + #.118 GLY + #.131 MGLY + #.41 AFG2 &
                                + #.74 RO2-R. + #.26 HO2. + #4.726 -C &
                                + #.74 RO2.
!
XYLM) 2.360E-11  0.000  0.000 ;XYLM + HO. = #.04 BALD + #.18 CRES &
                                + #.108 GLY + #.37 MGLY + #.666 AFG2 &
                                + #.82 RO2-R. + #.18 HO2. + #3.136 -C &
                                + #.82 RO2.
!
XYLO) 1.370E-11  0.000  0.000 ;XYLO + HO. = #.04 BALD + #.18 CRES &
                                + #.108 GLY + #.37 MGLY + #.666 AFG2 &
                                + #.82 RO2-R. + #.18 HO2. + #3.136 -C &
                                + #.82 RO2.
!
XYLP) 1.430E-11  0.000  0.000 ;XYLP + HO. = #.04 BALD + #.18 CRES &
                                + #.108 GLY + #.37 MGLY + #.666 AFG2 &
                                + #.82 RO2-R. + #.18 HO2. + #3.136 -C &
                                + #.82 RO2.
!
T135) 5.750E-11  0.000  0.000 ;T135 + HO. = #.03 BALD + #.18 CRES &
                                + #.62 MGLY + #.6 AFG2 + #.82 RO2-R. &
                                + #.18 HO2. + #3.87 -C + #.82 RO2.
!
T123) 3.270E-11  0.000  0.000 ;T123 + HO. = #.03 BALD + #.18 CRES &
                                + #.62 MGLY + #.6 AFG2 + #.82 RO2-R. &
                                + #.18 HO2. + #3.87 -C + #.82 RO2.
!
T124) 3.250E-11  0.000  0.000 ;T124 + HO. = #.03 BALD + #.18 CRES &
                                + #.62 MGLY + #.6 AFG2 + #.82 RO2-R. &
                                + #.18 HO2. + #3.87 -C + #.82 RO2.
!
IPOH) 2.540E-11 -0.815  0.000 ;ISOP + HO. = RO2-R. + RO2. + HCHO + RCHO &
                                + -C
!
IPO3) 1.230E-14  4.000  0.000 ;ISOP + O3 = #.135 RO2-R. + #.165 HO2. &
                                + #.135 RO2. + #.5 HCHO + #.15 CCHO + #.5 RCHO &
                                + #.21 MEK + #.295 CO + #1.565 -C + #.06 HO. &
                                + #.285 O3OL-SB + #.36 OLE-RI
!
IPN3) 3.030E-12  0.886  0.000 ;ISOP + NO3 = R2O2. + RO2. + HCHO + RCHO &
                                + -C + NO2
```

```
!
IPOA) 6.000E-11  0.000  0.000 ;ISOP + O = #.4 HO2. + #.5 RCHO + #.5 MEK &
                                + #1.5 -C + #.4 OLE-RI
!
APOH) 1.210E-11 -0.882  0.000 ;APIN + HO. = RO2-R. + RO2. + RCHO + #7 -C
!
APO3) 9.900E-16  1.366  0.000 ;APIN + O3 = #.135 RO2-R. + #.105 HO2. &
                                + #.15 R2O2. + #.285 RO2. + #.05 CCO-O2. &
                                + #.05 C2CO-O2. + #.1 RCO3. + #.05 HCHO &
                                + #.2 CCHO + #.5 RCHO + #.61 MEK + #.075 CO &
                                + #5.285 -C + #.16 HO. + #.1 O3OL-SB &
                                + #.5 OLE-RI
!
APN3) 1.190E-12 -0.974  0.000 ;APIN + NO3 = R2O2. + RO2. + RCHO + #7 -C &
                                + NO2
!
APOA) 3.000E-11  0.000  0.000 ;APIN + O = #.4 HO2. + #.5 RCHO + #.5 MEK &
                                + #6.5 -C + #.4 OLE-RI
!
BPOH) 2.380E-11 -0.709  0.000 ;BPIN + HO. = RO2-R. + RO2. + HCHO + RCHO &
                                + #6 -C
!
BPO3) 3.550E-15  3.187  0.000 ;BPIN + O3 = #.135 RO2-R. + #.165 HO2. &
                                + #.135 RO2. + #.5 HCHO + #.15 CCHO + #.5 RCHO &
                                + #.21 MEK + #.295 CO + #6.565 -C + #.06 HO. &
                                + #.285 O3OL-SB + #.36 OLE-RI
!
BPN3) 2.510E-12  0.000  0.000 ;BPIN + NO3 = R2O2. + RO2. + HCHO + RCHO &
                                + #6 -C + NO2
!
BPOA) 2.800E-11  0.000  0.000 ;BPIN + O = #.4 HO2. + #.5 RCHO + #.5 MEK &
                                + #6.5 -C + #.4 OLE-RI
!
MTBE) 6.129E-13 -0.914  2.000 ;MTBE + HO. = #.02 RO2-N. + #.98 RO2-R. &
                                + #.37 R2O2. + #.39 HCHO + #.41 MEK + #2.87 -C &
                                + #1.37 RO2.
!
TCA)  3.10E-12   3.30   0.00  ;TCA + HO. = RO2-R. + RO2. + CCHO
!  kinetic recommendations of Atkinson et al. (1992)
!
PERC) 9.40E-12   2.42   0.00  ;PERC + HO. = RO2-R. + RO2. + CCHO
!  kinetic recommendations of Atkinson et al. (1992)
```

B.2 Mechanism for toxic VOCs

Extensions to the core chemical mechanism [29] are listed for the modeling of toxic VOCs described in Chapter 6. Most of the data below are from Carter [29,127], except as indicated otherwise.

```
!-------------------------------------------------------------------------
! AIRTOXIC.RXN:
!-------------------------------------------------------------------------
!
.ACT
!          ---- Defaults for ----
!        Conc(0)   Mwt    #C's   #N's
!
CH4       0.0     16.04    1.0    0      methane
C2H6      0.0     30.07    2.0    0      ethane
ETHE      0.0     28.05    2.0    0      ethene
C6H6      0.0     78.11    6.0    0      benzene
TOLU      0.0     92.14    7.0    0      toluene
ETBZ      0.0    106.17    8.0    0      ethylbenzene
IPBZ      0.0    120.19    9.0    0      isopropylbenzene
XYLO      0.0    106.17    8.0    0      o-xylene
XYLM      0.0    106.17    8.0    0      m-xylene
XYLP      0.0    106.17    8.0    0      p-xylene
STYR      0.0    104.15    8.0    0      styrene
BD13      0.0     56.10    4.0    0      1,3-butadiene
ISOP      0.0     70.13    5.0    0      isoprene
APIN      0.0    136.24   10.0    0      alpha-pinene
BPIN      0.0    136.24   10.0    0      beta-pinene
TCA       0.0    133.40    2.0    0      1,1,1-trichloroethane
PERC      0.0    165.83    2.0    0      perchloroethylene
EGLY      0.0     62.07    2.0    0      ethylene glycol
PHEO      0.0     94.11    6.0    0      phenol
CREO      0.0    108.14    7.0    0      o-cresol
CREP      0.0    108.14    7.0    0      p-cresol
MIBK      0.0    100.16    6.0    0      methyl isobutyl ketone
ACRO      0.0     56.07    3.0    0      acrolein
H2CO      0.0     30.05    1.0    0      formaldehyde (directly emitted)
C2HO      0.0     44.05    2.0    0      acetaldehyde (directly emitted)
R2HO      0.0     58.08    3.0    0      propionaldehyde (directly emitted)
A2RO      0.0     56.07    3.0    0      acrolein (directly emitted)
ACE2      0.0     58.08    3.0    0      acetone (directly emitted)
MEK2      0.0     72.11    4.0    0      methyl ethyl ketone (directly emitted)
PHE2      0.0     94.11    6.0    0      phenol (directly emitted)
!
```

```
!
.RXN
BBOH) 2.500E-12  0.397  0.000 ;C6H6 + HO. = #.236 PHEO + #.207 GLY &
                               + #.49 AFG1 + #.764 RO2-R. + #.236 HO2. &
                               + #3.19 -C + #.764 RO2.
!
TTOH) 1.810E-12 -0.705  0.000 ;TOLU + HO. = #.085 BALD + #.204 CREO &
                               + #.118 GLY + #.131 MGLY + #.41 AFG2 &
                               + #.74 RO2-R. + #.26 HO2. + #2.726 -C &
                               + #.74 RO2. + #.048 CREP
!
PHOH) 2.63E-11                 ;PHEO + HO. = #.15 RO2-NP. + #.85 RO2-R. + &
                                 #.2 GLY + #4.7 -C + RO2.
!
PHN3) 3.92E-12                 ;PHEO + NO3 = HNO3 + BZ-O.
!
P2OH) 2.63E-11                 ;PHE2 + HO. = #.15 RO2-NP. + #.85 RO2-R. + &
                                 #.2 GLY + #4.7 -C + RO2.
!
P2N3) 3.92E-12                 ;PHE2 + NO3 = HNO3 + BZ-O.
!
CROH) 4.20E-11                 ;CREO + HO. = #.15 RO2-NP. + #.85 RO2-R. + &
                                 #.2 MGLY + #5.5 -C + RO2.
!
CRN3) 1.37E-11                 ;CREO + NO3 = HNO3 + BZ-O. + -C
!
CPOH) 4.70E-11                 ;CREP + HO. = #.15 RO2-NP. + #.85 RO2-R. + &
                                 #.2 MGLY + #5.5 -C + RO2.
!
CPN3) 1.07E-11                 ;CREP + NO3 = HNO3 + BZ-O. + -C
!
ETBZ) 7.100E-12                ;ETBZ + HO. = #.085 BALD + #.26 CRES &
                                 + #.118 GLY + #.131 MGLY + #.41 AFG2 &
                                 + #.74 RO2-R. + #.26 HO2. + #3.726 -C &
                                 + #.74 RO2.
!
IPBZ) 6.500E-12                ;IPBZ + HO. = #.085 BALD + #.26 CRES &
                                 + #.118 GLY + #.131 MGLY + #.41 AFG2 &
                                 + #.74 RO2-R. + #.26 HO2. + #4.726 -C &
                                 + #.74 RO2.
!
XYLO) 1.370E-11                ;XYLO + HO. = #.04 BALD + #.18 CRES &
                                 + #.108 GLY + #.37 MGLY + #.666 AFG2 &
                                 + #.82 RO2-R. + #.18 HO2. + #3.136 -C &
                                 + #.82 RO2.
!
XYLM) 2.360E-11                ;XYLM + HO. = #.04 BALD + #.18 CRES &
```

```
                                + #.108 GLY + #.37 MGLY + #.666 AFG2 &
                                + #.82 RO2-R. + #.18 HO2. + #3.136 -C &
                                + #.82 RO2.
!
XYLP) 1.430E-11                ;XYLP + HO. = #.04 BALD + #.18 CRES &
                                + #.108 GLY + #.37 MGLY + #.666 AFG2 &
                                + #.82 RO2-R. + #.18 HO2. + #3.136 -C &
                                + #.82 RO2.
!
BDOH) 1.480E-11 -0.890  0.000 ;BD13 + HO. = RO2-R. + RO2. + HCHO + ACRO
!
BDO3) 3.300E-14  4.968  0.000 ;BD13 + O3 = #.135 RO2-R. + #.165 HO2. &
                                + #.135 RO2. + #.5 HCHO + #.15 CCHO + ACRO &
                                + #.21 MEK + #.295 CO + #.565 -C + #.06 HO. &
                                + #.285 O3OL-SB + #.36 OLE-RI
!
BDN3) 1.480E-11  2.959  0.000 ;BD13 + NO3 = R2O2. + RO2. + HCHO + RCHO &
                                + NO2
!
BDOA) 2.100E-11  0.000  0.000 ;BD13 + O = #.4 HO2. + #.5 RCHO + #.5 MEK &
                                + #.5 -C + #.4 OLE-RI
!
SYOH) 1.070E-11 -1.000  0.000 ;STYR + HO. = RO2-R. + RO2. + HCHO + BALD
!
SYO3) 3.460E-15  3.144  0.000 ;STYR + O3 = #.06 HO2. + #.25 R2O2. &
                                + #.25 RO2. + #.5 HCHO + #.47 CO + #.5 BALD &
                                + #2.03 -C + #.25 HO. + #.435 O3OL-SB &
                                + #.31 OLE-RI + #.25 BZ-O.
!
SYN3) 6.550E-12  2.233  0.000 ;STYR + NO3 = R2O2. + RO2. + HCHO + BALD &
                                + NO2
!
SYOA) 1.210E-11 -0.235  0.000 ;STYR + O = #.4 HO2. + #.5 RCHO + #.5 MEK &
                                + #4.5 -C + #.4 OLE-RI
!
TCA)  3.10E-12   3.299  0.00  ;TCA + HO. = RO2-R. + RO2. + CCHO
!  kinetic recommendations of Atkinson et al. (1992)
!
PERC) 9.40E-12   2.385  0.00  ;PERC + HO. = RO2-R. + RO2. + CCHO
!  kinetic recommendations of Atkinson et al. (1992)
!
EGLY) 7.70E-12                 ;EGLY + HO. = HO2. + CCHO
!
S1) SAMEK C1            ;H2CO + HV = #2 HO2. + CO
!
S2) SAMEK C2            ;H2CO + HV = H2 + CO
!
```

```
S3) SAMEK C3            ;H2CO + HO. = HO2. + CO + H2O
!
S4) SAMEK C4            ;H2CO + HO2. = HOCOO.
!
S9) SAMEK C9            ;H2CO + NO3 = HNO3 + HO2. + CO
!
S10) SAMEK C10          ;C2HO + HO. = CCO-O2. + H2O + RCO3.
!
S11A) SAMEK C11A        ;C2HO + HV = CO + HO2. + HCHO + RO2-R. + RO2.
!
S12) SAMEK C12          ;C2HO + NO3 = HNO3 + CCO-O2. + RCO3.
!
S25) SAMEK C25          ;R2HO + HO. = C2CO-O2. + RCO3.
!
S26) SAMEK C26          ;R2HO + HV = CCHO + RO2-R. + RO2. + CO + HO2.
!
S27) SAMEK C27          ;NO3 + R2HO = HNO3 + C2CO-O2. + RCO3.
!
ACRO) 1.99E-11          ;ACRO + HO. = C2CO-O2. + RCO3.
! rate constant from Atkinson (1990)
! same reaction products as RCHO (propionaldehyde)
!
A2RO) SAMEK ACRO        ;A2RO + HO. = C2CO-O2. + RCO3.
!
ACO3) 2.80E-19          ;ACRO + O3 = #.5 "HCHO + GLY" + #1.5 -C
! rate constant from Atkinson (1990)
! products of the acrolein-ozone reaction include formic acid, glyoxal,
! formaldehyde and glyoxylic acid (Grosjean, 1990).  The organic acids
! are taken to be inert.
!
ACO4) SAMEK ACO3        ;A2RO + O3 = #.5 "HCHO + GLY" + #1.5 -C
!
ACN3) 1.20E-15          ;ACRO + NO3 = HNO3 + C2CO-O2. + RCO3.
!
ACN4) SAMEK ACN3        ;A2RO + NO3 = HNO3 + C2CO-O2. + RCO3.
!
S38) SAMEK C38          ;ACE2 + HO. = #.8 "MGLY + RO2-R." + #.2 "R2O2. + &
                                      HCHO + CCO-O2. + RCO3." + RO2.
!
S39) SAMEK C39          ;ACE2 + HV = CCO-O2. + HCHO + RO2-R. + RCO3. + RO2.
!
S44) SAMEK C44          ;MEK2 + HO. = H2O + #.5 "CCHO + HCHO + CCO-O2. + &
                                     C2CO-O2." + RCO3. + #1.5 "R2O2. + RO2."
!
S57) SAMEK C57          ;MEK2 + HV + #QY.MEK2 = CCO-O2. + CCHO + RO2-R. + &
                                                RCO3. + RO2.
.COE
```

```
QY.MEK2 0.1
!
.RXN
!
MIBK) 1.41E-11            ;MIBK + HO. = H2O + #.5 "CCHO + HCHO + CCO-O2. + &
                                        C2CO-O2." + RCO3. + #1.5 "R2O2. + RO2."
!
!  kinetic parameters from Atkinson (1990)
!  same reaction products as MEK
!
!
!
! The following species are not toxic, but I want them represented
! explicitly anyway rather than lumping them with other more reactive
! species:  methane, ethane, ethene.
!
CH4) 6.255E-13  2.548  2.000 ;CH4 + HO. = RO2-R. + HCHO + RO2.
!
C2H6) 1.278E-12  0.918  2.000 ;C2H6 + HO. = RO2-R. + CCHO + RO2.
!
EEOH) 1.960E-12 -0.870  0.000 ;ETHE + HO. = RO2-R. + RO2. + #1.56 HCHO &
                                  + #.22 CCHO
!
EEO3) 1.200E-14  5.226  0.000 ;ETHE + O3 = #.12 HO2. + HCHO + #.44 CO &
                                  + #.56 -C + #.37 O3OL-SB + #.12 OLE-RI
!
EEN3) 5.430E-12  6.043  0.000 ;ETHE + NO3 = R2O2. + RO2. + #2 HCHO + NO2
!
EEOA) 1.040E-11  1.574  0.000 ;ETHE + O = RO2-R. + HO2. + RO2. + HCHO + CO &
                                  + #2 OLE-RI
!
!  REACTIONS OF THE BIOGENIC HYDROCARBONS:
!
IPOH) 2.540E-11 -0.815  0.000 ;ISOP + HO. = RO2-R. + RO2. + HCHO + RCHO &
                                  + -C
!
IPO3) 1.230E-14  4.000  0.000 ;ISOP + O3 = #.135 RO2-R. + #.165 HO2. &
                                  + #.135 RO2. + #.5 HCHO + #.15 CCHO + #.5 RCHO &
                                  + #.21 MEK + #.295 CO + #1.565 -C + #.06 HO. &
                                  + #.285 O3OL-SB + #.36 OLE-RI
!
IPN3) 3.030E-12  0.886  0.000 ;ISOP + NO3 = R2O2. + RO2. + HCHO + RCHO &
                                  + -C + NO2
!
IPOA) 6.000E-11  0.000  0.000 ;ISOP + O = #.4 HO2. + #.5 RCHO + #.5 MEK &
                                  + #1.5 -C + #.4 OLE-RI
!
```

```
APOH) 1.210E-11 -0.882  0.000 ;APIN + HO. = RO2-R. + RO2. + RCHO + #7 -C
!
APO3) 9.900E-16  1.366  0.000 ;APIN + O3 = #.135 RO2-R. + #.105 HO2. &
                                + #.15 R2O2. + #.285 RO2. + #.05 CCO-O2. &
                                + #.05 C2CO-O2. + #.1 RCO3. + #.05 HCHO &
                                + #.2 CCHO + #.5 RCHO + #.61 MEK + #.075 CO &
                                + #5.285 -C + #.16 HO. + #.1 O3OL-SB &
                                + #.5 OLE-RI
!
APN3) 1.190E-12 -0.974  0.000 ;APIN + NO3 = R2O2. + RO2. + RCHO + #7 -C &
                                + NO2
!
APOA) 3.000E-11  0.000  0.000 ;APIN + O = #.4 HO2. + #.5 RCHO + #.5 MEK &
                                + #6.5 -C + #.4 OLE-RI
!
BPOH) 2.380E-11 -0.709  0.000 ;BPIN + HO. = RO2-R. + RO2. + HCHO + RCHO &
                                + #6 -C
!
BPO3) 3.550E-15  3.187  0.000 ;BPIN + O3 = #.135 RO2-R. + #.165 HO2. &
                                + #.135 RO2. + #.5 HCHO + #.15 CCHO + #.5 RCHO &
                                + #.21 MEK + #.295 CO + #6.565 -C + #.06 HO. &
                                + #.285 O3OL-SB + #.36 OLE-RI
!
BPN3) 2.510E-12  0.000  0.000 ;BPIN + NO3 = R2O2. + RO2. + HCHO + RCHO &
                                + #6 -C + NO2
!
BPOA) 2.800E-11  0.000  0.000 ;BPIN + O = #.4 HO2. + #.5 RCHO + #.5 MEK &
                                + #6.5 -C + #.4 OLE-RI
!
```

C Speciation profile listings

The new VOC emission speciation profiles described in Chapter 3 are listed in this appendix. Refer back to Chapter 3 for discussion of these profiles.

PROFILE NUMBER 602
NON-CATALYST GASOLINE ENGINE EXHAUST (COHU ET AL. [74])

SAROAD	CHEMICAL NAME	WT. PERCENT
43105	ISOMERS OF HEXANE	0.24
43106	ISOMERS OF HEPTANE	0.61
43107	ISOMERS OF OCTANE	0.35
43108	ISOMERS OF NONANE	0.30
43109	ISOMERS OF DECANE	0.65
43110	ISOMERS OF UNDECANE	1.02
43112	ISOMERS OF DODECANE	0.33
43121	ISOMERS OF PENTENE	0.02
43201	METHANE	9.51
43202	ETHANE	0.94
43203	ETHYLENE	10.15
43204	PROPANE	0.07
43205	PROPYLENE	4.30
43206	ACETYLENE	8.28
43208	PROPADIENE	0.33
43209	METHYLACETYLENE	0.18
43211	3-METHYL-1-PENTENE	0.06
43212	N-BUTANE	1.33
43213	1-BUTENE	0.75
43214	ISOBUTANE	0.17
43215	ISOBUTYLENE	0.95
43216	TRANS-2-BUTENE	0.47

43217	CIS-2-BUTENE	0.22
43218	1,3-BUTADIENE	1.17
43219	ETHYLACETYLENE	0.02
43220	N-PENTANE	1.89
43223	3-METHYL-1-BUTENE	0.06
43224	1-PENTENE	0.45
43225	2-METHYL-1-BUTENE	0.09
43226	TRANS-2-PENTENE	0.59
43227	CIS-2-PENTENE	0.20
43228	2-METHYL-2-BUTENE	0.69
43229	2-METHYLPENTANE	1.35
43230	3-METHYLPENTANE	1.13
43231	N-HEXANE	0.80
43232	N-HEPTANE	0.55
43233	N-OCTANE	0.19
43234	2,3-DIMETHYL-1-BUTENE	0.01
43235	N-NONANE	0.15
43238	N-DECANE	0.16
43241	N-UNDECANE	0.14
43242	CYCLOPENTANE	0.22
43243	ISOPRENE	0.07
43245	1-HEXENE	0.18
43248	CYCLOHEXANE	0.44
43261	METHYLCYCLOHEXANE	0.48
43262	METHYLCYCLOPENTANE	1.23
43270	3-METHYL-TRANS-2-PENTENE	0.07
43271	2,4-DIMETHYLPENTANE	0.35
43272	METHYLCYCLOPENTENE	0.06
43274	2,3-DIMETHYLPENTANE	0.63
43275	2-METHYLHEXANE	0.20
43276	2,2,4-TRIMETHYLPENTANE	0.81
43277	2,4-DIMETHYLHEXANE	0.48
43279	2,3,4-TRIMETHYLPENTANE	0.30
43280	2,3,3-TRIMETHYLPENTANE	0.33
43289	C6 OLEFINS	1.09
43290	C8 OLEFINS	0.75
43291	2,2-DIMETHYLBUTANE	0.29
43292	CYCLOPENTENE	0.22
43293	4-METHYL-TRANS-2-PENTENE	0.47

43294	C7 OLEFINS	1.33
43295	3-METHYLHEXANE	0.37
43296	2,2,3-TRIMETHYLPENTANE	0.14
43297	4-METHYLHEPTANE	0.03
43298	3-METHYLHEPTANE	0.29
43502	FORMALDEHYDE	2.27
43503	ACETALDEHYDE	0.63
43504	PROPRIONALDEHYDE	0.10
43505	ACROLEIN (PROPENAL)	0.47
43510	BUTYRALDEHYDE (BUTANAL)	0.04
43551	ACETONE	0.14
43552	METHYL ETHYL KETONE	0.04
45105	ISOMERS OF BUTYLBENZENE	0.16
45201	BENZENE	3.63
45202	TOLUENE	5.85
45203	ETHYLBENZENE	1.15
45204	O-XYLENE	1.56
45207	1,3,5-TRIMETHYLBENZENE	0.55
45208	1,2,4-TRIMETHYLBENZENE	1.76
45209	N-PROPYLBENZENE	0.68
45211	O-ETHYLTOLUENE	0.34
45212	M-ETHYLTOLUENE	0.21
45225	1,2,3-TRIMETHYLBENZENE	0.01
90029	METHYLHEXENE	0.22
90047	METHYLNONANE	0.03
90063	DIMETHYLPENTENE	0.79
90082	ETHYLMETHYLHEXANE	0.05
90095	TRIMETHYLHEXENE	0.16
90103	PENTADIENE	0.24
98001	2,3-DIMETHYLBUTANE	0.61
98004	2-METHYL-2-PENTENE	0.07
98033	2,2,5-TRIMETHYLHEXANE	0.38
98036	ISOBUTYRALDEHYDE	0.04
98038	C9 OLEFINS	0.67
98039	C10 OLEFINS	0.28
98043	ISOPROPYLBENZENE (CUMENE)	0.28
98044	INDAN	0.20
98045	M-DIETHYLBENZENE	0.24
98047	ISOBUTYLBENZENE	0.10

98050	C10 AROMATICS	1.19
98054	2,4,4-TRIMETHYL-1-PENTENE	0.09
98055	2,4,4-TRIMETHYL-2-PENTENE	0.14
98058	TRIMETHYLCYCLOPENTANE	0.06
98059	DIMETHYLCYCLOHEXANE	0.14
98090	METHYL HEPTENE	0.16
98132	ISOPENTANE	3.69
98133	2-BUTYNE	0.18
98135	4-METHYL-1-PENTENE	0.15
98139	2,3-DIMETHYLHEXANE	0.05
98140	2-METHYLHEPTANE	0.02
98141	2,3,5-TRIMETHYLHEXANE	0.12
98144	3,5-DIMETHYLHEPTANE	0.08
98145	2,3-DIMETHYLHEPTANE	0.03
98146	2-METHYLOCTANE	0.30
98147	2,4,5-TRIMETHYLHEPTANE	0.26
98149	2,4-DIMETHYLOCTANE	0.72
98152	1-METHYL-3N-PROPYLBENZENE	0.12
98154	O-DIETHYLBENZENE	0.04
98155	2-METHYLDECANE	0.24
98156	CROTONALDEHYDE	0.13
98157	BENZALDEHYDE	0.41
98159	HEXANALDEHYDE	0.13
99024	M- AND P-XYLENE	4.16
99999	UNIDENTIFIED	1.82

PROFILE NUMBER 603
CATALYST-EQUIPPED GASOLINE ENGINE EXHAUST (SIGSBY ET AL. [77], STUMP ET AL. [78, 79], AUTO/OIL STUDY-OLDER VEHICLES [80])

SAROAD	CHEMICAL NAME	WT. PERCENT
43106	ISOMERS OF HEPTANE	0.01
43109	ISOMERS OF DECANE	0.29
43110	ISOMERS OF UNDECANE	0.18
43120	ISOMERS OF 1-BUTENE	0.48
43201	METHANE	15.01
43202	ETHANE	2.94
43203	ETHYLENE	5.95
43204	PROPANE	0.13
43205	PROPYLENE	2.49
43206	ACETYLENE	2.64
43208	PROPADIENE	0.08
43209	METHYLACETYLENE	0.09
43211	3-METHYL-1-PENTENE	0.01
43212	N-BUTANE	4.37
43213	1-BUTENE	0.42
43214	ISOBUTANE	0.52
43215	ISOBUTYLENE	0.80
43216	TRANS-2-BUTENE	0.31
43217	CIS-2-BUTENE	0.56
43218	1,3-BUTADIENE	0.23
43220	N-PENTANE	1.85
43223	3-METHYL-1-BUTENE	0.12
43224	1-PENTENE	0.15
43225	2-METHYL-1-BUTENE	0.12
43226	TRANS-2-PENTENE	0.24
43227	CIS-2-PENTENE	0.14
43228	2-METHYL-2-BUTENE	0.50
43229	2-METHYLPENTANE	2.12
43230	3-METHYLPENTANE	1.27
43231	N-HEXANE	1.00
43232	N-HEPTANE	0.33

43233	N-OCTANE	0.24
43235	N-NONANE	0.05
43238	N-DECANE	0.09
43241	N-UNDECANE	0.24
43242	CYCLOPENTANE	0.19
43243	ISOPRENE	0.10
43245	1-HEXENE	0.16
43246	2-HEXENE	0.02
43248	CYCLOHEXANE	0.03
43255	N-DODECANE	0.01
43261	METHYLCYCLOHEXANE	0.38
43262	METHYLCYCLOPENTANE	0.54
43265	OCTENE	0.01
43266	CIS-2-OCTENE	0.01
43267	1-NONENE	0.01
43270	3-METHYL-TRANS-2-PENTENE	0.05
43271	2,4-DIMETHYLPENTANE	0.76
43272	METHYLCYCLOPENTENE	0.04
43273	CYCLOHEXENE	0.04
43274	2,3-DIMETHYLPENTANE	1.03
43275	2-METHYLHEXANE	0.48
43276	2,2,4-TRIMETHYLPENTANE	3.45
43277	2,4-DIMETHYLHEXANE	0.37
43278	2,5-DIMETHYLHEXANE	0.30
43279	2,3,4-TRIMETHYLPENTANE	1.88
43280	2,3,3-TRIMETHYLPENTANE	0.21
43288	ETHYLCYCLOHEXANE	0.00
43289	C6 OLEFINS	0.02
43290	C8 OLEFINS	0.00
43291	2,2-DIMETHYLBUTANE	0.63
43292	CYCLOPENTENE	0.12
43293	4-METHYL-TRANS-2-PENTENE	0.11
43295	3-METHYLHEXANE	0.75
43297	4-METHYLHEPTANE	0.23
43298	3-METHYLHEPTANE	0.37
43502	FORMALDEHYDE	1.25
43503	ACETALDEHYDE	0.62
43504	PROPRIONALDEHYDE	0.06
43505	ACROLEIN (PROPENAL)	0.14

43510	BUTYRALDEHYDE (BUTANAL)	0.06
43512	C5 ALDEHYDE	0.06
43551	ACETONE	0.39
43552	METHYL ETHYL KETONE	0.08
45104	ISOMERS OF ETHYLTOLUENE	0.66
45105	ISOMERS OF BUTYLBENZENE	0.08
45106	ISOMERS OF DIETHYLBENZENE	0.02
45201	BENZENE	3.72
45202	TOLUENE	8.90
45203	ETHYLBENZENE	1.29
45204	O-XYLENE	1.31
45207	1,3,5-TRIMETHYLBENZENE	1.29
45208	1,2,4-TRIMETHYLBENZENE	1.90
45209	N-PROPYLBENZENE	0.56
45211	O-ETHYLTOLUENE	0.33
45212	M-ETHYLTOLUENE	0.77
45213	P-ETHYLTOLUENE	0.14
45216	SEC-BUTYLBENZENE	0.12
45220	STYRENE	0.21
45225	1,2,3-TRIMETHYLBENZENE	0.50
45232	TETRAMETHYLBENZENE	0.10
45234	METHYLPROPYLBENZENE	0.02
46747	METHYLINDANS	0.07
90029	METHYLHEXENE	0.02
90047	METHYLNONANE	0.02
90063	DIMETHYLPENTENE	0.02
90064	DIMETHYLCYCLOPENTANE	0.18
90078	ETHYLPENTENE	0.00
90080	ETHYLMETHYLCYCLOPENTANE	0.05
90103	PENTADIENE	0.05
90120	PROPYLCYCLOHEXANE	0.00
98001	2,3-DIMETHYLBUTANE	1.01
98002	2-ETHYL-1-BUTENE	0.03
98003	CIS-3-HEXENE	0.01
98004	2-METHYL-2-PENTENE	0.08
98005	1-HEPTENE	0.00
98032	3,5,5-TRIMETHYLHEXANE	0.00
98033	2,2,5-TRIMETHYLHEXANE	0.63
98034	TRANS-2-HEXENE	0.03

98035	CIS-2-HEXENE	0.03
98037	1-METHYLCYCLOHEXENE	0.05
98038	C9 OLEFINS	0.14
98040	2-METHYL-1-PENTENE	0.01
98041	3-HEPTENE	0.02
98043	ISOPROPYLBENZENE (CUMENE)	0.01
98044	INDAN	0.24
98045	M-DIETHYLBENZENE	0.19
98046	NAPHTHALENE	0.04
98047	ISOBUTYLBENZENE	0.09
98050	C10 AROMATICS	1.12
98054	2,4,4-TRIMETHYL-1-PENTENE	0.01
98056	ISOVALERALDEHYDE	0.02
98057	ETHYLCYCLOPENTANE	0.04
98058	TRIMETHYLCYCLOPENTANE	0.00
98059	DIMETHYLCYCLOHEXANE	0.11
98060	TRIMETHYLCYCLOHEXANE	0.01
98091	DIMETHYLHEPTANE	0.04
98095	C6 ALDEHYDE	0.08
98130	2,2-DIMETHYLPROPANE	0.00
98132	ISOPENTANE	4.19
98134	2-METHYL-1,3-BUTADIENE	0.05
98135	4-METHYL-1-PENTENE	0.03
98136	TRANS-3-HEXENE	0.12
98137	DIMETHYLHEXENE	0.04
98138	2,2-DIMETHYLHEXANE	0.14
98139	2,3-DIMETHYLHEXANE	0.33
98140	2-METHYLHEPTANE	0.33
98141	2,3,5-TRIMETHYLHEXANE	0.09
98142	2,4-DIMETHYLHEPTANE	0.05
98143	2,5-DIMETHYLHEPTANE	0.06
98144	3,5-DIMETHYLHEPTANE	0.03
98145	2,3-DIMETHYLHEPTANE	0.00
98146	2-METHYLOCTANE	0.24
98147	2,4,5-TRIMETHYLHEPTANE	0.10
98149	2,4-DIMETHYLOCTANE	0.05
98150	C10 PARAFFIN	0.08
98151	3,4-DIMETHYLOCTANE	0.44
98152	1-METHYL-3N-PROPYLBENZENE	0.18

98153	1-METHYL-3-ISOPROPYLBENZENE	0.14
98154	O-DIETHYLBENZENE	0.22
98155	2-METHYLDECANE	0.30
98156	CROTONALDEHYDE	0.03
98157	BENZALDEHYDE	0.20
98158	PARA-TOLUALDEHYDE	0.09
99024	M- AND P-XYLENE	3.50
99999	UNIDENTIFIED	1.88

PROFILE NUMBER 604
SOLVENT-BORNE ARCHITECTURAL SURFACE COATINGS
(SEE SECTION 3.2.5 FOR DESCRIPTION AND REFERENCES)

SAROAD	CHEMICAL NAME	WT. PERCENT
43108	ISOMERS OF NONANE	3.20
43109	ISOMERS OF DECANE	11.02
43110	ISOMERS OF UNDECANE	8.37
43111	ISOMERS OF TRIDECANE	2.40
43112	ISOMERS OF DODECANE	1.75
43235	N-NONANE	3.20
43238	N-DECANE	9.17
43241	N-UNDECANE	3.25
43255	N-DODECANE	0.80
43301	METHYL ALCOHOL	0.10
43302	ETHYL ALCOHOL	0.10
43304	ISOPROPYL ALCOHOL	2.30
43305	N-BUTYL ALCOHOL	1.80
43306	ISOBUTYL ALCOHOL	0.40
43367	GLYCOL ETHER	1.20
43435	N-BUTYL ACETATE	2.70
43445	METHYL AMYL ACETATE	0.20
43446	ISOBUTYL ACETATE	0.20
43551	ACETONE	0.10
43552	METHYL ETHYL KETONE	1.20
43560	METHYL ISOBUTYL KETONE	1.60
43561	METHYL AMYL KETONE	1.00
43814	1,1,1-TRICHLOROETHANE	2.20
45102	ISOMERS OF XYLENE	1.00
45202	TOLUENE	3.20
98050	C10 AROMATICS	1.60
98068	C3 ALKYL CYCLOHEXANE	8.79
98070	C4 SUBSTITUTED CYCLOHEXANE	20.54
98071	C5 SUBSTITUTED CYCLOHEXANE	3.39
98072	C6 SUBSTITUTED CYCLOHEXANE	3.13

PROFILE NUMBER 605
COMPOSITE INDUSTRIAL SURFACE COATINGS
(ROGOZEN ET AL. [96], TABLE 6.1-1)

SAROAD	CHEMICAL NAME	WT. PERCENT
43108	ISOMERS OF NONANE	0.88
43109	ISOMERS OF DECANE	3.08
43110	ISOMERS OF UNDECANE	2.14
43111	ISOMERS OF TRIDECANE	0.63
43112	ISOMERS OF DODECANE	0.24
43235	N-NONANE	0.91
43238	N-DECANE	2.62
43241	N-UNDECANE	0.93
43255	N-DODECANE	0.22
43302	ETHYL ALCOHOL	2.73
43304	ISOPROPYL ALCOHOL	3.52
43305	N-BUTYL ALCOHOL	6.36
43367	GLYCOL ETHER	6.59
43433	ETHYL ACETATE	1.98
43435	N-BUTYL ACETATE	3.06
43446	ISOBUTYL ACETATE	1.55
43551	ACETONE	3.12
43552	METHYL ETHYL KETONE	8.13
43560	METHYL ISOBUTYL KETONE	5.90
45102	ISOMERS OF XYLENE	15.78
45202	TOLUENE	14.67
98050	C10 AROMATICS	4.94
98068	C3 ALKYL CYCLOHEXANE	2.44
98070	C4 SUBSTITUTED CYCLOHEXANE	5.82
98071	C5 SUBSTITUTED CYCLOHEXANE	0.92
98072	C6 SUBSTITUTED CYCLOHEXANE	0.87

PROFILE NUMBER 607
MILITARY JET ENGINE EXHAUST
(SPICER ET AL. [94], SPECIATION DATA SYSTEM [63])

SAROAD	CHEMICAL NAME	WT. PERCENT
43112	ISOMERS OF DODECANE	0.51
43113	ISOMERS OF TETRADECANE	0.20
43114	ISOMERS OF PENTADECANE	0.18
43121	ISOMERS OF PENTENE	0.76
43201	METHANE	9.38
43202	ETHANE	0.91
43203	ETHYLENE	18.37
43204	PROPANE	0.19
43205	PROPYLENE	5.44
43206	ACETYLENE	4.41
43213	1-BUTENE	2.06
43217	CIS-2-BUTENE	0.50
43218	1,3-BUTADIENE	1.89
43220	N-PENTANE	0.22
43224	1-PENTENE	0.89
43228	2-METHYL-2-BUTENE	0.21
43229	2-METHYLPENTANE	0.41
43232	N-HEPTANE	0.07
43233	N-OCTANE	0.05
43235	N-NONANE	0.13
43238	N-DECANE	0.44
43241	N-UNDECANE	0.54
43245	1-HEXENE	0.86
43255	N-DODECANE	1.07
43258	N-TRIDECANE	0.67
43259	N-TETRADECANE	0.59
43260	N-PENTADECANE	0.26
43265	OCTENE	0.30
43267	1-NONENE	0.26
43268	1-DECENE	0.17
43281	HEXADECANE	0.28

43282	HEPTADECANE	0.01
43294	C7 OLEFINS	0.54
43502	FORMALDEHYDE	15.48
43503	ACETALDEHYDE	4.83
43504	PROPRIONALDEHYDE	0.98
43505	ACROLEIN (PROPENAL)	2.38
43510	BUTYRALDEHYDE (BUTANAL)	1.24
43551	ACETONE	2.41
45105	ISOMERS OF BUTYLBENZENE	0.26
45201	BENZENE	2.02
45202	TOLUENE	0.55
45203	ETHYLBENZENE	0.18
45204	O-XYLENE	0.20
45220	STYRENE	0.41
45245	C5 ALKYLBENZENES	0.21
45300	PHENOL	0.26
98010	METHYLNAPHTHALENE	0.52
98046	NAPHTHALENE	0.60
98157	BENZALDEHYDE	0.57
98159	HEXANALDEHYDE	0.22
99024	M- AND P-XYLENE	0.30
99999	UNIDENTIFIED	13.57

PROFILE NUMBER 608
COMMERCIAL JET ENGINE EXHAUST
(SPICER ET AL. [94], SPECIATION DATA SYSTEM [63])

SAROAD	CHEMICAL NAME	WT. PERCENT
43112	ISOMERS OF DODECANE	0.48
43113	ISOMERS OF TETRADECANE	0.19
43114	ISOMERS OF PENTADECANE	0.17
43121	ISOMERS OF PENTENE	0.73
43201	METHANE	9.57
43202	ETHANE	0.88
43203	ETHYLENE	17.43
43204	PROPANE	0.18
43205	PROPYLENE	5.15
43206	ACETYLENE	4.17
43213	1-BUTENE	1.97
43217	CIS-2-BUTENE	0.48
43218	1,3-BUTADIENE	1.80
43220	N-PENTANE	0.21
43224	1-PENTENE	0.84
43228	2-METHYL-2-BUTENE	0.20
43229	2-METHYLPENTANE	0.39
43232	N-HEPTANE	0.06
43233	N-OCTANE	0.05
43235	N-NONANE	0.13
43238	N-DECANE	0.42
43241	N-UNDECANE	0.53
43245	1-HEXENE	0.82
43255	N-DODECANE	1.07
43258	N-TRIDECANE	0.66
43259	N-TETRADECANE	0.58
43260	N-PENTADECANE	0.26
43265	OCTENE	0.28
43267	1-NONENE	0.24
43268	1-DECENE	0.17
43281	HEXADECANE	0.26

43282	HEPTADECANE	0.01
43294	C7 OLEFINS	0.54
43502	FORMALDEHYDE	15.01
43503	ACETALDEHYDE	4.65
43504	PROPRIONALDEHYDE	0.95
43505	ACROLEIN (PROPENAL)	2.27
43510	BUTYRALDEHYDE (BUTANAL)	1.20
43551	ACETONE	2.45
45105	ISOMERS OF BUTYLBENZENE	0.24
45201	BENZENE	1.94
45202	TOLUENE	0.52
45203	ETHYLBENZENE	0.17
45204	O-XYLENE	0.19
45220	STYRENE	0.39
45245	C5 ALKYLBENZENES	0.19
45300	PHENOL	0.24
98010	METHYLNAPHTHALENE	0.49
98046	NAPHTHALENE	0.57
98157	BENZALDEHYDE	0.55
98159	HEXANALDEHYDE	0.21
99024	M- AND P-XYLENE	0.29
99999	UNIDENTIFIED	16.54

PROFILE NUMBER 609
LIQUID GASOLINE-COMPOSITE OF PRODUCT-SUMMER BLEND
(OLIVER AND PEOPLES [68], WEIGHTED BY 1987 SALES)

SAROAD	CHEMICAL NAME	WT. PERCENT
43105	ISOMERS OF HEXANE	0.01
43106	ISOMERS OF HEPTANE	1.61
43107	ISOMERS OF OCTANE	0.84
43108	ISOMERS OF NONANE	2.05
43109	ISOMERS OF DECANE	0.96
43120	ISOMERS OF 1-BUTENE	0.10
43212	N-BUTANE	3.34
43214	ISOBUTANE	0.79
43216	TRANS-2-BUTENE	0.12
43217	CIS-2-BUTENE	0.13
43220	N-PENTANE	2.68
43223	3-METHYL-1-BUTENE	0.08
43224	1-PENTENE	0.34
43225	2-METHYL-1-BUTENE	0.39
43226	TRANS-2-PENTENE	0.70
43227	CIS-2-PENTENE	0.34
43228	2-METHYL-2-BUTENE	1.34
43229	2-METHYLPENTANE	3.28
43230	3-METHYLPENTANE	2.10
43231	N-HEXANE	2.00
43232	N-HEPTANE	2.03
43233	N-OCTANE	0.98
43235	N-NONANE	0.58
43238	N-DECANE	0.20
43241	N-UNDECANE	0.17
43242	CYCLOPENTANE	0.47
43245	1-HEXENE	0.30
43248	CYCLOHEXANE	0.58
43261	METHYLCYCLOHEXANE	0.98
43262	METHYLCYCLOPENTANE	2.46
43265	OCTENE	0.20

43266	CIS-2-OCTENE	0.11
43267	1-NONENE	0.18
43269	1-UNDECENE	0.13
43270	3-METHYL-TRANS-2-PENTENE	0.16
43271	2,4-DIMETHYLPENTANE	1.13
43275	2-METHYLHEXANE	4.07
43276	2,2,4-TRIMETHYLPENTANE	3.94
43278	2,5-DIMETHYLHEXANE	1.49
43279	2,3,4-TRIMETHYLPENTANE	1.57
43289	C6 OLEFINS	0.10
43290	C8 OLEFINS	0.32
43291	2,2-DIMETHYLBUTANE	0.22
43292	CYCLOPENTENE	0.19
43293	4-METHYL-TRANS-2-PENTENE	0.17
43294	C7 OLEFINS	0.04
43295	3-METHYLHEXANE	1.96
43298	3-METHYLHEPTANE	1.51
45105	ISOMERS OF BUTYLBENZENE	0.67
45106	ISOMERS OF DIETHYLBENZENE	0.02
45201	BENZENE	1.87
45202	TOLUENE	10.19
45203	ETHYLBENZENE	1.87
45204	O-XYLENE	3.12
45207	1,3,5-TRIMETHYLBENZENE	1.19
45208	1,2,4-TRIMETHYLBENZENE	3.21
45209	N-PROPYLBENZENE	0.53
45211	O-ETHYLTOLUENE	1.10
45212	M-ETHYLTOLUENE	2.64
45225	1,2,3-TRIMETHYLBENZENE	0.86
98001	2,3-DIMETHYLBUTANE	1.09
98025	A-PINENE	0.08
98026	B-PINENE	0.18
98032	3,5,5-TRIMETHYLHEXANE	1.53
98033	2,2,5-TRIMETHYLHEXANE	0.76
98034	TRANS-2-HEXENE	0.61
98035	CIS-2-HEXENE	0.76
98037	1-METHYLCYCLOHEXENE	0.48
98038	C9 OLEFINS	0.63
98039	C10 OLEFINS	0.08

98043	ISOPROPYLBENZENE (CUMENE)	0.18
98044	INDAN	0.35
98045	M-DIETHYLBENZENE	0.51
98046	NAPHTHALENE	0.03
98047	ISOBUTYLBENZENE	0.04
98048	INDENE	0.04
98050	C10 AROMATICS	0.60
98054	2,4,4-TRIMETHYL-1-PENTENE	0.14
98132	ISOPENTANE	6.87
99024	M- AND P-XYLENE	8.32

PROFILE NUMBER 610
GASOLINE VAPORS-COMPOSITE OF PRODUCT-SUMMER BLEND
(OLIVER AND PEOPLES [68], WEIGHTED BY 1987 SALES)

SAROAD	CHEMICAL NAME	WT. PERCENT
43106	ISOMERS OF HEPTANE	0.25
43107	ISOMERS OF OCTANE	0.03
43108	ISOMERS OF NONANE	0.01
43120	ISOMERS OF 1-BUTENE	1.32
43202	ETHANE	0.18
43204	PROPANE	2.14
43212	N-BUTANE	29.95
43214	ISOBUTANE	11.41
43216	TRANS-2-BUTENE	1.74
43217	CIS-2-BUTENE	1.36
43220	N-PENTANE	6.29
43223	3-METHYL-1-BUTENE	0.43
43224	1-PENTENE	1.03
43225	2-METHYL-1-BUTENE	1.27
43226	TRANS-2-PENTENE	1.72
43227	CIS-2-PENTENE	0.86
43228	2-METHYL-2-BUTENE	2.55
43229	2-METHYLPENTANE	2.80
43230	3-METHYLPENTANE	1.55
43231	N-HEXANE	1.14
43232	N-HEPTANE	0.23
43233	N-OCTANE	0.02
43242	CYCLOPENTANE	0.52
43245	1-HEXENE	0.24
43248	CYCLOHEXANE	0.34
43261	METHYLCYCLOHEXANE	0.10
43262	METHYLCYCLOPENTANE	1.11
43270	3-METHYL-TRANS-2-PENTENE	0.08
43271	2,4-DIMETHYLPENTANE	0.40
43275	2-METHYLHEXANE	0.77
43276	2,2,4-TRIMETHYLPENTANE	0.56

43278	2,5-DIMETHYLHEXANE	0.10
43279	2,3,4-TRIMETHYLPENTANE	0.09
43289	C6 OLEFINS	0.12
43290	C8 OLEFINS	0.01
43291	2,2-DIMETHYLBUTANE	0.25
43292	CYCLOPENTENE	0.28
43293	4-METHYL-TRANS-2-PENTENE	0.19
43294	C7 OLEFINS	0.06
43295	3-METHYLHEXANE	0.33
43298	3-METHYLHEPTANE	0.05
45201	BENZENE	0.66
45202	TOLUENE	0.65
45203	ETHYLBENZENE	0.03
45204	O-XYLENE	0.04
45207	1,3,5-TRIMETHYLBENZENE	0.01
45208	1,2,4-TRIMETHYLBENZENE	0.34
45212	M-ETHYLTOLUENE	0.02
45225	1,2,3-TRIMETHYLBENZENE	0.05
98001	2,3-DIMETHYLBUTANE	1.07
98032	3,5,5-TRIMETHYLHEXANE	0.06
98033	2,2,5-TRIMETHYLHEXANE	0.02
98034	TRANS-2-HEXENE	0.30
98035	CIS-2-HEXENE	0.38
98037	1-METHYLCYCLOHEXENE	0.05
98038	C9 OLEFINS	0.01
98054	2,4,4-TRIMETHYL-1-PENTENE	0.01
98132	ISOPENTANE	22.32
99024	M- AND P-XYLENE	0.13

PROFILE NUMBER 614
INDUSTRIAL ADHESIVE (ROGOZEN ET AL. [96])

SAROAD	CHEMICAL NAME	WT. PERCENT
43105	ISOMERS OF HEXANE	7.78
43106	ISOMERS OF HEPTANE	1.76
43108	ISOMERS OF NONANE	1.94
43109	ISOMERS OF DECANE	6.75
43110	ISOMERS OF UNDECANE	4.69
43111	ISOMERS OF TRIDECANE	1.38
43112	ISOMERS OF DODECANE	0.54
43235	N-NONANE	2.01
43238	N-DECANE	5.75
43241	N-UNDECANE	2.04
43255	N-DODECANE	0.48
43264	CYCLOHEXANONE	1.72
43301	METHYL ALCOHOL	0.29
43302	ETHYL ALCOHOL	0.06
43304	ISOPROPYL ALCOHOL	0.43
43305	N-BUTYL ALCOHOL	0.07
43370	ETHYLENE GLYCOL	0.21
43433	ETHYL ACETATE	0.25
43435	N-BUTYL ACETATE	0.36
43450	DIMETHYL FORMAMIDE	1.82
43551	ACETONE	2.55
43552	METHYL ETHYL KETONE	14.60
43802	DICHLOROMETHANE	1.98
43814	1,1,1-TRICHLOROETHANE	11.06
43824	TRICHLOROETHYLENE	0.70
45102	ISOMERS OF XYLENE	0.14
45202	TOLUENE	6.63
98068	C3 ALKYL CYCLOHEXANE	5.35
98070	C4 SUBSTITUTED CYCLOHEXANE	12.77
98071	C5 SUBSTITUTED CYCLOHEXANE	2.01
98072	C6 SUBSTITUTED CYCLOHEXANE	1.90

PROFILE NUMBER 617
WATER-BORNE ARCHITECTURAL SURFACE COATINGS
(ROGOZEN ET AL. [96])

SAROAD	CHEMICAL NAME	WT. PERCENT
43367	GLYCOL ETHER	27.40
43369	PROPYLENE GLYCOL	29.08
43370	ETHYLENE GLYCOL	43.51

PROFILE NUMBER 618
COMPOSITE THINNING SOLVENT (ROGOZEN ET AL. [96])

SAROAD	CHEMICAL NAME	WT. PERCENT
43108	ISOMERS OF NONANE	0.48
43109	ISOMERS OF DECANE	1.69
43110	ISOMERS OF UNDECANE	1.17
43111	ISOMERS OF TRIDECANE	0.35
43112	ISOMERS OF DODECANE	0.13
43235	N-NONANE	0.50
43238	N-DECANE	1.44
43241	N-UNDECANE	0.51
43255	N-DODECANE	0.12
43302	ETHYL ALCOHOL	11.84
43304	ISOPROPYL ALCOHOL	4.99
43305	N-BUTYL ALCOHOL	0.33
43433	ETHYL ACETATE	3.68
43435	N-BUTYL ACETATE	1.40
43446	ISOBUTYL ACETATE	0.87
43551	ACETONE	10.31
43552	METHYL ETHYL KETONE	15.96
43560	METHYL ISOBUTYL KETONE	0.55
45102	ISOMERS OF XYLENE	11.57
45202	TOLUENE	20.68
98050	C10 AROMATICS	5.90
98068	C3 ALKYL CYCLOHEXANE	1.34
98070	C4 SUBSTITUTED CYCLOHEXANE	3.19
98071	C5 SUBSTITUTED CYCLOHEXANE	0.50
98072	C6 SUBSTITUTED CYCLOHEXANE	0.47

PROFILE NUMBER 629
LIQUID GASOLINE-COMPOSITE OF PRODUCT-WINTER BLEND
(OLIVER AND PEOPLES [68], WEIGHTED BY 1987 SALES)

SAROAD	CHEMICAL NAME	WT. PERCENT
43105	ISOMERS OF HEXANE	0.03
43106	ISOMERS OF HEPTANE	0.82
43107	ISOMERS OF OCTANE	3.97
43108	ISOMERS OF NONANE	1.48
43109	ISOMERS OF DECANE	2.79
43120	ISOMERS OF 1-BUTENE	0.21
43202	ETHANE	0.06
43204	PROPANE	0.08
43212	N-BUTANE	5.88
43214	ISOBUTANE	2.20
43216	TRANS-2-BUTENE	0.24
43217	CIS-2-BUTENE	0.23
43220	N-PENTANE	2.66
43223	3-METHYL-1-BUTENE	0.08
43224	1-PENTENE	0.31
43225	2-METHYL-1-BUTENE	0.38
43226	TRANS-2-PENTENE	0.60
43227	CIS-2-PENTENE	0.32
43228	2-METHYL-2-BUTENE	1.02
43229	2-METHYLPENTANE	2.97
43230	3-METHYLPENTANE	1.83
43231	N-HEXANE	1.75
43232	N-HEPTANE	1.63
43233	N-OCTANE	0.92
43235	N-NONANE	0.60
43238	N-DECANE	0.22
43241	N-UNDECANE	0.21
43242	CYCLOPENTANE	0.49
43245	1-HEXENE	0.35
43248	CYCLOHEXANE	0.50
43261	METHYLCYCLOHEXANE	0.86

43262	METHYLCYCLOPENTANE	2.21
43265	OCTENE	0.14
43266	CIS-2-OCTENE	0.02
43267	1-NONENE	0.06
43269	1-UNDECENE	0.16
43271	2,4-DIMETHYLPENTANE	1.01
43275	2-METHYLHEXANE	3.42
43278	2,5-DIMETHYLHEXANE	1.16
43279	2,3,4-TRIMETHYLPENTANE	1.15
43289	C6 OLEFINS	0.51
43290	C8 OLEFINS	0.38
43291	2,2-DIMETHYLBUTANE	0.14
43292	CYCLOPENTENE	0.19
43293	4-METHYL-TRANS-2-PENTENE	0.08
43294	C7 OLEFINS	0.37
43295	3-METHYLHEXANE	1.56
43298	3-METHYLHEPTANE	1.24
45105	ISOMERS OF BUTYLBENZENE	0.83
45201	BENZENE	1.76
45202	TOLUENE	9.18
45203	ETHYLBENZENE	1.93
45204	O-XYLENE	3.28
45207	1,3,5-TRIMETHYLBENZENE	1.20
45208	1,2,4-TRIMETHYLBENZENE	3.73
45209	N-PROPYLBENZENE	0.62
45211	O-ETHYLTOLUENE	1.17
45212	M-ETHYLTOLUENE	3.00
45225	1,2,3-TRIMETHYLBENZENE	1.20
98001	2,3-DIMETHYLBUTANE	0.95
98025	A-PINENE	0.11
98026	B-PINENE	0.19
98032	3,5,5-TRIMETHYLHEXANE	1.22
98033	2,2,5-TRIMETHYLHEXANE	0.82
98034	TRANS-2-HEXENE	0.56
98035	CIS-2-HEXENE	0.16
98037	1-METHYLCYCLOHEXENE	0.64
98038	C9 OLEFINS	0.41
98043	ISOPROPYLBENZENE (CUMENE)	0.22
98044	INDAN	0.46

98045	M-DIETHYLBENZENE	0.45
98046	NAPHTHALENE	0.23
98047	ISOBUTYLBENZENE	0.05
98048	INDENE	0.04
98049	C9 AROMATICS	1.40
98050	C10 AROMATICS	0.03
98054	2,4,4-TRIMETHYL-1-PENTENE	0.09
98132	ISOPENTANE	6.45
99024	M- AND P-XYLENE	8.28

PROFILE NUMBER 630
GASOLINE VAPORS-COMPOSITE OF PRODUCT-WINTER BLEND
(OLIVER AND PEOPLES [68], WEIGHTED BY 1987 SALES)

SAROAD	CHEMICAL NAME	WT. PERCENT
43106	ISOMERS OF HEPTANE	0.67
43107	ISOMERS OF OCTANE	1.12
43108	ISOMERS OF NONANE	0.23
43109	ISOMERS OF DECANE	0.04
43120	ISOMERS OF 1-BUTENE	1.86
43202	ETHANE	0.10
43204	PROPANE	2.06
43212	N-BUTANE	30.14
43214	ISOBUTANE	17.22
43216	TRANS-2-BUTENE	1.68
43217	CIS-2-BUTENE	1.23
43220	N-PENTANE	4.37
43223	3-METHYL-1-BUTENE	0.27
43224	1-PENTENE	0.72
43225	2-METHYL-1-BUTENE	0.92
43226	TRANS-2-PENTENE	1.12
43227	CIS-2-PENTENE	0.57
43228	2-METHYL-2-BUTENE	1.62
43229	2-METHYLPENTANE	2.45
43230	3-METHYLPENTANE	1.49
43231	N-HEXANE	1.19
43232	N-HEPTANE	0.53
43233	N-OCTANE	0.13
43235	N-NONANE	0.01
43238	N-DECANE	0.01
43242	CYCLOPENTANE	0.55
43245	1-HEXENE	0.33
43248	CYCLOHEXANE	0.28
43261	METHYLCYCLOHEXANE	0.30
43262	METHYLCYCLOPENTANE	1.52
43265	OCTENE	0.04

43266	CIS-2-OCTENE	0.01
43267	1-NONENE	0.01
43271	2,4-DIMETHYLPENTANE	0.57
43275	2-METHYLHEXANE	1.44
43278	2,5-DIMETHYLHEXANE	0.27
43279	2,3,4-TRIMETHYLPENTANE	0.19
43289	C6 OLEFINS	0.51
43290	C8 OLEFINS	0.11
43291	2,2-DIMETHYLBUTANE	0.22
43292	CYCLOPENTENE	0.25
43293	4-METHYL-TRANS-2-PENTENE	0.19
43294	C7 OLEFINS	0.03
43295	3-METHYLHEXANE	0.62
43298	3-METHYLHEPTANE	0.23
45201	BENZENE	1.33
45202	TOLUENE	1.86
45203	ETHYLBENZENE	0.16
45204	O-XYLENE	0.24
45207	1,3,5-TRIMETHYLBENZENE	0.01
45208	1,2,4-TRIMETHYLBENZENE	0.05
45209	N-PROPYLBENZENE	0.01
45211	O-ETHYLTOLUENE	0.01
45212	M-ETHYLTOLUENE	0.04
45225	1,2,3-TRIMETHYLBENZENE	0.02
98001	2,3-DIMETHYLBUTANE	0.89
98004	2-METHYL-2-PENTENE	0.06
98032	3,5,5-TRIMETHYLHEXANE	0.22
98033	2,2,5-TRIMETHYLHEXANE	0.12
98034	TRANS-2-HEXENE	0.36
98035	CIS-2-HEXENE	0.12
98037	1-METHYLCYCLOHEXENE	0.16
98038	C9 OLEFINS	0.11
98041	3-HEPTENE	0.01
98046	NAPHTHALENE	0.01
98049	C9 AROMATICS	0.03
98054	2,4,4-TRIMETHYL-1-PENTENE	0.03
98055	2,4,4-TRIMETHYL-2-PENTENE	0.01
98132	ISOPENTANE	14.21
99024	M- AND P-XYLENE	0.55